

**“The exploration of whitening and sun
screening compounds in bengkoang roots
(*Pachyrhizus erosus*)”**

Dissertation zur Erlangung des naturwissenschaftlichen Doktorgrades Der
Bayerischen Julius-Maximilians-Universität Würzburg

Vorgelegt von

Endang Lukitaningsih
Aus Jogjakarta, Indonesien

Würzburg 2009

Eingereicht am:.....
bei der Fakultät für Chemie und Pharmazie

1. Gutachter:
2. Gutachter:
der Dissertation

1. Prüfer:
2. Prüfer:
3. Prüfer:
des Öffentlichen Promotionskolloquiums

Tag des Öffentlichen Promotionskolloquiums:

Doktorurkunde ausgehändigt am:

Gedruckt mit Unterstützung des Deutschen Akademischen Austauschdienstes
(DAAD)

ACKNOWLEDGEMENTS

First, I wish to express my deep gratitude and sincere appreciation to Prof. Dr. Ulrike Holzgrabe, *Lehrstuhl für Pharmazie und Lebensmittel Chemie der Julius-Maximilians-Universität Würzburg*, for your continuous support and encouragement in my Ph.D study. I thank you also for giving me so much your time and teaching me to dissolve a research problem. Without your guidance, this dissertation could not be completed.

I also wish to express my special thanks to my examiners, Prof. Dr. Matthias Unger and Prof. Dr. Tanja Schirmeister.

My gratitude and acknowledgements are due to the *Deutscher Akademischer Austauschdienst* (DAAD) for financial support and the *Pharmazie und Lebensmittel Chemie Institut, Universität Würzburg*, for providing me with research facilities.

Special thanks go to the Dean of Pharmacy Faculty of Gadjah Mada University, who gives me the permission to continue my study. I also wish to express my sincere thank to Prof. Dr. Sri Noegrohati, Apt, Faculty of Pharmacy, Gadjah Mada University. Your patience to hear my complaints and frustration were very helpful.

The appreciation and greatest honours are assigned to my beloved husband, Agus Supriyanto, and to my daughters Eky Purbaningtyas and Erika Padmaningtyas for their love, patience, understanding and prayers. Your support was most valuable as I struggled to translate my ideas into a final this dissertation. I thank you so much also for my mother, father R. Mulyono Padmo Wardoyo, brothers and sisters for their continuous moral support and unending encouragement.

Finally, I wish to express my gratitude to all my friends, my colleagues in Würzburg (the present and those already graduated) for the peaceful and friendly academic environment and also my colleagues in Jogjakarta which have helped me to finish this research.

To:

*my husband Agus Supriyanto
my daughters Eky Purbaningtyas and Erika Padmaningtyas
my mother and my father R. Mulyono Padmowardoyo*

for your love, patience, understanding and prayers

TABLE OF CONTENTS

Aknowledgements.....	iii
Table of Contents.....	v
List of Tables.....	vii
List of Figures.....	viii
List of Appendices.....	xi
Abbreviations.....	xii
I. Introduction.....	1
I.1. Background of research.....	1
I.2. Literature Review	2
I.2.1. Bengkoang (<i>Pachyrhizus sp</i>).....	2
I.2.2. Secondary metabolites : Fatty acid, Flavonoid and.....	3
I.2.3. Sunscreen and Whitening Agent.....	12
1.2.3.1. Tyrosinase and its structure.....	12
1.2.3.2. Melanin biosynthesis.....	16
1.2.3.3. Sun screening, antioxidative and tyrosinase.....	21
1.2.3.4. Tyrosinase inhibition assay.....	28
I.3. Statement of the Objectives.....	29
II. Materials and Methods.....	30
II.1. Plant materials.....	30
II.2. Laboratory chemicals and instruments.....	30
II.3. Framework of the research.....	31
II.4. Chromatography.....	32
II.4.1. Thin Layer Chromatography.....	32
II.4.2. Column Chromatography.....	33
II.4.3. Analytical HPLC.....	33
II.4.4. Semi Preparative HPLC.....	33
II.4.5. Liquid Chromatography/Mass Spectroscopy.....	35
II.4.6. Gas Chromatography/Mass Spectroscopy.....	35
II.5. Extraction and fractionation.....	35
II.6. Isolation of secondary metabolites from bengkoang root.....	37
II.6.1 Compound isolation of petroleum ether extract.....	37
II.6.2. Compound isolation of ethyl acetate extract.....	40
II.6.3 Compound isolation of butanol extract.....	43
II.6.4. Compound isolation of ethyl acetate after hydrolysis.....	44
II.7. Structure elucidation.....	45
II.8. Determination of UV absorption activity.....	46
II.9. Determination of whitening activity.....	46
II.9.1. Determination of total phenol contents.....	46
II.9.2. Determination of total flavonoid contents.....	46
II.9.3. Determination of antioxidative activity.....	47
II.9.4. Tyrosinase inhibition assay.....	47
II.9.5. Determination of tyrosinase inhibition type.....	48
III. Results and discussion.....	49
III.1. Profil chromatogram of bengkoang root extract.....	49
III.2. Compound 101 (9,12-Tricosandiene).....	52
III.3. Compound 102 (Trilinolein).....	56
III.4. Compound 109a and 109b (β -Sitosterol and Stigmasterol).....	59
III.5. Compound G1 (Hexadecyl pentanoate).....	66
III.6. Compound WuPe (Palmitic acid).....	69

III.7.	Compound W2Et (Dihydrofran-2,5-dione).....	72
III.8.	Compound C1 (Daidzein).....	75
III.9.	Compound Wu1a (Daidzein-7-O- β -glucopyranose).....	79
III.10.	Compound Wu3a (5-Hydroxy-daidzein-7-O- β -glucopyranose)...	84
III.11.	Compound A182 ((8,9)-Pterocarpan-3-ol).....	91
III.12.	Compound HWu10 (4-(2'-(Furane-2-yl)-2-methyl-2,5-dihydrofurane-3-carbaldehyde).....	99
III.13.	Compound WuBuOH (2-Butoxy-2,5-bis(hydroxymethyl)-tetrahydrofurane-3,4-diol).....	107
III.14.	UV absorption activity assay.....	113
III.15.	Total phenol contents assay.....	114
III.16.	Total flavonoid contents assay.....	115
III.17.	Antioxidative activity assay.....	117
III.18.	Tyrosinase inhibitory activity assay.....	124
III.19.	Determination of tyrosinase inhibition type.....	131
IV.	Summary.....	135
	Zusammenfassung.....	139
	Abstract.....	141
	List of references.....	142
	Appendices.....	155

LIST OF TABLES

Tab.II.4.1.	Elution systems of thin layer chromatography.....	32
Tab.II.4.2.	Elution systems of column chromatography.....	33
Tab.II.4.3.	Elution programs of semi preparative HPLC.....	34
Tab.III.1.1.	The chemical structure of isolated compounds.....	52
Tab.III.2.1.	Chemical shift value (δ) of compound 101.....	53
Tab.III.3.1.	NMR Spectroscopic data of compound 102.....	57
Tab.III.4.1.	NMR Spectroscopic data of compound 109a and 109b.....	62
Tab.III.5.1.	NMR Spectroscopic data of compound G1.....	66
Tab.III.6.1.	NMR Spectroscopic data of compound WuPe.....	70
Tab.III.7.1.	NMR Spectroscopic data of compound W2Et.....	73
Tab.III.8.1.	NMR Spectroscopic data of compound C1.....	76
Tab.III.9.1.	NMR Spectroscopic data of compound Wu1a.....	80
Tab.III.10.1.	NMR Spectroscopic data of compound Wu3a.....	88
Tab.III.11.1.	NMR Spectroscopic data of compound A182.....	95
Tab.III.12.1.	NMR Spectroscopic data of compound HWu10.....	101
Tab.III.13.1.	NMR Spectroscopic data of compound WuBuOH.....	110
Tab.III.14.1.	The results of the UV Absorption activity assay.....	111
Tab.III.15.1.	The total phenol contents in crude extracts.....	114
Tab.III.16.1.	The total flavonoid contents in crude extracts.....	117
Tab.III.17.1.	The SC ₅₀ of antioxidative activity of crude extract and.....	122
Tab.III.18.1.	The IC ₅₀ of tyrosinase inhibitory activity of crude extract and...	128
Tab.III.19.1.	Result of tyrosinase inhibition type of isolated compounds.....	134
Tab.IV.1.	Summary of isolated compounds from bengkoang root.....	137

LIST OF FIGURES

Fig.I.2.2.1.	The secondary metabolite biosynthesis.....	4
Fig.I.2.2.2.	The saturated fatty acid biosynthesis pathway.....	5
Fig.I.2.2.3.	The triglyceride biosynthesis pathway.....	6
Fig.I.2.2.4.	Basic flavonoid structure.....	8
Fig.I.2.2.5.	Scheme of general flavonoid biosynthesis pathway.....	9
Fig.I.2.2.6.	The chemical structure of phytosterols.....	11
Fig.I.2.3.1.	Reaction of tyrosinase and catecholase.....	12
Fig.I.2.3.2.	Röntgencrystall structure of tyrosinase.....	14
Fig.I.2.3.3a.	The scheme of redox reaction of tyrosinase.....	15
Fig.I.2.3.3b.	The scheme of mechanism reaction of tyrosinase with.....	16
Fig.I.2.3.4.	The skin anatomy.....	18
Fig.I.2.3.5.	Melanin biosynthesis.....	20
Fig.II.3.1.	The framework of the research.....	31
Fig.II.5.1.	Extraction and fractionation scheme.....	36
Fig.II.6.1.1.	The isolation scheme of compounds in PE extract.....	39
Fig.II.6.2.1.	The isolation scheme of compounds in EtOAc extract.....	42
Fig.II.6.3.1.	Chromatogram of the compound WuBuOH.....	43
Fig.II.6.3.2.	The isolation scheme of compound in butanol extract.....	43
Fig.II.6.4.1.	The isolation scheme of compounds in EtOAc after.....	45
Fig.III.1.1.	TLC chromatogram of the bengkoang extracts.....	49
Fig.III.1.2.	HPLC chromatogram of the ethyl acetate extract.....	50
Fig.III.1.3.	HPLC chromatogram of the butanol extract.....	51
Fig.III.1.4.	HPLC chromatogram of the ethyl acetate after hydrolysis.....	51
Fig.III.2.1.	The chemical structure of compound 101.....	52
Fig.III.2.2.	Mass fragmentation pattern of compound 101.....	54
Fig.III.2.3.	COSY diagram of compound 101.....	55
Fig.III.2.4.	HMBC diagram of compound 101.....	56
Fig.III.3.1.	The chemical structure of compound 102.....	56
Fig.III.3.2.	COSY diagram of compound 102.....	58
Fig.III.3.3.	HMBC diagram of compound 102.....	59
Fig.III.4.1.	The chemical structure of compound 109a and 109b.....	59
Fig.III.4.2.	GC/MS chromatogram of compound 109a and 109b.....	60
Fig.III.4.3.	COSY diagram of compound 109a and 109b.....	61
Fig.III.4.4.	HMBC diagram of compound 109a and 109.....	63
Fig.III.4.5.	Mass fragmentation pattern of compound 109a.....	64
Fig.III.4.6.	Mass fragmentation pattern of compound 109b.....	65
Fig.III.5.1.	The chemical structure of compound G1.....	66
Fig.III.5.2.	COSY diagram of compound G1.....	67
Fig.III.5.3a.	HMBC diagram of compound G1.....	67
Fig.III.5.3b.	The ¹ H- ¹³ C-long range correlation of the compound G1.....	68
Fig.III.5.4.	ESI-MS data and fragmentation pattern of compound G.....	68
Fig.III.6.1.	The chemical structure of compound WuPe.....	69
Fig.III.6.2a.	ESI-MS spectrum of compound WuPe.....	69
Fig.III.6.2b.	Fragmentation pattern of compound WuPe.....	70
Fig.III.6.3.	COSY diagram of compound WuPe.....	71
Fig.III.6.4.	HMBC diagram of compound WuPe.....	71
Fig.III.7.1.	The chemical structure of compound W2Et.....	72
Fig.III.7.2.	The GC/MS spectrum of compound W2Et.....	72
Fig.III.7.3.	HMBC diagram of compound W2Et.....	73

Fig.III.7.4.	EI-MS spectrum of compound W2Et.....	73
Fig.III.7.5.	The fragmentation pattern of compound w2Et.....	74
Fig.III.8.1.	The chemical structure of compound C1.....	75
Fig.III.8.2.	The GC/MS spectrum of compound C1.....	75
Fig.III.8.3.	COSY diagram of compound C1.....	77
Fig.III.8.4.	HMBC diagram of compound C1.....	77
Fig.III.8.5.	The ¹ H- ¹³ C NMR long range correlation of compound C1.....	78
Fig.III.8.6.	EI-MS spectrum of compound C1.....	78
Fig.III.8.7.	The fragmentation pattern of compound C1.....	79
Fig.III.9.1.	The chemical structure of compound Wu1a.....	79
Fig.III.9.2.	COSY diagram of compound Wu1a.....	81
Fig.III.9.3.	HMBC diagram of compound Wu1a.....	82
Fig.III.9.4.	ESI-MS spectrum of compound Wu1a.....	83
Fig.III.9.5.	The fragmentation pattern of compound Wu1a.....	83
Fig.III.10.1.	The chemical structure of compound Wu3a.....	84
Fig.III.10.2.	Analytical HPLC chromatogram of compound Wu3a.....	84
Fig.III.10.3.	IR spectrum of compound Wu3a.....	85
Fig.III.10.4.	UV spectrum of compound Wu3a.....	85
Fig.III.10.5.	¹ H NMR spectrum of compound Wu3a.....	86
Fig.III.10.6.	¹³ C NMR spectrum of compound Wu3a.....	86
Fig.III.10.7.	COSY diagram of compound Wu3a.....	89
Fig.III.10.8.	ESI-MS data of compound Wu3a.....	89
Fig.III.10.8.	The fragmentation pattern of compound Wu3a.....	90
Fig.III.11.1.	The chemical structure of compound A182.....	91
Fig.III.11.2.	Analytical HPLC chromatogram of compound A182.....	91
Fig.III.11.3.	UV spectrum of compound A182.....	92
Fig.III.11.4.	IR spectrum of compound A182.....	92
Fig.III.11.5.	¹ H NMR spectrum of compound A182.....	93
Fig.III.11.6.	¹³ C NMR spectrum of compound A182.....	94
Fig.III.11.7.	DEPT spectrum of compound A182.....	95
Fig.III.11.8.	COSY diagram of compound A182.....	96
Fig.III.11.9.	The HMBC of compound A18.....	96
Fig.III.11.10a.	ESI-MS spectrum of compound A182.....	97
Fig.III.11.10b.	ESI-MS2 spectrum of compound A182.....	97
Fig.III.11.11.	The fragmentation pattern of compound A182.....	98
Fig.III.12.1	The chemical structure of compound HWu10.....	99
Fig.III.12.2.	UV spectrum of compound HWu10.....	99
Fig.III.12.3.	IR spectrum of compound HWu10.....	100
Fig.III.12.4.	GC/MS spectrum of compound HWu10.....	101
Fig.III.12.5.	¹ H NMR spectrum of compound HWu10.....	102
Fig.III.12.6.	¹³ C NMR spectrum of compound HWu10.....	102
Fig.III.12.7.	COSY diagram of compound HWu10.....	103
Fig.III.12.8.	HMBC diagram of compound HWu10.....	104
Fig.III.12.9.	EI-MS spectrum of compound HWu1a.....	105
Fig.III.12.10.	Mass fragmentation pattern of compound HWu10.....	106
Fig.III.13.1.	The chemical structure of compound WuBuOH.....	107
Fig.III.13.2.	HPLC chromatogram of compound WuBuOH.....	107
Fig.III.13.3.	IR spectrum of compound WuBuOH.....	108
Fig.III.13.4.	¹ H NMR spectrum of compound WuBuOH.....	108
Fig.III.13.5.	¹³ C NMR spectrum of compound WuBuOH.....	109
Fig.III.13.6.	COSY diagram of compound WuBuOH.....	110

Fig.III.13.7.	HMBC diagram of compound WuBuOH.....	111
Fig.III.13.8.	¹ H- ¹³ C long range correlation of compound WuBuOH.....	111
Fig.III.13.9.	EI-MS spectrum of compound WuBuOH.....	112
Fig.III.13.10.	Mass fragmentation pattern of compound WuBuOH.....	112
Fig.III.15.1.	Wavelength scans of the reaction gallic acid with Folin-Ciocalteu.....	114
Fig.III.15.2.	Calibration curve of the gallic acid.....	114
Fig.III.16.1.	The reaction of catechin with AlCl ₃	116
Fig.III.16.2.	Wavelength scans of the reaction catechin with AlCl ₃	116
Fig.III.16.3.	Calibration curve of catechin.....	116
Fig.III.17.1.	The structure of DPPH free radical and DPPH non radical.....	118
Fig.III.17.2.	Wavelength scans of product reaction of ascorbic acid and....	118
Fig.III.17.3a.	Concentration-Scavenging activity curve of crude extract.....	119
Fig.III.17.3b.	Concentration-Scavenging activity curve of isolated	120
Fig.III.18.1.	The oxidation pathway of tyrosine.....	125
Fig.III.18.2.	Wavelength scans of the product reaction DOPAchrome.....	125
Fig.III.18.3a.	Concentration-Tyrosinase Inhibition curve of crude extracts..	126
Fig.III.18.3b.	Concentration-Tyrosinase Inhibition curve of isolated.....	127
Fig.III.18.4.	Chemical structures of isoflavonoids and a pterocarpan isolated from the bengkoang roots.....	130
Fig.III.19.1.	Chemical structure of compound A182.....	132
Fig.III.19.2.	The lineweaver-Burk plots of isolated compounds.....	133

LIST OF APPENDICES

App.1.	IR spectrum, UV spectrum, ¹ H NMR and ¹³ C NMR of compound 101.	155
App.1.1.	IR spectrum of compound 101.....	155
App.1.2.	UV spectrum of compound 101.....	155
App.1.3.	¹ H NMR spectrum of compound 101.....	156
App.1.4.	¹³ C NMR spectrum of compound 101.....	156
App.2.	IR spectrum, UV spectrum, ¹ H NMR and ¹³ C NMR of compound 102.	157
App.2.1.	IR spectrum of compound 102.....	157
App.2.2.	UV spectrum of compound 102.....	157
App.2.3.	¹ H NMR spectrum of compound 102.....	158
App.2.4.	¹³ C NMR spectrum of compound 102.....	158
App.3.	IR spectrum, ¹ H NMR and ¹³ C NMR of compound 109a and a09b....	159
App.3.1.	IR spectrum of compound 109a and 109b.....	159
App.3.2.	¹ H NMR spectrum of compound 109a and 109b.....	159
App.3.3.	¹³ C NMR spectrum of compound 109a and 109b.....	160
App.4.	IR spectrum, UV spectrum, ¹ H NMR and ¹³ C NMR.....	161
App.4.1.	IR spectrum of compound WuPe.....	161
App.4.2.	UV spectrum of compound WuPe.....	161
App.4.3.	¹ H NMR spectrum of compound WuPe.....	162
App.4.4.	¹³ C NMR spectrum of compound WuPe.....	162
App.5.	IR spectrum, UV spectrum, ¹ H NMR and ¹³ C NMR of compound G1..	163
App.5.1.	IR spectrum of compound G1.....	163
App.5.2.	UV spectrum of compound G1.....	163
App.5.3.	¹ H NMR spectrum of compound G1.....	163
App.5.4.	¹³ C NMR spectrum of compound G1.....	164
App.6.	IR spectrum, ¹ H NMR and ¹³ C NMR of compound W2Et.....	165
App.6.1.	IR spectrum of compound W2Et.....	165
App.6.2.	UV spectrum of compound W2Et.....	165
App.6.3.	¹ H NMR spectrum of compound W2Et.....	165
App.6.4.	¹³ C NMR spectrum of compound W2Et.....	166
App.7.	IR spectrum, UV spectrum, ¹ H NMR and ¹³ C NMR of compound C1..	167
App.7.1.	IR spectrum of compound C1.....	167
App.7.2.	UV spectrum of compound C1.....	167
App.7.3.	¹ H NMR spectrum of compound C1.....	168
App.7.4.	¹³ C NMR spectrum of compound C1.....	169
App.7.5.	HPLC chromatogram of compound C1.....	169
App.8.	IR spectrum, UV spectrum, ¹ H NMR and ¹³ C NMR.....	170
App.8.1.	IR spectrum of compound Wu1a.....	170
App.8.2.	UV spectrum of compound Wu1a.....	170
App.8.3.	¹ H NMR spectrum of compound Wu1a.....	171
App.8.4.	¹³ C NMR spectrum of compound Wu1a.....	171

ABBREVIATIONS

APCI	: atmospheric pressure chemical ionisation
Anisaldehyde	: anisaldehyde-H ₂ SO ₄
AU	: absorbance unit
AUC	: area under curve
br	: broad signal
CC	: column chromatography
CDCl ₃	: deuterated chloroform
COSY	: correlation spectroscopy
d	: doublet
dd	: doublet of doublet
ddd	: doublet of doublet of doublet
Dopa	: 3,4-dihydroxyphenylalanine
DEPT	: distortionless enhancement by polarization transfer
DMSO-d ₆	: deuterated dimethylsulfoxide
DPPH	: 2,2-diphenyl-1-picrylhydrazil
dt	: doublet of triplet
EI-MS	: electron ionization mass spectrometry
ESI-MS	: electron spray ionization mass spectrometry
EtOAc	: ethyl acetate
EtOH	: ethanol
eV	: electron volt
GC/MS	: gas chromatography mass spectrometry
HMBC	: heteronuclear multiple bond correlation
HMQC	: heteronuclear multiple quantum coherence
HPLC	: high performance liquid chromatography
Hz	: hertz
IC ₅₀	: the concentration of a compound that is required for 50% inhibition in vivo
IR	: infra red
LC/MS	: liquid chromatography/ mass spectrometry
m	: multiplet
MeOH-d ₄	: deuterated methanol
m.p.	: melting point
MS	: mass spectrometry
m/z	: mass per charge
n-BuOH	: normal-butanol
NMR	: nuclear magnetic resonance
p.a.	: pro analysis
PBS	: phosphate buffer saline
ppm	: part per million
q	: quartet
RP-18	: reverse phase C-18
Rf	: retention factor
s	: singlet
SC ₅₀	: the concentration of a compound that is required for scavenging 50%
t	: triplet
TLC	: thin layer chromatography
Tr	: time of retention

Abbreviations

UV : ultra violet
Vis : visible

CHAPTER I INTRODUCTION

I.1. Background of research

The development of life style, drugs and cosmetics initiated by the increasing desire to live healthy and to appear more attractive, influences the cosmetics industry. In about 20 years, cosmetic industries have been developing rapidly. Innumerable chemical substances both synthetic materials and biological materials were found and every year new products appear. Most materials used for cosmetics are derived from scientific researches. However, several cosmetic materials are based on the experience of ancestors, or in other words, they are known as traditional cosmetics. In Indonesia, the bengkoang roots are one of these traditional cosmetics.

The Bengkoang is a species of a *Pachyrizus* and grows naturally in many tropical and subtropical countries in America. It is usually eaten raw, sometimes with salt, lemon juice and powdered chili. In Indonesia, bengkoang roots have also been traditionally used as a cosmetics material for centuries based on ancestor's experience. They are used as sun screening and skin whitening materials. However, the active compounds in bengkoang roots which have skin whitening and sun screening activity have not been discovered yet.

The sun screen preparation has been developed rapidly since it was found that the ultraviolet ray causes several damages on skin; for examples, sunburn, cancer, abnormally pigmented skin, wrinkling and coarsening of the skin surface. To avoid effects of ultraviolet, it is important to use sun screen preparations. These preparations contain compounds which have the activity to prevent ultraviolet rays penetrating the skin. There are three kinds of sunscreen compounds grouped according to their mechanism, i.e.: ultraviolet absorbent, ultraviolet reflector and tanning compounds. Tanning compounds are compounds that, together with the keratin of corneal layer, forms brown complex.

Additionally, whitening preparations are needed to minimize abnormally pigmented skin. They prevent new melanin synthesis by inhibiting the oxidative polymerase enzyme. As it is known, melanin is a brown skin pigment. The bengkoang root extracts may contain a substance which has the activity to inhibit oxidative polymerization, so that it can reduce the melanin production.

According to the above explanation, bengkoang roots possibly contain many substances which have the activity to absorb and to reflect ultraviolet rays, to form a brown complex with keratin and to inhibit melanin synthesis. Thus, bengkoang roots can be used for raw materials in both sunscreen and skin whitening preparations. To prove the hypothesis, the study on "The exploration of whitening and sun screening compounds in bengkoang roots (*Pachyrhizus sp*)" was initiated.

I.2. Literature review

I.2.1. Bengkoang (*Pachyrhizus sp*)

This is the botanical classification of the bengkoang.

Kingdom	: Plantae
Division	: Magnoliophyta
Class	: Magnoliopsida
Order	: Fabales
Family	: Fabaceae
Subfamily	: Faboideae
Genus	: <i>Pachyrhizus</i>
Species	: <i>P. erosus</i>
Binomial name	: <i>Pachyrhizus erosus</i> (L) Urb

Bengkoang plant grows as a vine that can reach a height of 4-5 m when it is given suitable support. Its root can attain the length of 2 m and can weigh up to 2 kg. It is a component in the Indonesian traditional salad called "rujak". It is eaten raw, sometimes with lemon juice and powdered chilli. In contrast with the edible root, the remaining part of the bengkoang plant is very poisonous, for example the seed contains rotenone, which is very toxic and is used to poison insects and fishes. Bengkoang consists of 86-90 % water. It contains only trace amounts of protein and lipids. Its sweet flavour comes from the oligofructose inulin. It is suitable for diabetics and people on diet program. There are other compounds in bengkoang, such as adenine, choline, saponine and flavonoids (Anonim 2006). Flavonoids and saponins serve as natural "sunscreen" in preventing damage caused by free-radical excitement as the result of absorption of ultra-violet rays (UV) (Sandler 2005). Therefore, it is possible that the bengkoang roots can be used as a sun screening materials, especially as UV absorbance materials. Besides, there are also many phenolic compounds in

bengkoang. According to Wang et al. (2005), phenolic compounds may be used as depigmenting agents because they have a similar chemical structure to tyrosine, the substrate of the tyrosinase. Tyrosinase enzyme is an important enzyme that plays a major role in melanin synthesis. Melanin is well known as a dark pigment in human and animals.

I.2.2. Secondary metabolites: fatty acid, flavonoid and phytosterol

All organisms need to transform and interconvert a vast number of organic compounds to enable them to live, grow and reproduce through integrated chemical reactions or metabolism processes. There are two important metabolism processes, namely primary metabolism and secondary metabolism. The primary metabolism is a process to synthesize, degrade or modify all important molecules, such as carbohydrates, proteins, fats and nucleic acids. These compounds are found in all organisms with the same structure or with minor variations (Dewick 2002).

In contrast to the primary metabolism, the second metabolism is specific for organisms, or groups of organisms, and is an expression of the individuality of species. Some of secondary metabolites produced for easily appreciated reasons, e.g. as toxic materials providing defence against predators, as volatile attractants towards the same or other species, or as colouring agents to attract or warn other species (Dewick 2002).

The building blocks for secondary metabolites are derived from primary metabolism as indicated in Fig. I.2.2.1. By far the most important building blocks employed in the biosynthesis of secondary metabolites are derived from the intermediates acetyl coenzyme A, shikimic acid, mevalonic acid, and 1-deoxyxylulose 5-phosphate. These are utilized respectively in the acetate, shikimate, mevalonate and deoxyxylulose phosphate pathways. Important secondary metabolites formed from the acetate pathway include phenols, prostaglandins, and macrolide antibiotics, together with various fatty acids and derivatives at the primary/secondary metabolism interface. The shikimate pathway leads to a variety of phenols, cinnamic acid derivatives, lignans and alkaloids. The mevalonate and deoxyxylulose phosphate pathways are together responsible for the biosynthesis of a vast array of terpenoid and steroid metabolites (Dewick 2002).

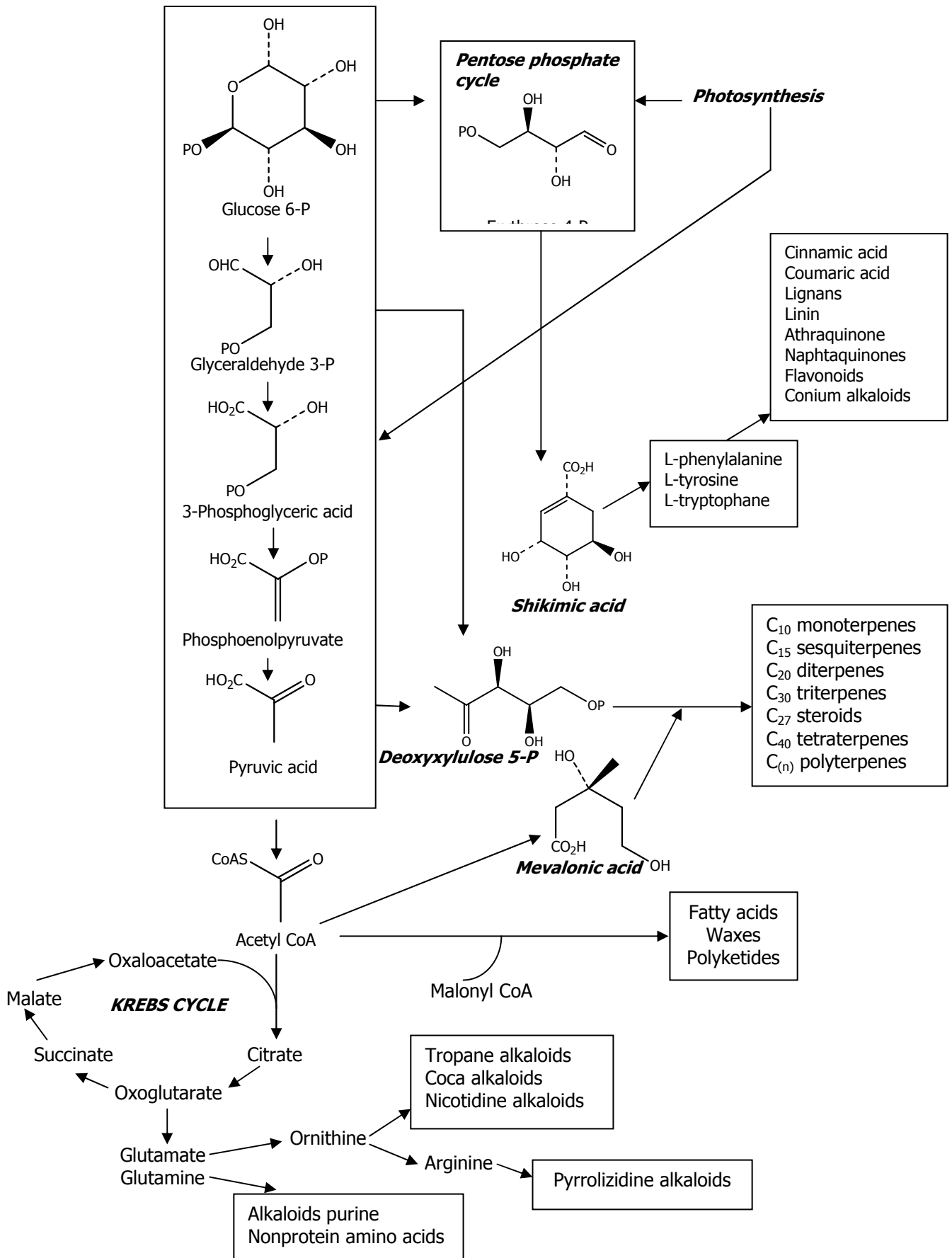


Fig. I.2.2.1. The secondary metabolite biosynthesis (Dewick 2002; Wing 1999)

Fatty Acids

The processes of fatty acid biosynthesis are well studied and displayed in Figure I.2.2.2. Naturally fatty acids may contain 4 to 30, or even more carbon atoms, the most abundant being those with 16 or 18 carbons. Fatty acids containing an odd number of carbon atoms are rare. From the Figure I.2.2.2 can be seen that the combination of one acetate starter unit with seven malonates gives the C16 fatty acid, palmitic acid, and with eight malonates the C18 fatty acid, stearic acid (Dewick 2002).

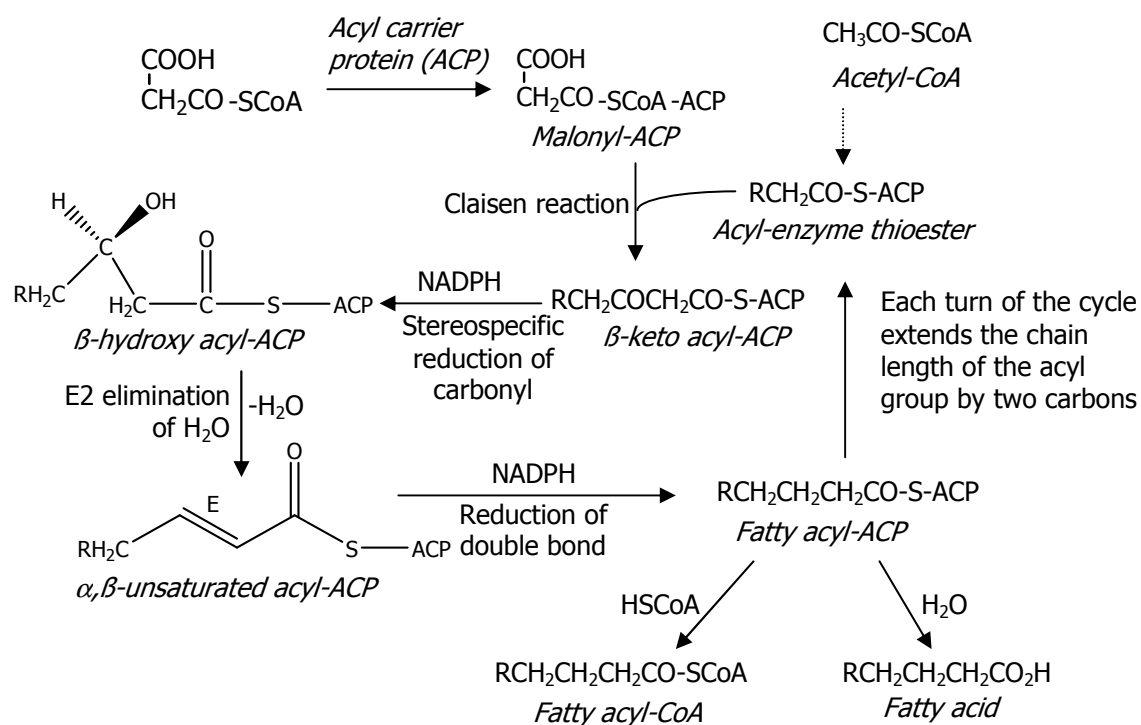


Fig. I.2.2.2. The saturated fatty acid biosynthesis pathway (Dewick 2002)

Fatty acids are mainly found as glycerol esters called triglycerides. These materials are called fats or oils, depending on whether they are solid or liquid at room temperature. Most natural fats and oils are composed of mixed triglycerides. Each triglyceride species may contain up to three distinct fatty acid substituents, which can vary in chain length, degree of unsaturation and position of double bonds. Triglycerides play a major role in energy storage in animals. (Hvattum 2001).

In human body, triglycerides are stored in the adipocyte cell and will be released again as free fatty acids when needed by the body. Mobilization of

stored lipid is controlled by the action of hormone sensitive lipase, which catalyzes the sequential hydrolysis of triglyceride to diglyceride and monoglyceride. Monoglyceride is hydrolyzed by a specific monoglyceride lipase (Soma et al. 1992).

The triglyceride biosynthesis can be found in the Fig I.2.2.3 (Dewick 2002). The glyceride compounds are metabolized much less than the fatty acids (fats or oils) due to the polyol chain between the glycerol backbone and the fatty acids, which prevents lipase cleavage (Thayer 1992).

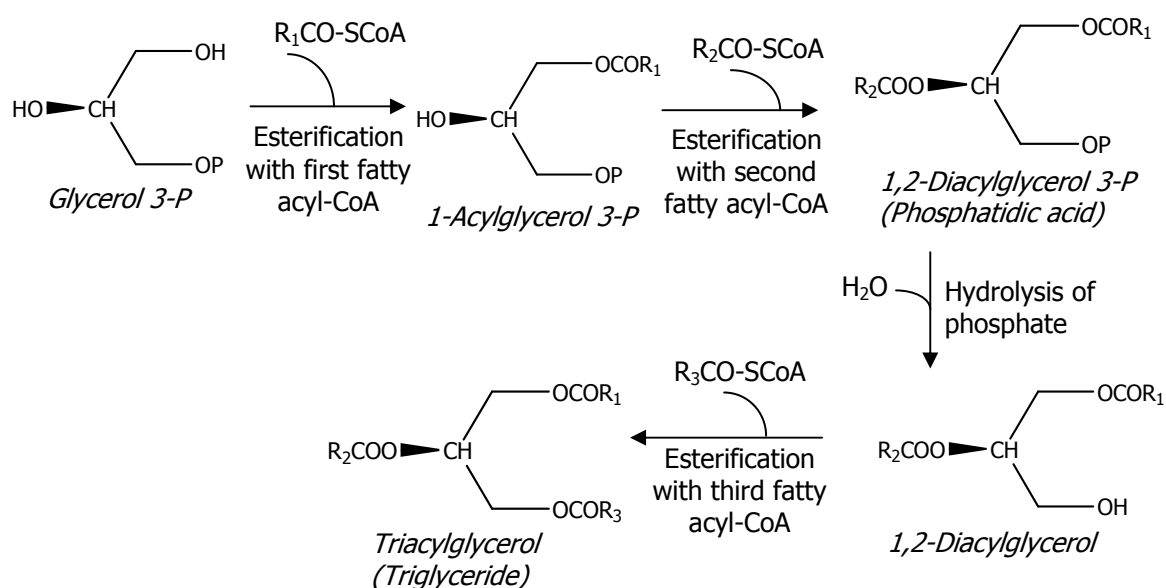


Fig. I.2.2.3. The triglyceride biosynthesis pathway (Dewick 2002)

Unsaturated fatty acids can be found in abundant concentration in living organisms primarily in animals. Trilinolein and also alkene compounds have been reported as pheromone components in *Captotermes formosanus* (Bland et al. 2004; Blomquist et al. 1980). Gibb et al. (2006) has reported that (Z)-7-tricosene and monosaturated ketones are the main components of sex pheromone of the *Cossinoptycha improbana*. (Z)-11-Hexadecenal and (3Z,6Z,9Z)-tricosatriene have been reported by Gibb et al. (2008) as sex pheromone components of the red banded mango *Caterpillar deanolis sublimbalis*.

The number and position of unsaturated carbon depends on the species of the organism and also on the climate. Most eukaryotic organisms possess a unsaturated fatty acid at C9. In colder climates, a higher proportion of polyunsaturated fatty acids are produced, so that the plant can maintain the

fluidity of its storage fats and membranes (Dewick 2002). Oxidation occurs readily in unsaturated fatty acids, because hydrogen abstraction from a carbon atom adjacent to a double bond is favored due to the formation of a stable allylic radical (Frankel et al. 1984; Kanner et al. 1987; Kubow 1992; Mahungu et al. 1999). The initial compounds produced by oxidation are hydroperoxides and cyclic hydroperoxides (Neff and Byrdwell 1998). The hydroperoxide decomposition products may have negative health implications regarding cancer, heart disease, and aging (Neff and Byrdwell 1998).

Fatty acids have many pharmacology effects, such as antioxidative activity, transcription inhibition of sterol regulatory element binding protein-1C (Qu et al. 2001), carry fat soluble vitamins, supply linoleic acid and essential fatty acids (Mahungu et al. 1999). Trilinolein has been reported by Liu et al. (2004) that it has various beneficial effects, including the ability to reduce thrombogenicity, erythrocyte deformability, arrhythmias, antioxidative and also myocardial protective effect. The myocardial protective effect is thought to be related to the antioxidative activity via potentiation of superoxide dismutase (SOD) (Liu et al. 2004; Chan et al. 2002). In addition, trilinolein has also the inhibitory effect on adrenaline induced platelet aggregation (Shen and Hong 1995).

Flavonoids

Flavonoids represent a highly diverse class of secondary plant metabolites with about 9000 structures which have been identified so far. These compounds are found in all vascular plants as well as in some mosses (Harborne and Baxter 1999; Williams and Grayer 2004). They exhibit a wide range of properties in physiology, biochemistry and ecology, for example in UV-protection, flower coloration, interspecies interaction and plant defence (Martens 2005).

'Flavonoid' is a collective noun used to describe several classes of compounds having a common C₆-C₃-C₆ flavone skeleton in which the three carbon bridge between the phenyl groups is commonly cyclised with oxygen as in Fig I.6 (Cavaliere et al. 2007). Flavonoids are products from a cinnamoyl-CoA starter unit, with chain extension using three molecules of malonyl-CoA (Dewick 2002). The biosynthesis pathway of flavonoid can be read in Fig. I.2.2.5. The crucial biosynthetic reaction is the condensation of three molecules malonyl-CoA

with one molecule p-coumaryl-CoA to chalcone intermediates (Martens 2005). The major classes of flavonoids are flavones, isoflavones, flavonols, flavanones, anthocyanins, catechins and chalcones (Cavaliere et al. 2007).

Chalcones and dihydrochalcones are classes of flavonoids that consist of two phenol groups which are connected by three carbons. Derived from the chalcone structure, a flavonoid-class containing three rings, the flavanones, can be formed. Based on these flavanones, all other flavonoid-classes are generated, including isoflavones, flavanols, anthocyanidines, flavonols and flavones (Martens 2005). The latter flavonoid-class is characterized by the presence of a double bond between C2 and C3 in the heterocycle of the flavan skeleton. The B-ring is attached to C2 and usually no substituent is present at C3. This constitutes the difference between flavone and flavonols. In flavonols a hydroxyl group can be found at the C3 position. A basic flavonoid structure and general flavonoid pathway can be found in Figure I.2.2.4 and Figure I.2.2.5 (Martens 2005).

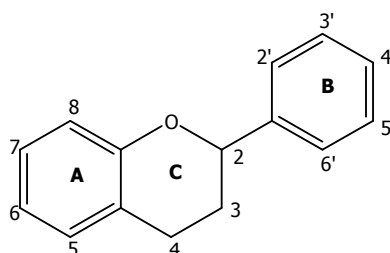


Fig. I.2.2.4. Basic flavonoid structure (Martens 2005)

Flavones can be classified into several subgroups based on the presence of substituents and the solubility of the flavones in water. There are many substituents, for example hydroxylation, O-methylation, C-methylation, isoprenylation, or methylenedioxy substitution. According to the solubility, we find an aglycon structure and glycosides. Flavones mostly occur as 7-O-glycosides (Harborne and Baxter 1999; Williams and Grayer 2004).

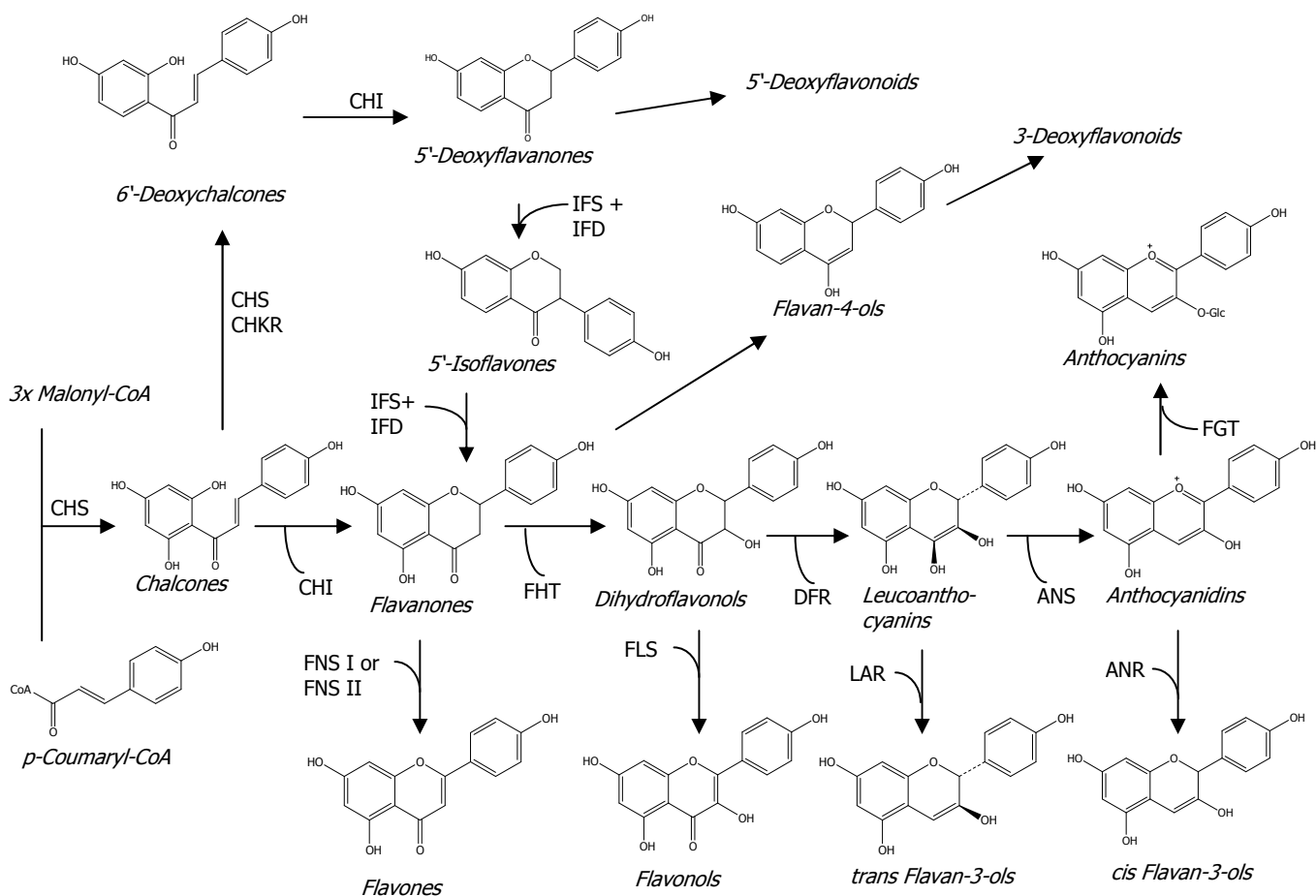


Fig. 1.2.2.5. Scheme of general flavonoid biosynthesis pathway. Enzymes are abbreviated as follows : ChS, chalcone synthase; ChKR, chalcone polyketide reductase; CHI, chalcone isomerase; FHT, flavanone 3- β -hydroxylase; DFR, dihydroflavonol 4-reductase; ANS, anthocyanidin synthase; FGT, flavonoid glycosyltransferase; FNS, flavone synthase; FLS, flavonol synthase; LAR, leucoanthocyanidin reductase; ANR, anthocyanidin reductase; leucoanthocyanidin reductase; ANR, anthocyanidin reductase; IFS, isoflavone synthase; IFD, isoflavone dehydratase (Martens 2005)

Isoflavones, coumestans and lignans are classified into phytoestrogenic compounds (Urasopon et al. 2008). They have estrogen-like properties (Nikander et al. 2004; Knight and Eden 1996; Santos et al. 2006), anti estrogen activity (Ito et al. 2006) and have been associated with lesser incidence of steroid-hormone dependent cancers (Falcao et al. 2005; Lang'at-Thoruwa et al. 2003), e.g. those of the breast, prostate (Wu et al. 2004) and colon (Wijeratne and Cuppet 2007). Isoflavonoids primarily daidzein, genistein, daidzin, genistin are found in the Fabaceae family, and are distributed in edible plants and derived products (Coward et al. 1993; Kang et al. 2006; Cavaliere et al. 2007).

Foods rich of isoflavonoids, for example soybean (Coward et al. 1993), are valuable in countering some of side effects of the menopause women, such as hot flushes, tiredness and mood swings. In addition, there is mounting

evidence that phytoestrogens also provide a range of other beneficial effects, helping to prevent heart attacks and other cardiovascular diseases (Nikander et al. 2004), angiogenesis (Wu et al. 2004), protecting against osteoporosis (Clarkson et al. 1995 in Lamartiniere et al. 2002; Blair et al. 1996; Choi 2006), decreasing the risk of breast and uterine cancer (Wang et al. 2009), and leukemia (Raynal et al. 2008), and also displaying significant antioxidative activity which may reduce the risk of Alzheimer's disease (Dewick 2002). The antioxidative activity is caused by the presence of multiple hydroxyl groups in their structure (Ruiz Larrea et al. 1997; Wijeratne and Cuppet 2007). Mao et al. (2007) have reported that daidzein in soybean has anti-apoptosis effects; therefore it was a potential drug candidate for neurodegeneration therapy. Mximo et al. (2002) have investigated antifungal activity of isoflavonoids isolated from *Ulex airensis* and *Ulex europaeus* ssa *europaeus*. The isoflavonoids have appeared good antifungal activity against *Cladosporium cucumerinum*. However, many other applications are known for flavonoids and related compound.

Phytosterol

The term phytosterols refers to sterols synthesized in plants; the most prevalent ones are β -sitosterol and campesterol as in Figure I.2.2.6 (Dewick 2002; Lee et al. 2007). Phytosterols are generally present in plant cell membranes (De-Eknamkul and Potduang 2003) and affect the permeability of these membranes (Hac-Wydro 2007). In addition, they also play a role in cell proliferation (Dewick 2002).

Phytosterols are a class of natural products which possesses the tetracyclic ring system (Nes and Venkatramesh 1999). The main phytosterols are similar to cholesterol, sterols produced by animals, with the addition one or two carbon substituent on the side chain, attached at C-24. Consequently, the phytosterols may undergo oxidation process similar to cholesterol oxidations and yield therefore similar products. Cholesterol oxidation products (COP's) have well documented adverse effects, including a harmful role in the development of arteriosclerosis (Brown and Jessup 1999). The consumption of dietary phytosterols in increased quantities has lead to the possibility of increased levels of phytosterol oxides in the blood (McCarthy et al. 2005)

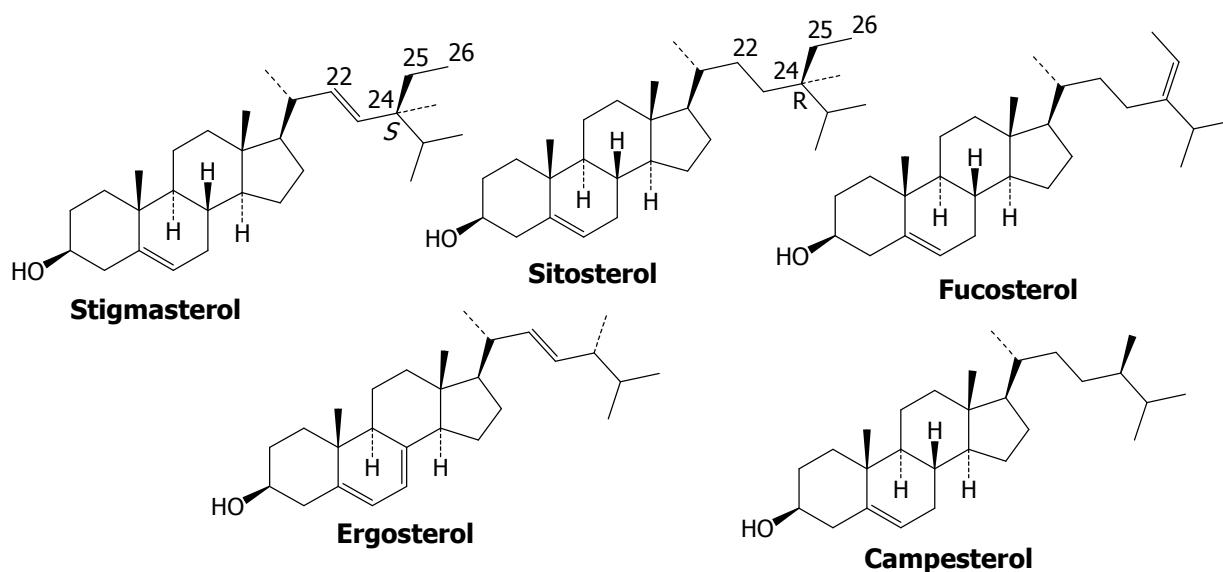


Fig. I.2.2.6. The chemical structure of some of phytosterols (Dewick 2002)

Biosynthetically, it has been proposed that the isoprene building blocks of the phytosterols are originated mainly from the mevalonate pathway rather than the deoxyxylulose pathway (the non-mevalonate pathway) which has been shown to be involved in the biosynthesis of various terpenoid natural products (reviewed in Eisenreich et al. 1998; Rohmer 1999).

The phytosterols are not synthesized in humans endogenously but are intestinal absorbed solely. Previous studies have shown that phytosterols have anticarcinogenic activity, e.g. colon, prostate and breast (Moon et al. 2007), antiinflammatory activity, reducing cholesterol levels activity (Huang et al. 2007), cardiovascular risk prevention, antiangiogenic (Fassbender et al. 2006), immunomodulating (Park et al. 2007), antineoplastic (Lee et al. 2007; Patrick and Lamprecht 1999), and anti-asthma properties (Yuk et al. 2007).

Phytosterols have been used not only in pharmaceuticals, such as antiinflammatory drugs (Parra-Delgado et al. 2004; Dickson et al. 2007), hormones, vitamins (Dewick 2002), but also in nutrition (anti cholesterol additives) and cosmetics (for creams and lipstick) (Berezin et al. 2001). Gomes et al. (2007) have reported that β -sitosterol and stigmasterol isolated from *Pluchea indica* Less have an inhibition snake-venom activity.

I.2.3. Sun screening and skin whitening

I.2.3.1. Tyrosinase and its structure

Tyrosinase (polyphenol oxidase, EC 1.14.18.1) also known as polyphenol oxidase (PPO) (Kubo and Kinst-Hori 1998a) is a copper containing enzyme widely distributed in nature (Khatib et al. 2005). Over the past 30 years the enzyme tyrosinase has received considerable attention as an indispensable tool in the performance of studies on a wide range a topics. Since the first biochemical investigations were carried out in 1895 on the mushroom *Russula nigricans*, the cut flesh of which turned red and then black on exposure to air, a number of studies have been performed to find the culprit mainly responsible for the colour change (Parvez et al. 2007).

Tyrosinase occurs in different microorganisms, plants and animals (Matsuura et al. 2006) and is mainly involved in the biosynthesis of melanin (Lerch 1983). Tyrosinase catalyzes both the hydroxylation of monophenols, such as tyrosine to o-diphenols by monooxygenase, and the oxidation of o-diphenols to o-quinones (catechol oxidase) (Lee 2002; Sasaki et al. 2002; Salzbrunn 2007; Kubo and Kinst-Hori 1998a). The o-quinones further polymerize and undergo a series of subsequent enzymatic and nonenzymatic reactions (Matsuura et al. 2006) to produce brown and red pigment (Friedman 1996) and black melanin (Sasaki et al. 2002).

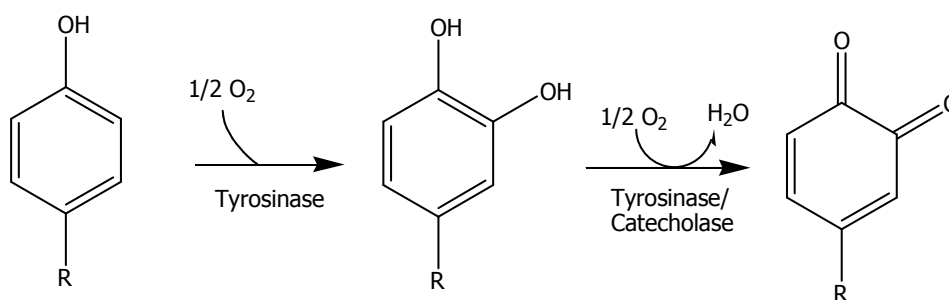


Fig. I.2.3.1. Reaction of tyrosinase and catecholase. Tyrosinase catalyzes hydroxylation of monophenol to form o-diphenol and the oxidation of o-diphenol to o-quinone. Both reactions, hydroxylation and oxidation, need the presence of oxygen (Salzbrunn 2007)

In insects, several functions of this enzyme have been reported in the generation of o-diphenols and quinones for pigmentation, wound healing, parasite encapsulation and sclerotization. Because these functions are effectively utilized in various types of developmental and defensive processes in insects, the enzyme may be an alternative target site for the control of insect pests (Lee 2002; Kubo and Kinst-Hori 1998a). In food, tyrosinase is responsible for undesired enzymatic browning of fruits and vegetables (Martinez and Whitaker 1995; Parvez et al. 2007) during post-harvest handling and processing (Lee 2002; Chang 2007). This reaction produces undesirable changes in colour, flavour and nutritive value of the product. Unfavourable browning of raw fruits, vegetables, and beverages is a major problem in the food industry and is believed to be one of main causes of quality loss (Friedmann 1996; Kubo and Kinst-Hori 1998a; Matsuura et al. 2006). The degree of browning among different fruit cultivars is variable because of differences in phenol content and tyrosinase activity (Lee 2002). The application of polyphenol oxidase inhibitors has been one of the most popular and desirable strategies adopted by the food industry to prevent food browning (Zheng et al. 2008) and also in agriculture as an insecticide (Likhitiwitayuwid 2008). Kojic acid was speculated by Kahn et al. (1997) as insecticide because of its activity to prevent sclerotization in several insects. Similarly, the unfavourable browning caused by tyrosinase on the surface of seafood product has also been of great concern (Ogawa et al. 1984).

In humans, tyrosinase catalyzes the melanin biosynthesis (Briganti 2003; Kubo and Kinst-Hori 1999). Melanin pigments are also found in the mammalian brain. In the human brain, tyrosinase plays an important role in neuromelanin formation, which could be of central importance to dopamine neurotoxicity and may contribute to the neurodegeneration associated with Parkinson's disease (Chen and Kubo 2002; Matsuura et al. 2006). The melanin is the major pigment for colour of skin, hair and eye. Melanin may be overproduced with chronic sun exposure, melasma or other hyperpigmentation disease (Briganti et al. 2003). Tyrosinase inhibitors have become increasingly important in cosmetics (Maeda 1991; Kubo and Kinst-Hori 1998a; Parvez et al. 2007) and drugs for the treatment of some skin disorders associated with melanin hyperpigmentation (Parvez et al. 2007) and to prevent spots and freckles due to sunburn (Tanimoto et al. 2006).

Tyrosinases have been isolated and studied from a wide variety of plant, animal, fungi species and microorganisms (Kubo and Kinst-Hori 1999). More than 20 species of Lichens from the sub-order Peltigerineae has been investigated and the result displayed significant tyrosinase activity (Laufer et al. 2006). Tyrosinases from different species are diverse in terms of their structural properties, tissue distribution and cellular location (Mayer 1987). The enzymes found in plant, animal and fungi tissue frequently differ with respect to their primary structure, size, glycosylation pattern and activation characteristics. However, all tyrosinases have in common a binuclear type 3 copper centre within their active site. Here two copper atoms are each coordinated with three histidine residue (Mirica et al. 2005; Matoba et al. 2006; Kim et al. 2006; Salzbrunn 2007).

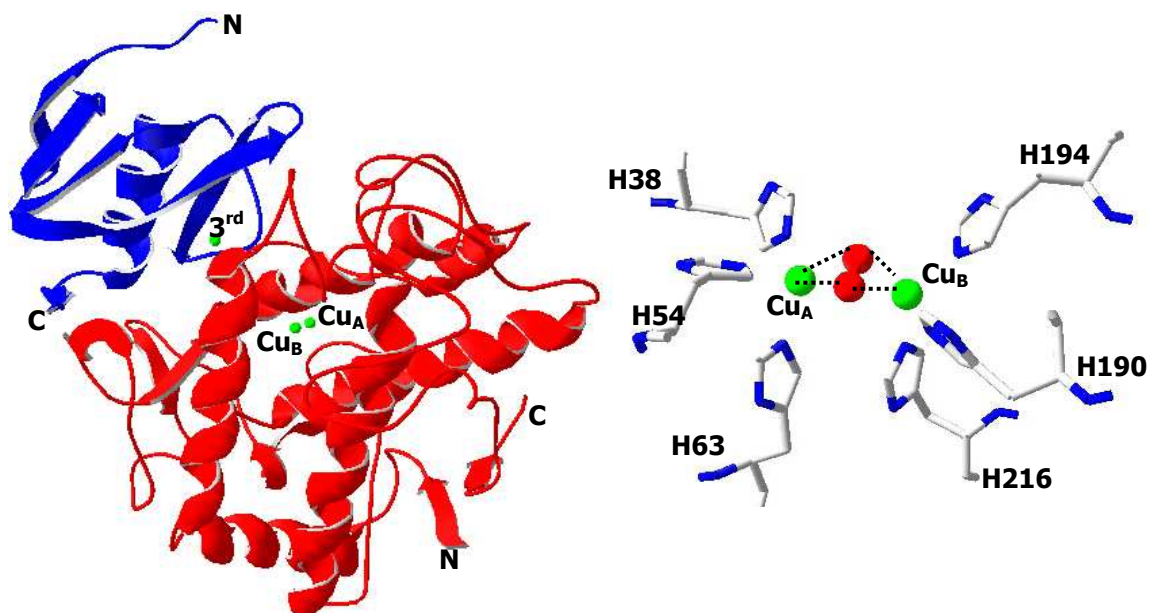


Fig. I.2.3.2. Röntgencrystall structure of tyrosinase obtained from *Streptomyces castaneoglobisporus* (Salzbrunn 2007), reproduced with a permission from the Autor

Tyrosinase has three domains, of which the central domain contains two copper binding sites as displayed in Fig I.2.3.2. Copper binding sites are the active site in the tyrosinase catalytic reaction (Matsuura et al. 2006). The two copper atoms within the active site of tyrosinase enzymes interact with oxygen to form a highly reactive chemical intermediate which oxidizes the substrate. Six histidine residues bind a pair of copper ions in the active site of tyrosinase (Jackman et al. 1991; Hirota et al. 2005; Parvez et al. 2007). The location of

cysteine also plays an important role in the formation of disulfide linkages, which stabilize protein structure (Parvez et al. 2007).

Tyrosinase catalyses two oxidation reactions. Three tyrosinase isoforms exist, namely mettyrosinase, oxytyrosinase and deoxytyrosinase (Likhitwitayawuid 2008). According to Land et al. (2003) and Palavicini et al. (2005), native tyrosinase occurs in the inactive *met*-form in which the binuclear copper site is in the wrong oxidation state [Cu(II)] to bind oxygen. Two-electron reduction by a catechol converts *met*-tyrosinase to *deoxy*-tyrosinase, which readily binds oxygen giving *oxy*-tyrosinase (Fig.I.2.3.3a). Both phenols and catechols are oxidized to *ortho*-quinones by the *oxy*-tyrosinase but the mechanisms of these oxidations are different. Oxidation of a catechol leads to *met*-tyrosinase, which cannot bind oxygen to regenerate *oxy*-tyrosinase. Only in the presence of a second catechol molecule, the *met*-tyrosinase is reduced to *deoxy*-tyrosinase which then regenerates the *oxy* form (Fig.I.2.3.3b).

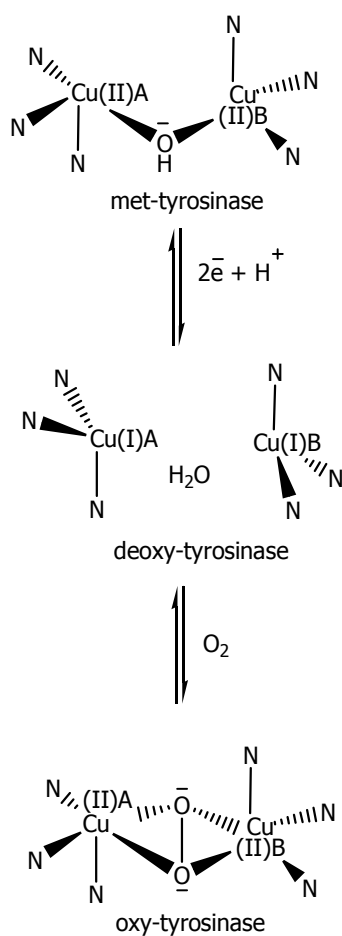


Fig.I.2.3.3a. The scheme of redox reaction of the tyrosinase (Land et al. 2003)

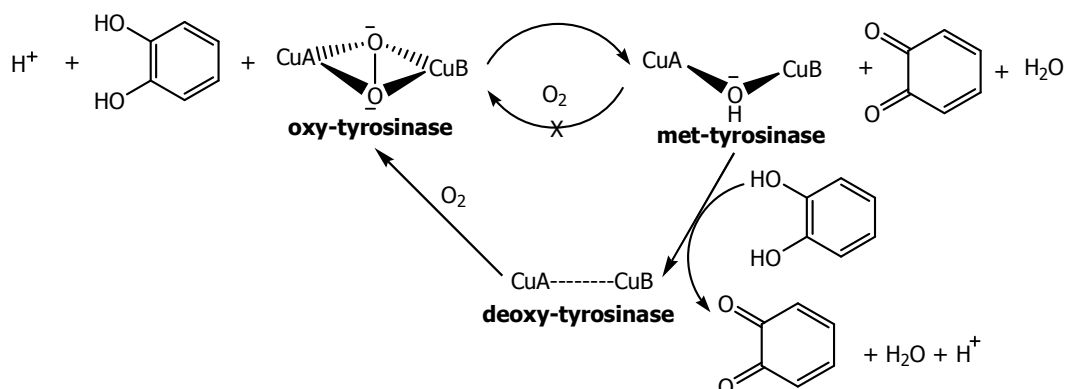
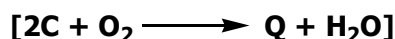
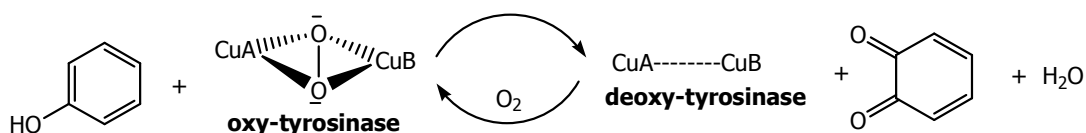
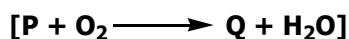
(a) Catecholic Substrate Oxidation cycle**(b) Phenolic Substrate Oxidation Cycle**

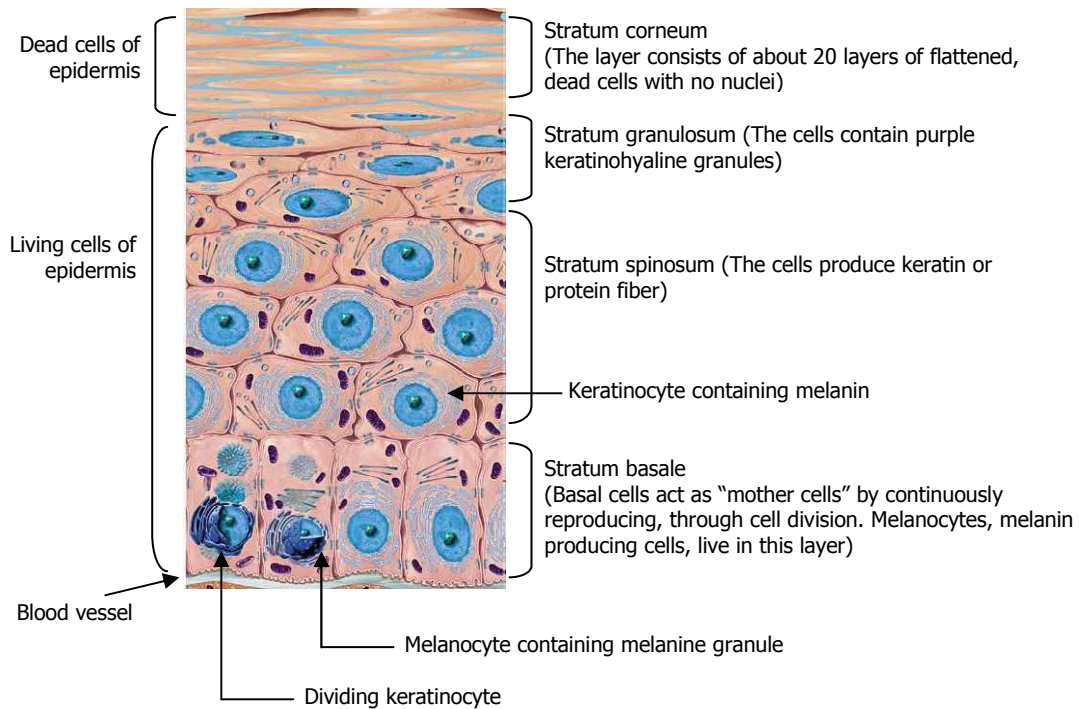
Fig. I.2.3.3b. Scheme of mechanism reaction of tyrosinase with monophenol and diphenol substances. Three forms of tyrosinase deoxytyrosinase (TY_{red}), mettyrosinase (TY_{met}) and oxytyrosinase (TY_{oxy}) are involved in this reaction (Land et al. 2003)

I.2.3.2. Melanin biosynthesis

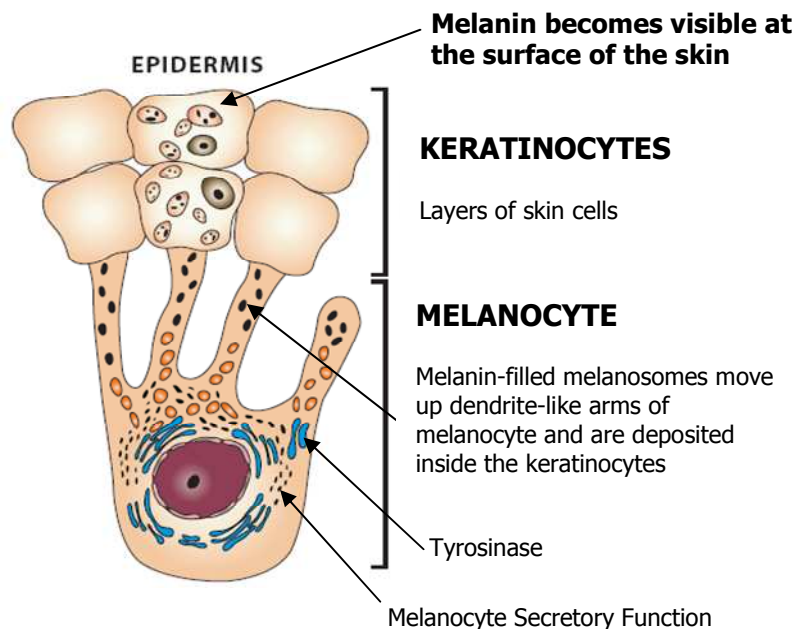
Normal skin colour is dependent on haemoglobin (in both the oxygenated and reduced state), carotenoids and melanin pigment. The major colour determinant is melanin and racial and ethnic differences in skin colour are related to the number, size, shape, distribution and degradation of melanin-containing organelles called melanosomes (Bleehen et al. 1995). The production of melanin by melanocyte within the skin or hair is called melanogenesis (Kim et al. 2004a).

Production of melanin is dependent on UV light or sun exposure. It is a natural protective mechanism of the skin against too much UV light penetrating in the human skin, where too much UV cause sunburn, disrupts the synthesis of precursors necessary to make human DNA and also increase free radicals. Melanin will attach the free radicals and also participate in other oxidation-reduction processes in the human body (Bleehen et al. 1995).

The process of pigmentation consists of three phases : activation, synthesis and expression phases. The first step is the activation of the melanocyte by several triggers such as UV light and free radical exposure. The second step is the synthesis of melanin phase. The melanocyte actually makes the melanin granules called melanosomes through several reactions as displayed in the Figure I.2.3.4. The last step is an expression phase. During this step, the melanosomes are transferred from the melanocytes to upper skin cell layers. Once the melanin has been synthesized and filled into the melanosomes, the melanosomes travel out into the arms of the melanocyte. When the melanosomes reach the end of these dendrite-like tentacles, they are actually pushed out of the melanocyte and taken up by keratinocytes, which are the skin cells located above the melanocytes in the epidermis. The keratinocytes take these melanosomes and carry them all the way up to surface of the skin, where they are, in essence, expressed. After this transfer has taken place, the melanin colour will eventually become visible on the surface of the skin (Williams et al. 1995).



Note : Reproduced from <http://www.eucerin.co.uk/media/epidermis.jpg> with modifications



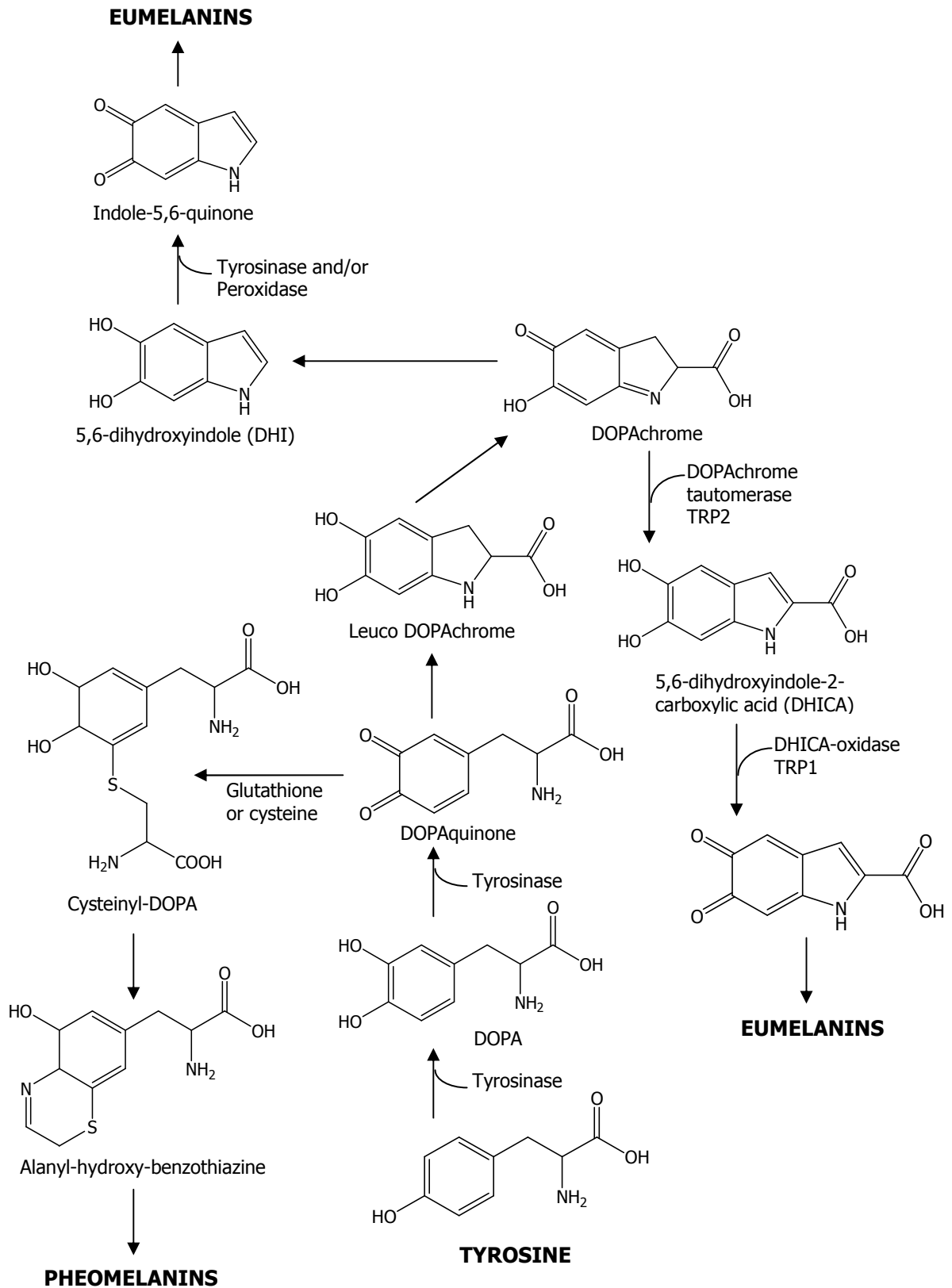
Note : Reproduced with modifications from http://www.nuskin.com/corp/library/pdf/clinical/tpw_pigmentation_clinical.pdf

Fig.I.2.3.4. The skin anatomy. Melanocyte containing melanin granule is in basal layer of epidermis. If the skin exposed by UV light, the melanin production will be increased and the melanin migrates to the skin surface to protect skin from the radiation damage

Melanins are usually classified into two main groups : the black and brown eumelanins which are insoluble, and the yellow and reddish-brown phaeomelanins, which are alkali soluble. Both eumelanins and phaeomelanins are derived from tyrosine, by the same initial steps (Bleehen et al. 1995; Parvez et al. 2007; Kobayashi et al. 1994).

Synthesis of melanin started from the conversion of the amino acid L-tyrosine to L-3,4-dihydroxyphenylalanine (L-DOPA) and then oxidation of L-DOPA to produce an ortho-quinone (dopaquinone) by tyrosinase. Dopaquinone is further transformed through several reactions to yield brown to black melanin which is responsible for the colour of mammal's skin (Okombi 2006; Lee 2002; Ohguchi et al. 2003, Wang and Hebert 2006). Two other melanogenic enzymes, tyrosine-related protein1 (TRP1) enzyme and tyrosine-related protein2 (TRP2) enzyme also named dopachrome tautomerase (DCT) enzyme (Solano et al. 1994), are involved in the melanin biosynthesis (Kobayashi et al. 1994; Parvez et al. 2007) as in Figure I.2.3.5.

The quinone-generating activity of tyrosinase explains its cytotoxicity and antiproliferative activity. Tyrosinase-generated quinones may cause substantial cytotoxicity because of the ability to bind covalently with free –SH groups and to alkylates DNA. Tyrosinase could be modified by mutation techniques to find tyrosinase mutants that can be used as prodrugs for tumoral therapy primarily for melanoma therapy (Simonova et al. 2000)



I.2.3.5. Melanin biosynthesis (Kobayashi et al. 1994; Parvez et al. 2007)

I. 2.3.3. Sun screening, antioxidative and tyrosinase inhibitor

Sun screening

Chronic sun exposure, melasma or other hyperpigmentation diseases may overproduce melanin (Wang et al. 2006). According to Seiberg et al. (2000), melanin biosynthesis can be prevented by:

- Avoiding ultraviolet rays exposure
- Inhibition the melanocyte metabolism and proliferation
- Inhibition the tyrosinase activity
- Removing melanin by corneal ablation

The ultraviolet ray can be classified into 3 groups. They are UV_A, UV_B and UV_C. The UV_A has a wave length between 315 and 400 nm. It is less dangerous than UV_B and UV_C, but it can cause loss of collagen and has alteration effect. The UV_B has the wave length between 290 and 315 nm. It causes sunburn and activates the melanocytes in the skin, so that they produce melanin and cause tanning effect. The UV_C has the wave length between 100 and 290 nm. It is very dangerous, but it is absorbed by the atmosphere (ozone layer and other gases) (Walters 1997).

The UV_A band has been an important subject of research on the protection of skin from damage caused by sunlight because several cutaneous effects of UV irradiation including wrinkles, pigmentation and skin cancer are found to be attributed not only to UV_B but also to UV_A exposure. It has been well known that the best way to protect skin from sun damage is to apply sunscreens. Many UV_B filters are now commercially available, but very few UV_A filters have been developed. Since it is not practical to use a UV_A filter only, the combination of UV_B and UV_A filters is always recommended for sunscreen formulation (Imokawa 1990).

Sunscreens are classified into two groups, chemical or physical sunscreens. The classification is based on their mode of action whether they absorb, reflect or scatter specific wavelength bands of radiation. When chemical sunscreens are applied on the skin, they usually do not modify the appearance of the skin. When physical sunscreens are applied on the skin, they can be seen on the skin's surface because they reflect and scatter light. Because physical sunscreens are not selective to absorb UV wave length, they are recognized as

broad spectral protection. Examples of physical sunscreens are titanium dioxide, talc, zinc oxide, and iron oxide. On the other hand examples of chemical sunscreens are p-aminobenzoic acid, coumarin, hydroquinone, dioxyacetone. The physical sunscreen is more safely than the chemical sunscreen because the physical sunscreen does not react with the skin material and some of them are not be absorbed by skin layers (Sayre 1994). In addition, the chemical sunscreens may produce allergy.

Most important for maintaining skin whiteness is to avoid ultraviolet exposure. UV radiation can also induce formation of various radicals (Matsuura et al. 2006), primarily reactive oxygen species (ROS) in the skin such as singlet oxygen and superoxide anion, promoting biological damage in exposed tissues via iron-catalyzed oxidative reactions. These radicals included ROS playing important roles in the activation of tyrosinase in human skin (Matsuura et al. 2006) and then enhance melanin biosynthesis via induction of the proliferation of the melanocytes. These radicals also cause the DNA damage. Furthermore the ROS scavengers or inhibitors such as antioxidatives may reduce hyperpigmentation and can be also used as whitening materials. Not only ROS, but also the hydroxyl radical can damage living cells. The hydroxyl radical is one of the most reactive radicals generated from biological molecules (Wang et al. 2006). Therefore, it is necessary to combine sun screen compounds and antioxidative compounds in cosmetics products to achieve an optimal whitening effect.

Antioxidative

There is an increasing interest in antioxidatives, particularly in those intended to prevent the presumed deleterious effects of free radicals not only in the human body, but also foodstuff. In both cases, there is a preference for antioxidatives from natural rather than from synthetic sources (Abdalla and Roozen 1999; Molyneux 2004).

Some plant extracts may have the ability to scavenge hydroxyl radicals and oxygen radicals and may protect cellular lipids against free radical reaction. Geraniol, terpinolene and gamma-terpinene were reported as radical scavengers in lemon oil (Matsuura et al. 2006). Marxen et al. (2007) have reported that some Microalga extracts from methanol (*Anabaena* sp, *Isochrysis galbana*,

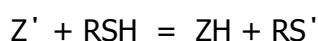
Synechocystis sp, *Phaedodactylum tricornutum*, *Porphyridium purpureum*) have antioxidative activity. Antioxidative activity of *Rosa damascene* flower extract (fresh flower and spent flower) has been investigated by Özkan et al. (2004). The antioxidative activity was measured by the formation of phosphomolybdenum complex. The extent of the antioxidative effects of this extract could be attributed to their phenol composition and essential oil contents (Aridogan et al. 2002; Özkan et al. 2004). Miliauskas et al. (2003) have observed the antioxidative activity of some medicinal and aromatic plant extracts (*Salvia sclarea*, *Salvia glutinosa*, *Salvia pratensis*, *Lavandula angustifolia*, *Calendula officinalis*, *Matricaria recutia*, *Echinacea purpurea*, *Rhaponticum carthamoides*, *Juglans regia*, *Melilotus officinalis*, *Geranium machorrhizum* and *Potentilla fruticosa*) using DPPH and ABTS radicals. The results indicate that the amount of total phenol compounds in investigated plant extracts in most cases correlated with their antiradical activity.

Active-oxygen scavenging activity of traditional nourishing-tonic herbal medicines and active constituents of *Rhodiola sacra* has been investigated by Ohsugi et al. (1999) using superoxide anion radical and hydroxyl radical. There are 19 compounds found in this species. Hydroquinone, caffeic acid, gallic acid, protocatechic acid, epigallocatechin-3-o-gallate, gallic acid-4-O- β -D-glucopyranoside showed inhibitory activity against superoxide radicals, while hydrocinnamic acid and 4-hydroxybenzoic acid inhibited hydroxyl radical. Antioxidative activity of two major acylated flavonoid quercetin-3-O-[2G-(E)-coumaroyl-3G-O- β -D-glucopyranosyl-3R-O- β -glusylrutinoside] and kaempferol-3-O-[2G-(E)-coumaryl-3G-O- β -D-glucosyl-3R-O- β -D-glucosylrutinoside] in methanol extract of oolong tea has been evaluated by Lee et al. (2007). Rangkadilok et al. (2006) have reported the antioxidative activity of longan fruit extract is similar to those of Japanese green tea extract. The activities were attributed to the polyphenol compounds in this plant. The antioxidative properties of violacein, a violet pigment produced by *Chromobacterium violaceum*, against DPPH, nitric oxide and superoxide radicals has been observed by Konzen et al. (2006). The efficiency of flavonoids in polar extracts of *Lycium chinense* Mill fruits as free radical scavenger has been investigated by Qian and Huang (2004). The major constituents of this extract are rutin, chlorogenic acid and protocatechuic. Other compounds having antioxidative activity, such as camphor, parthenolide, luteolin

and apigenin, have been reported by Wu et al. (2006). In an other paper, Silva et al. (2005) have investigated the antioxidative properties of *Hypericum perforatum*. Its antioxidative activity is due to their flavonoid contents.

For estimating the antioxidative potential of chemical components, different experimental approaches were used (Prior et al. 2005). Most of them require a spectrophotometric measurement and a certain reaction time in order to obtain reproducible results (Kulisic et al. 2004; Marxen et al. 2007). For example, the β -carotene bleaching test (BCB) is based on the decolorization of β -carotene by its reaction with radicals. This effect is measured at a wavelength of 470 nm after a reaction time of about 120 min. Other methods like the 2,2-diphenylpicrylhydrazyl (DPPH, $C_{18}H_{12}N_5O_6$) scavenging method or the thiobarbituric acids reactive species (TBARS) assay work similar to the BCB test (Marxen et al. 2007). The TBARS assay uses the production of a pink pigment produced by the reaction of thiobarbituric acid (TBA, $C_4H_4N_2O_2S$) with malondialdehyd (MDA, $C_3H_4O_2$) and other secondary lipid peroxidation products. Absorbance measurements at 532 nm serve as an indicator of the extent of lipid degradation (Kulisic et al. 2004). Another method is TEAC method (the ferryl myoglobin/ABTS assay). The principle of this reaction is the pre-formed radical monocation of 2,2'-azinobis-(3-ethylbenzothiazoline-6-sulfonic acid) ($ABTS^{\cdot+}$, $C_{18}H_{24}N_6O_6S_4^+$) is generated by oxidation of ABTS with potassium persulfate and is reduced in the presence of such hydrogen-donating antioxidatives (Re et al. 1999).

One such method that is currently popular is the DPPH method, because this method is simple, rapid and convenient and independent of sample polarity (Koleva et al. 2001; Marxen et al. 2007). This method has been introduced by Marsden-Blois about 50 years ago. He used the DPPH to analyse antioxidative of the thiol of the amino acid cystein through titration. He has accounted the stoichiometry of the reaction between DPPH and cysteine, and the result is a 1:1 stoichiometry. The reaction can be written :

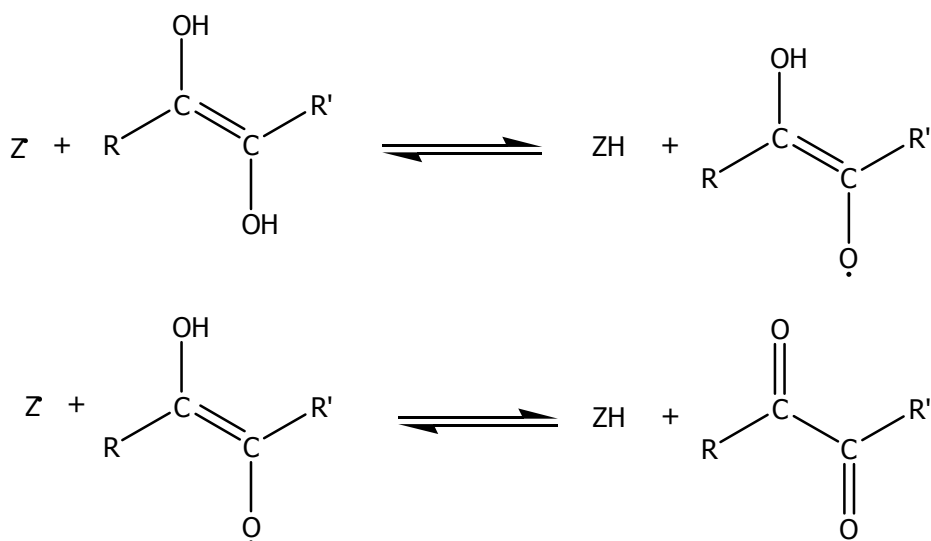


Z' is DPPH radical; RSH is cysteine molecule

The free radical RS' then reacts with another molecule that was produced by a parallel reaction.



Based on the reaction above, it can be shown that two molecules of DPPH are reduced by two molecules of cysteine with an 1:1 stoichiometry. However, if the molecule has two adjacent sites for hydrogen abstraction, such as in Vitamin C molecule, the stoichiometry of the reaction is 2:1. The same stoichiometry is true for the reaction of DPPH and hydroquinone (1,4-dihydroxybenzene) which leads to the production of quinone (1,4-benzoquinone) by a similar two step mechanism (Molyneux 2004).



The original Blois method has been used by several workers. The UV spectrophotometer was used to measure the reaction between DPPH and the substances. The product formation is measured at 517 nm. A linear curve of the changes in absorbance versus the concentration of the substance is used to calculate the parameter EC_{50} or SC_{50} . The parameters are used to express the antioxidative activity and defined as the concentration of the substance that cause 50% loss of DPPH activity. Thus, the lower the SC_{50} value, the higher the antioxidative activity (Molyneux 2004; Marxen et al. 2007).

Tyrosinase inhibition

Tyrosinase inhibition is one of methods to reduce the melanin synthesis (Khatib et al. 2005). In recent years, with the nature orientation of consumers, functional cosmetics such as antiwrinkle solutions and whitening agents have been combined with compounds from natural medicines or herbal medicines (Tanimoto et al. 2006). However, only a few natural and synthetic compounds, which have activity as tyrosinase inhibitors, were used as skin whitening agents due to safety concerns (Okombi et al. 2006).

A number of tyrosinase inhibitors from natural sources that inhibited monophenolase, diphenolase or both, have been identified. Plants are a rich source of bioactive chemicals, which are often free from harmful side effects (Lee and Lee 1977; Chang 2007). Some inhibitors from higher plants have been found and can be classified into two groups, polyphenols and aldehyde derivatives (Parvez 2007). Phenol compounds are important materials and can be used as depigmenting agents, because they have a chemical structure similar to tyrosine, the starting material of the melanin and the substrate of the tyrosinase (Wang et al. 2006; Sandler 2005; Sudjaroen et al. 2005).

Flavonoids are one of important plant phenol groups that have strong tyrosinase inhibitory activity. All flavonoids inhibit the enzyme due to their ability to chelate copper in the active site of the tyrosinase. However, they are only applicable if the 3-hydroxyl group of the isoflavonoid is free. Flavonoids containing a keto group possess potent tyrosinase inhibitory activity. This may be explained by the similarity between the dihydroxyphenyl skeleton in L-DOPA and the keto group in flavonoid. Green tea catechins, belonging to the group of flavonoids, exhibit biological and pharmacological effects including anti-tyrosinase and antioxidative activity (Kim et al. 2004). Nithitanakool et al. (2009) found that pentagalloyl glucopyranose from seed kernels of Thai Mango (*Mangifera indica*, L. cv, 'Fahlun') has anti-tyrosinase activity which involve an ability to chelate the copper atoms of active site of the enzyme. Tannic acid and gallic acid from *Rhus javanica* leaves have also been investigated by Kubo et al. (2003) and the results indicated that the tyrosinase inhibitory activity of tannic acid is more potent than gallic acid. Tyrosinase inhibitory studies of cycloartane and cucurbitane glycosides from Astragalus (Leguminosae) and Bryonia (Cucurbitaceae) plants have been investigated by Khan et al. (2006). Isoflavone derivatives (included

daidzein, glycitein, daidzin and genistin) isolated from soybean, have been studied by Chang (2007), and the result displayed that they have a high potential to inhibit the tyrosinase. Gilly et al. (2001) have reported that resveratrol found in Carignan Grape juice has tyrosinase inhibition activity. Galangin, kaempferol, and quercetin have been identified as potent tyrosinase inhibitory polyphenols (Matsuura et al. 2006).

A large number of aldehydes and other derivatives were also characterized as tyrosinase inhibitors, because they can react with nucleophilic groups such as sulfhydryl, amino and hydroxyl groups. Its inhibitory effect is e.g. due to the formation of a Schiff base with the primary amino group of the enzyme. (Kubo and Kinst-Hori 1998b; Schauenstein et al. 1977; Parvez 2007). Cuminaldehyde extracted from the seed of *Cuminum cyminum* L, has reported to be a tyrosinase inhibitor which has activity being about 16 fold higher than that of benzaldehyde. 6-Hydroxy-2H-pyran-3-carbaldehyde, haemanthamine and 1,1'-bis(1,1'-carboxyethyl) were isolated from *Crinum yemense* showed competitive tyrosinase inhibitory activity (Abdel-Hakim et al. 2008). A series (2E)-alkenals were also isolated and characterized as tyrosinase inhibitors (Kubo and Kins-Hori 1999). Anisaldehyde characterized in the seed of *Pimpinella anisum* disrupts the tertiary structure of the enzyme not only through forming a Schiff base with a primary amino group in the enzyme, but also via hydrogen-bonding interactions (Joung-Ha et al. 2005).

Chalcones containing a phenol moiety may exhibit antioxidative activity as a result of their ability to donate an electron (or receive hydrogen atom) and/or chelate transition metals, such as copper or ferrous ions, and thereby eliminating reactive oxygen and nitrogen species (ROS and RNS) and decay-free radical propagation reaction. When both reactions are strong, they are known to induce melanine synthesis (Nerya et al. 2004; Khatib et al. 2005). Hydroquinone has been known as tyrosinase inhibitor since 1896 (Gregg and Nelson 1940). Gnetol from genus gnetum is also tyrosinase inhibitor (Ohguchi 2003). Stilbene, related 4-substituted resorcinols and several flavonoids, were tested for their inhibitory activity against tyrosinase to clarify the structural-activity relationship (Sasaki et al. 2002; Likhitwitayawuid 2008). Kojic acid and azelaic acid are tyrosinase inhibitor from fungi which are good chelators of transition metal ions and good scavenger of free radicals. Linoleic acid, hinokitiol, arbutin, catechins, naturally

occurring hydroquinone and aloesin have been also reported to act as tyrosinase inhibitors (Parvez 2007, Okombi et al. 2006). Free fatty acids have been shown to have remarkable regulatory effects on melanogenesis in cultured B16F10 murine melanoma cells. Unsaturated fatty acids, such as oleic acid (C18:1), linoleic acid (18:2) or gamma-linolenic acid (C18:3), decrease melanin synthesis and tyrosinase activity, while saturated fatty acids, such as palmitic acid (C16:0) or stearic acid (18:0), increase it (Ando et al. 1999).

I.2.3.4. Tyrosinase inhibition Assay

There are two main methods to evaluate tyrosinase inhibition, either in vitro assay or in vivo assay. The in vitro assay is easy to handle, accurate, but can't be exploited from developing products for human use. It is done by using the commercially available mushroom tyrosinase as a model. Although mushroom tyrosinase differs somewhat from other sources (van Gelder et al. 1997), this fungal source was used for some experiments because it is readily available. On the other hand, the in vivo assay is relative good and can be exploited for human use, but rather complex in its procedure. This assay is performed by using a cellular test indicating the decrease of the tyrosinase activity. This assay can also be done by using human melanocytes obtained from healthy individuals. The inhibitory potency is evaluated by measuring the transformation rate of L-DOPA to L-Dopaquinone. Then L-dopaquinone can be trapped by 3-methyl-2-benzothiazolinone hydrazone MBTH. The absorbance of this solution is measured by spectrophotometer at 490 nm. The absorbance will be lower than normal value when there is a tyrosinase inhibitor compound (Okombi et al. 2006).

I.3. STATEMENT OF THE OBJECTIVES

The objectives of the research were :

1. isolation of compounds from bengkoang roots which have UV absorption and whitening activities
2. elucidation of the chemical structures of active compounds in bengkoang roots which have a sunscreen ability and skin whitening activity based on the spectroscopy data involving one and two dimensional NMR spectroscopy data as well as mass spectrometry data
3. determination of whitening activity in bengkoang roots extracts by measuring antioxidative activity and tyrosinase inhibitory activity

CHAPTER II MATERIALS AND METHODS

II.1. Plant materials

The bengkoang belongs to the taxonomic class of Magnoliopsida; order Fabales; family Fabaceae; subfamily Faboideae; genus *Pachyrhizus*; species *Pachyrhizus erosus*. The bengkoang *Pachyrhizus erosus* (L) Urb roots were collected from Purworejo, Central Java, Indonesia in dry season (November 2006).

II.2. Laboratory chemicals and instruments

Chemicals and solvents

The chemicals used in the detection and isolation methods were anisaldehyde (4-methoxybenzaldehyde), glacial acetic acid, aluminium chloride, hydrochloric acid and concentrated sulphuric acid (all purchased from Merck, Darmstadt, Germany), mushroom tyrosinase 4187 IU/mg, Folin-Ciocalteu's phenol reagent, L-DOPA (dihydroxy phenyl alanine), kojic acid (Fluka, Seelze, Germany), sodium nitrite, sodium hydroxide (purchased from Grüssing, Filsum, Germany), dimethylsulfoxide extra pure (Acros[®] organic, Geel, Belgium), DPPH (2,2-diphenyl-1-picrylhydrazine), catechin, Dulbeco's phosphate buffered saline, (purchased from Sigma Aldrich, Steinheim Germany), ascorbic acid (Sigma Aldrich, Steinheim, Germany), gallic acid, PABA (p-aminobenzoic acid) (Fluka, Seelze, Germany), sodium carbonate (Grüssing, Filsum, Germany), Sephadex LH20 (Aldrich, Steinheim, Germany), Silica gel 60 (particle sizes 0.063-0.200mm, Merck, Darmstadt, Germany), TLC Aluminium sheets, silica gel 60 F254 (layer thickness 0.2 mm, Merck, Darmstadt, Germany).

Solvents for separation techniques were petroleum ether, ethyl acetate (Fisher Scientific, Leicestershire, UK), methanol (Merck, Darmstadt, Germany), chloroform, dichloromethane, n-butanol and were purchased from the Fluka, Seelze, Germany.

Instruments

Melting point SMP3 Stuart[®] apparatus (Staffordshire, UK), Cary 50 Bio UV-Visible spectrophotometer (Varian, California, USA), JASCO FT/IR-6100 Spectrophotometer (Gross-Umstadt, Germany), Thermo Mixer Comfort 5355 V.2.12 Eppendorf (Hamburg, Germany), ALPHA II-12 Freeze dryer (Osterode,

Germany), Bruker Avance 400 NMR spectrometer (Rheinstetten, Germany), Shimadzu GC/MS-QP 20105 gas chromatography (Kyoto, Japan), Agilent 1100 series HPLC apparatus (California, USA) equipped by column Zorbax SB-C18 (25 cm, i.d. 0,46 cm, 5 μ m, Agilent, California, USA), UV and MS detectors, Agilent 1100 series preparative-HPLC (California, USA) equipped by column Zorbax SB-C18 (7 μ m, 21,2X150 mm, Agilent, California, USA), Büchi rotavapor (Flawil, Switzerland).

II.3. Framework of the research

The framework of the research consisted of several steps as in the figure II.3.1.

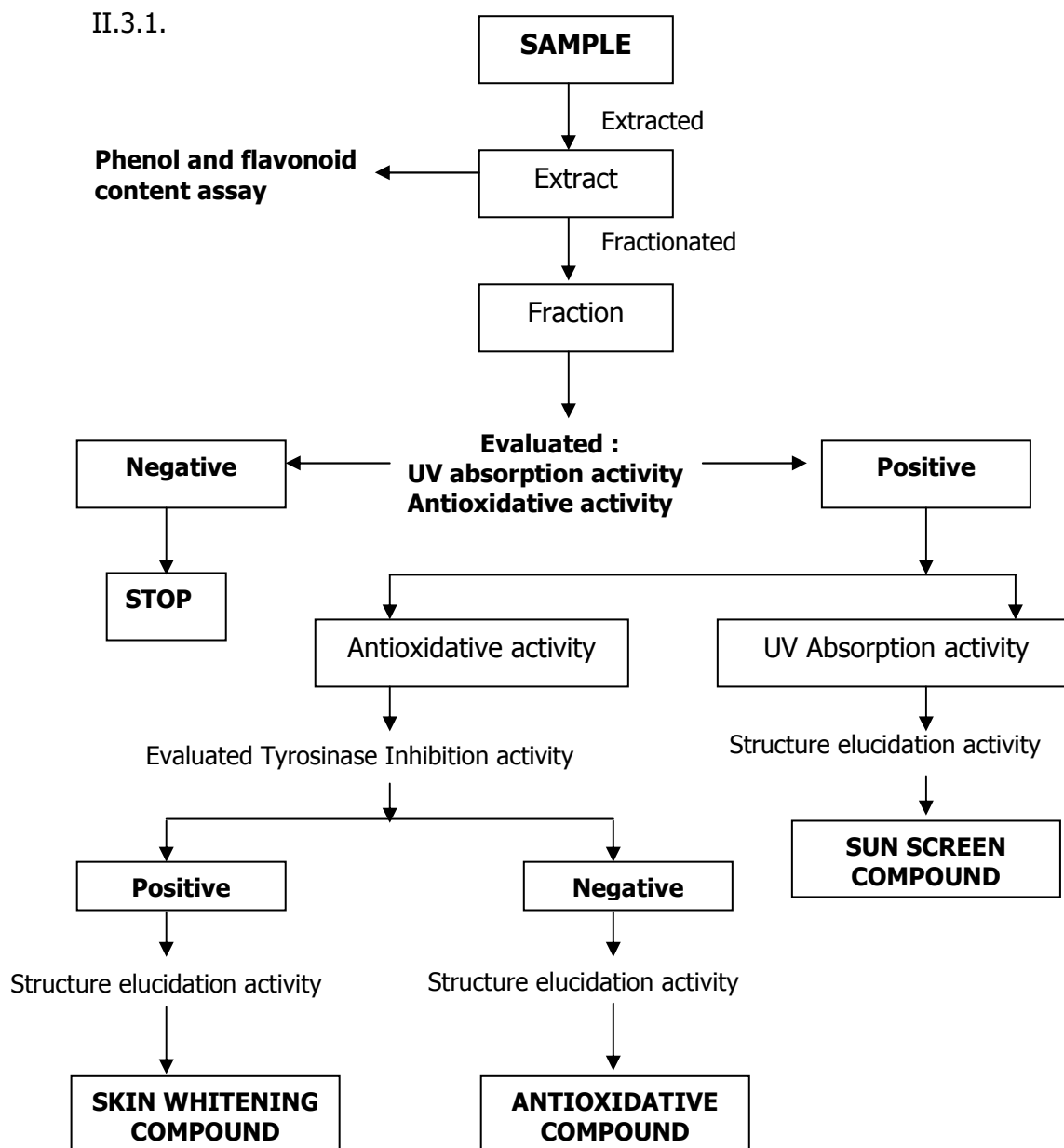


Fig. II.3.1. The framework of the research

II.4. Chromatography

II.4.1. Thin layer chromatographic

Analytical Thin Layer Chromatography (TLC) was carried out by using the commercially available Merck TLC plastic sheet pre-coated Kieselgel 60 F₂₅₄ (layer thickness 0.2 mm, Merck, Darmstadt, Germany) for semi polar to non polar substances and with precoated TLC RP 18 F₂₅₄ plates (layer thickness 0.25 mm, Merck, Darmstadt, Germany) for more polar substances.

Detection was performed by UV light at 254 and 366 nm, followed by spraying the TLC plates with anisaldehyde-H₂SO₄ reagent and subsequent heating at 110°C, or followed by spraying with DPPH solution in MeOH according to Cacha et al. (2005) and Torres et al. (2006). After developing and drying, the TLC plates (sample ranging from 0.1-100 µg) were sprayed with 0.2% solution of DPPH dissolved in MeOH. The DPPH solution was stored in a dark bottle and kept refrigerated until used. The reagent is no longer usable when the colour has turned to yellow. Active compounds appeared as yellow spots against a purple background after 90 minutes of spraying.

The anisaldehyde-H₂SO₄ reagent: for 100 ml reagent, 10 ml glacial acetic acid was added to 85 ml MeOH followed by 5 ml concentrated H₂SO₄ (added slowly) and 0.5 ml anisaldehyde. The reagent was stored in a coloured bottle and kept refrigerated until used. The reagent is no longer usable when the colour has turned to red-violet.

Thin layer chromatography was carried out in 5 elution system as described in Table II.4.1.

Table. II.4.1. Elution systems of thin layer chromatography (silica gel)

System	Mobile Phase	Detection
TLC-1	CHCl ₃ -EtOAc (6:4)	UV 254; DPPH; Anisaldehyde-H ₂ SO ₄
TLC-2	CHCl ₂ -EtOAc (6:4)	UV 254; DPPH; Anisaldehyde-H ₂ SO ₄
TLC-3	EtOAc-MeOH-H ₂ O (61:31:8)	UV 254; DPPH; Anisaldehyde-H ₂ SO ₄
TLC-4	Upper phase of BuOH-CH ₃ COOH-H ₂ O (4:1:5)	UV 254; DPPH; Anisaldehyde-H ₂ SO ₄
TLC-5	CHCl ₃ -EtOAc (2:8)	UV 254; DPPH; Anisaldehyde-H ₂ SO ₄

II.4.2. Column Chromatography

Column chromatography was conducted in several systems as described in Table II.4.2.

Table II.4.2. Elution systems of column chromatography

System	Stationary phase	Mobile phase
SG-1	Silica gel	Gradient mixture of PE-EtOAc (from 100% of PE to 100% of EtOAc) and followed by gradient mixture of EtOAc-MeOH (from 100% of EtOAc to 100% of MeOH)
SG-2	Silica gel	CHCl ₃ 100%
SG-3	Silica gel	CH ₂ Cl ₂ -EtOAc (60:40)
SG-4	Silica gel	CH ₂ Cl ₂ -EtOAc (50:50)
SG-5	Silica gel	PE-EtOAc (60:40; 25:75), EtOAc 100%, EtOAc-MeOH (50:50)
SG-6	Silica gel	PE-EtOAc (30:70), EtOAc 100%, EtOAc-MeOH (70:30)
PC-1	Sephadex LH20	MeOH 100%

II.4.3. Analytical HPLC

The Agilent 110 series HPLC apparatus (California, USA) equipped with two solvent delivery systems, an auto sampler and an UV detector was used in this study. The column Zorbax SB-C18 (25 cm, i.d. 0.46 cm, 5 µm particle size) from Agilent was used. Chemicals used in this research for HPLC were millipore water, methanol for HPLC (VWR, Leuven, Belgium), formic acid 98-100% (Riedel-de Häen[®], Sigma Aldrich, Seelze, Germany).

II.4.4. Semi preparative HPLC

The Agilent 1100 series HPLC (California, USA) with column Zorbax SB-C18 (150 mm, i.d. 21.2 mm, 7 µm particle size) equipped with an auto sampler and UV detector was used. The sample dissolved in an appropriate solvent with maximal concentration 2 mg/ml was injected into the system. The solvent systems and the elution programs used in the semi preparative HPLC were based on the previously performed analytical HPLC data. The flow rate was 10 ml/min. Table II.4.3 displays the elution program used in this research.

Table II.4.3. The elution programs of semi preparative HPLC (Flow rate 10 ml/min)

System	Elution Program										
Prep-1	Gradient elution of acetonitrile and water										
	<table border="1"> <thead> <tr> <th>Time (min)</th> <th>% Acetonitrile</th> </tr> </thead> <tbody> <tr> <td>0</td> <td>70</td> </tr> <tr> <td>10</td> <td>70</td> </tr> <tr> <td>20</td> <td>100</td> </tr> <tr> <td>40</td> <td>100</td> </tr> </tbody> </table>	Time (min)	% Acetonitrile	0	70	10	70	20	100	40	100
	Time (min)	% Acetonitrile									
	0	70									
	10	70									
20	100										
40	100										
Prep-2	Gradient elution of methanol and water										
	<table border="1"> <thead> <tr> <th>Time (min)</th> <th>% MeOH</th> </tr> </thead> <tbody> <tr> <td>0</td> <td>20</td> </tr> <tr> <td>5</td> <td>20</td> </tr> <tr> <td>20</td> <td>100</td> </tr> <tr> <td>25</td> <td>100</td> </tr> </tbody> </table>	Time (min)	% MeOH	0	20	5	20	20	100	25	100
	Time (min)	% MeOH									
	0	20									
	5	20									
20	100										
25	100										
Prep-3	Gradient elution of acetonitrile and water										
	<table border="1"> <thead> <tr> <th>Time (min)</th> <th>% Acetonitrile</th> </tr> </thead> <tbody> <tr> <td>0</td> <td>5</td> </tr> <tr> <td>10</td> <td>50</td> </tr> <tr> <td>30</td> <td>50</td> </tr> </tbody> </table>	Time (min)	% Acetonitrile	0	5	10	50	30	50		
	Time (min)	% Acetonitrile									
	0	5									
10	50										
30	50										
Prep-4	MeOH - water (30:70)										
Prep-5	Gradient elution of methanol and water										
	<table border="1"> <thead> <tr> <th>Time (min)</th> <th>% MeOH</th> </tr> </thead> <tbody> <tr> <td>0</td> <td>5</td> </tr> <tr> <td>20</td> <td>50</td> </tr> <tr> <td>30</td> <td>100</td> </tr> <tr> <td>35</td> <td>100</td> </tr> </tbody> </table>	Time (min)	% MeOH	0	5	20	50	30	100	35	100
	Time (min)	% MeOH									
	0	5									
	20	50									
30	100										
35	100										
Prep-6	Gradient elution of methanol and water										
	<table border="1"> <thead> <tr> <th>Time (min)</th> <th>% MeOH</th> </tr> </thead> <tbody> <tr> <td>0</td> <td>20</td> </tr> <tr> <td>20</td> <td>100</td> </tr> <tr> <td>30</td> <td>100</td> </tr> </tbody> </table>	Time (min)	% MeOH	0	20	20	100	30	100		
	Time (min)	% MeOH									
	0	20									
20	100										
30	100										

II.4.5. Liquid chromatography / mass spectroscopy (LC/MS)

An Agilent 1100 series HPLC equipped with an ESI-ion trap mass detector was used. The detector parameter was : nebulizer pressure 50 psi, dry gas flow rate 10 ml/min, dry temperature 350°C and capture power 25nA.

II.4.6. Gas chromatography / mass spectroscopy (GC/MS)

The GC/MS analysis was carried out on a Shimadzu GC/MS-QP 2010S mass spectrometer (Kyoto, Japan) with Rtx-5 MS capillary column (30 m, i.d. 0.25mm). The carrier gas was helium with flow rate 0.5 ml/min. The column temperature was programmed from 120 °C (5 min) and then continued to 300 °C (37 min) with an increasing temperature velocity 10 °C/min. The ion source temperature was 250 °C with electron energy 70 eV. Spectra were acquired and processed by WILEY.7 GC/MS Library, which produced standard bar graphs for direct comparison with published spectra.

II.5. Extraction and fractionation

The roots (45 kg) were peeled and washed with water, subsequently dried at 60°C and milled into fine powder. The fine powder (4.75 kg) was extracted by soxhlet using petroleum ether. The residue was extracted using methanol to achieve the semi polar and polar compounds. The extracts were filtered and concentrated in vacuo. The concentrated methanol extract was divided into two parts. One part was hydrolyzed with 2N HCl at 100°C in 2 hours and then extracted with ethyl acetate. This extract was called as the ethyl acetate after hydrolysis extract. To the other part of the concentrated methanol extract, water was added and also extracted with ethyl acetate. The ethyl acetate phase was further concentrated and the water phase was extracted with n-butanol. The residue methanol/water phase was obtained by evaporating using freeze dryer. The fractionation scheme can be shown in Figure II.5.1.

Crude extracts and fractions were then chemically investigated and analyzed by using thin layer chromatography, analytical HPLC, semipreparative-HPLC, GC/MS and LC/MS to determine further isolation work.

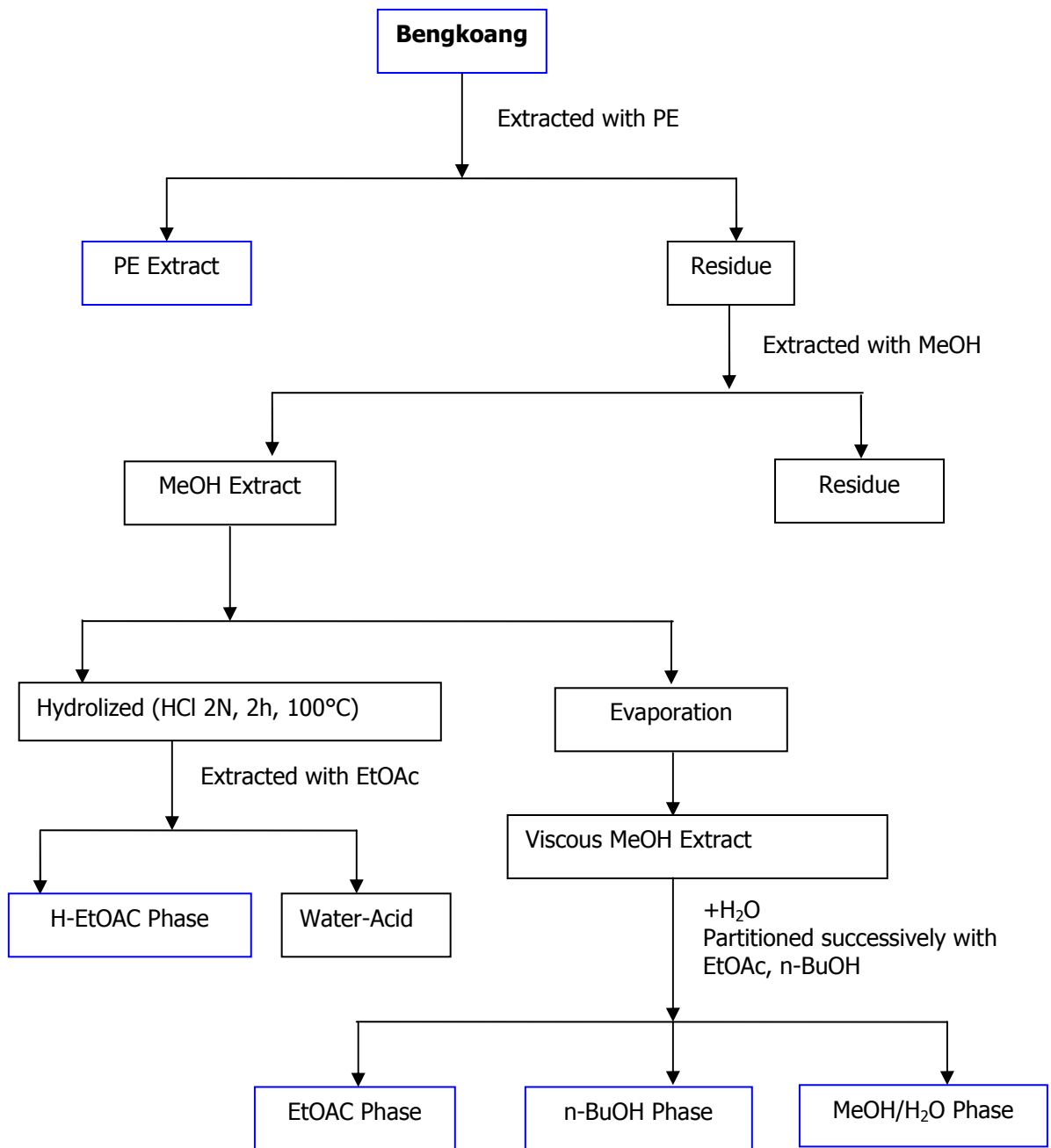


Fig. II.5.1. Extraction and fractionation scheme of bengkoang

II.6. Isolation of secondary metabolites from bengkoang root

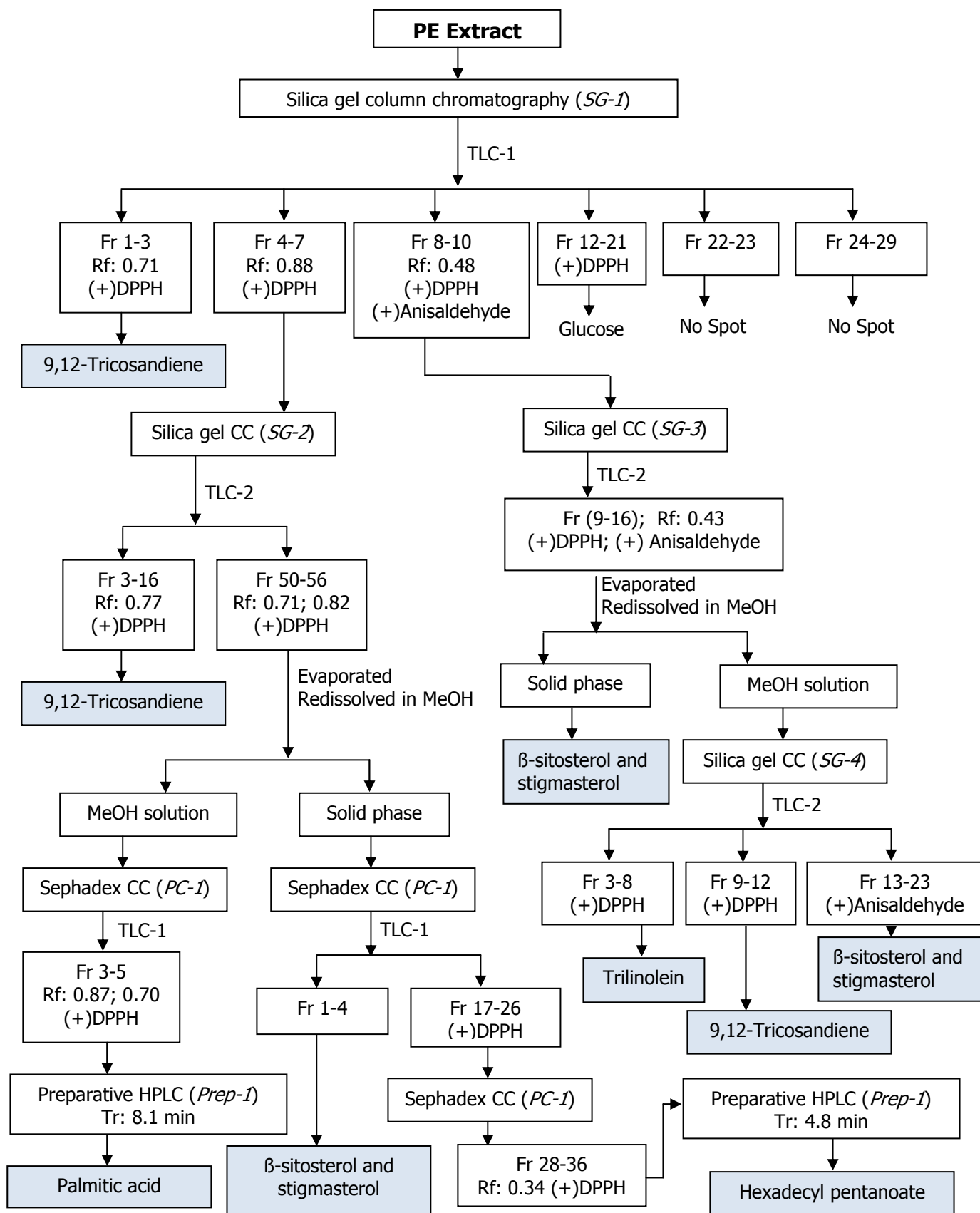
II.6.1. Compound isolation of petroleum ether extract

The petroleum ether extract (26.3 gram) was further subjected to silica gel chromatography (*SG-1*) as described in Table II.4.2 (p. 33). 29 fractions of 100 ml were collected according to the TLC results. TLC was conducted to each fraction respectively using silica gel as a stationary phase, chloroform-ethyl acetate (6:4) as a mobile phase (*TLC-1*). Detection was performed with UV light at 254 and 366 nm, followed by spraying the TLC plates with anisaldehyde-H₂SO₄ reagent and subsequent heating at 110°C or by spraying with DPPH reagent to determine the antioxidative activity of compounds.

Fractions 1, 2, 3 with an R_f value of 0.71 (positive with DPPH) were collected and evaporated. The obtained brown powder was washed with ethyl acetate. The pure brown powder (3.9 gram) was found to be **9,12-tricosandiene (101)**.

Fractions 4, 5, 7 with an R_f value of 0.88 (positive with DPPH) were collected and evaporated. To purify the fractions, the concentrated fraction was subjected to another silica gel column chromatography (*SG-2*) and eluted using chloroform. 29 fractions of 10 ml eluents were obtained. Fractions 50-56 which have 2 spots on *TLC-2* with R_f values of 0.71 and 0.82 (both of them positive with DPPH) were collected and evaporated to achieve a yellowish solid. The obtained solid then was washed with MeOH. The solid phase was subsequently subjected to sephadex column chromatography (*PC-1*) and eluted by methanol producing 26 fractions. Fractions 1-4 were collected and evaporated. These fractions contained the mixture of β-sitosterol and stigmaterol. Fractions 17-26 were also collected and evaporated, then subjected to another sephadex column chromatography (*PC-1*). The elution was performed by methanol producing 27 fractions. Fractions 28-36 which have an R_f value of 0.34 (positive with DPPH) were collected and purified through semipreparative-HPLC (*Prep-1*) giving **compound G1 (Hexadecyl pentanoate)**. The methanol washing was evaporated and then subjected to another sephadex column chromatography using methanol as eluent (*PC-1*) to get 7 fractions. Fractions 3-5 which have R_f values of 0.87 and 0.70, respectively, (both of them positive with DPPH) were collected and purified using semipreparative-HPLC (*Prep-1*) and giving **compound WuPe**, being **Palmitic acid**.

Fractions 8, 9, 10 have the same spot on *TLC-1* with an R_f value of 0.48 (positive with DPPH). Therefore, they were combined and then subjected to another silica gel column chromatography using dichloromethane-ethyl acetate (60:40) as a mobile phase (*SG-3*). Ten millilitre fractions were collected and evaluated by *TLC-2*. Fractions 9-16 have the same retention factor ($R_f = 0.43$) on TLC. They were combined and evaporated. The obtained solid was washed with methanol and recrystallized from petroleum ether and ethyl acetate to get a mixture (727 mg) which was identified as **stigmasterol (109a) and β -sitosterol (109b)**. The MeOH washing was evaporated to dryness and then subjected to another silica column chromatography (*SG-4*). Elution was performed by a mixture of dichloromethane-ethyl acetate (50:50). 28 fractions of 10 ml were collected and checked by TLC using silica gel as stationary phase, dichloromethane-ethyl acetate (6:4) as a mobile phase (*TLC-2*). Fractions 3-8 with an R_f value of 0.60 (positive with DPPH) were collected and evaporated, giving yellowish oil (364 mg), which could be assigned to **trilinolein (102)**. The isolation scheme of compounds in petroleum ether extract is displayed in Fig.II.6.1.1.



Note: detail elution systems of column chromatography, thin layer chromatography and preparative HPLC can be found on pages 32-34

Fig. II.6.1.1. The isolation scheme of compounds in petroleum ether extract

II.6.2. Compound isolation of the ethyl acetate extract

The isolation of compounds from the ethyl acetate extract has been conducted according to the Fig.II.6.2.1.

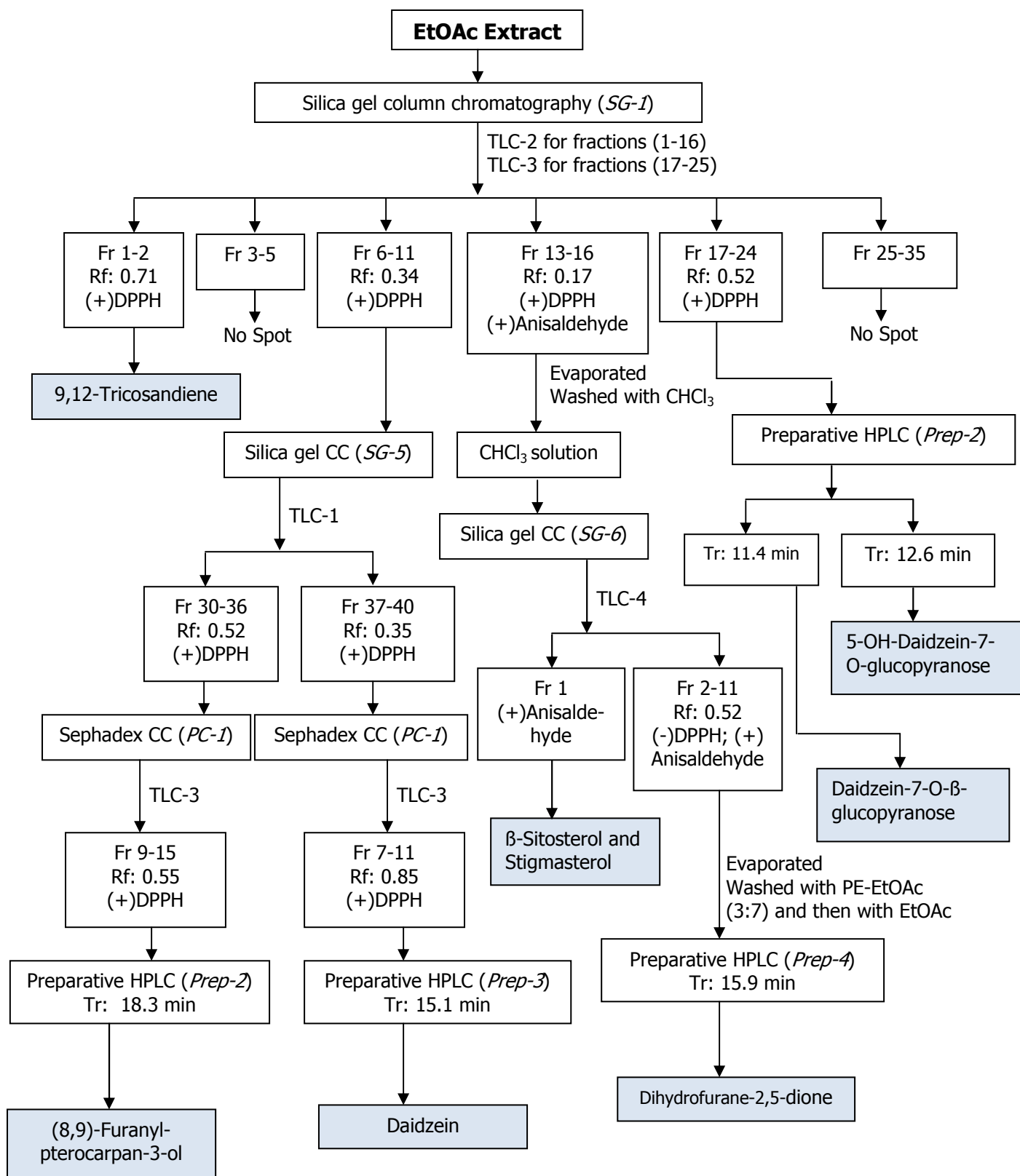
The ethyl acetate extract (31.1 gram) obtained from the scheme in Fig. II.5.1 (p. 36) was subjected to silica gel column chromatography (*SG-1*) and eluted using the gradient mixture of petroleum ether-ethyl acetate and ethyl acetate-methanol producing 35 fractions of 100 ml eluents. There were 6 groups based on their profile TLC chromatograms.

Fractions 6-11 which have an R_f value of 0.17 (positive with DPPH) were collected and evaporated. The fractions may contain antioxidative compounds because the spot was able to reduce DPPH. The concentrated fraction was then purified via another silica gel column chromatography (*SG-5*) using a mixture of petroleum ether-ethyl acetate (60:40, 25:75), ethyl acetate 100%, and then ethyl acetate-methanol (50:50) giving 44 fractions. Fractions 30-36 with an R_f value of 0.52 (positive with DPPH) on TLC-1 were evaporated and purified from impurities that have similar polarity to the target compound but different molecular size. The purification was carried out using column sephadex chromatography (*PC-1*). Fractions 9-15 from PC-1 were further subjected into preparative HPLC (*Prep-2*). 670 mg yellow crystal (**A182**) were obtained and identified as **(8,9)-furanyl-pterocarpan-3-ol**. Fractions 37-40 from column chromatography SG-5 with an R_f value of 0.35 on *TLC-3* were collected and purified. The purification was conducted by other sephadex column chromatography giving 19 fractions. Fractions 7-11 of this chromatography had the R_f value of 0.85 (positive with DPPH). The fractions were evaporated and purified via preparative-HPLC (*Prep-3*) giving 33 mg of **compound C1**. Based on the GC/MS and NMR spectroscopic data, compound C1 was identified as **daidzein**.

Fractions 13-16 from the first column chromatography *SG-1* were collected and evaporated. The concentrated fraction contained white yellowish suspended materials and a brown solution. After filtration, the obtained solid phase was washed with chloroform, followed with methanol. The chloroform solution gave two spots on TLC-4 with R_f values of 0.70 and 0.49. Therefore, the solution was then purified by silica gel column chromatography (*SG-6*) and eluted using petroleum ether-ethyl acetate (3:7), ethyl acetate 100% and ethyl acetate-

methanol (7:3) giving 14 fractions. Fractions 2-11 with an R_f value of 0.52 (positive with Anisaldehyde-H₂SO₄) were collected and purified via preparative-HPLC (*Prep-4*) producing 180 mg of **compound W2Et**. The structure of this compound was assigned to **dihydrofurane-2,5-dione**.

Fractions 17-24 of the first column chromatography *SG-1* with an R_f value of 0.52 (TLC-3) were collected and evaporated. The concentrated fraction was analyzed by analytical HPLC using a gradient mixture of methanol-water as a mobile phase. The chromatogram has two peaks at 11.4 min and 12.6 min, respectively. To isolate the compounds, the preparative HPLC (*Prep-2*) has been conducted using the same program as in analytical HPLC. The isolated compounds were then elucidated. Based on their spectroscopic data, the compound with a retention time of 11.4 min (Wu1a) was assigned to **daidzein-7-O-β-glucopyranose**, while the other compound having a retention time of 12.6 was assigned to **5-hydroxy-daidzein-7-O-β-glucopyranose**.

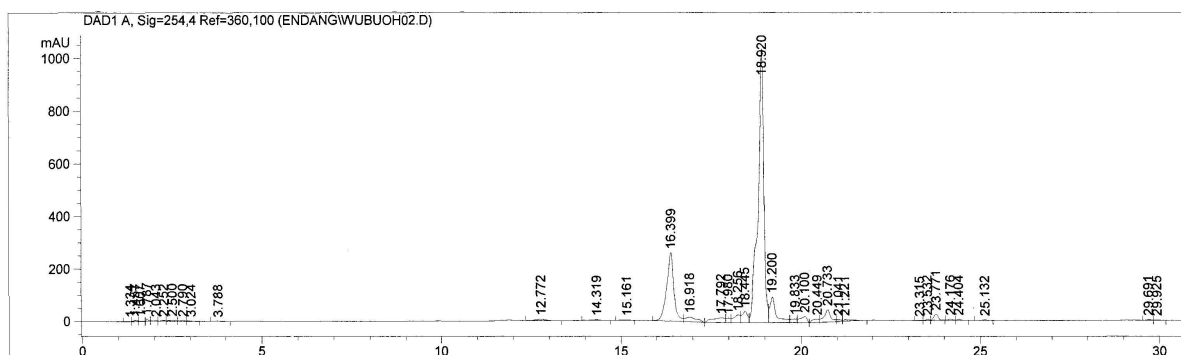


Note: detail elution systems of column chromatography, thin layer chromatography and preparative HPLC can be found on pages 32-34

Fig. II.6.2.1. The isolation scheme of compounds in the ethyl acetate extract

II.6.3. Compound isolation of the butanol extract

The isolation of compounds in butanol extract obtained from the scheme in Fig II.5.1 (p. 36) has been conducted according to the scheme in Fig.II.6.3.2. A small quantity of the butanol extract was analyzed by analytical HPLC using a gradient mixture of methanol-water as a mobile phase. The chromatogram has a main peak at 18.9 min (fig. II.6.3.1). The butanol extract was then purified through the semipreparative-HPLC using the same elution program to get 70 mg **compound WuBuOH** that was assigned to **(2-Butoxy-2,5-bis-(hydroxyl-methyl)-tetrahydrofuran-3,4-diol)**.

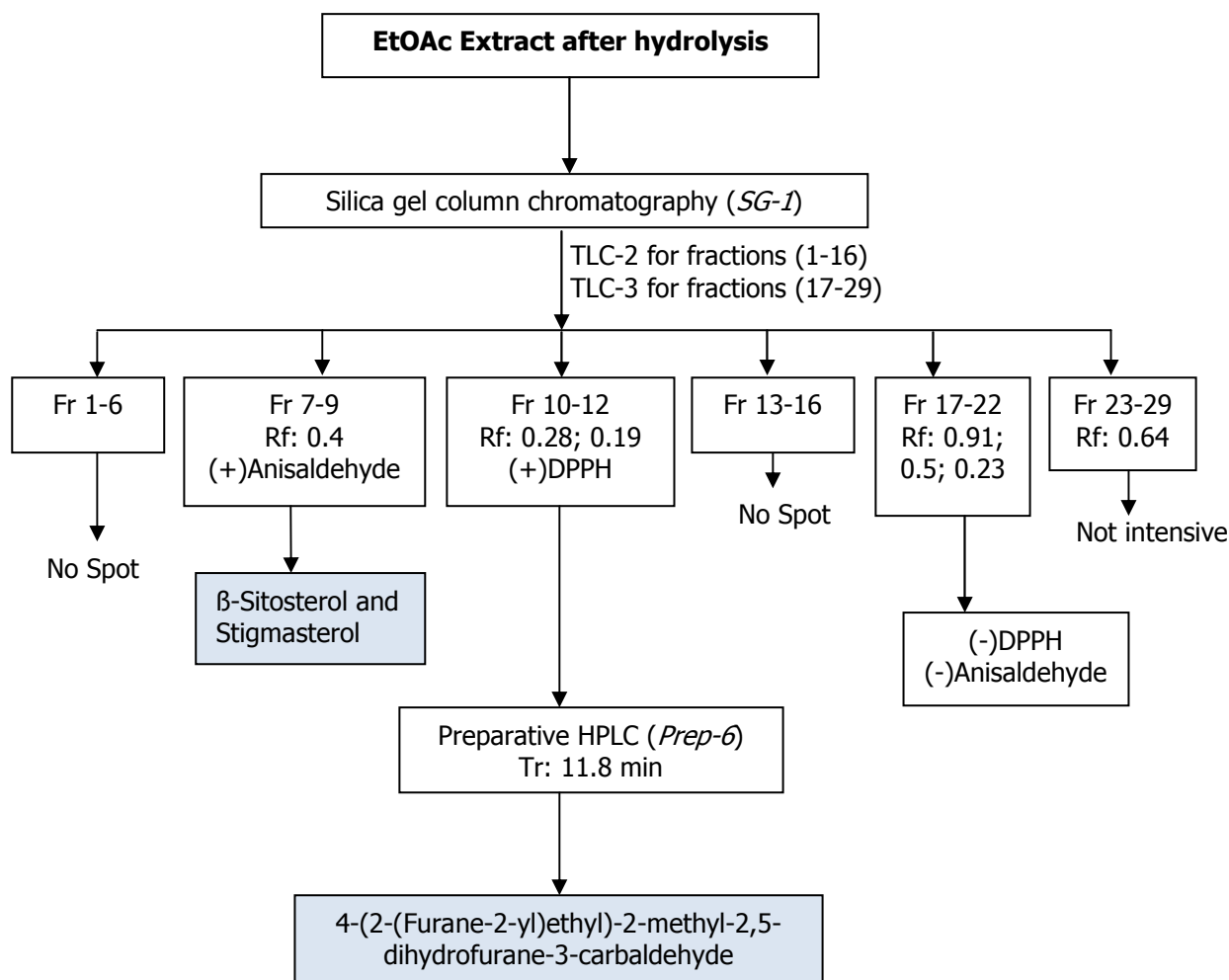


II.6.4. Compound isolation of the ethyl acetate extract after hydrolysis

The isolation of compounds in the ethyl acetate extract after hydrolyzation has been conducted to get the active compounds in aglycon forms. The procedure was performed according to the scheme II.6.4.1.

The ethyl acetate extract after hydrolyzation (10.08 gram) was subjected to silica gel column chromatography (*SG-1*) and eluted with a gradient mixture of petroleum ether-ethyl acetate and ethyl acetate-methanol producing 29 fractions of 100 ml eluents.

Fractions 10-12 from the silica column chromatography (*SG-1*) were collected and evaporated. The small quantity of the concentrated fraction was analyzed by analytical-HPLC using column C18 and a gradient mixture of methanol-water as a mobile phase. There was a main peak on the chromatogram at 11.8 min. Therefore, the concentrated fraction was purified via preparative-HPLC (*Prep-6*) using the same elution program obtained in analytical-HPLC. From this step, the **compound HWu10** (30 mg) was obtained and was identified as 4-(2-(furan-2-yl)ethyl)-2-methyl-2,5-dihydrofuran-3-carbaldehyde (C₁₂H₁₄O₃).



Note: detail elution systems of column chromatography, thin layer chromatography and preparative HPLC can be found on pages 32-34

Fig. II.6.4.1. The isolation scheme of compounds in the ethyl acetate after hydrolysis extract

II.7. Structure elucidation

The structure elucidation of the isolated compounds was based on spectroscopic data, including UV spectra, IR spectra, ^1H NMR (400.13 MHz) spectra, ^{13}C NMR (100.61 MHz) and mass spectra.

II.8. Determination of UV absorption activity

The isolated compounds were analyzed by HPLC using C18 as a stationary phase and a mixture of methanol-water as a mobile phase and UV detector. As a standard, p-aminobenzoic acid was used. By comparing AUC (area under the curve) value of the chromatograms of isolated compounds and p-aminobenzoic acid, the UV absorption activity can be described.

II.9. Determination of whitening activity

The step of determining the whitening activity consists of 5 parts, namely determination of total phenol contents, determination of total flavonoid contents, antioxidative activity, determination of tyrosinase inhibition and determination of tyrosinase inhibition type.

II.9.1. Determination of total phenol contents :

The amount of phenol compounds in the extracts was determined by the Folin-Ciocalteu colorimetric method as described by Singleton and Rossi (1965) with a slight modification. An aliquot (200 μ l) of the extracts or a standard solution of gallic acid (20, 40, 60, 80 and 100 ppm) was added to 5 ml volumetric flask, containing 2 ml of distilled deionised water. A reagent blank using deionised H₂O was prepared. 200 μ l of Folin-Ciocalteu phenol reagent was added to the mixture and shaken. After 5 min, 2 ml of 7% Na₂CO₃ solution was added to the mixture. The solution was diluted to 5 ml with deionised H₂O and mixed. After incubation for 90 min at room temperature, the absorbance was measured against a blank solution at wavelength 755 nm with an UV-Vis 1240 spectrophotometer. The total phenol content of the extracts was expressed as gallic acid equivalent (GAE) in mg/g extract. Determinations were carried out in triplicate.

II.9.2. Determination of total flavonoid contents :

Total flavonoid content was measured by the aluminium chloride colorimetric assay as described by Zhisen et al. (1999) with a slight modification. An aliquot (1 ml) of the extracts or standard solution of catechin (20, 40, 60, 80 and 100 ppm) was added to a 10 ml volumetric flask containing 4 ml of deionised H₂O and then 0.3 ml of 5% NaNO₂ was added. After 5 min, 0.3 ml of 10% AlCl₃

was added and followed by 2 ml of 1M NaOH at the sixth minutes. The total volume was made up to 10 ml with deionised H₂O. The solution was mixed well and the absorbance was measured against a blank at 500 nm (obtained from Figure III.15.1). Determinations were carried out in triplicate and calculated from a calibration curve obtained with catechin. The total flavonoid contents were expressed as mg catechin equivalents (CE)/g extract.

II.9.3. Antioxidative activity assay :

The antioxidative activities of crude extracts and isolated compounds were evaluated by measure the scavenging activity assay against DPPH radical with ascorbic acid as a positive control (IC₅₀ 7.24 ppm) according to Wang et al. (2006) and Dickson et al. (2007). 4 ml of 100 µM 1,1-Diphenyl-2-picrylhydrazyl (DPPH) solution in methanol was thoroughly mixed with 1 ml of a sample solution at various concentration. The mixture was kept in the dark for 30 minute. The absorbance of these solutions was measured at 517 nm. The concentration in ppm at which the absorbance decreases to 50% of its initial value was used as the SC₅₀ value for each test solution. All tests were done in triplicate.

II.9.4. Tyrosinase inhibition assay :

Tyrosinase inhibitory activity of crude extracts and isolated compounds was measured according to Hearing (1987) and Rangkadilok et al. (2006) with a slight modification, using mushroom tyrosinase as the enzyme, L-DOPA as a substrate and kojic acid as a positive control. An aliquot (50 µl) of samples in DMSO was mixed with 100 µl of 200 IU/ml of mushroom tyrosinase and 100 µl of phosphate buffered saline (pH 6.8). The assay mixture was pre-incubated at 37 °C for 10 min and then 100 µl of L-1,4-dihydroxyphenylalanine (L-DOPA) solution 7.6 mM was added. The reaction was then further incubated for 15 min at 37 °C. The dopachrome was measured at 475 nm using a UV/Vis spectrophotometer (A). As a blank, DMSO was used, being B. As a colour control test, phosphate buffer was used instead of the enzyme tyrosinase, being C. The percentage of tyrosinase inhibitions were expressed as a percentage of inhibition of tyrosinase activity and calculated as follows:

Tyrosinase inhibition (%) = {B-(A-C)}/B X 100%

Kojic acid was used as a standard inhibitor for tyrosinase. All tests were done in triplicate.

II.9.5. Determination of the tyrosinase inhibition type :

Determination of the tyrosinase inhibition type of isolated compounds was carried out according to Chen and Kubo (2002) with a little modification. Enzyme activity was determined at 25°C by following the increase in absorbance at 475 nm accompanying the oxidation of the substrate (L-DOPA). One unit (U) of enzymatic activity was defined as the amount of enzyme that increasing 0.001 absorbance at 475 nm in this condition. The progress of substrate reaction was applied to the current study of the inhibition kinetics of mushroom tyrosinase by isolated compounds. In this method, the mushroom tyrosinase (1.0 mg/mL in 0.1 M phosphate buffer pH 6.8) was first diluted 50 times with water, and then 50 µl of the solution was added to 200 µl of an assay substrate solution with 25 µl DMSO containing different concentrations of the isolated compounds. The increasing UV/Vis absorbance of this mixture was immediately measured at 475 nm for 20 min for detection of dopachromed formed. The concentrations of substrate solutions (DOPA solution in phosphate buffer pH 6.8) used in this experiment were 0.6; 0.8; 1.0; 1.5 and 2.0 mM. The substrate reaction progress curve was analysed to obtain the reaction rate constants (V) expressed in (unit/min). The reaction rate constant (V) was the slope of the plots of the absorption value (as Y axis) and time (as X axis). The Lineweaver-Burk plot, the correlation between $1/[\text{concentration of the DOPA solution}]$ versus $1/V$ in the presence of different concentrations of the isolated compounds, was performed to evaluate the type of the tyrosinase inhibition of the isolated compounds. The compound could be included in a competitive inhibitor group, if the increase of the compound concentration produced a series of lines with a common intercept on the $1/V$ axis but with different slopes. If the increase of the compound concentration produced a series lines with the same intercept on the $1/S$ axis with also different slopes, the compounds were assigned to be a non-competitive inhibitor.

CHAPTER III RESULTS AND DISCUSSIONS

III.1. Profil Chromatogram of bengkoang extracts

The TLC analysis of bengkoang extracts (petroleum extract, ethyl acetate, butanol and ethyl acetate after hydrolysis extract) has been carried out to find out how many compounds are in each extracts and their distribution. This step was necessary before doing isolation and determination. Figure III.1.1 displays the TLC chromatogram of bengkoang extract. The TLC was performed on silica gel with a mixture of petroleum ether-ethyl acetate (6:4) as an eluent and detected under UV light at 254 nm.

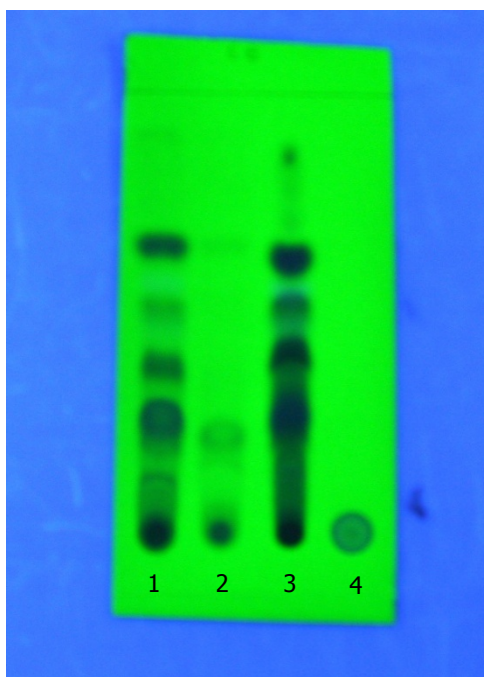


Fig. III.1.1 The TLC chromatogram. Spots from left to right were ethyl acetate extract (1), ethyl acetate after hydrolysis extract (2), petroleum ether extract (3) and butanol extract (3)

The chromatogram did not show any separation for the butanol extract and the ethyl acetate after hydrolysis extract. This result might be due to the fact that both extracts have only polar compounds. The ethyl acetate extract contained the same apolar compounds as found in the petroleum ether extract, but their concentrations were lower than in the petroleum ether. After purification and structure elucidation, the compounds could be assigned to 9,12-

having a retention time of 7.1 min wasn't further analyzed, because it had no antioxidative activity.

The HPLC analysis has been carried out with the butanol extract and also with the ethyl acetate after hydrolysis extract. The results can be seen in Figures III.1.3 and III.1.4.

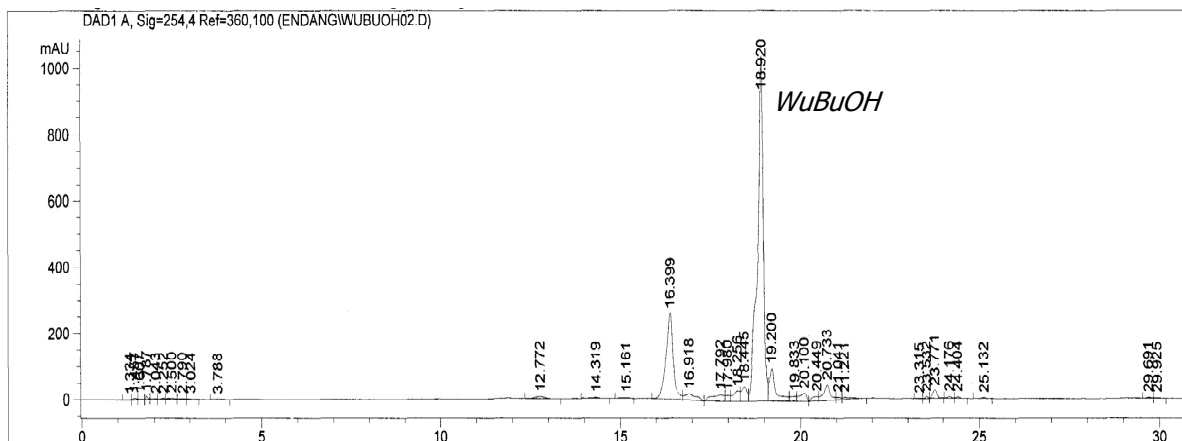


Fig. III.1.3. Chromatogram of the butanol extract obtained with a column Zorbax SB-C18 (25 cm, i.d. 0,46 cm, 5 µm particle size) using a gradient mixture methanol-water as a mobile phase and UV detection at 254 nm

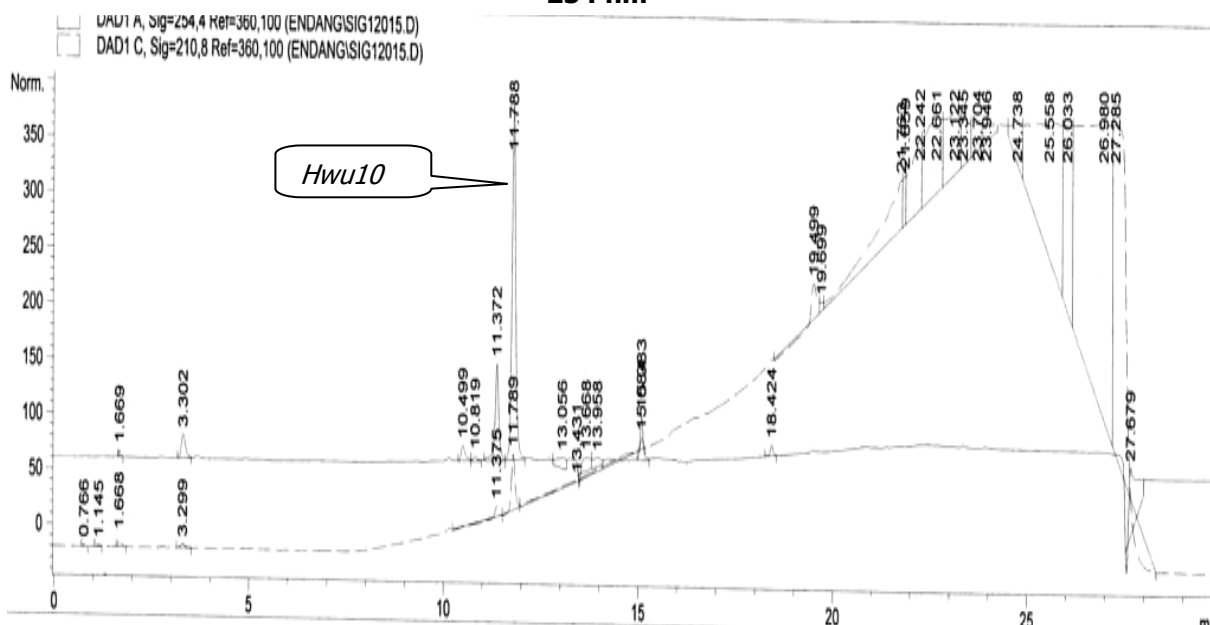


Fig.III.1.4. Chromatogram of the ethyl acetate after hydrolysis extract obtained with a column Zorbax SB-C18 (25 cm, i.d. 0,46 cm, 5 µm particle size) using a gradient mixture of MeOH-water as mobile phase and UV detection at 254 nm

Isolation and structure elucidation revealed 2-butoxy-2,5-bis(hydroxymethyl)-tetrahydrofuran-3,4-diol (WuBuOH) from the butanol

extract and the 4-(2'-(furane-2yl)-2-methyl-2,5-dihydrofurane-3-carbaldehyde (HWu10) in the ethyl acetate after hydrolysis extract. Table III.1.1 summarizes the isolated compounds of the bengkoang extract.

Table III.1.1 The chemical structure of isolated compounds

Code of compound	Chemical structure of compound
Petroleum ether extract	
101	9,12-Tricosandiene
102	Trilinolein
109a and 109b	β -Sitosterol and Stigmasterol
WuPe	Palmitic acid
G1	Hexadecyl pentanoate
Ethyl acetate extract	
C1	Daidzein
W2Et	Dihydrofurane-2,5-dione
Wu1a	Daidzein-7-O- β -glucopyranose
Wu3a	5-hydroxy-daidzein-7-O- β -glucopyranose
A182	(8,9)-Furanyl-pterocarpan-3-ol
n-butanol extract	
WuBuOH	2-Butoxy-2,5-bis(hydroxymethyl)-tetrahydrofurane-3,4-diol
Ethyl acetate after hydrolysis	
HWu10	4-(2-(Furane-2-yl)ethyl)-2-methyl-2,5-dihydrofurane-3-carbaldehyde

III.2. Compound 101 (9,12-Tricosandiene)

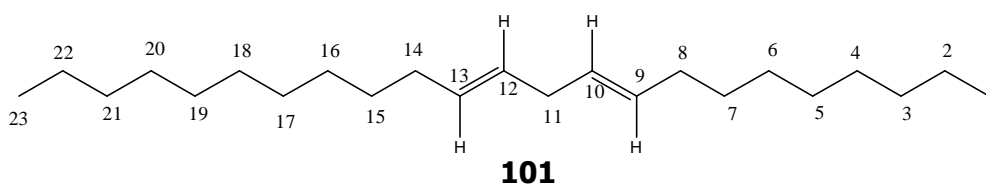


Fig. III.2.1. The chemical structure of compound 101 (9,12-Tricosandiene)

Compound (101) was obtained from petroleum ether extract as brown powder. The EI-MS of the compound 101 (Fig.III.2.2) shows a molecular ion signal at m/z 320. The molecular formula was confirmed as $C_{23}H_{44}$. In the UV spectrum, a maximum absorption was observed at 275 nm suggesting the presence of at least a C-C double bond. The IR spectrum indicated the presence of C-C double bond (1737 cm^{-1}), $-\text{CH}$ aliphatic groups (2921 cm^{-1}), and $-\text{CH}_2$ (1464 cm^{-1}).

The chemical shift values of ^1H NMR and ^{13}C NMR spectra in Table III.2.1 show typical signals of olefin hydrocarbon. The ^1H NMR spectrum displays a signal for double bond group (δ_{H} 5.12; q). The δ_{C} 128 and 131 ppm in the ^{13}C NMR spectrum are indicative of the double bonds. The presence of double bonds at C^9 and C^{12} was also deduced from the characteristic fragment ion peaks in the mass spectrum as in Figure III.2.2.

Table III.2.1. Chemical shift value (δ) in ppm of compound 101 measured in CDCl_3

C/H	δ H (ppm)	δ C (ppm)	δ^* C (ppm)
1	0.66 (3H, t)	14.11	14.10
2	1.18 (2H, m)	22.70	22.70
3	1.18 (2H, m)	31.52	31.80
4	1.18 (2H, m)	25.63	29.30
5	1.18 (2H, m)	29.35	29.70
6	1.18 (2H, m)	29.35	29.70
7	1.18 (2H, m)	29.79	29.90
8	1.92 (2H, q)	31.94	33.80
9	5.12 (1H, q)	130.20	132.10
10	5.12 (1H, q)	127.88	127.30
11	2.55 (2H, t)	34.12	37.60
12	5.12 (1H, q)	127.88	127.30
13	5.12 (1H, q)	130.20	132.10
14	1.92 (2H, q)	31.94	33.80
15	1.18 (2H, m)	29.79	29.90
16	1.18 (2H, m)	29.35	29.70
17	1.18 (2H, m)	29.35	29.70
18	1.18 (2H, m)	29.79	29.60
19	1.18 (2H, m)	29.79	29.60
20	1.18 (2H, m)	25.63	29.30
21	1.18 (2H, m)	31.52	31.80
22	1.18 (2H, m)	22.70	22.70
23	0.66 (3H, t)	14.11	14.10

Note : δ^* C are estimated values using ChemDraw Ultra 9.0 Software

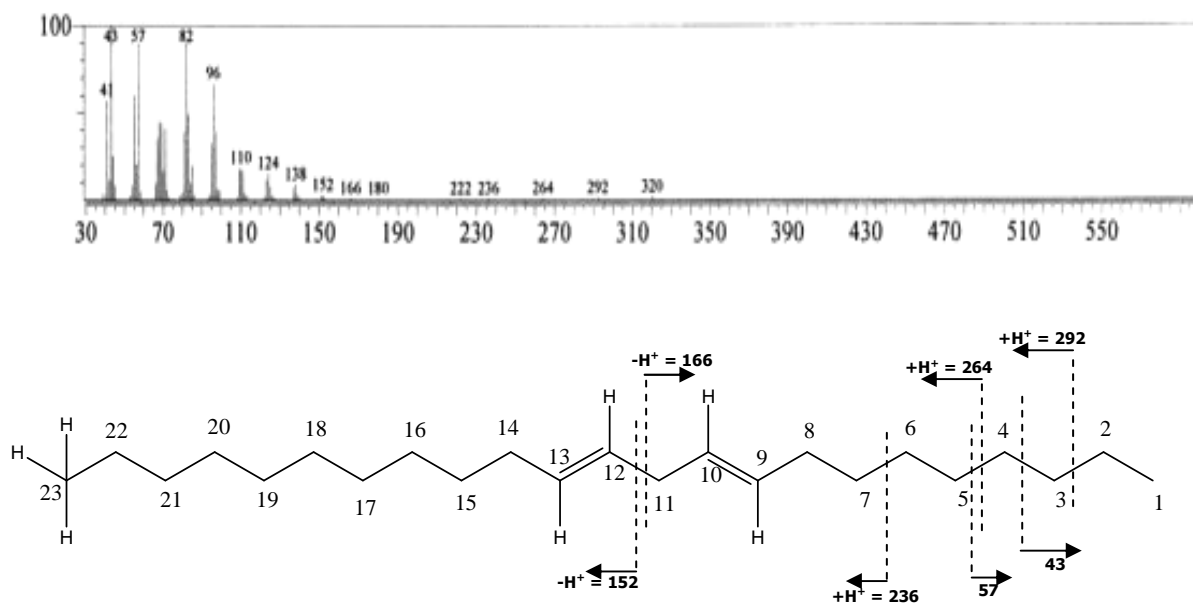


Fig. III.2.2. Mass fragmentation patterns of compound 101

These observations were further confirmed by the analysis of the HMQC, HMBC and COSY experiments. The COSY experiments (Fig.III.2.2) show the expected correlations between the protons H⁸ at δ 1.92 ppm with H⁹ at δ 5.12 ppm, H¹³ at δ 5.12 ppm with H¹⁴ at δ 1.92 ppm, H¹³ at δ 5.12 ppm with H¹² at δ 5.12 ppm, H⁷ at δ 1.18 ppm with H⁸ at δ 1.92 ppm, H¹⁴ at δ 1.92 ppm with H¹⁵ at δ 1.18 ppm. Based on the COSY data, it could be concluded that the position of two double bonds is separated by one $-\text{CH}_2$ moiety.

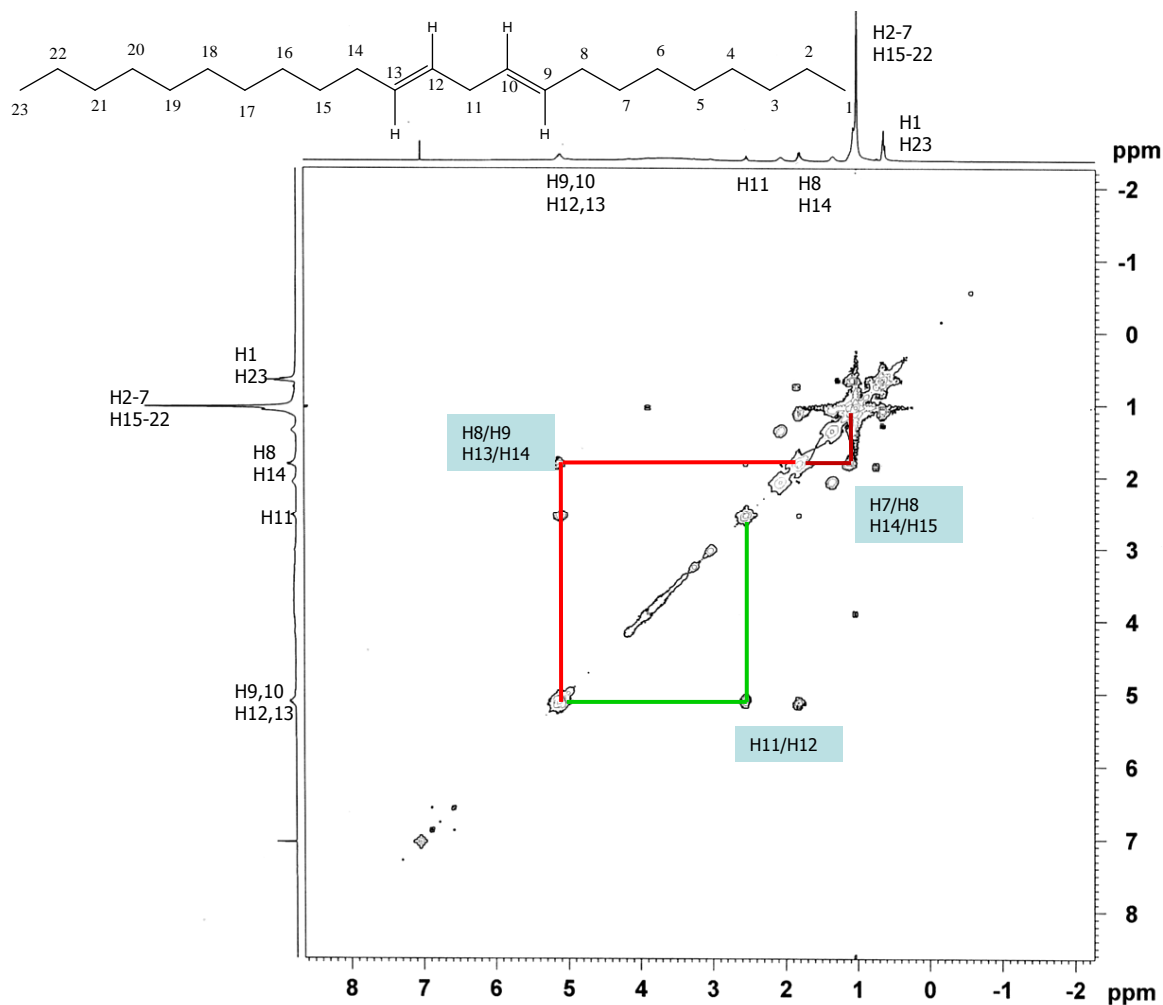


Fig.III.2.3. COSY diagram of compound 101

The HMBC diagram (Fig.III.2.4) reveals significant correlations between H^{10} and C^8 , H^{12} and C^{14} , H^{11} and C^9 , H^{11} and C^{13} , H^3 and C^1 , H^{21} and C^{23} , H^8 and C^9 , H^{14} and C^{13} , H^1 and C^3 , H^{23} and C^{21} . The selected HMBC correlation of compound 101 can be found in Figure III.2.5. All of the data above proved the structure of 101 as 9,12-tricosandiene.

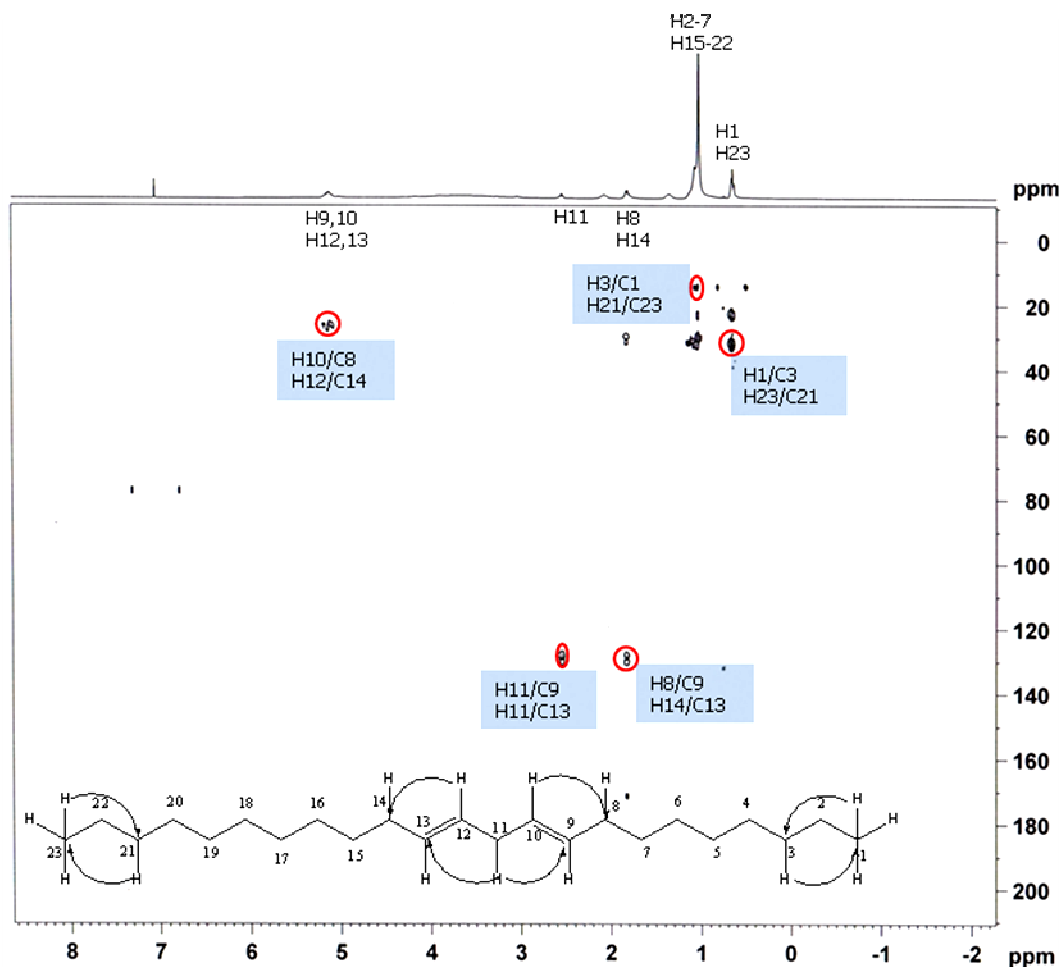


Fig. III.2.4. HMBC diagram of compound 101

III.3. Compound 102 (Trilinolein)

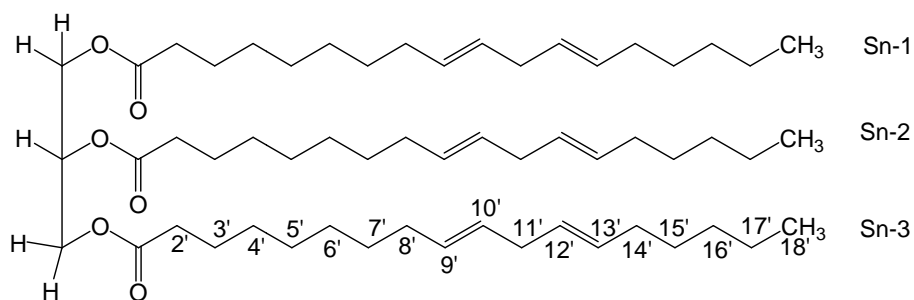


Fig. III.3.1. Chemical structure of compound 102 (Trilinolein)

Compound 102 was isolated as yellowish oil. The UV spectrum displays a maximum absorption at 247 nm. The EI-MS gives a molecular ion peak at m/z 879 corresponding to the molecular formula $C_{57}H_{98}O_6$. The IR spectrum shows a

signal at 1742 cm^{-1} indicating the presence of -C=O group, 1162 cm^{-1} indicating an ester group and 1647 cm^{-1} indicating a C-C double bond.

Table III.3.1. ^1H NMR and ^{13}C NMR spectroscopic data of compound 102 measured in CDCl_3

C/H	δH (ppm)	$\delta^*\text{H}$ (data base)	δC (ppm)	$\delta^*\text{C}$ (data base)
1a	4.27 (dd)	4.295	62.90	62.14
1b	4.12 (dd)	4.147	62.09	62.14
2	5.25 (m)	5.270	68.89	69.00
3a	4.27 (dd)	4.295	62.90	62.14
3b	4.12 (dd)	4.147	62.09	62.14
1'	-	-	173.33	173.13
2'	2.29 (t)	2.315	34.28	34.05
3'	1.58 (m)	1.610	25.07	24.87
4'	1.25 (m)	1.301	29.24	29.12
5'	1.25 (m)	1.301	29.24	29.12
6'	1.25 (m)	1.301	29.24	29.12
7'	1.29 (m)	1.360	29.86	29.63
8'	2.05 (q)	2.049	27.32	27.22
9'	5.32 (m)	5.351	130.11	129.99
10'	5.32 (m)	5.351	128.21	128.12
11'	2.78 (t)	2.769	25.73	25.68
12'	5.32 (m)	5.351	128.03	127.95
13'	5.32 (m)	5.351	130.34	130.21
14'	2.05 (q)	2.049	27.32	27.22
15'	1.29 (m)	1.361	29.86	29.63
16'	1.25 (m)	1.301	31.45	31.54
17'	1.25 (m)	1.301	22.62	22.58
18'	0.87 (m)	0.889	14.27	14.04

Note : δ^* is obtained from data base SDBS AIST Japan

The ^{13}C NMR spectrum of compound 102 in Table III.3.1 showed six double bonds (δ_{C} 128.21 ppm and δ_{C} 130.11 ppm) and three quaternary carbon atoms (δ_{C} 173.33; 172.97; 173.33 ppm). The ^1H NMR spectrum of compound 102 showed a signal at δ_{H} 5.32 ppm indicating the presence of H double bonds. Signals at δ_{H} 4.27 and 4.12 ppm indicated protons that were close with the atom oxygen probably in the glycerol chain.

The COSY, HMQC and HMBC experiments allowed the identification of all protons of the compound and the corresponding carbons. The COSY correlations (Fig. III.3.2) between H^8 and H^9 ; $\text{H}^{13'}$ and $\text{H}^{14'}$; H^2 and H^1 ; H^2 and H^3 ; H^{11} and $\text{H}^{12'}$; $\text{H}^{11'}$ and $\text{H}^{10'}$; $\text{H}^{14'}$ and $\text{H}^{15'}$; H^8 and H^7 ; $\text{H}^{3'}$ and $\text{H}^{2'}$ and $\text{H}^{17'}$ and $\text{H}^{18'}$ supported the compound 102 as trilinolein.

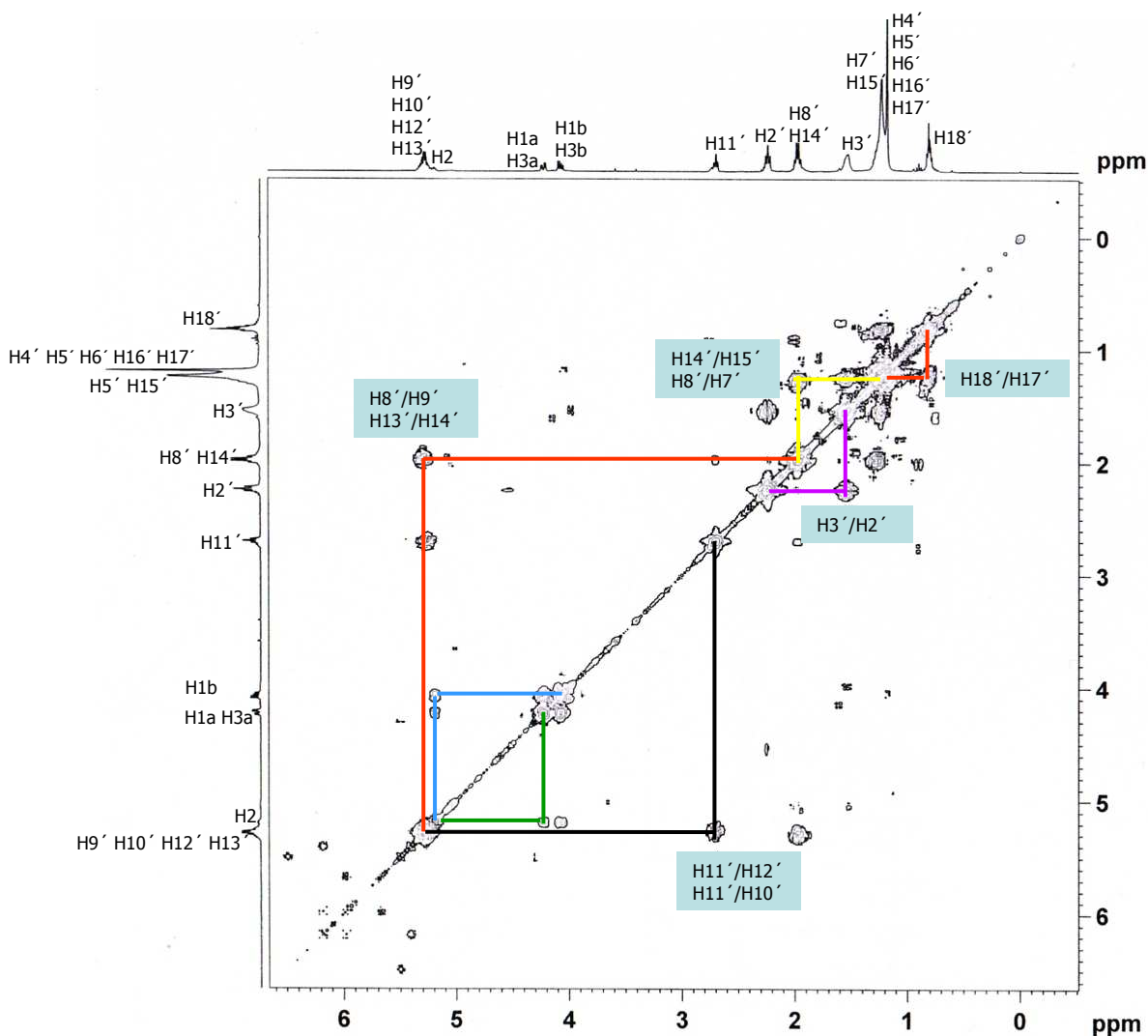
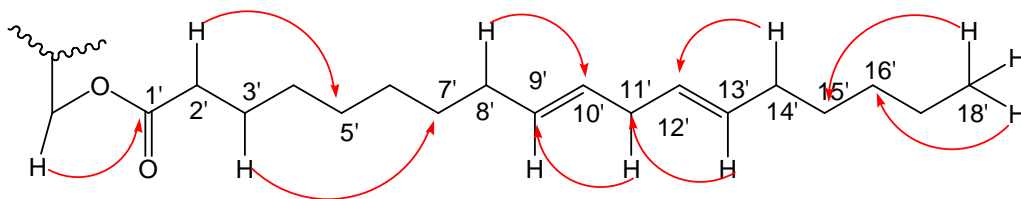


Fig. III.3.2. COSY diagram of compound 102 measured in CDCl_3

Some of the ^1H - ^{13}C -long range correlations observed in the HMBC diagram (Fig. III.3.3) confirmed that the structure of 102 was trilinolein or 1,2,3-propanetriyl-tris(cis-9,12-octadecadienoate). All of these data proved the structure of the compound 102 as trilinolein.



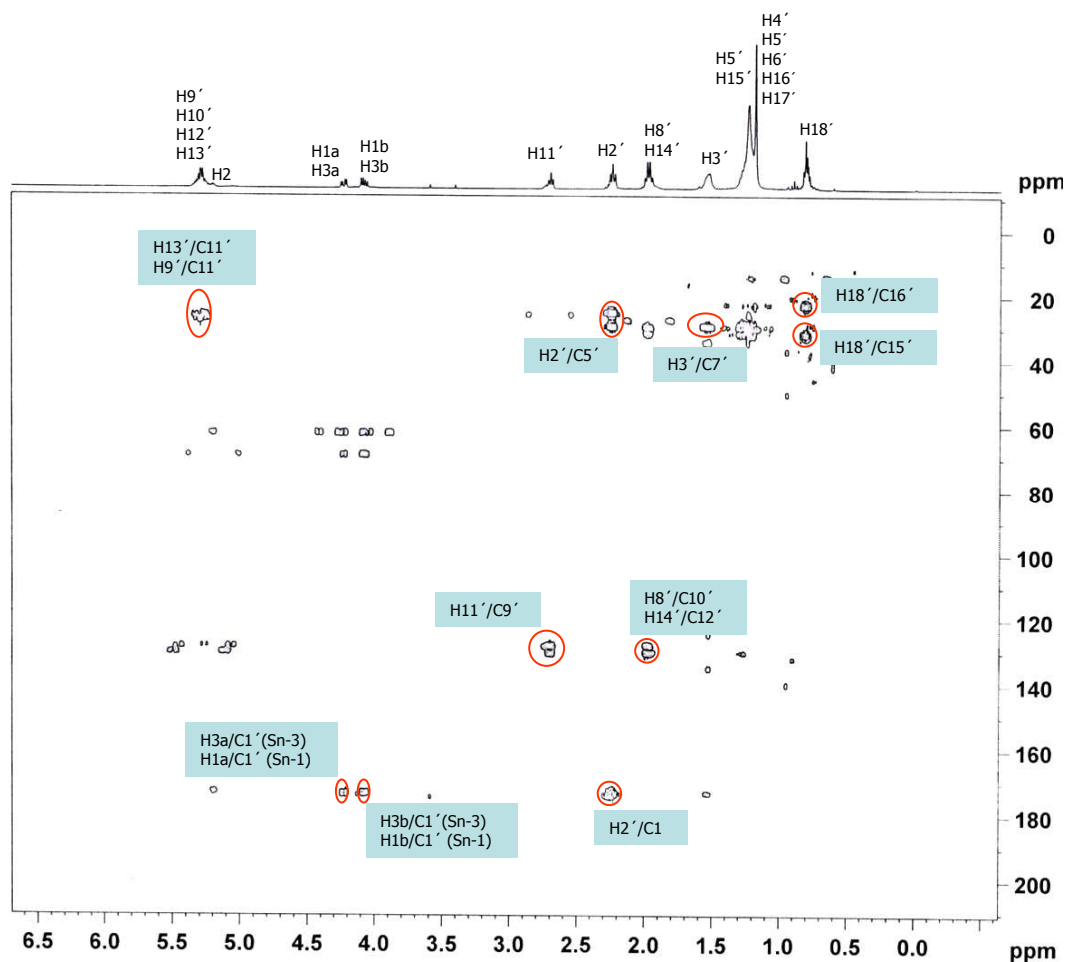


Fig. III.3.3. HMBC diagram of compound 102

III.4. Compound 109a and 109b (β -sitosterol and stigmasterol)

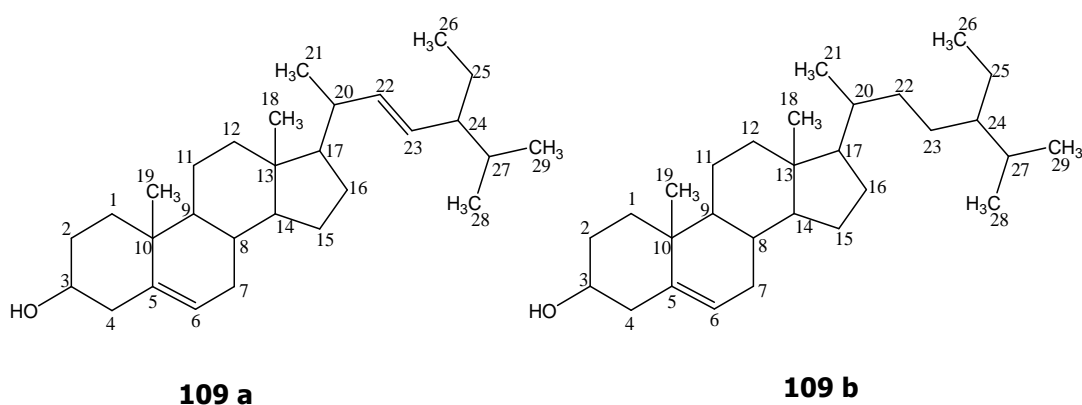


Fig. III.4.1. The chemical structure of compounds 109a and 109b

The mixture of compounds 109a and 109b has been isolated from fractions 8, 9, 10 of the petroleum ether extract as white needle crystals having a melting point of 136-139 °C. UV maximum absorptions were found at 245 nm

and 291 nm indicating the presence of a chromophor, such as a C-C double bond. The band at 1699 cm^{-1} of the IR spectrum indicated the presence of C=C or C=O. Additionally the IR spectrum showed 3364 cm^{-1} (-OH group), 2925 cm^{-1} (-C-H aliphatic group), 1463 cm^{-1} (-CH group), 1375 cm^{-1} (-CH group) and 1051 cm^{-1} (-C-O-C group).

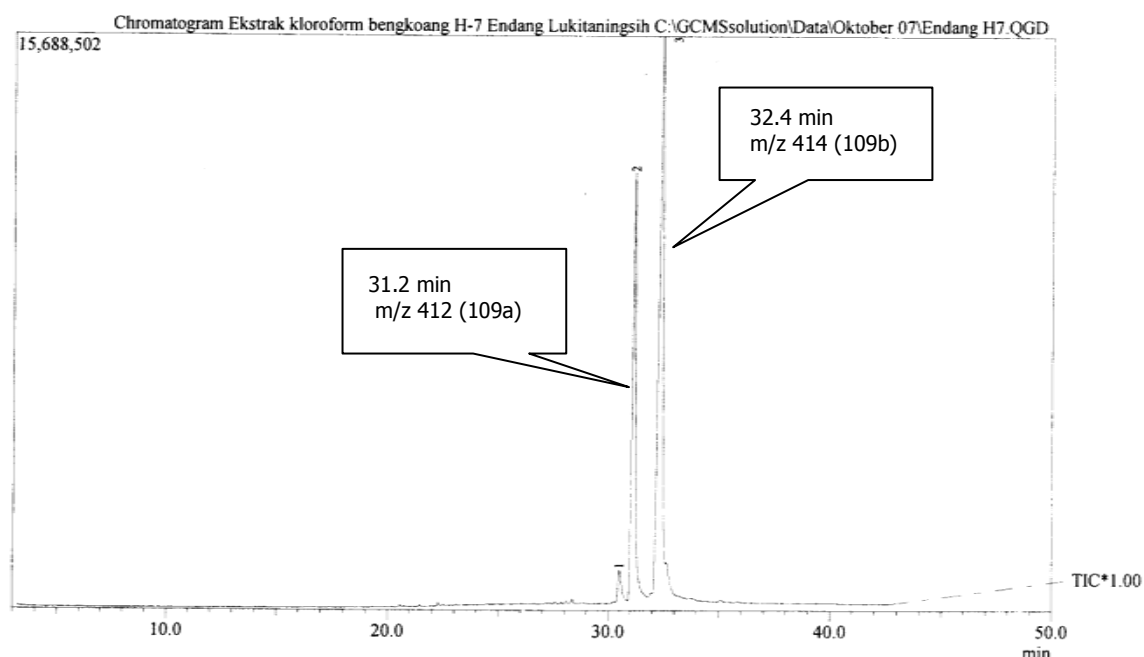


Fig. III.4.2. GC/MS chromatogram of the mixture of compound 109a and 109b

The GC/MS chromatogram in Figure III.4.2 shows two peaks with retention times of 31.2 and 32.4 min, corresponding to the molecular ion peaks at m/z 412 and 414, respectively. They are consistent with the molecular formula $C_{29}H_{48}O$ (e.g. stigmasterol) and $C_{29}H_{50}O$ (e.g. β -sitosterol).

The presence of the hydroxyl group was supported by the strong loss of 18 mass units in both EI mass spectrums. The existence of a double bond of C-C was represented in the ^{13}C -NMR by four downfield signals at δ 140.9 ppm (quarternary carbon), 121.9 ppm (CH), 129.4 ppm (CH) and 138.5 ppm (CH). The carbon chemical shift data of 109a was similar to 109b, except δ C^{22} and C^{23} . The carbon chemical shifts of C^{22} from 109a and 109b were 33.9 ppm and 138.5 ppm, respectively. Meanwhile the carbon chemical shifts of C^{23} of 109a and 109b were 28.3 ppm and 129.4 ppm, respectively. All the carbon chemical shift data of the ^{13}C NMR spectrum (Table III.4.1) were in a close agreement with those of stigmasterol and β -sitosterol in literature reported (Kovganko et al. 2000) and also with the database in SDBS AIST Japan.

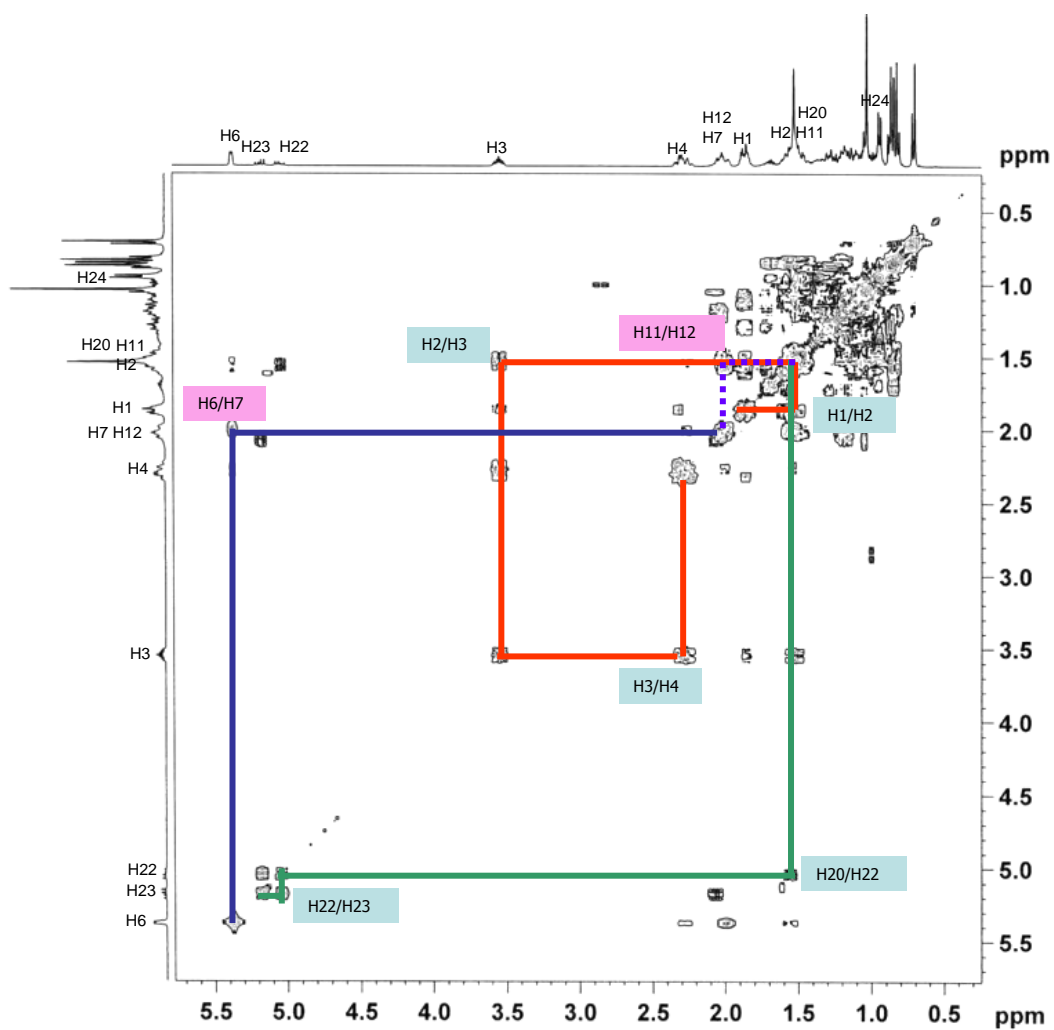


Fig. III.4.3. COSY diagram of the mixture of compound 109a and 109b

Tabel III.4.1. ^1H NMR and ^{13}C NMR spectroscopic data of the mixture of compound 109a and 109b measured in CDCl_3

C	Compound 109a (Stigmasterol)			Compound 109b (β -sitosterol)		
	δH	δC	δC^*	δH	δC	δC^*
1	1.84 (1H, m); 1.30 (1H, m)	37.4	37.2	1.84 (1H, m); 1.30 (1H, m)	37.4	37.3
2	1.50 (2H, m)	28.4	31.3	1.50 (2H, m)	28.4	31.6
3	3.50 (3H, m)	71.9	70.3	3.50 (3H, m)	71.9	71.7
4	2.27 (2H, m)	42.5	42.0	2.27 (2H, m)	42.5	42.3
5	-	140.9	141.6	-	140.9	140.8
6	5.34 (1H, dd)	121.9	120.2	5.34 (1H, dd)	121.9	121.6
7	1.98 (2H, m)	32.0	31.6	1.98 (2H, m)	32.0	31.9
8	1.70 (1H, m)	32.1	31.8	1.70 (1H, m)	32.1	31.9
9	0.92 (1H, m)	50.3	50.1	0.92 (1H, m)	50.3	50.2
10	-	36.7	36.3	-	36.7	36.5
11	1.50 (2H, m)	20.0	20.8	1.50 (2H, m)	20.0	21.1
12	2.01 (2H, m)	39.9	39.4	2.01 (2H, m)	39.9	39.8
13	-	46.0	42.4	-	46.0	42.3
14	1.10 (1H, m)	56.9	56.5	1.10 (1H, m)	56.9	56.8
15	1.09 (1H, m), 1.70 (1H, m)	23.2	23.9	1.09 (1H, m), 1.70 (1H, m)	23.2	24.3
16	1.70 (2H, m)	26.3	28.1	1.70 (2H, m)	26.3	28.3
17	1.20 (1H, m)	56.2	55.9	1.20 (1H, m)	56.2	56.1
18	0.68 (3H, s)	12.0	11.8	0.68 (3H, s)	12.0	11.9
19	1.01 (3H, s)	19.2	19.1	1.01 (3H, s)	19.2	19.4
20	1.28 (1H, m)	40.6	40.3	1.28 (1H, m)	40.6	36.2
21	0.92 (3H, s)	19.6	20.6	0.92 (3H, s)	19.6	18.8
22	5.01 (1H, dd)	138.5	137.7	1.20 (2H, m)	33.90	33.9
23	5.16 (1H, dd)	129.4	129.3	1.7 (2H, m)	28.30	26.1
24	1.50 (2H, m)	51.4	50.6	1.50 (2H, m)	51.4	45.9
25	1.20 (2H, m)	24.5	24.7	1.2 (2H, m)	24.5	23.1
26	0.83 (3H, d)	12.3	11.9	0.83 (3H, d)	12.3	12.3
27	1.90 (1H, m)	29.3	31.50	1.90 (1H, m)	29.3	29.2
28	0.83 (3H, d)	18.9	18.90	0.83 (3H, d)	18.9	19.1
29	0.83 (3H, d)	21.2	21.04	0.83 (3H, d)	21.2	19.8

Note : δC^* is data base of carbon chemical shift from SDBS AIST Japan

The downfield signal in the ^1H -NMR spectrum at δ 5.34 (1H, dd) was due to an olefinic proton at C^6 and a methine proton at C^3 was represented by multiplet signal at 3.50 (1H, m). The presence of a pair of doublets at δ 5.01 and δ 5.16 was due to the sp^2 methine protons at C^{22} and C^{23} in molecule 109a. The existence of six methyl signals was also noted at δ 0.68 ($\text{H}^3\text{-C}^{18}$), 1.01 ($\text{H}^3\text{-C}^{19}$), 0.92 ($\text{H}^3\text{-C}^{21}$), 0.83 ($\text{H}^3\text{-C}^{28}$), 0.83 ($\text{H}^3\text{-C}^{29}$).

The COSY correlations between H^6 and H^7 ; H^{22} and H^{23} ; H^3 and H^4 ; H^{11} and H^{12} ; H^1 and H^2 ; H^2 and H^3 ; H^{20} and H^{22} supported the stigmasterol and β -sitosterol (Fig. III.4.3). Some of the ^1H - ^{13}C -long range correlations (Figure

III.4.4) observed in the HMBC diagram confirmed that the structures of 109a and 109b were stigmasterol and β -sitosterol.

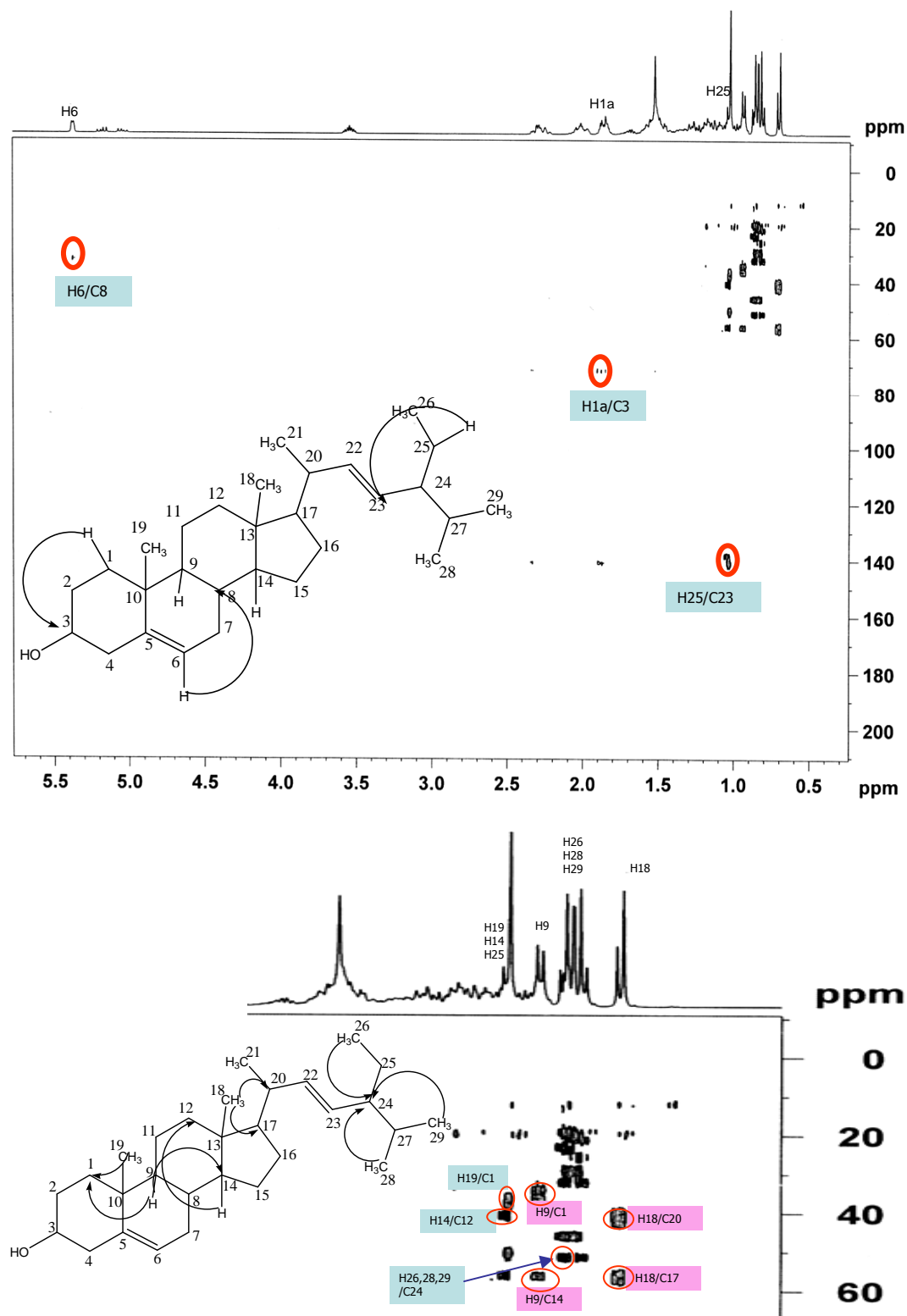


Fig. III.4.4. HMBC diagram of the mixture of compounds 109a and 109b

The mass fragmentation pattern of the 109a is displayed in Figure III.4.5. The molecular ion of 109a was observed at m/z 412. The loss of water from 109a was indicated by the presence of a fragment ion at m/z 394. The subsequent fragment at m/z 379 might be due to the loss of a methyl group. The signal at m/z 271 was the characteristic of the stigmasterol fragmentation due to the loss of side chain followed by the loss of two hydrogen atoms.

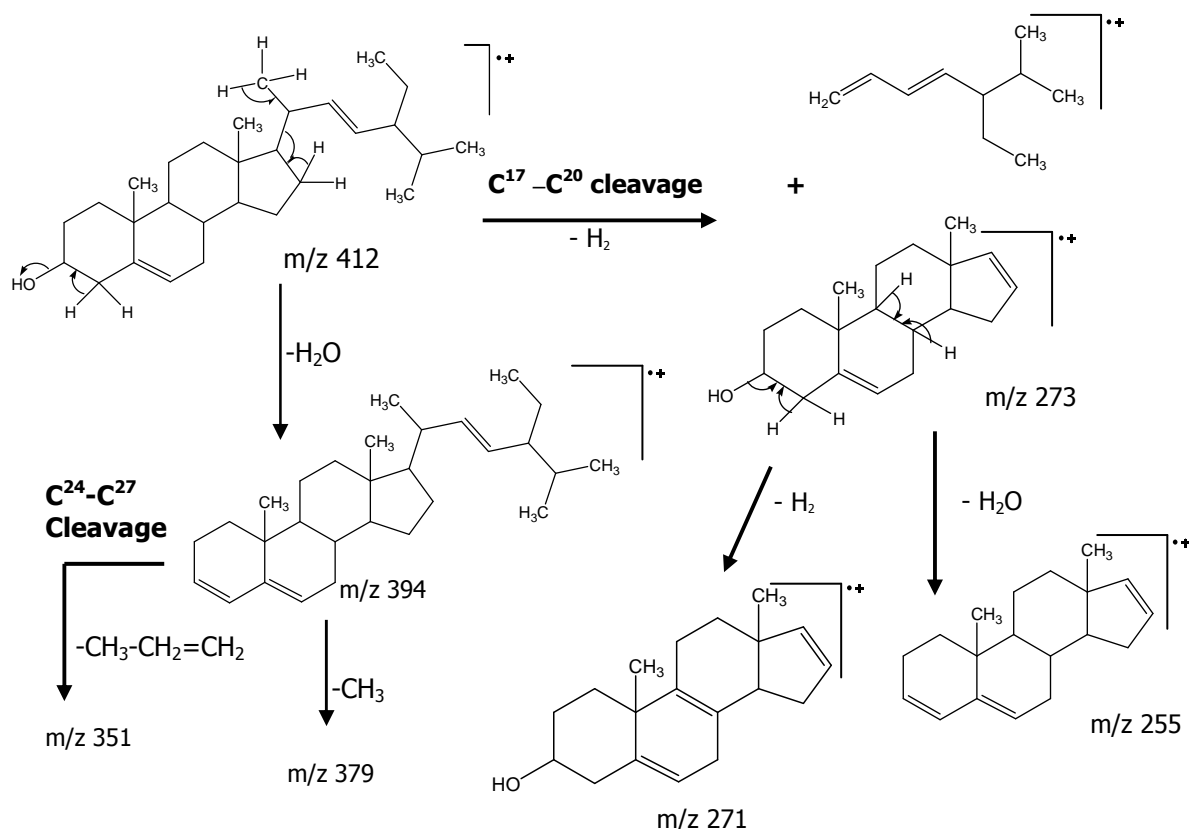


Fig. III.4.5. Mass fragmentation pattern of compound 109a

The mass fragmentation pattern above was in accordance with previously paper. Chaves et al. (2004) found in GC/MS the fragments with m/z value of 412 (M^+), 271 and 273. Based on the above fragmentation, this substance 109a was identified as stigmasterol.

The Figure III.4.6 displays a mass fragmentation pattern of 109b having a molecular ion m/z 414. The fragment ions at m/z 396 and 381 were due to the loss of water and followed by a methyl group from the molecular ion. The characteristic observed in the mass spectrum of 109b was the presence of a fragment ion peak at m/z 273. This signal was in a close agreement with the loss of side chain caused by the fission of $C^{17}-C^{20}$ bond. This was further fragmented producing water. From this process, the signal at m/z 255 was observed.

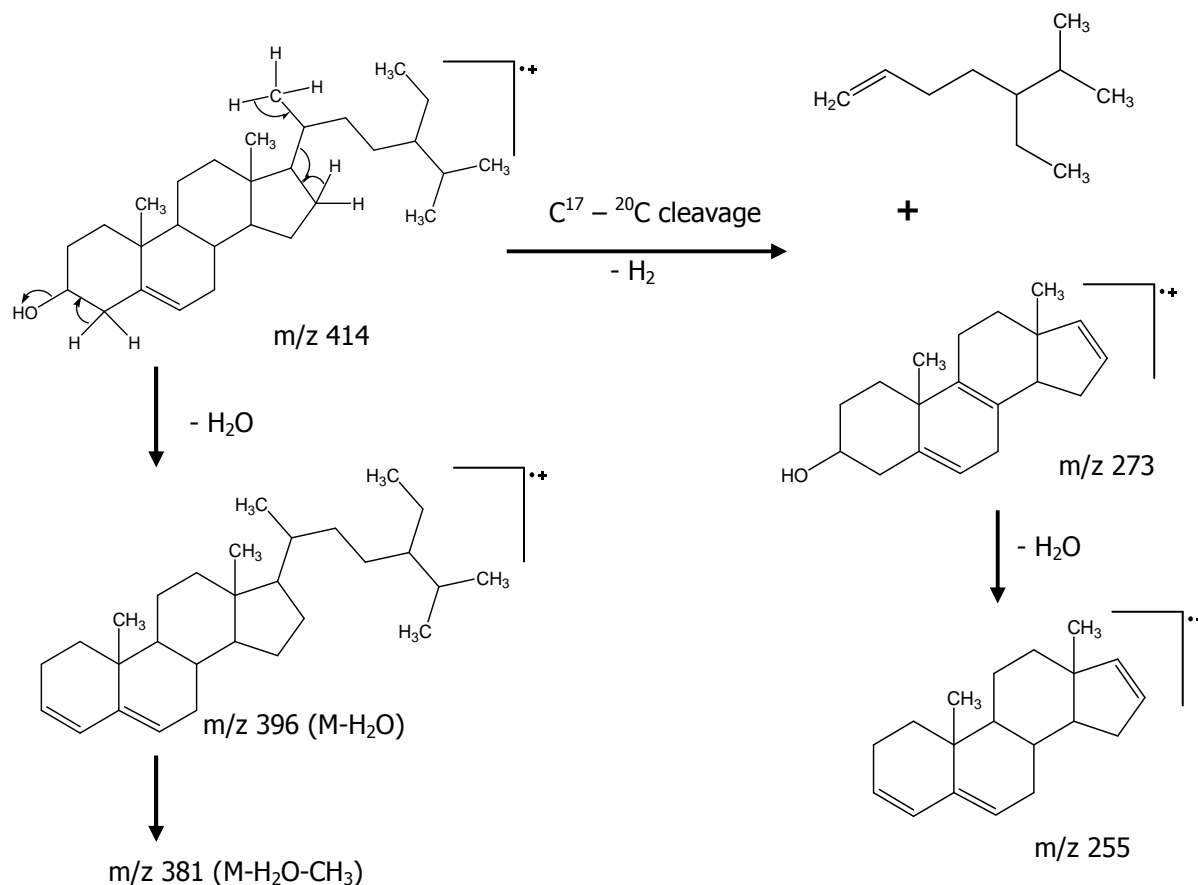


Fig. III.4.6. Mass fragmentation pattern of compound 109b

The fragmentation pattern above is in accordance to Zhang (2005): β -sitosterol in acid solution produces positive signals at m/z 382 and 397 with intensities 52 and 100, respectively. The signal at m/z 397 was assigned to $(M+H^+ - H_2O)$ and the signal at m/z 382 to $(M+H^+ - H_2O - CH_3)$. In addition, Berezin et al. (2004) and Huang et al. (2007) have investigated the fragmentation of β -sitosterol and stigmastrol using HPLC-MS equipped with APCI. The result showed that β -sitosterol and stigmastrol were protonated by a reactive species in the plasma of ion source. β -Sitosterol had an exact mass of 414.39, which became 397.38 after protonation and loss of water. While stigmastrol had an exact mass of 412.41 which became 395.4 after protonation and loss of water.

All these spectroscopy data proved the structure of the substance 109b as β -sitosterol. The concentration ratio of stigmastrol and β -sitosterol from this fraction was 35 : 65 (Fig. III.4.2).

III.5. Compound G1 (Hexadecyl pentanoate)

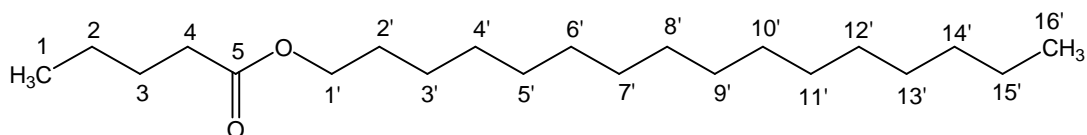


Fig. III.5.1. The chemical structure of compound G1 (hexadecyl pentanoate)

Compound G1 was isolated from the petroleum extract as yellowish oil. In IR spectrum a signal at 2925 cm^{-1} was observed due to aliphatic C-H stretching. The peak at 1739 cm^{-1} (C=O) and 1175 cm^{-1} (C-O) indicates the presence of the ester group. In ^1H NMR spectrum, the downfield δ at 4.07 ppm appears as a triplet due to $-\text{COOCH}_2\text{CH}_2-$ group while the signal δ at 2.28 as a triplet appears due to $-\text{CH}_2-\text{COO}-$. The complete data of ^1H NMR and ^{13}C NMR of the compound G1 can be found in Table III.5.1. The result of ESI-LCMS experiment which can be found in Figure III.5.2 shows the peak at m/z 327.7 due to ($M+1$) which is confirmed as $\text{C}_{21}\text{H}_{42}\text{O}_2$. The peak at 284 was due to the loss of C_3H_7 (39).

Table III.5.1. NMR spectroscopic data of compound G1 measured in CDCl_3

C/H	δ H (ppm)	δ^* H (ppm)	δ C (ppm)
1	0.81	0.85	14.06
2	1.23	1.25	22.64
3	1.56	1.62	24.85
4	2.28	2.32	34.06
5	-	-	173.88
1'	4.07	4.07	65.01
2'	1.56	1.62	24.85
3'	1.23	1.37	29.08
4'	1.23	1.37	29.08
5'	1.18	1.27	29.65
6'	1.18	1.27	29.65
7'	1.18	1.27	29.65
8'	1.18	1.27	29.65
9'	1.18	1.27	29.65
10'	1.18	1.27	29.65
11'	1.18	1.27	29.65
12'	1.18	1.27	29.65
13'	1.18	1.27	29.65
14'	1.18	1.27	31.88
15'	1.18	1.27	22.64
16'	0.81	0.85	14.06

Note : δ^* H was obtained from Sharma, 2008

The COSY experiments (Fig. III.5.2) show the expected correlations between the protons of H¹-H², H^{15'}-H^{16'}, H³-H², H^{2'}-H^{3'} and H³-H⁴.

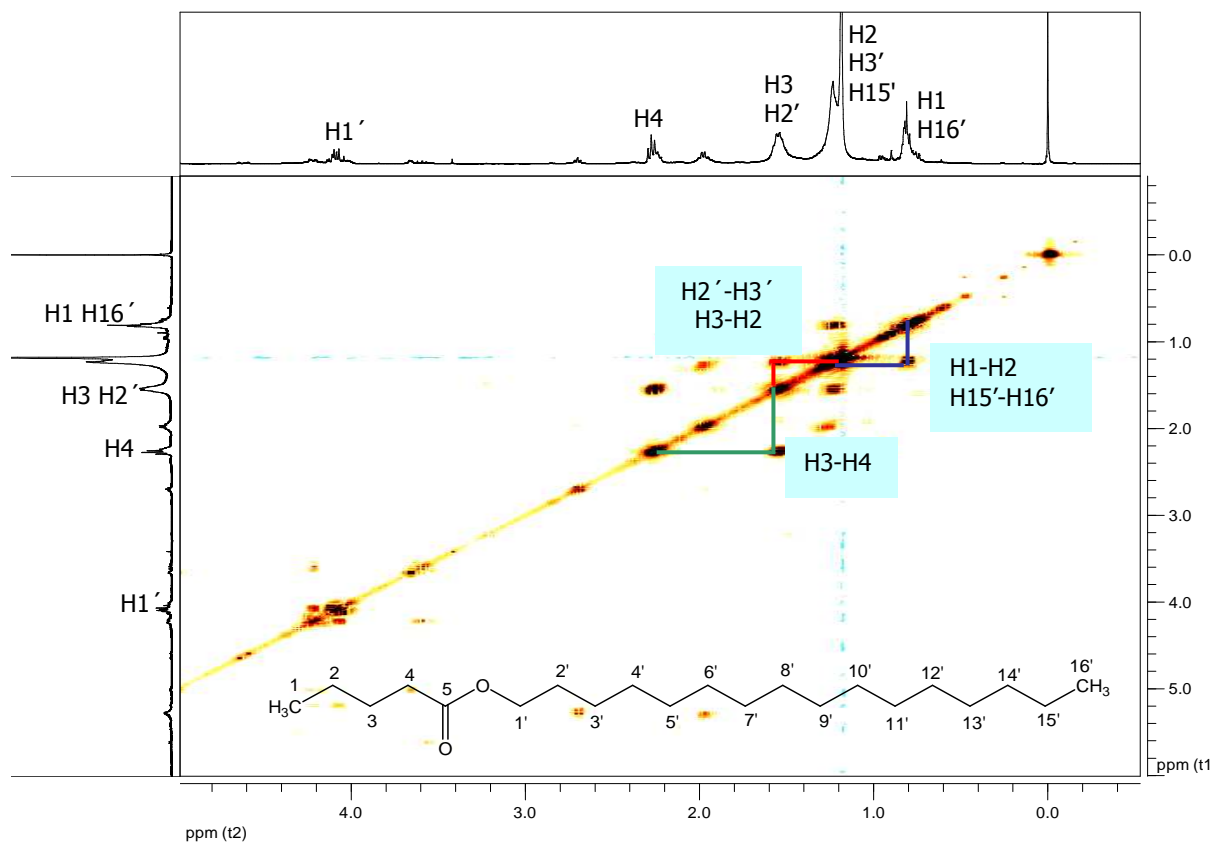


Fig. III.5.2. The COSY diagram of compound G1

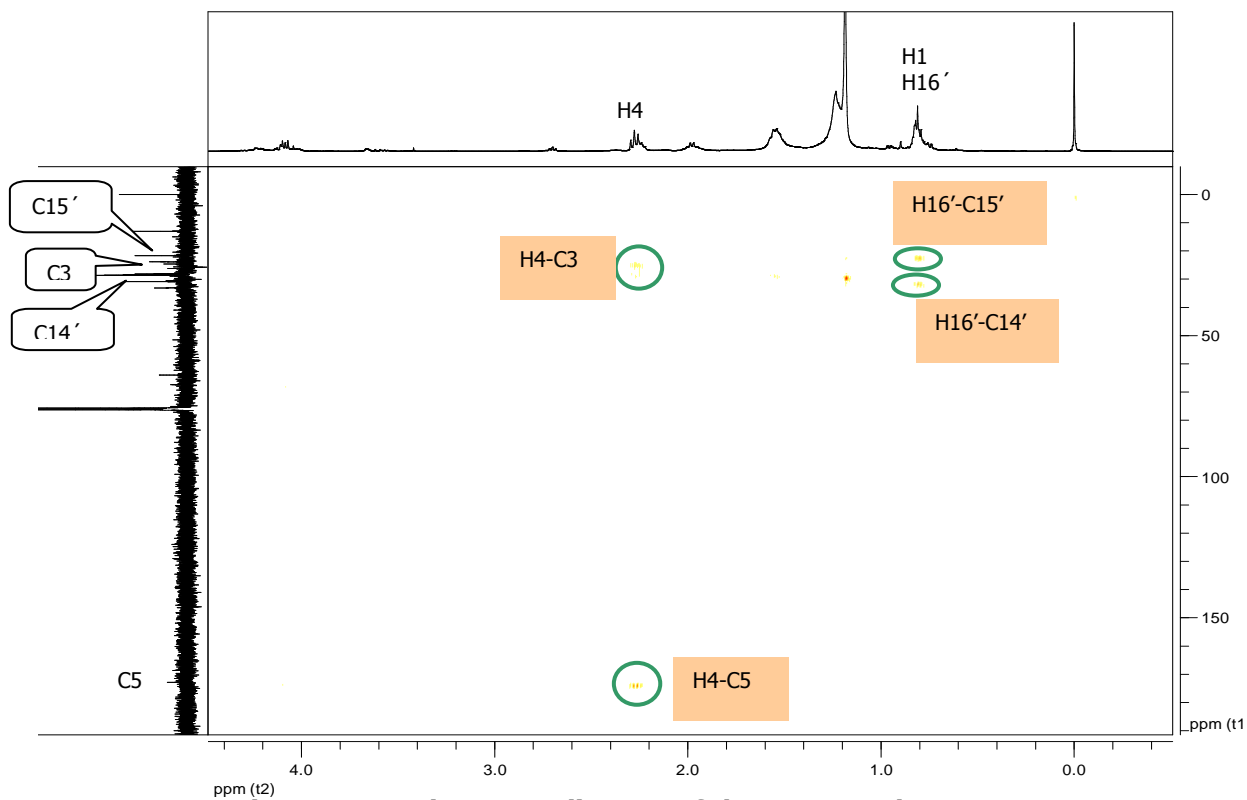


Fig. III.5.3a. The HMBC diagram of the compound G1

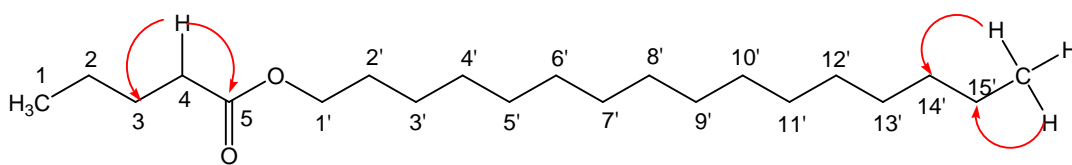


Fig. III.5.3b. The ^1H - ^{13}C -long range correlation of the compound G1

The HMBC diagram (Fig. III.5.3a) above reveals significant correlations between $\text{H}^{16'}$ and $\text{C}^{15'}$, $\text{H}^{16'}$ and $\text{C}^{14'}$, H^4 and C^3 and H^4 and C^5 .

Figure III.5.4 displays the ESI-MS data. Signal at 327.7 and 284.0 were due to (M+1) and (M+1)-39, respectively. The signal at 414.8 might be due to the contamination of β -sitosterol, because the retention factor of β -sitosterol (0.52) was very close to retention factor of compound G1 (0.6). Therefore both of the compounds cannot be separated perfectly by column chromatography.

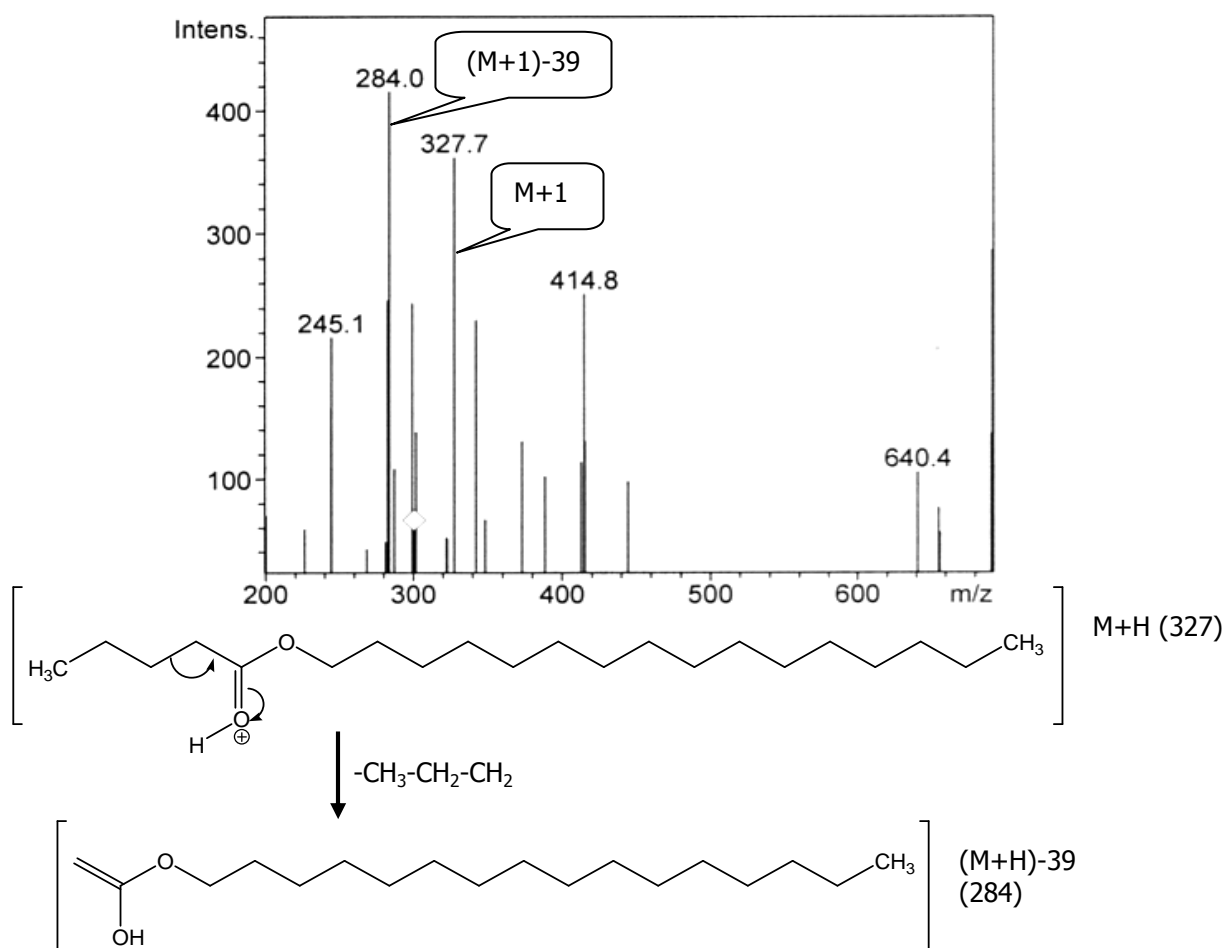


Figure. III.5.4. ESI-MS data and fragmentation pattern of the compound G1

Based on all of the data above, the structure of the compound G1 was determined as hexadecyl pentanoate.

III.6. Compound WuPe (Palmitic acid)

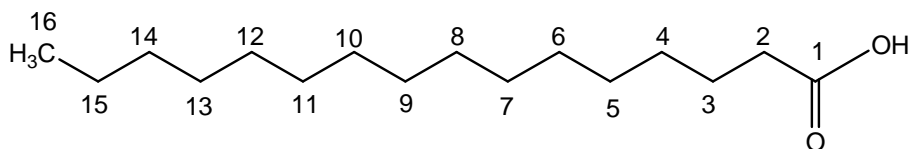


Fig. III.6.1. The chemical structure of compound WuPe

Compound WuPe was isolated from the petroleum extract as white crystals. The IR spectrum shows peaks at 2914 cm^{-1} and 2847 cm^{-1} due to aliphatic C-H and signal at 1699 cm^{-1} indicating the presence of -C=O group. The presence of carbonyl group can be deduced from the ^{13}C NMR spectrum by the signal at $\delta 176.31\text{ ppm}$. The signal corresponds to carboxylic acid. The EI-MS experiment (Fig.III.6.2a) exhibits a signal at $m/z 60$ in high intensity, corresponding to the $\text{-CH}_2=\text{C}(\text{OH})_2^+$. The ion was a fragmentation result from acids containing gamma-hydrogens through the McLafferty rearrangement process. Beside that, the EI-MS experiment also displayed the molecule ion signal at $m/z 256$ was confirmed as $\text{C}_{16}\text{H}_{32}\text{O}_2$.

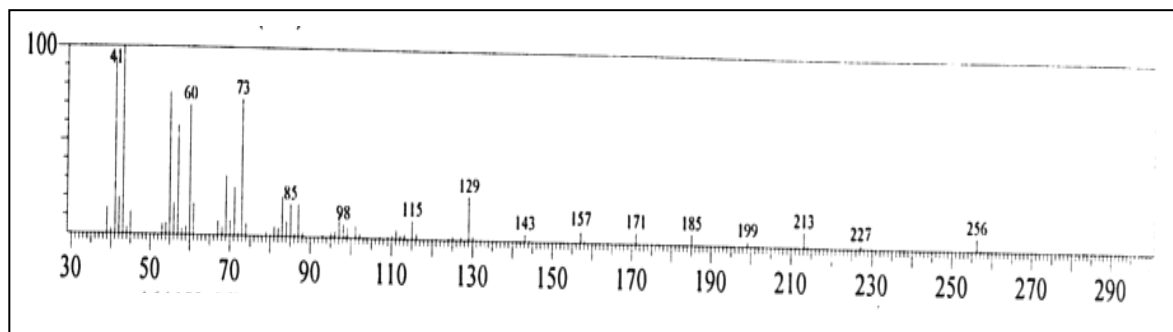


Fig. III.6.2a. ES-MS spectrum of compound WuPe

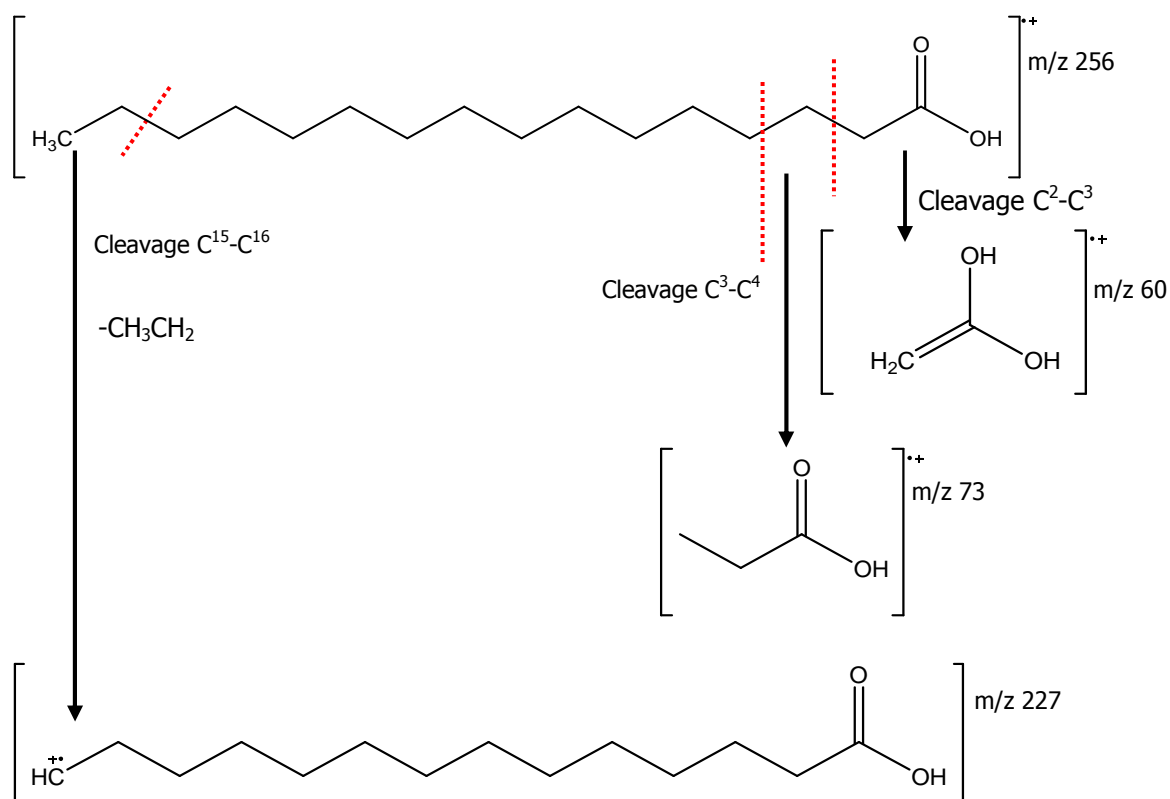


Figure. III.6.2b. Fragmentation pattern of compound WuPe

Table III.6.1. NMR spectroscopic data of compound WuPe measured in MeOH-d₄

C/H	δ H (ppm)	δ C (ppm)	δ^* C (ppm)
1	-	176.32	180.58
2	2.17	33.57	34.23
3	1.49	24.71	24.80
4	1.19	29.31	29.80
5	1.19	29.31	29.80
6	1.19	29.31	29.80
7	1.19	29.31	29.80
8	1.19	29.31	29.80
9	1.19	29.31	29.80
10	1.19	29.31	29.80
11	1.19	29.31	29.80
12	1.19	29.31	29.80
13	1.19	29.31	29.80
14	1.19	31.68	32.05
15	1.19	22.34	22.79
16	0.80	13.03	14.14

Note : δ^* C was obtained from SDBS Aist database Japan

The COSY diagram as in Figure III.6.2 shows the correlation of H²-H³, H³-H⁴ and H¹⁵-H¹⁶. Meanwhile, ¹H-¹³C HMBC experiment as in Figure III.6.3 demonstrates correlations between H²-C¹, H²-C³, H²-C⁴, H³-C⁴, H¹⁶-C¹⁵ and H¹⁶-C¹³.

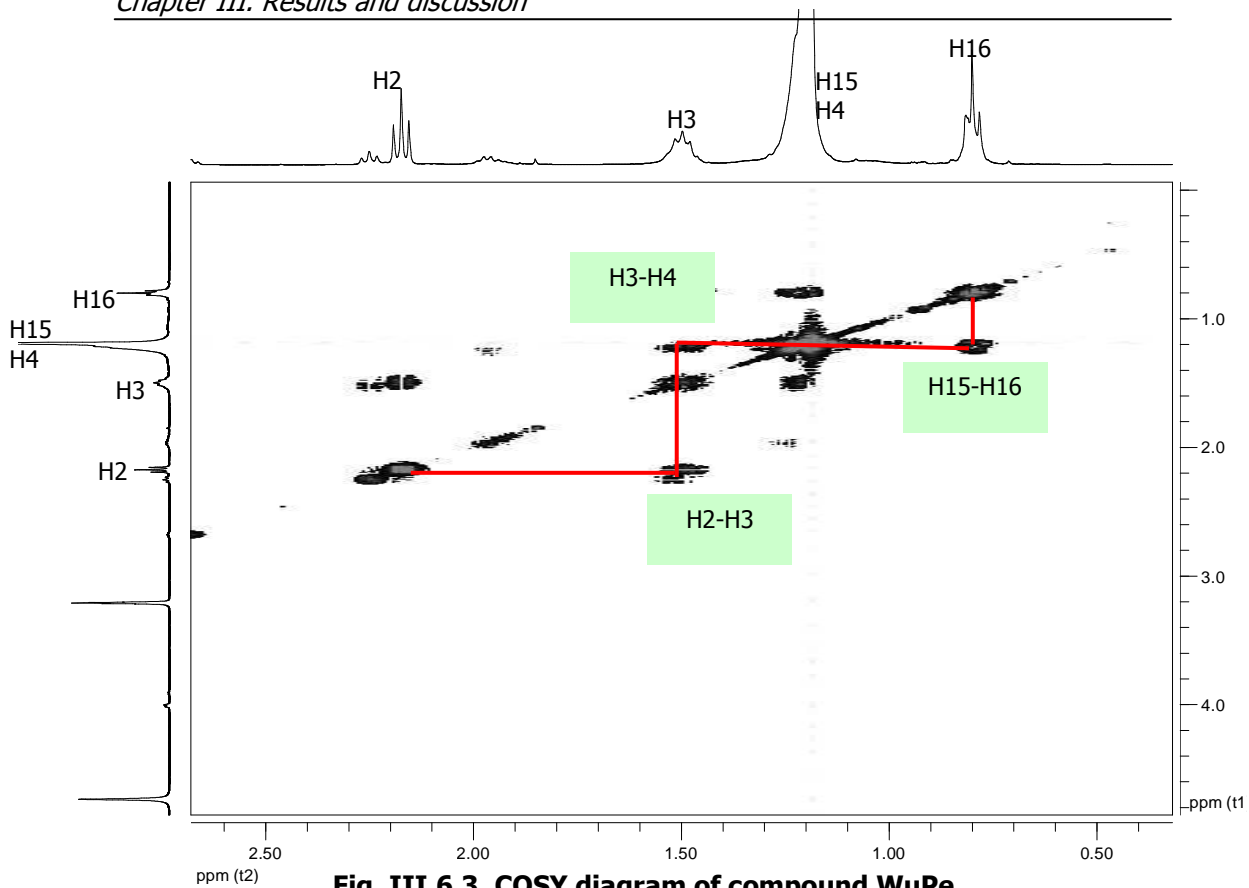


Fig. III.6.3. COSY diagram of compound WuPe

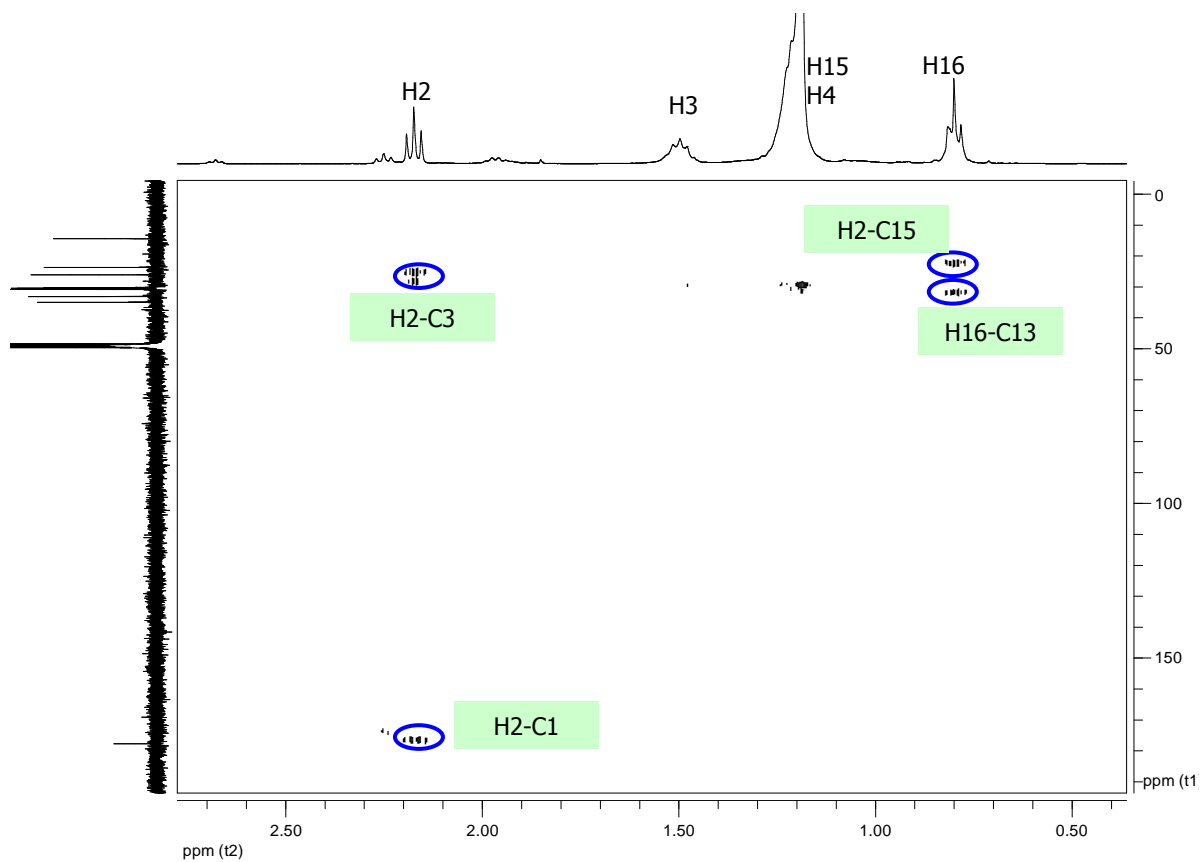
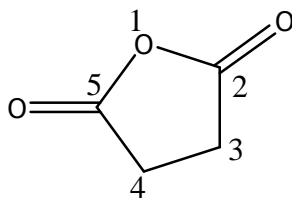
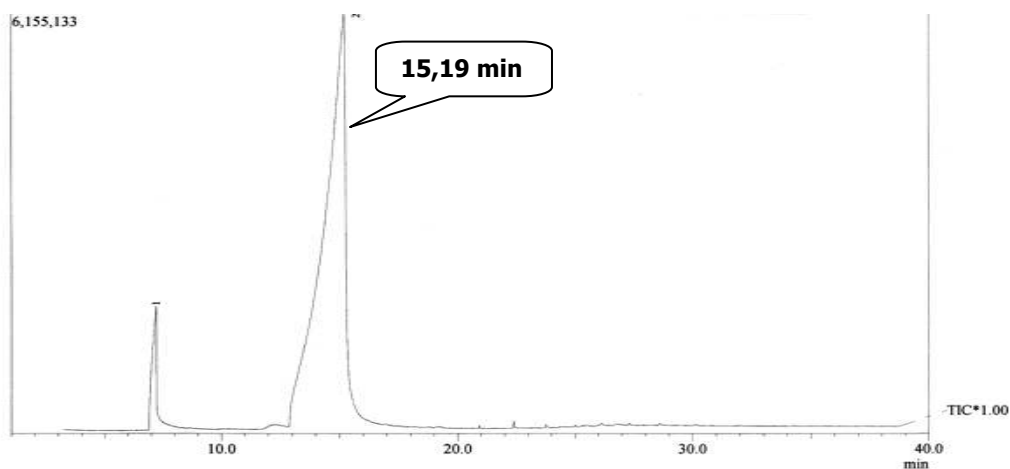


Fig. III.6.3. HMBC diagram of compound WuPe

According to all data above, the compound WuPe was confirmed as palmitic acid.

III.7. Compound W2Et (dihydrofurane-2,5-dione)**Dihydrofurane-2,5-dione****Fig. III.7.1. The chemical structure of compound W2Et (dihydrofurane-2,5-dione)**

Compound W2Et was isolated from the ethyl acetate extract after hydrolysis as a white powder having a melting point of 188°C. The ^1H NMR spectrum of the compound W2Et shows signals at 1680 cm^{-1} (C=O group), 1197 cm^{-1} (-C-O-C ether), 1410 cm^{-1} (-CH group) and 1306 cm^{-1} (-CH group). The result of GC/MS experiment which can be found in Figure III.7.2 and III.7.4 shows the molecular ion peaks at m/z 100 which can be assigned to $\text{C}_4\text{H}_4\text{O}_3$.

**Fig. III.7.2. The GC/MS spectrum of compound W2Et**

The ^1H NMR spectrum displays that there is only one signal at δ 2.58 ppm (H^4 and H^5). The signal of ^{13}C NMR spectrum shows signals at δ 176.16 ppm and 29.84 ppm are assigned to C^2 and C^5 , respectively. The complete data of ^1H NMR and ^{13}C NMR can be found in Table III.7.1.

Table III.7.1. NMR spectroscopic data of the compound W2Et measured in MeOH-d₄

C/H	δ C (ppm)	δ H (ppm)
1	-	-
2	176.16	-
3	29.84	2.58
4	29.84	2.58
5	176.16	-

The HMBC diagram as in Figure III.7.3 shows the correlations of H⁴ and C² or H³ and C⁵.

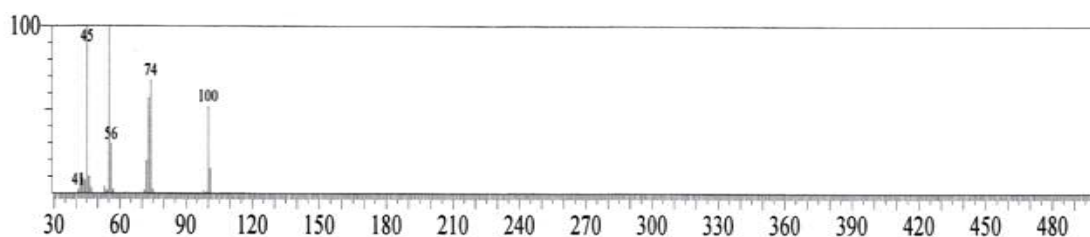
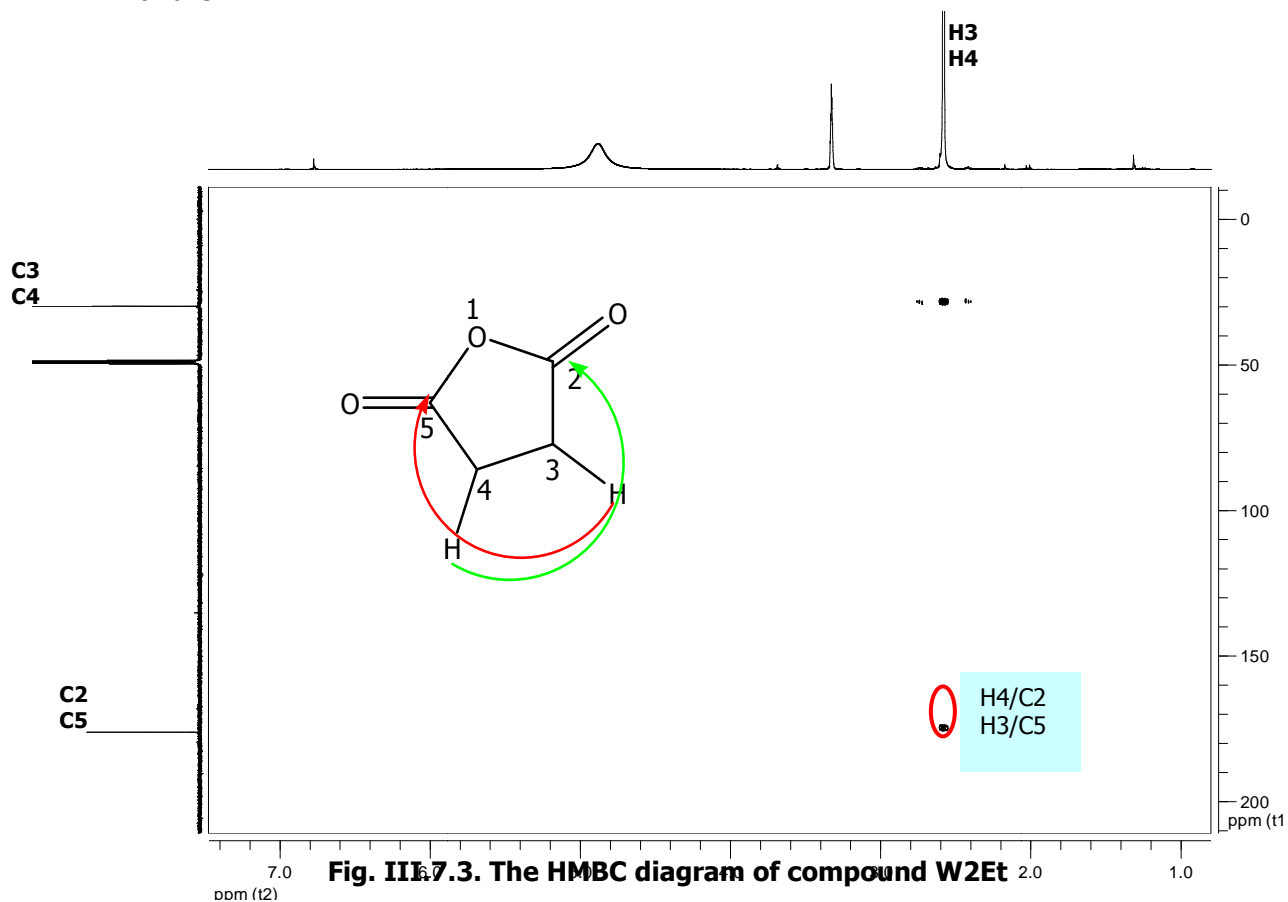


Figure III.7.5 displays the mass fragmentation pattern of compound W2Et.

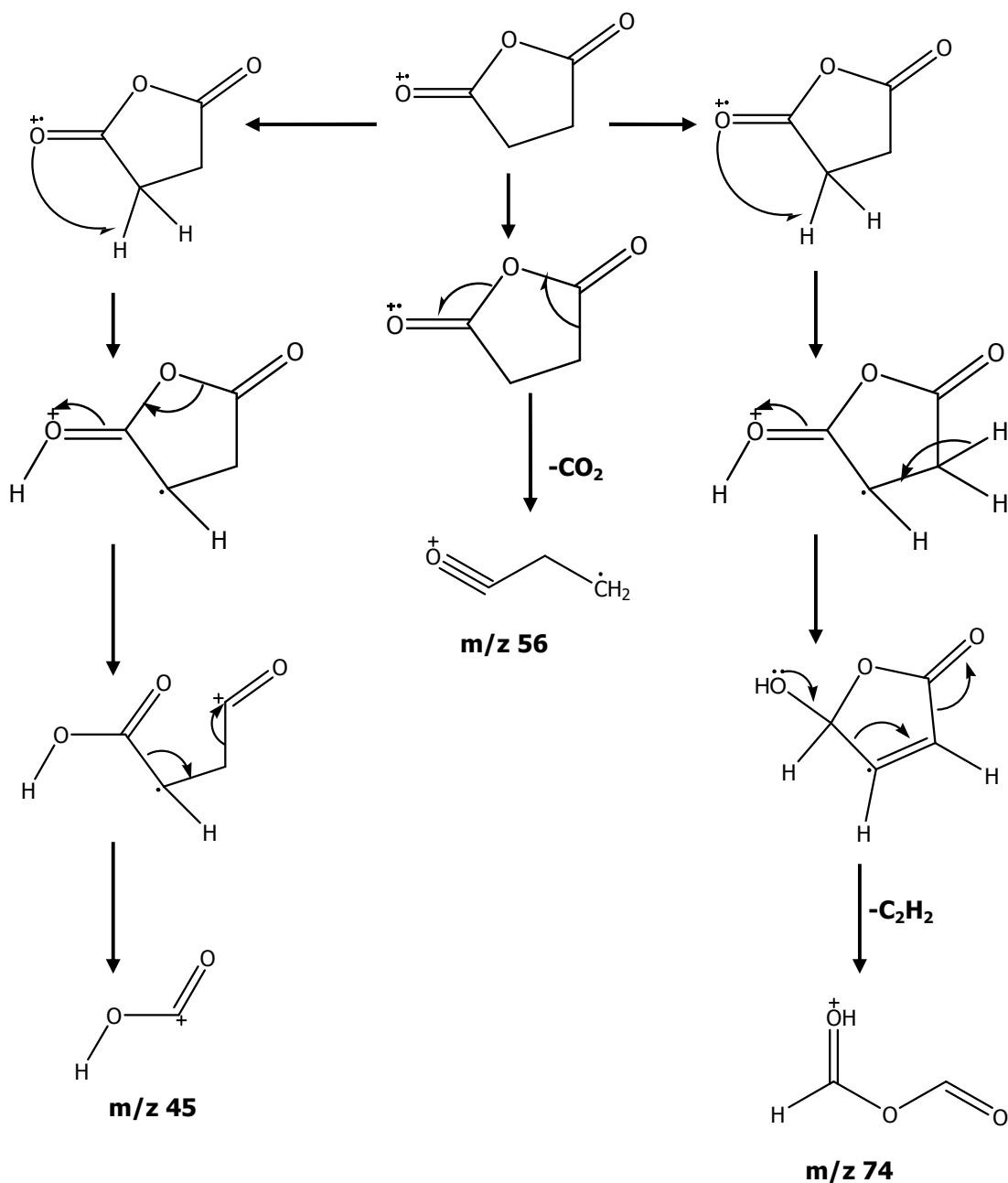


Fig. III.7.5. The fragmentation pattern of compound W2Et

Based on all the data, the compound W2Et can be identified as dihydrofuran-2,5-dione.

III.5. Compound C1 (Daidzein)

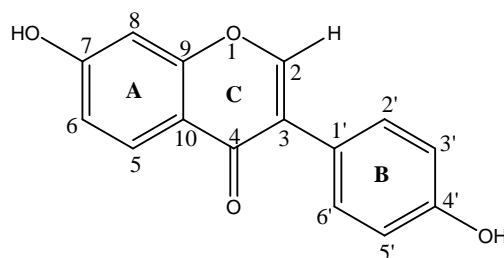


Fig.III.8.1. The chemical structure of compound C1 (daidzein)

Compound C1 was isolated from the ethyl acetate extract as brown powder having a melting point of 295 °C – 297 °C. Because compound C1 was able to reduce the DPPH, it was further investigated by GC/MS and NMR spectroscopy to elucidate the chemical structure. The results of GC/MS experiment displayed in Figures III.8.2 and III.8.6 show the molecular ion peaks at m/z 254 which is in agreement with $C_{15}H_{10}O_4$. The 1H NMR spectrum of the compound C1 shows the five signals in aromatic region with the pattern typical for isoflavonoids. The IR spectrum indicates also the presence of the aromatic group at 1592 cm^{-1} , 1514 cm^{-1} , 1381 cm^{-1} and 1456 cm^{-1} . Additionally the IR spectrum shows peaks at 3149 cm^{-1} ($-OH$ group), 1621 cm^{-1} ($C=O$ group) and 1234 cm^{-1} ($-C-O-C$ group).

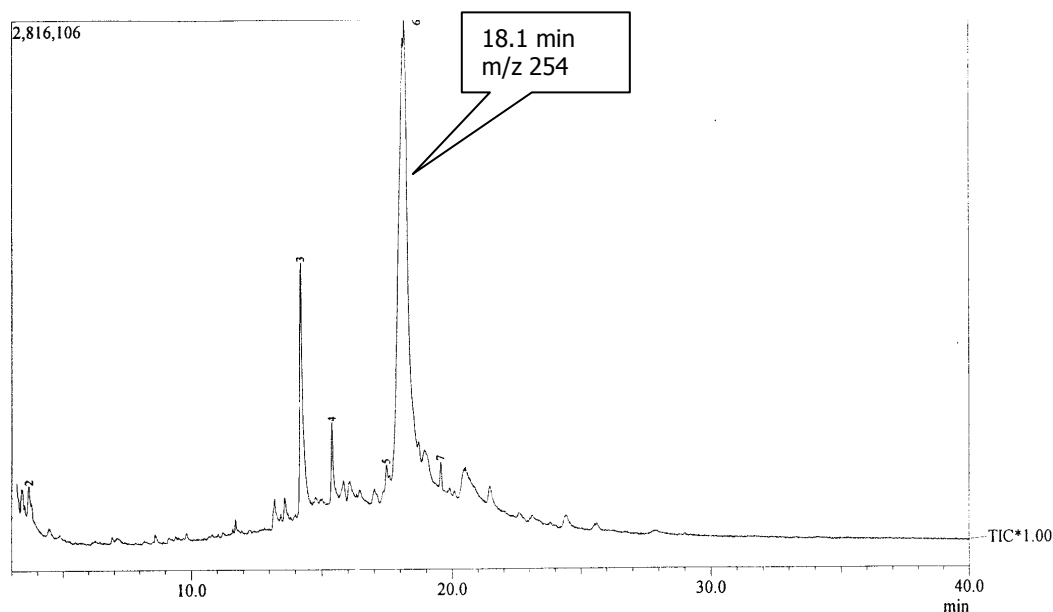


Fig. III.8.2. The GC/MS chromatogram of compound C1 (daidzein)

The chemical shift values of the ^1H NMR and ^{13}C NMR spectra of compound C1 described in Table III.8.1 show typical signals of isoflavonoid. The ^1H NMR spectrum shows only signals for aromatic protons at δ 6.76 – 8.02 ppm. The signal at δ 8.02 ppm (s) was assigned to H^2 , and the signal at δ 6.76 ppm (s) to H^8 . The presence of $-\text{OH}$ can not be deduced from the ^1H NMR spectrum but from the IR spectrum and also the ^{13}C NMR spectrum. The presence of a carbonyl and an ether was confirmed by the signals at δ 178.19 ppm and δ 158.72 ppm, respectively. Meanwhile other signals of ^{13}C NMR are in agreement with aromatic moiety. The complete information about the NMR spectroscopic data of compound C1 can be seen in Table III.8.1.

Table III.8.1. NMR spectroscopic data of the compound C1 (in MeOH- d_4)

C/H	δ C (ppm)	δ^* C (ppm)	δ H (ppm)	δ^* H database (ppm)
2	153.04	152.78	8.02 (s)	8.29 (s)
3	124.32	123.44	-	-
4	176.57	174.65		
5	128.53	127.23	7.95 (d, J = 8)	7.96 (d, J = 8.6)
6	116.47	115.09	6.85 (d, J = 6.7)	6.94 (d, J = 8.6)
7	164.62	162.49	-	-
8	103.24	102.06	6.74 (s)	6.87 (s)
9	158.72	157.38	-	-
10	118.23	116.59	-	-
1'	125.98	122.49	-	-
2'	131.42	130.02	7.26 (d, J = 7.3)	7.38 (d, J = 8.6)
3'	116.24	114.91	6.76 (d, J = 6.76)	6.81 (d, J = 8.6)
4'	159.82	157.14	-	-
5'	116.24	114.91	6.76 (d, J = 6.7)	6.81 (d, J = 8.6)
6'	131.42	130.02	7.26 (d, J = 7.3)	7.38 (d, J = 8.6)

Note : δ^* H is proton chemical shift value obtained in DMSO- d_6 (Goto, et al., 2009)

Three spin systems were detected in ^1H - ^1H COSY (Fig. III.8.3). One spin system was located in ring A (i.e. δ_{H} 7.94 and δ_{H} 6.84) and two spin systems were identical and located in ring B (i.e. δ_{H} 7.26 and δ_{H} 6.76). The long-range correlation between δ_{H} 7.94 to δ 158.72 (C^9) and δ 164.62 (C^8) supported that δ_{H} 7.94 (H^5) and δ_{H} 6.84 (H^6) were located in ring A. Another ^1H - ^{13}C correlation between δ_{H} 7.26 to δ 125.98 ($\text{C}^{1'}$) and δ 159.82 ($\text{C}^{4'}$) supported that δ_{H} 7.26 ($\text{H}^{2'}$ and $\text{H}^{6'}$) and δ_{H} 6.76 ($\text{H}^{3'}$ and $\text{H}^{5'}$) were located in ring B.

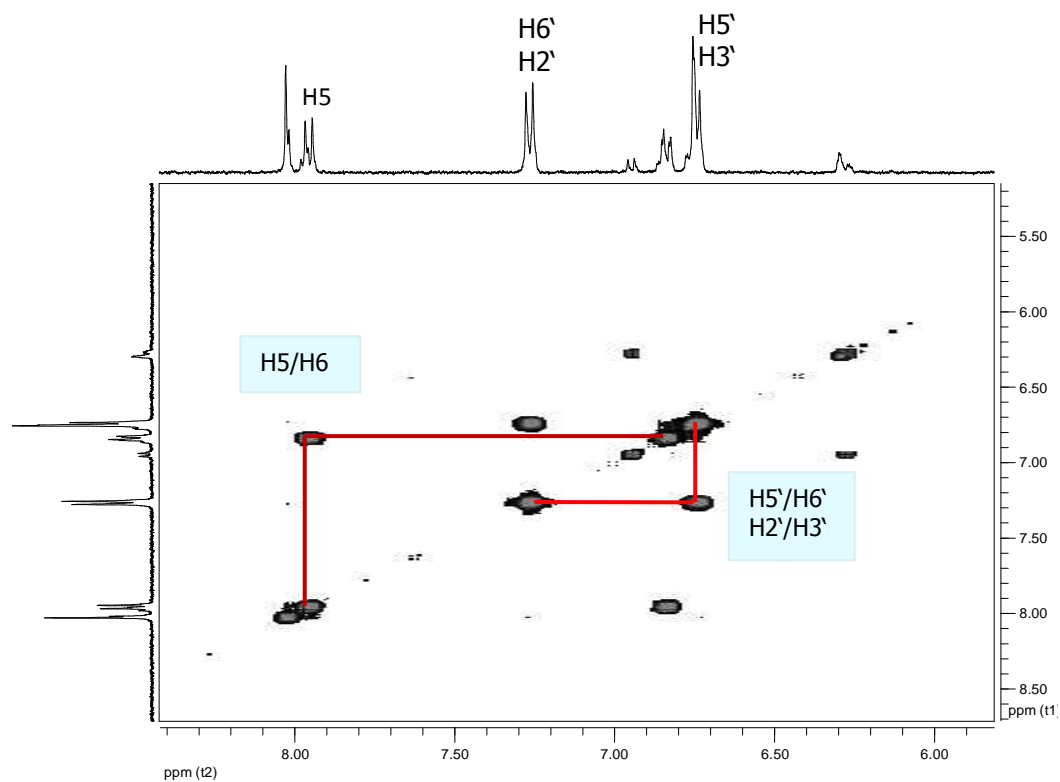


Fig. III.8.5. The COSY diagram of the compound C1

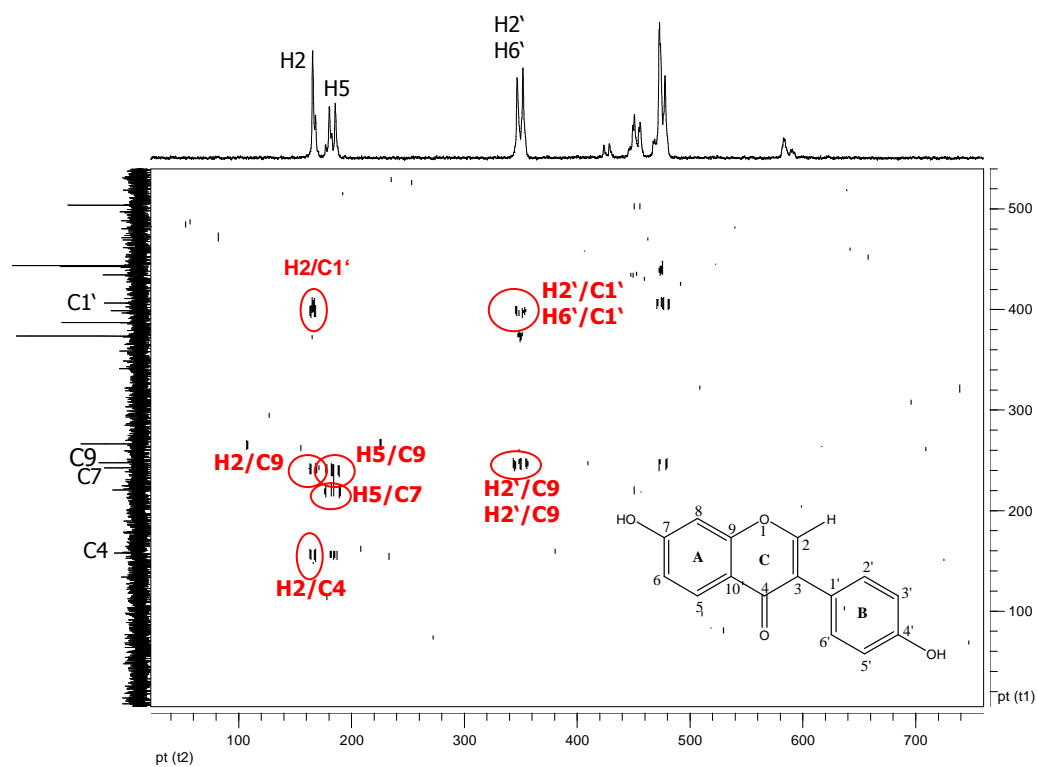


Fig. III.8.4. The HMBC diagram of the compound C1

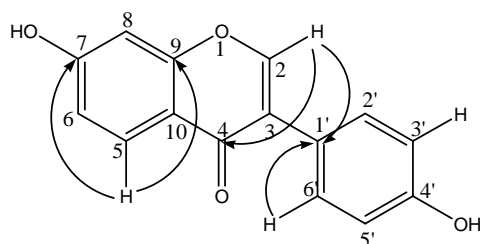


Fig. III.8.5. The ^1H - ^{13}C NMR long range correlation of compound C1 (daidzein)

The HMBC diagram (Fig.III.4) reveals significant correlations between H^2 and $\text{C}^{1'}$ ($^3J_{\text{C-H}}$), H^2 and C^4 ($^3J_{\text{C-H}}$), H^2 and C^9 ($^3J_{\text{C-H}}$), H^5 and C^7 ($^3J_{\text{C-H}}$), $\text{H}^{2'}$ and $\text{C}^{1'}$ ($^2J_{\text{C-H}}$), and $\text{H}^{6'}$ and $\text{C}^{1'}$ ($^2J_{\text{C-H}}$). Three correlations of them confirmed the presence of the isoflavone skeleton, i.e. the bond coupling of the proton at δ_{H} 8.13 (H^2) with the carbonyl group at 176.57 (C^4), 158.72 (C^9) and also 125.98 ($\text{C}^{1'}$). This finding is in accordance with Falco et al. (2005).

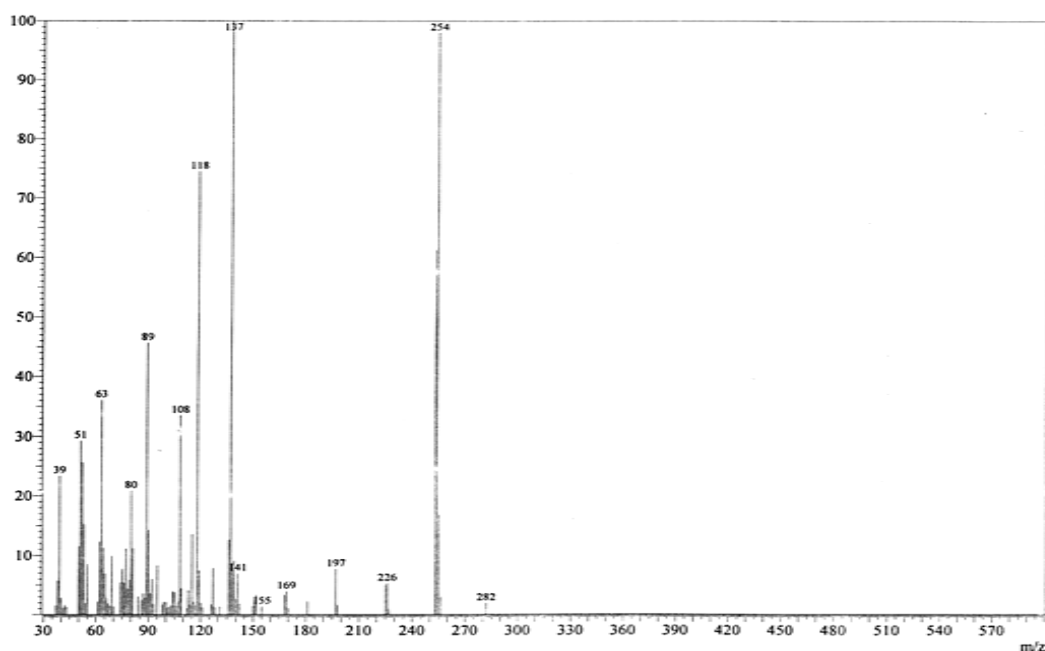


Fig. III.8.6. The EI-MS spectrum of compound C1 (Daidzein)

The EI-MS spectrum (Fig.III.8.6) shows a main signal at m/z 254 indicating the positive charged radical of daidzein $[\text{M}]^+$. This finding was supported by previously paper. Santos et al. (2005) have analyzed daidzein using ESI-MS in the negative ion mode, and the result showed a negative peak at m/z 253 that was assigned to $(\text{daidzein-H})^{-1}$. Thus, the molecular weight of daidzein can be concluded as 254.

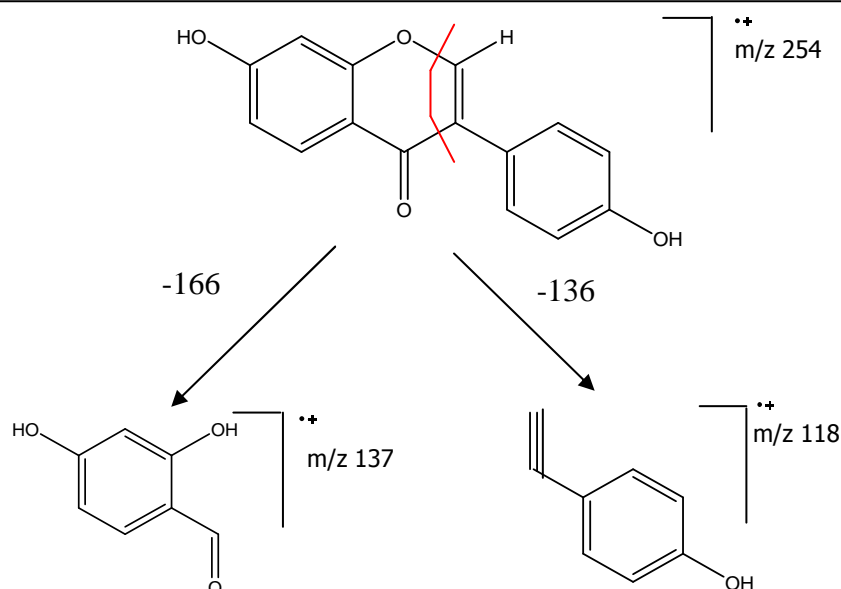


Fig. III.8.7. The fragmentation pattern of compound C1

The fragmentation scheme is according to Setchell 1987, who already observed the fragment producing the main signal at m/z 118.

After careful interpretation of the experimental data, compound C1 could be assigned to daidzein.

I.9.1. Compound Wu1a (Daidzein-7-O- β -glucopyranose)

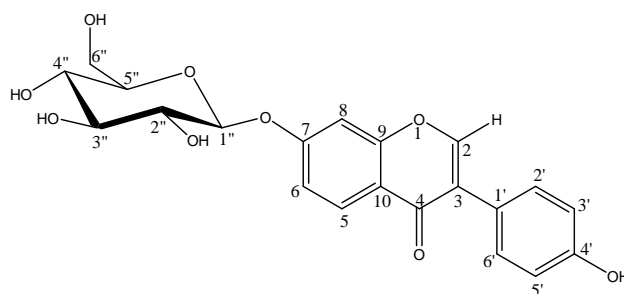


Fig. III.9.1. The chemical structure of compound Wu1a (Daidzein-7-O- β -glucopyranose)

Compound Wu1a was isolated from the ethyl acetate extract as yellow powder. This compound has high activities, absorbing UV light and reducing the DPPH. Therefore, it was further investigated by LC/MS and NMR spectrometer. The result of LC/MS experiment can be read in Figure III.9.4. The molecular formula of Wu1a was established as $C_{21}H_{20}O_9$ based on its ESI-MS spectrum. The fragmentation spectrum suggested that Wu1a was composed of daidzein aglycon (signal at 255) and hexose. The 1H NMR spectrum of the compound Wu1a shows the group signals (at δ 3.38 – 5.03 ppm) with the pattern of glucopyranose and five signals in aromatic region (signals at δ 6.78 – 8.11 ppm) with the pattern of an isoflavonoid. This pattern was similar to compound C1 (daidzein). The IR

spectrum indicates also the presence of the aromatic group at 1515 cm^{-1} , 1445 cm^{-1} and 1374 cm^{-1} . Additionally, the IR spectrum showed peaks at 3324 cm^{-1} (–OH group), 1617 cm^{-1} (C=O group) and 1248 cm^{-1} (–C–O–C group).

The ^1H NMR spectrum showed the pattern of isoflavonoid that was similar to compound C1 (daidzein) with the exception of the chemical shift values of the proton H^6 and H^8 . They were shifted relatively upfield, from 6.85 ppm (H^6) and 6.74 ppm (H^8) in compound C1 to 7.12 ppm (H^6) and 7.16 ppm (H^8) in compound Wu1a. This evidence supported that the substituent attached of C^7 in compound Wu1a was not a hydroxyl group but a glucose. The presence of the glucose is supported by a β -anomeric proton signal at δ 5.03 ppm (1H, d, $J = 7.4$), while an anomeric carbon signal can be found in the ^{13}C NMR spectrum at δ 100.42 ppm. The glucose component of compound Wu1a was determined to be β -glucopyranose. This finding was in accordance with Shimoda et al. (2008) that the proton signal and the carbon signal of β -anomeric in ^1H NMR spectrum were 5.17 (d, $J = 7.6$) and 101.8 ppm, respectively.

Table III.9.1. The spectroscopic data of compound Wu1a measured in MeOH- d_4

C/H	δ C (ppm)	δ^* C (ppm)	δ H (ppm)	δ^* H database (ppm)
2	154.04	153.2	8.11 (1H, s)	8.39 (1H, s)
3	124.87	123.5	-	-
4	177.09	175.3	-	-
5	127.14	131.2	8.06 (1H, d, $J = 8.0$)	8.04 (1H, d, $J = 8.6$)
6	115.89	109.1	7.12 (1H, d, $J = 7.1$)	7.13 (1H, dd, $J = 8.6 ; 2.0$)
7	162.13	163.9	-	-
8	103.79	103.9	7.16 (1H, s)	7.24 (1H, s)
9	157.97	157.8	-	-
10	118.94	115.5	-	-
1'	124.87	125.1	-	-
2'	130.23	127.8	7.29 (1H, d, $J = 7.3$)	7.40 (1H, d, $J = 6.4$)
3'	115.15	115.8	6.78 (1H, d, $J = 6.8$)	6.82 (1H, d, $J = 6.4$)
4'	157.19	157.7	-	-
5'	115.15	115.8	6.78 (1H, d, $J = 6.8$)	6.82 (1H, d, $J = 6.4$)
6'	130.23	127.8	7.29 (1H, d, $J = 7.3$)	7.40 (1H, d, $J = 6.4$)
Gly-1''	100.42	101.8	5.03 (1H, d, $J = 7.4$)	5.17 (1H, d, $J = 7.6$)
Gly-2''	73.41	73.4	3.38 – 3.86 (6H, m)	3.18 – 3.71 (6H, m)
Gly-3''	76.42	73.4		
Gly-4''	69.93	71.5		
Gly-5''	77.00	77.7		
Gly-6''	61.10	62.2		

δ^* measured in DMSO- d_6 (obtained from Shimoda et al, 2008)

The COSY experiments (Fig. III.9.2) show the expected correlations between the protons of H^5 - H^6 , $\text{H}^{2'}$ - $\text{H}^{3'}$ and $\text{H}^{5'}$ - $\text{H}^{6'}$.

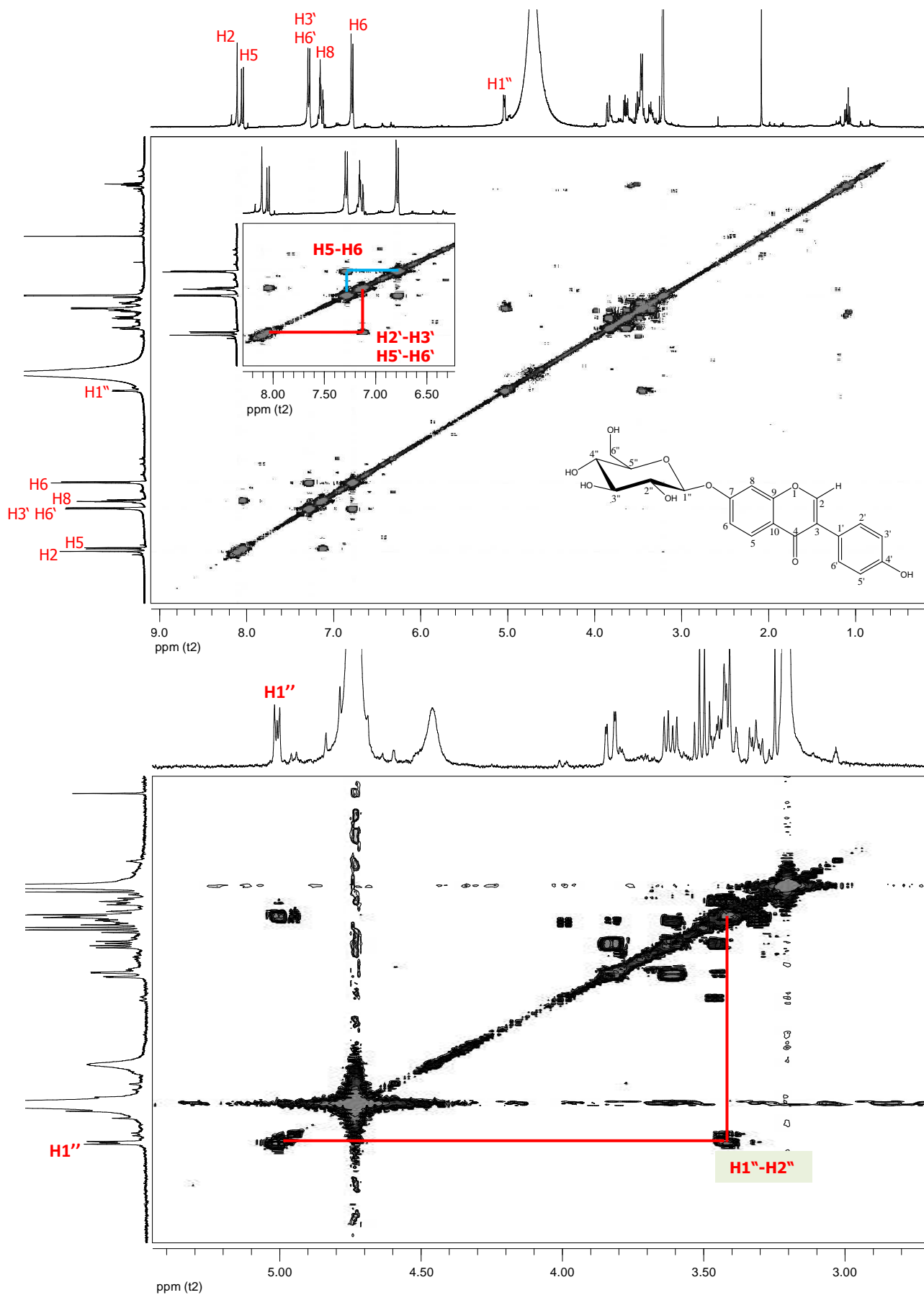


Fig. III.9.2. The COSY diagram of compound Wu1a

The HMBC correlations were observed between the anomeric proton signal at δ_H 5.03 ppm ($H^{1''}$) and the carbon resonance at δ 162,13 (C^7) as can be seen in Figure III.9.3. This finding confirmed that the glucopyranose residue was attached to the hydroxyl group at C^7 of daidzein. The other correlations were also observed between $H^{3'}-C^{1'}$ ($^3J_{C-H}$), H^6-C^9 ($^4J_{C-H}$), $H^2-C^{1'}$ ($^3J_{C-H}$), H^2-C^9 ($^3J_{C-H}$) and H^2-C^4 ($^3J_{C-H}$). Three correlations $H^2-C^{1'}$, H^2-C^9 and H^2-C^4 were typical for isoflavon skeleton.

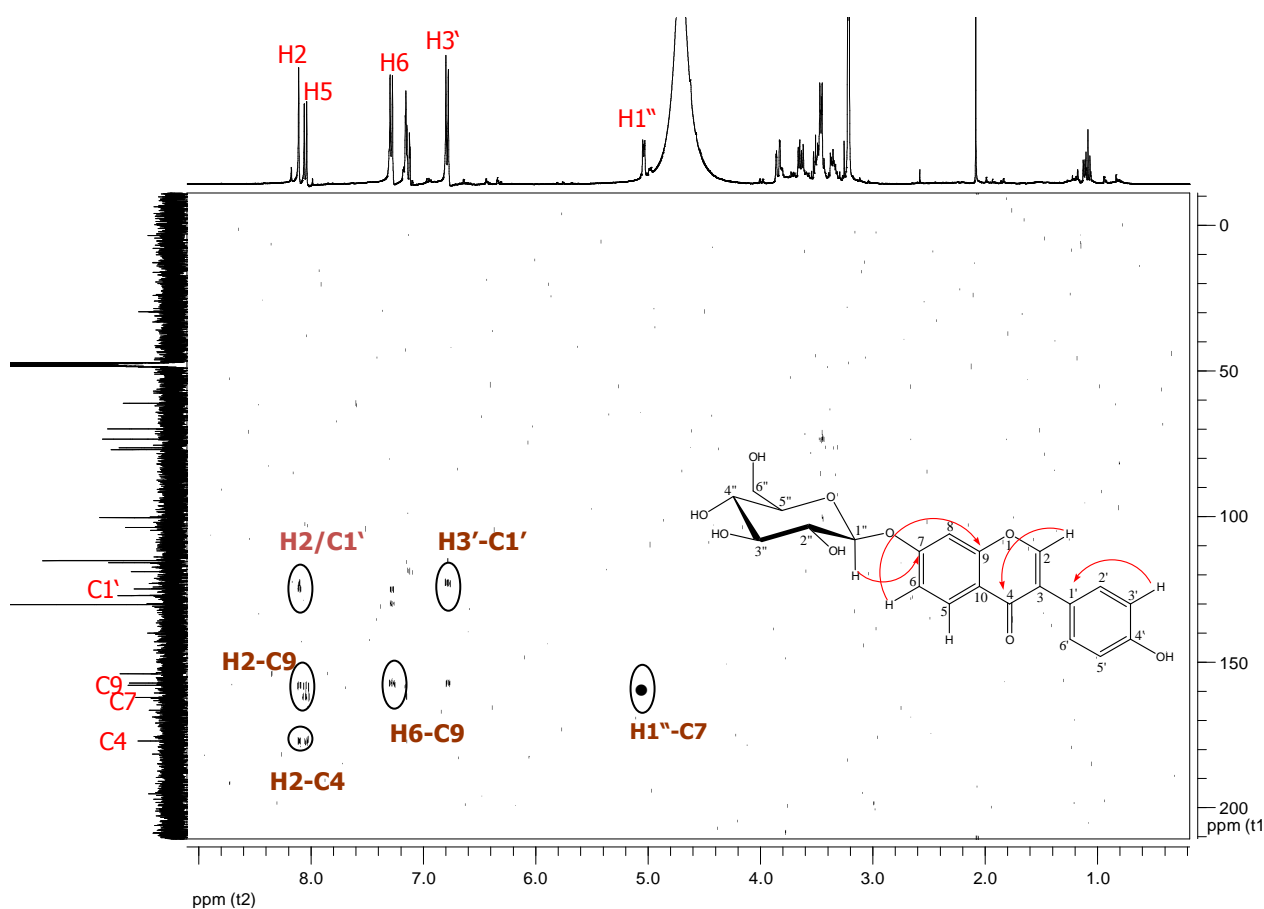


Fig. III.9.3. The HMBC diagram of compound Wu1a

Figure III.9.5 describes the fragmentation pattern of compound Wu1a according to the ESI-MS spectrum. Compound Wu1a was protonated producing signal at 417.2 $[M+H]^{+1}$ and fragmented producing the positively charged ion of $[daidzein+H]^{+1}$ at m/z 255.0.

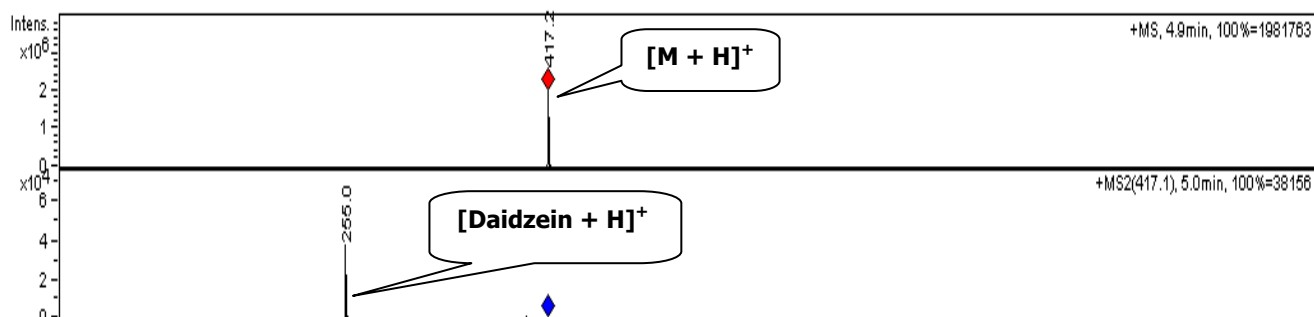


Fig. III.9.4. ESI-MS (above) and ESI-MS-MS spectrum of compound Wu1a

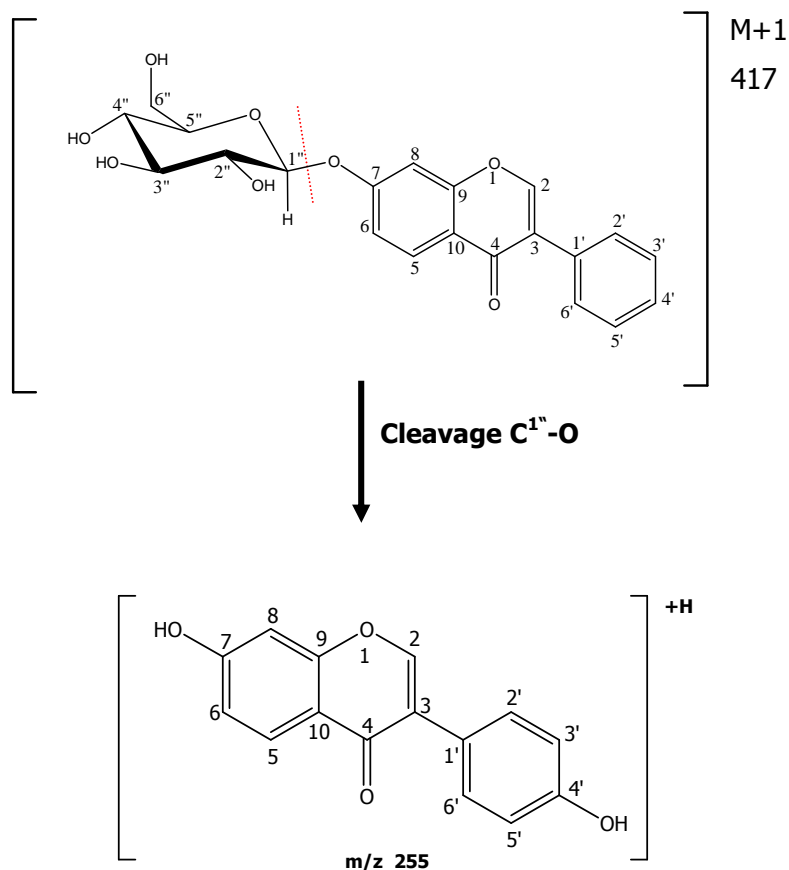


Fig III.9.5. The fragmentation pattern of compound Wu1a

Based on all data above, the compound Wu1a was identified as **daidzein-7-O- β -glucopyranose**.

III.10. Compound Wu3a (5-hydroxy-daidezine-7-O- β -glucopyranose)

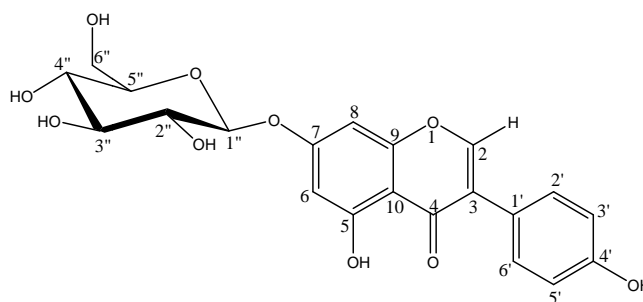


Fig. III.10.1. The chemical structure of compound Wu3a

Compound Wu3a was isolated as a yellow-brown powder from the ethyl acetate extract. This compound has high activities to absorb UV light and to reduce DPPH.

The molecular formula of $C_{21}H_{20}O_{10}$ was deduced from ESI-MS data and the ^{13}C NMR analysis. This compound was assigned to a glycosidic derivative of a hydroxylated daidezine. 1H NMR (MeOH- d_4) of the compound Wu3a showed five signals in aromatic regions (δ 6.60 – 7.29 ppm) with the pattern of daidezine. The other signals at δ 3.38 – 4.95 ppm revealed the presence of glucopyranose group. The presence of aromatic group was also deduced from the IR spectrum (Fig III.10.3). The IR spectrum showed the signals of $-C=C-$ aromatic (1651 cm^{-1} , 1444 cm^{-1} and 1516 cm^{-1}), $-C=O$ (1614 cm^{-1}), $-C-O-C$ (1069 cm^{-1}), $-C-H$ (2927 cm^{-1}) and $-OH$ (3330 cm^{-1}).

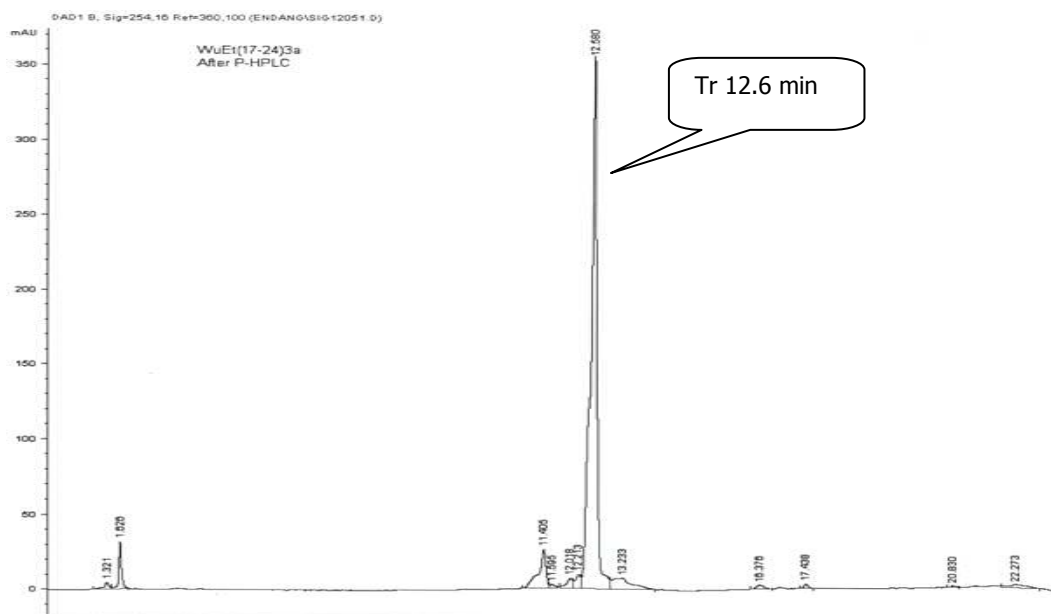


Fig. III.10.2. Analytical HPLC of compound Wu3a, Tr : 12.6 min.

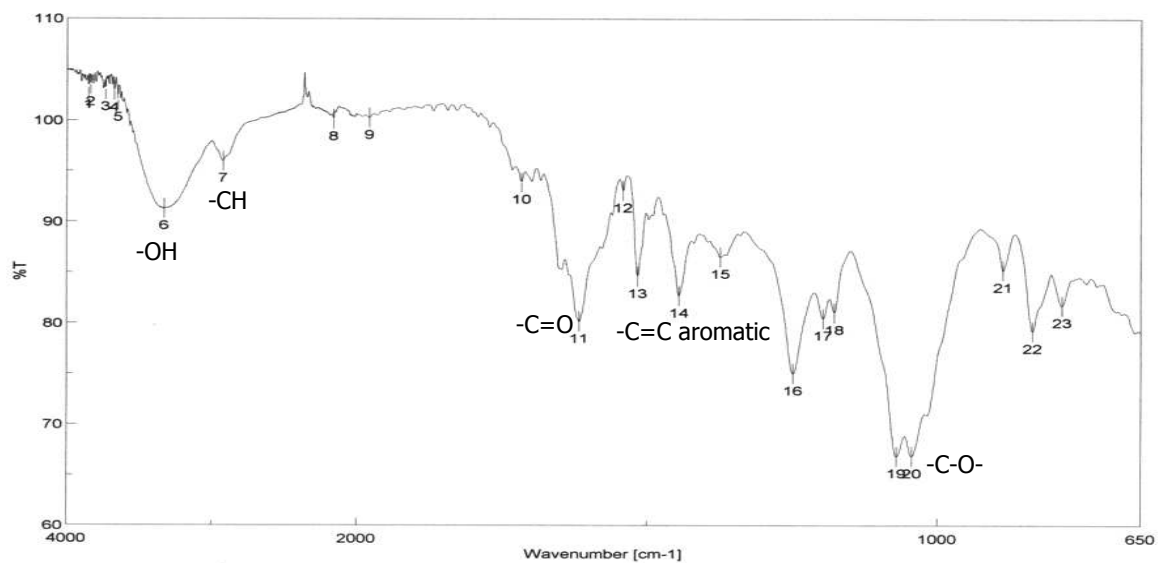


Fig. III.10.3. IR spectrum of compound Wu3a

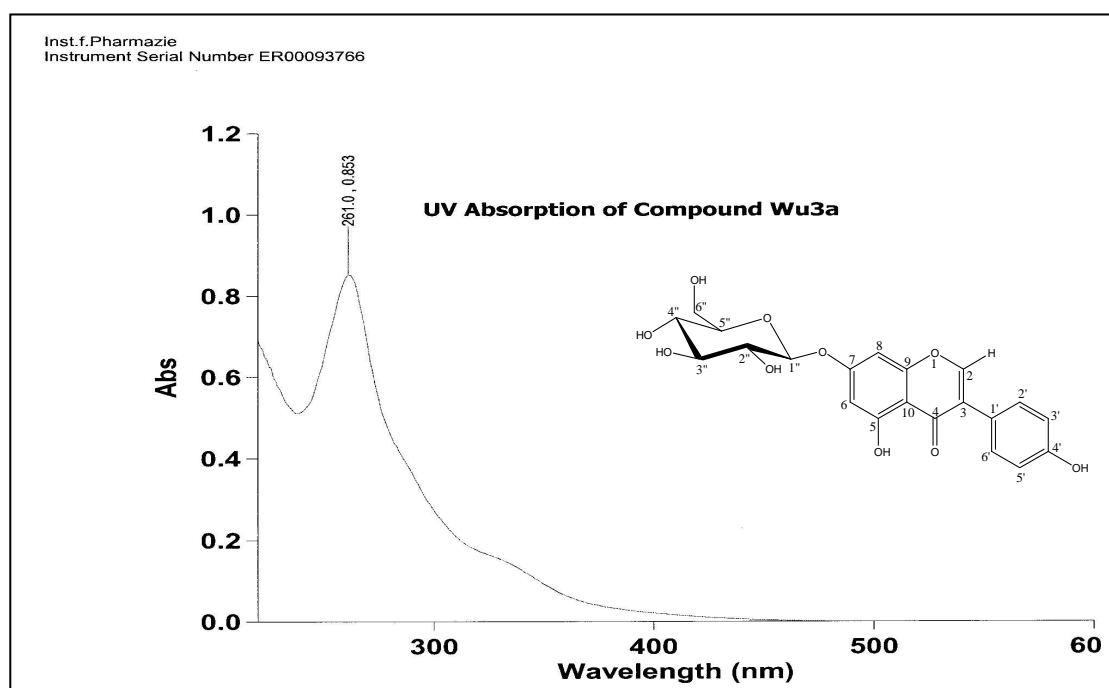


Fig. III.10.4. UV spectrum of compound Wu3a

For the measurement of the ¹H NMR spectrum only a low amount of the compound Wu3a was available. Thus, the quality of the spectra is low.

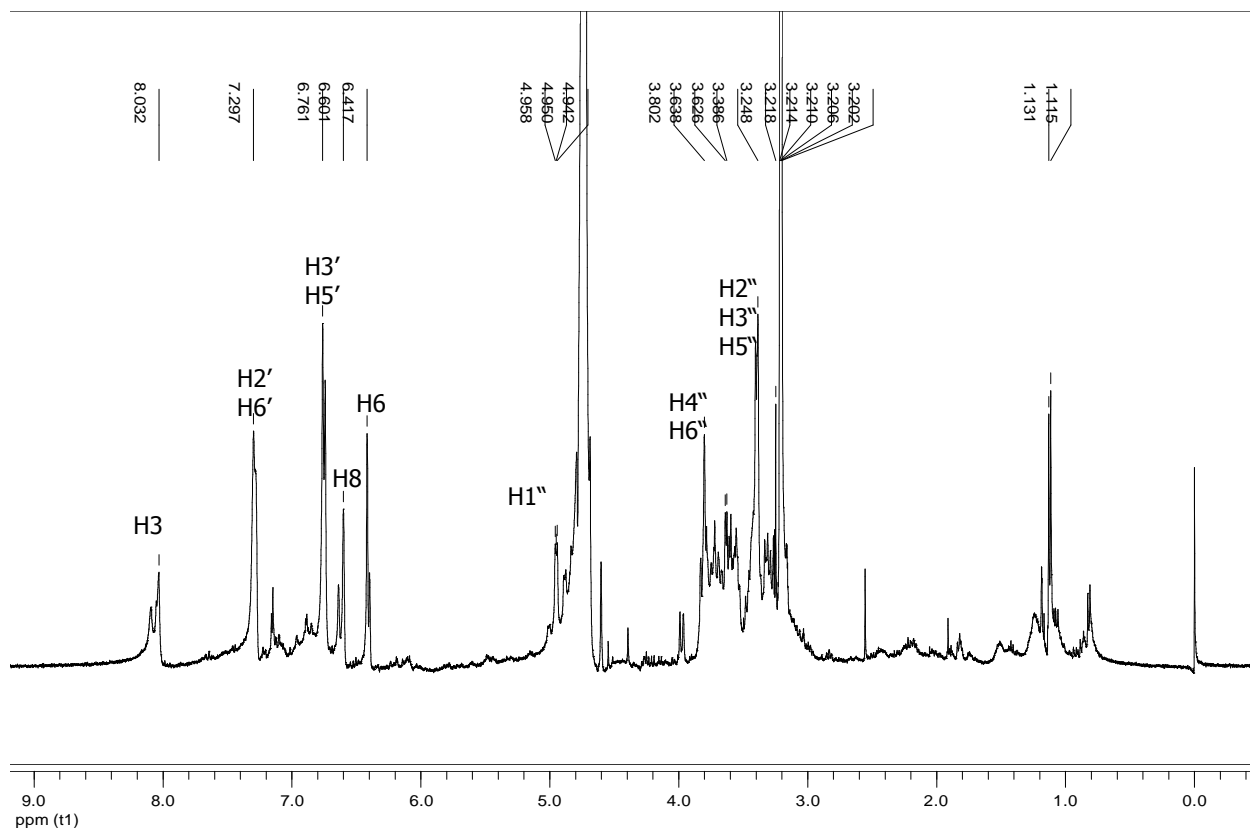


Fig III.10.5. ^1H NMR spectrum of compound Wu3a (MeOH- d_4 , 500MHz)

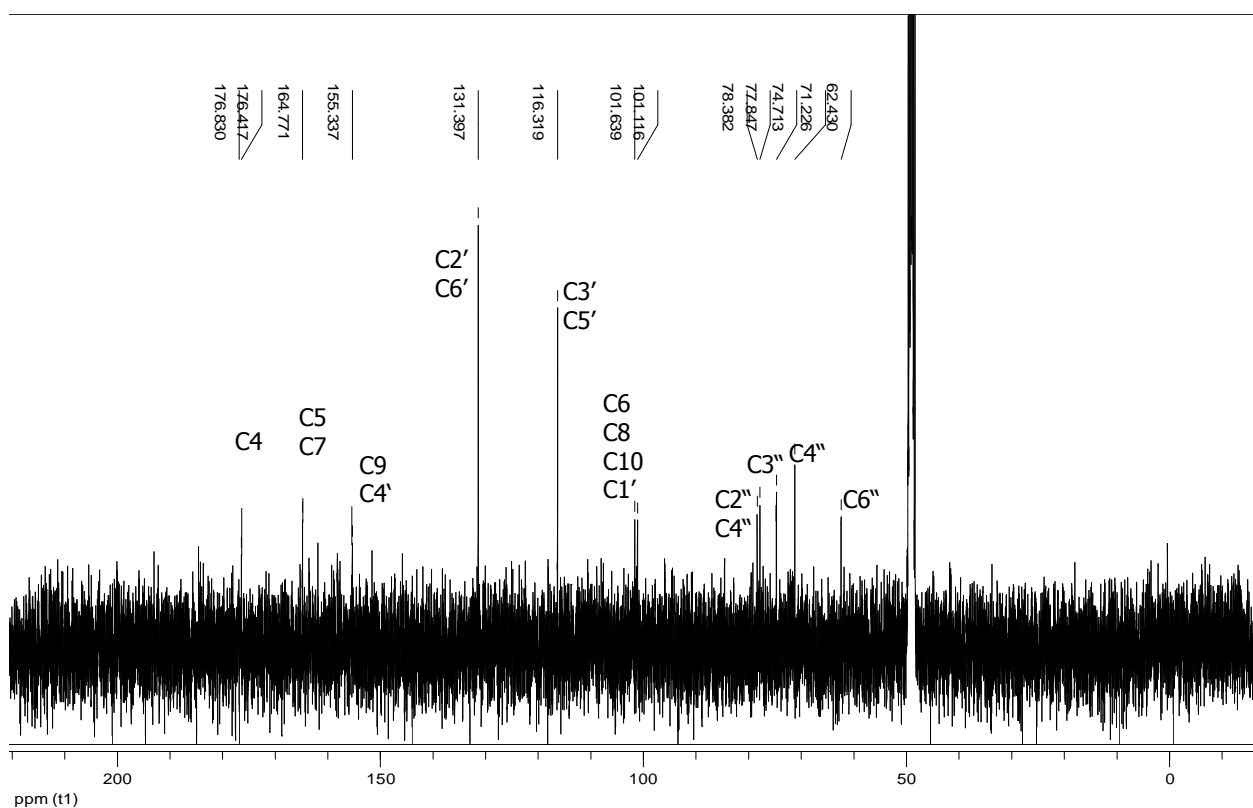


Fig III.10.6. ^{13}C NMR spectrum of compound Wu3a (MeOH- d_4 , 125 MHz)

The signal at δ 4.95 (d, $J = 6.37$) ppm in ^1H NMR spectrum (Fig. III.10.5) and the signal at δ 100.41 ppm in ^{13}C NMR demonstrated the presence a β -anomeric proton of the glucopyranose ($\text{H}^{1''}$). The correlation between $\text{H}^{1''}$ with the carbon aromatic at δ 164.7 ppm (C^7) in HMBC spectrum (Fig.III.10.8) revealed that the glucopyranose residue was attached to the phenolic hydroxyl group at C^7 of daidzein. The typical ^1H - ^{13}C correlation for skeleton isoflavonoid also appeared in the HMBC diagram, i.e. H^2 - $\text{C}^{1'}$ ($^3J_{\text{C-H}}$), H^2 - C^4 ($^3J_{\text{C-H}}$) and H^2 - C^9 ($^3J_{\text{C-H}}$).

The hydroxyl substituent in the daidzein moiety can be deduced from ESI-MS data. The signal at 271 in the fragmentation spectrum exhibited that daidzein was bound to one hydroxyl substituent. The signals at δ 6.58 ppm and 6.39 ppm in the ^1H NMR spectrum were correlated to protons in the aromatic ring (H^6 and H^8). These signals were different from the signal of daidzein without hydroxyl at position C^5 . The chemical shift value of H^6 in molecule Wu3a was shifted relatively downfield because of the presence $-\text{OH}$ at C^5 . The ^1H - ^1H correlation in COSY diagram of compound Wu3a showed two identical correlations, i.e. $\text{H}^{2'}$ - $\text{H}^{3'}$ and $\text{H}^{5'}$ - $\text{H}^{6'}$ in ring B. The fact also supported that C^5 attached a $-\text{OH}$ substituent. Thus, the compound Wu3a was elucidated as 5-hydroxy-daidzein-7-O- β -glucopyranose.

Table III.10.1. The spectroscopic data of compound Wu3a measured in MeOH-d₄

C/H	δ C (ppm)	δ^* C (ppm)	δ H (ppm)	δ^* H database (ppm)
2	156.32	154.01	8.03 (d, J = 8.1)	8.02
3	84.38	123.88	-	
4	174.21	181.37	-	
5	164.77	163.70	-	
6	101.64	99.73	6.58 (d, J = 6.4)	6.52
7	163.07	164.73	-	
8	94.00	94.34	6.39 (d, J = 6.6)	6.48
9	157.68	158.82	-	
10	115.08	106.05	-	
1'	127.93	122.90	-	
2'	130.16	130.97	7.29 (d, J = 7.3)	7.46
3'	115.08	115.82	6.76 (d, J = 6.8)	6.68
4'	157.69	158.20	-	
5'	115.08	115.82	6.76 (d, J = 6.8)	6.68
6'	130.16	130.97	7.29 (d, J = 7.3)	7.46
Gly-1''	100.41	101.8	4.95 (d, J = 6.37)	5.08
Gly-2''	73.48	73.4	3.39 – 3.80 (6H, m)	3.40 – 3.91 (6H, m)
Gly-3''	76.61	73.4		
Gly-4''	69.98	71.5		
Gly-5''	77.15	77.7		
Gly-6''	62.43	62.2		

δ^* obtained from Murthy and Rao (1986) measured in acetone-d₆

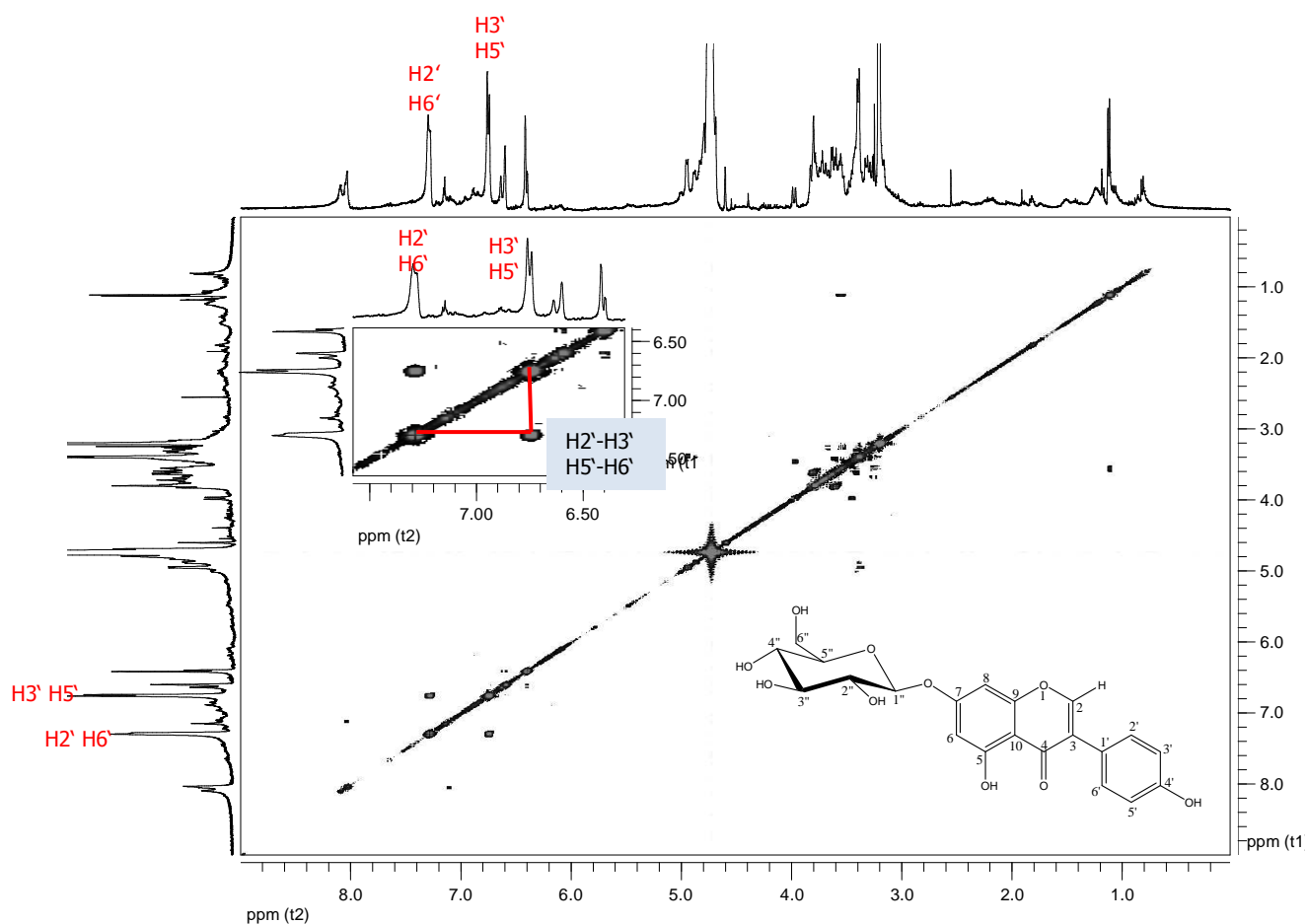


Fig III.10.6. The COSY diagram of compound Wu3a

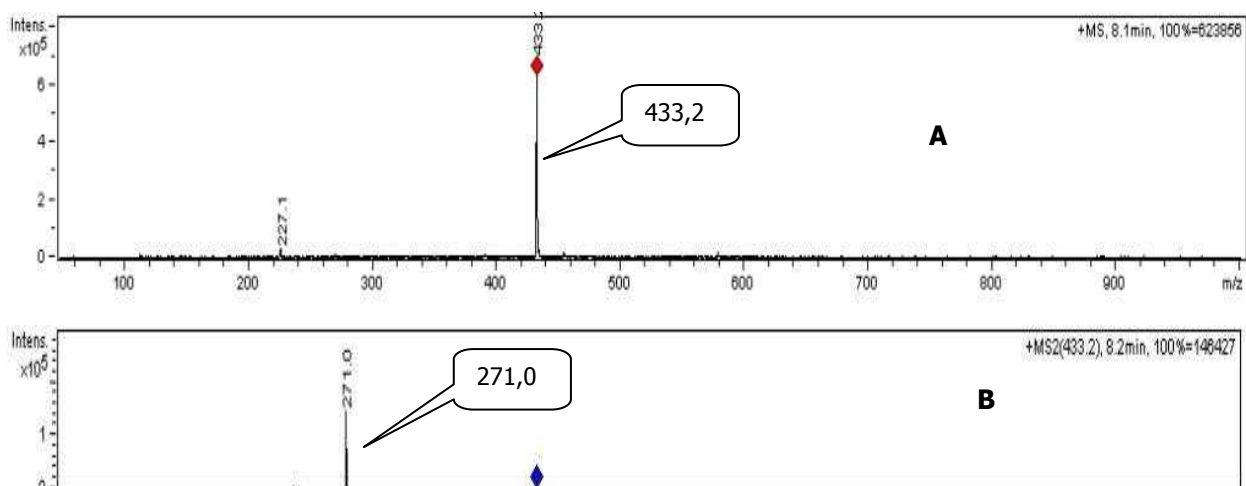


Fig. III.10.7. ESI-MS data (A) and ESI-MS-MS spectrum (B) of compound Wu3a

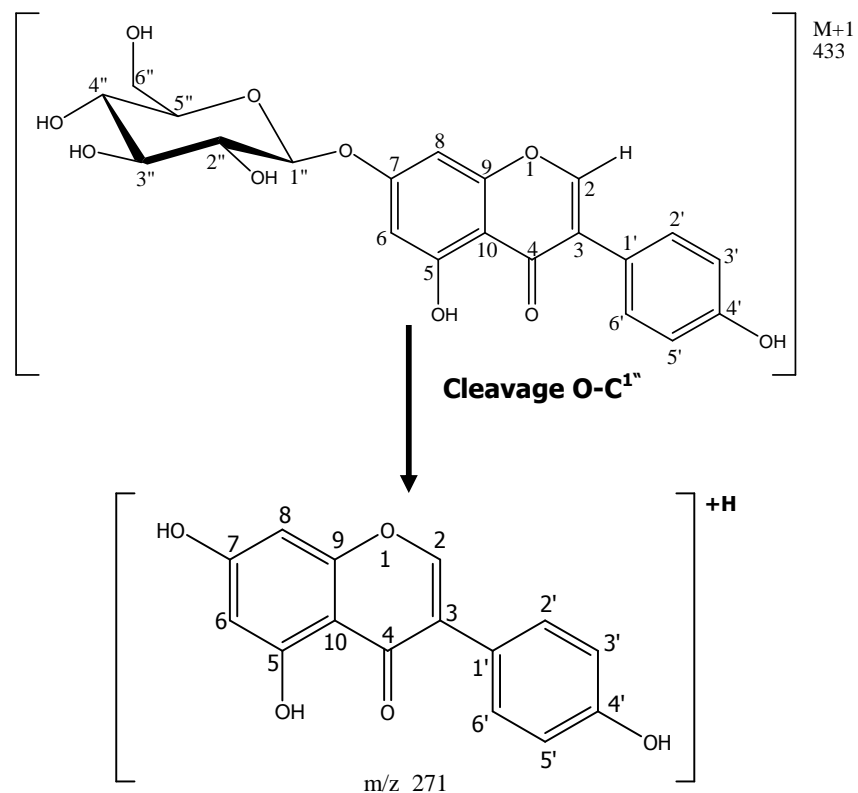
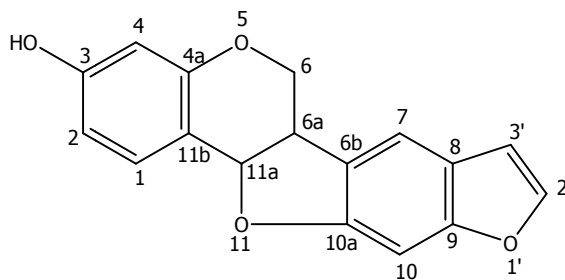


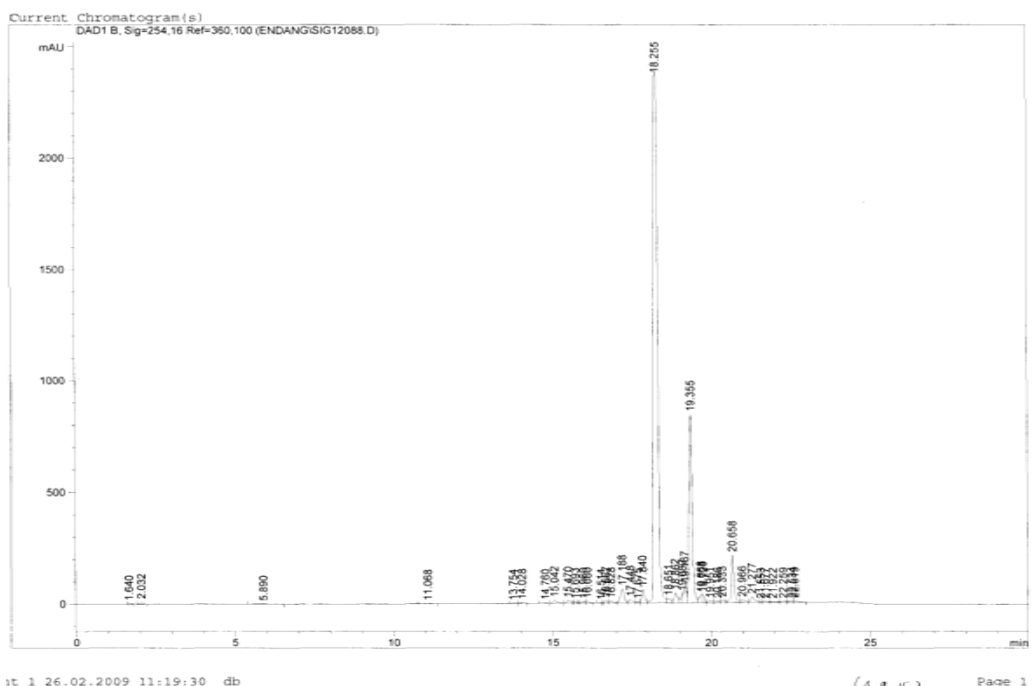
Fig. III.10.8. The fragmentation pattern of compound Wu3a

Compound Wu3a was protonated and fragmented producing signals at 433.2 $[M+H]^+$ and 271 $[M+H-\text{glucose}]^+$. Santos et al. (2006) reported that the molecule 5-hydroxy-daidzein had a main signal at m/z 269 in the negative mode of ESI-MS that was assigned to $[M-H]^{-1}$. Thus, the molecular weight of 5-hydroxy-daidzein, the aglycon of compound Wu3a, was 270 as the result of this experiment.

Based on the NMR data and LC/MS data, it could be concluded that the compound Wu3a was **5-hydroxy-daidzein-7-O- β -glucopyranose**.

III. 11. Compound A182 (8,9)-Furanyl-pterocarpan-3-ol**Fig. III.11.1. The chemical structure of compound A182 ((8,9)-Furanyl-pterocarpan-3-ol)**

Compound A182 was isolated from the ethyl acetate extract as yellow crystals. The UV spectrum (Fig III.11.3) showed that the compound A182 had a high activity to absorb the UV light at a maximum wavelength 293 nm, therefore it was predicted that compound A182 had many conjugated C-C bounds. This compound had also the potential to reduce the DPPH reagent. Thus, it was necessary to further examine to get more information about its antioxidative activity and tyrosinase inhibitory activity. The SC_{50} value (parameter for antioxidative activity) and the IC_{50} value (parameter for tyrosinase inhibitory) were 2.1 mM and 7.19 mM, respectively.

**Fig. III.11.2. Analytical HPLC chromatogram of compound A182 Tr: 18.3 min**

Inst.f.Pharmazie
Instrument Serial Number ER00093766

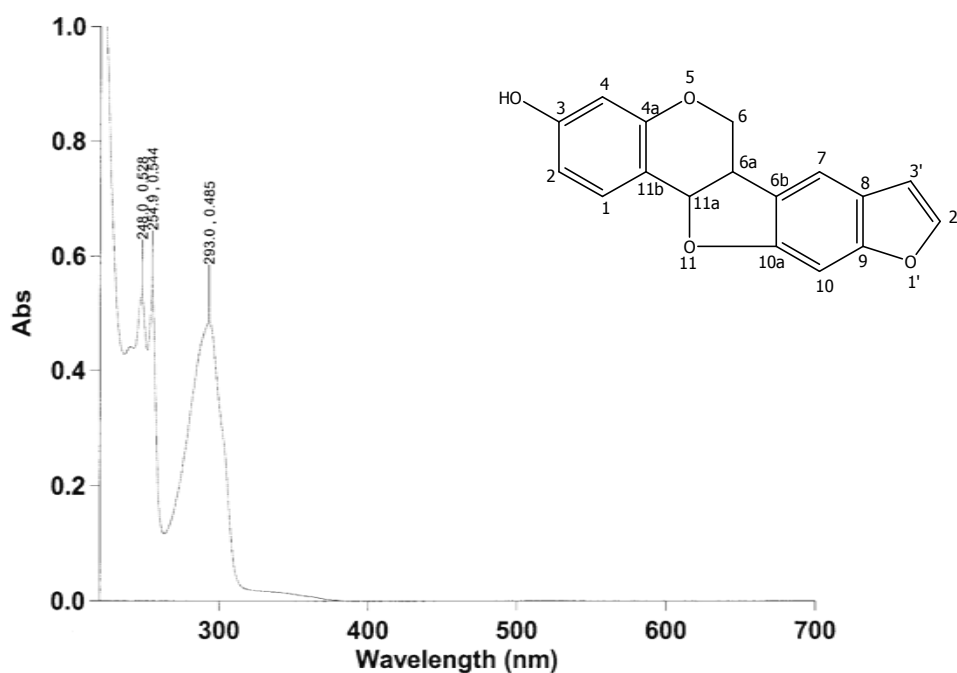


Fig. III.11.3. UV spectrum of compound A182 (λ_{max} 293 nm, measured in methanol)

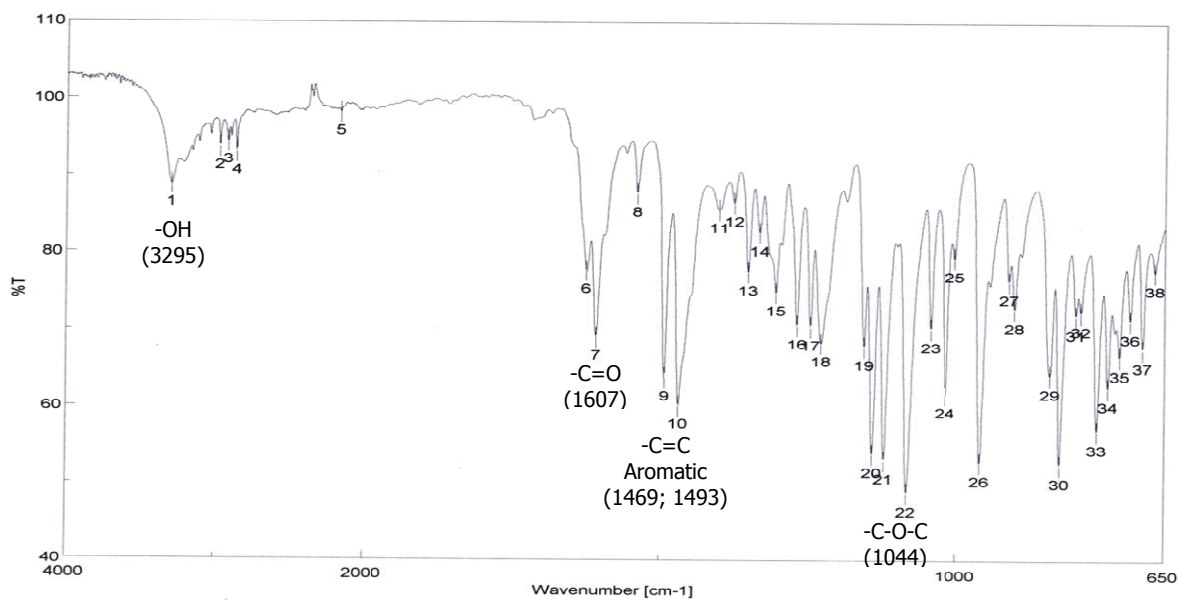


Fig. III.11.4. IR spectrum of compound A182

The molecular formula of compound A182, $C_{17}H_{12}O_4$ was determined by ESI-LC/MS m/z $[M+H]^+$ 281.3. Its 1H NMR spectrum (Fig. III.11.5) exhibited five aromatic protons at δ_H 7.6 (s, H^7), 6.9 (d, $J = 8.06$ Hz; H^1), 6.9 (s, H^{10}), 6.2 (dd, $J = 8.06$; 2.20; H^2), 6.2 (d, $J = 2.23$, H^4). There were a coupling of ortho-related protons (H^1 - H^2) and a coupling of meta-related protons (H^2 - H^4). The signals at δ_H 7.5 (d, $J = 2.25$, $H^{2'}$) and 6.7 (d, $J = 2.23$, $H^{3'}$) were characteristic for ortho-related protons in a furane system. The finding was also supported by the correlation of δ 7.5 ($H^{2'}$) and δ 6.7 ($H^{3'}$) in the COSY diagram. Four protons appeared at δ_H 4.1 (d, $J = 9.68$, H^6), 3.5 (d, $J = 10.30$, H^6), 3.4 (dd, $J = 5.63$; 2.85, H^{6a}), 5.5 (d, $J = 6.71$, H^{11a}) are characteristic for $-O-CH_2-CH-CH-O$. This fact was also supported by δC data. Detailed 1H NMR spectrum can be found in Fig III.11.6. The presence of hydroxyl group was indicated by signal at 3295 cm^{-1} in IR spectrum (Fig III.11.4). In addition, the IR spectrum showed main signals at 1607 , 1469 , 1493 cm^{-1} ($-C=C-$ aromatic) and 1084 cm^{-1} ($-C-O-C-$).

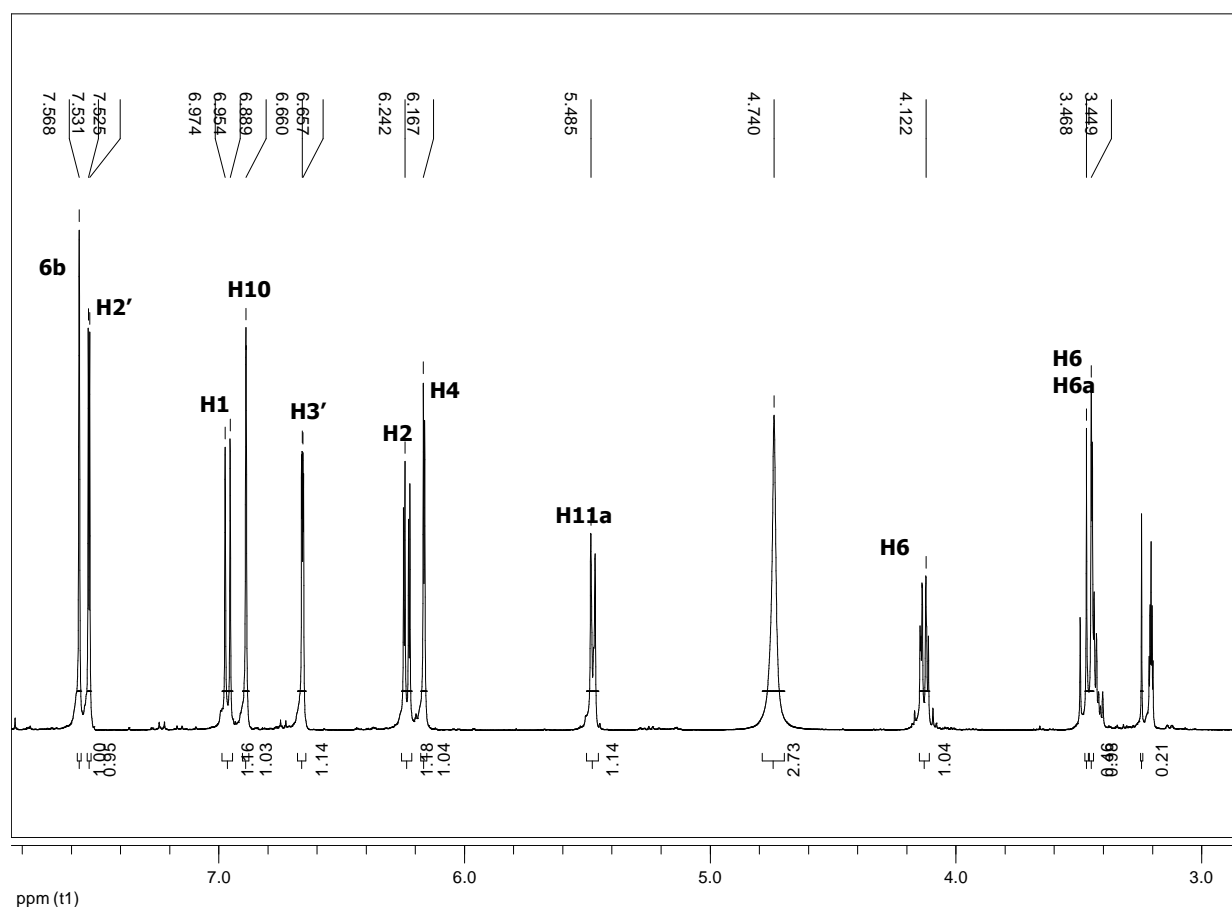


Fig. III.11.5. 1H NMR spectrum of compound A182 (MeOH- d_4 , 500 MHz)

Figure III.11.6 and III.11.7 display the ^{13}C NMR and DEPT spectrum. From the spectrum, we know that the compound A182 had 17 carbons that divided into 3 groups: 9 (-CH), 1 (-CH₂) and 7 carbon quaternary (C). Detailed NMR spectroscopy data can be found in Table III.11.1.

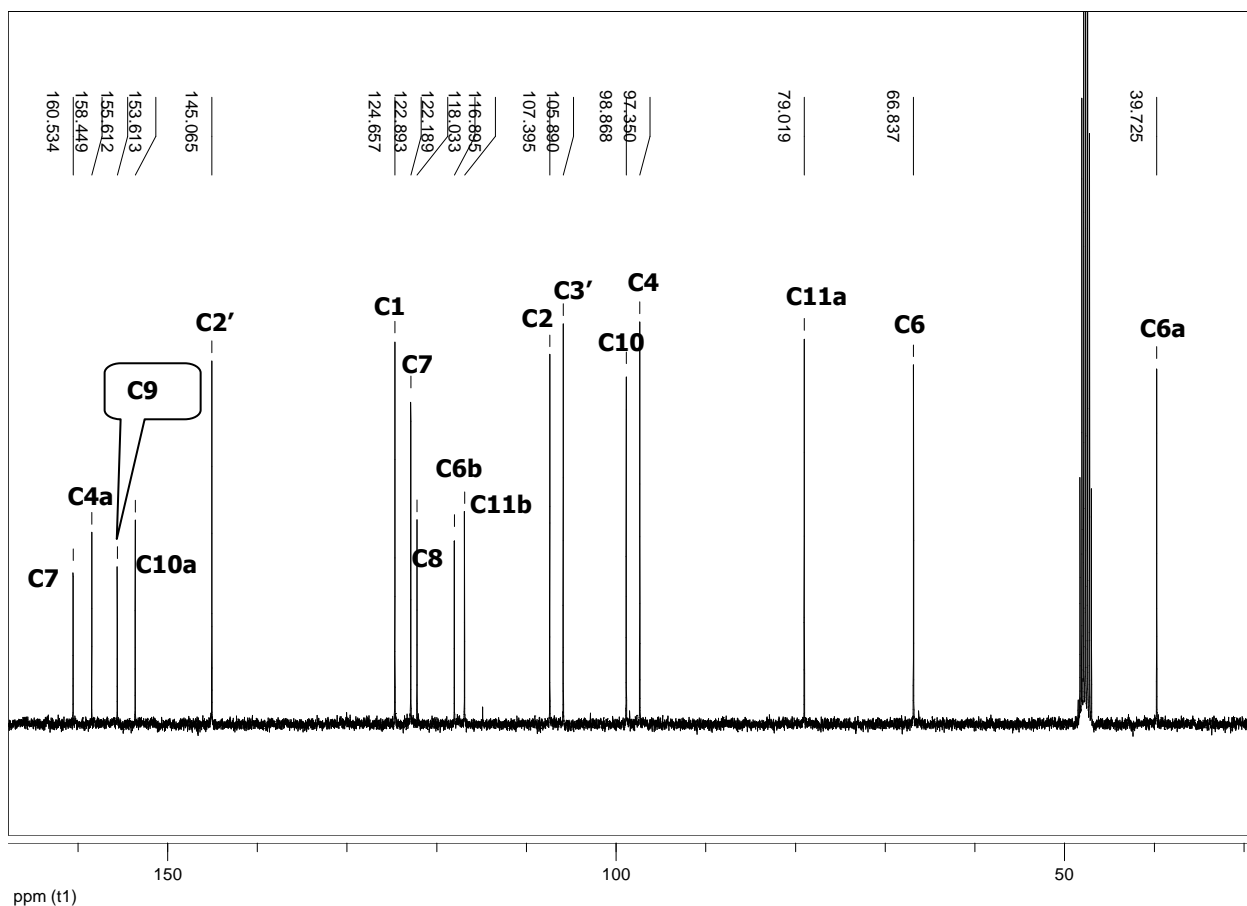


Figure III.11.6. The ^{13}C NMR spectrum of compound A182 (MeOH-d₄, 125 MHz)

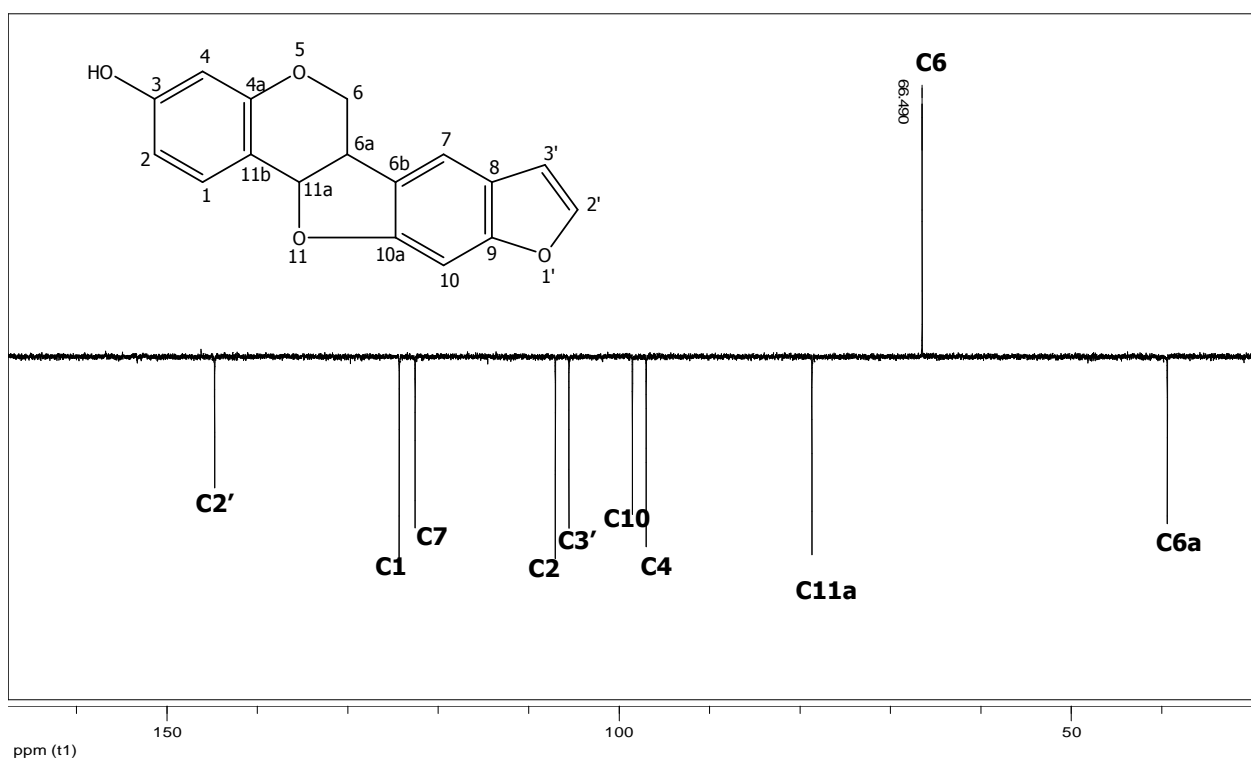


Figure. III.11.8. The DEPT spectrum of compound A182

Table III.11.1. NMR spectroscopy data of compound A182 (measured in MeOH-d₄)

C/H	δ C (ppm)	δ H (ppm)
1	124.66	6.95 (d, J = 8.06 Hz)
2	107.40	6.22 (dd, J = 8.06; 2.20 Hz)
3	160.53	-
4	97.35	6.17 (d, J = 2.15 Hz)
4a	158.45	-
6	66.84	4.14 (d, J = 9.68 Hz) 3.48 (d, J = 10.30 Hz)
6a	39.73	3.44 (dd, J = 5.63; 2.85 Hz)
6b	116.90	-
7	122.89	7.57 (s)
8	122.19	-
9	155.61	-
10	98.87	6.89 (s)
10a	153.61	-
11a	79.02	5.49 (d, J = 6.71 Hz)
11b	118.03	-
2'	145.07	7.53 (d, J = 2.25 Hz)
3'	105.89	6.66 (d, J = 2.23 Hz)

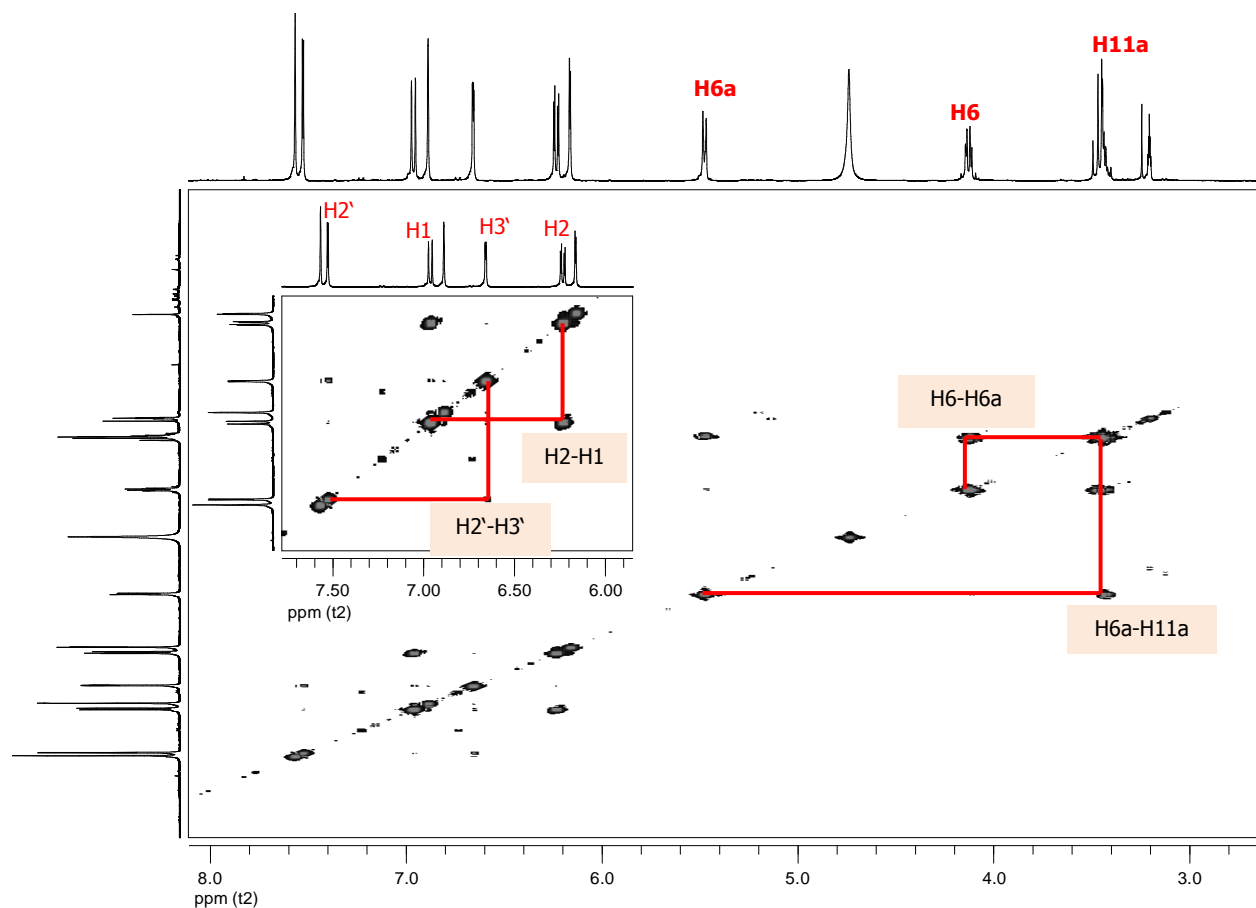


Fig. III.11.8. The COSY diagram of compound A182

Figure III.11.9 below displayed the ^1H - ^{13}C long-range correlations in compound A182 observed in HMBC spectra.

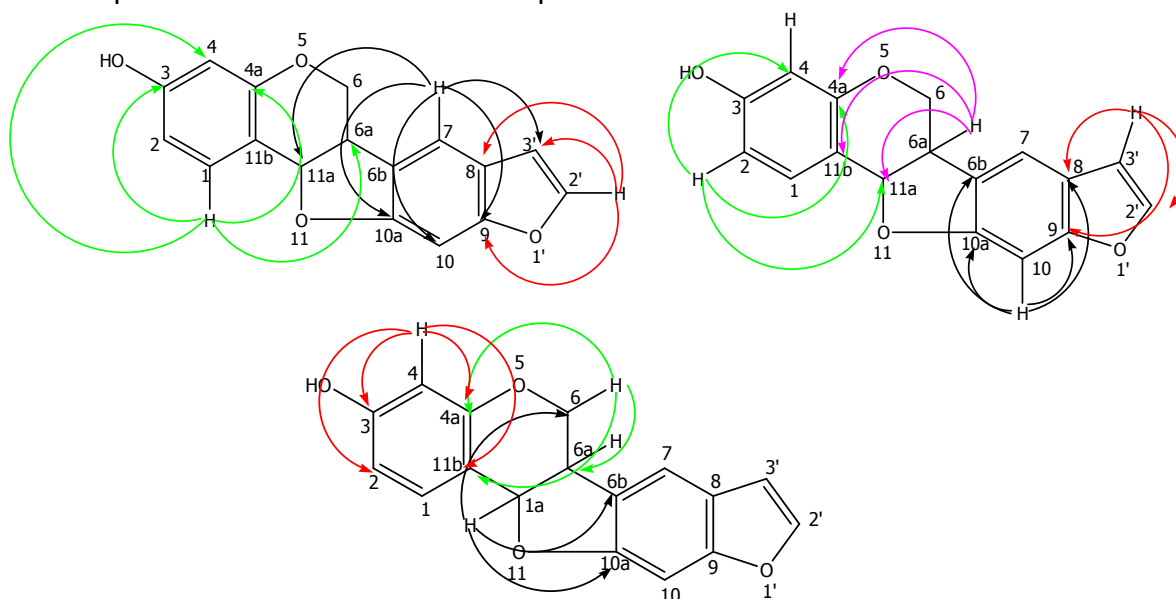


Figure. III.11.9. ^1H - ^{13}C long-range correlations observed from HMBC diagram of compound A182

ESI-MS spectra show that the compound A182 was fragmented producing signal m/z at 123 (in positive detection) and m/z at 121 (in negative detection). Figure III.11.10 displays the fragmentation pattern of compound 182.

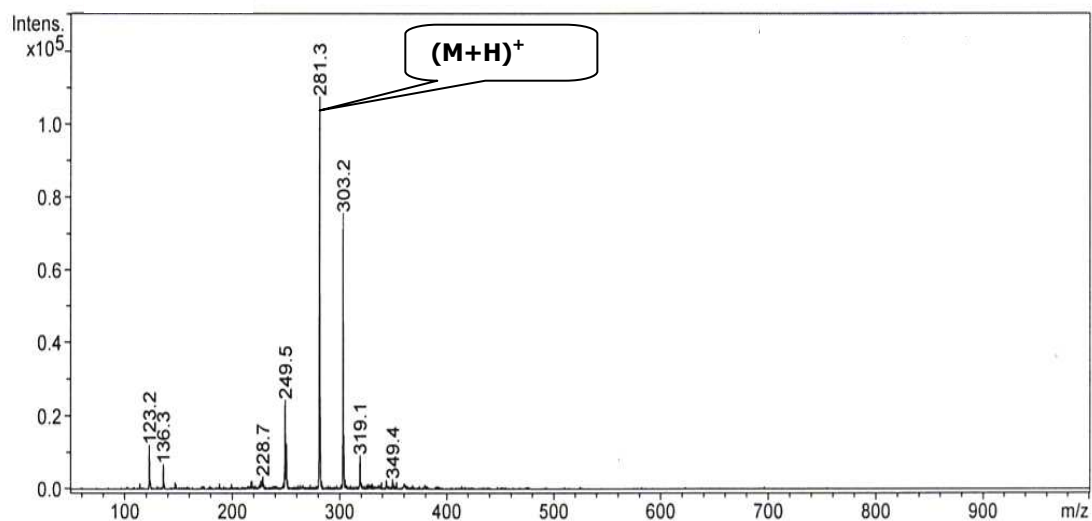


Fig.III.10a. ESI-MS spectrum of compound A182

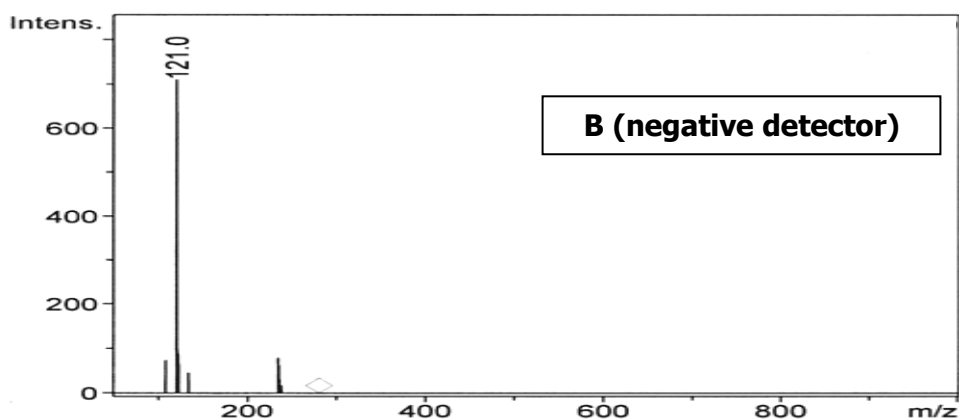
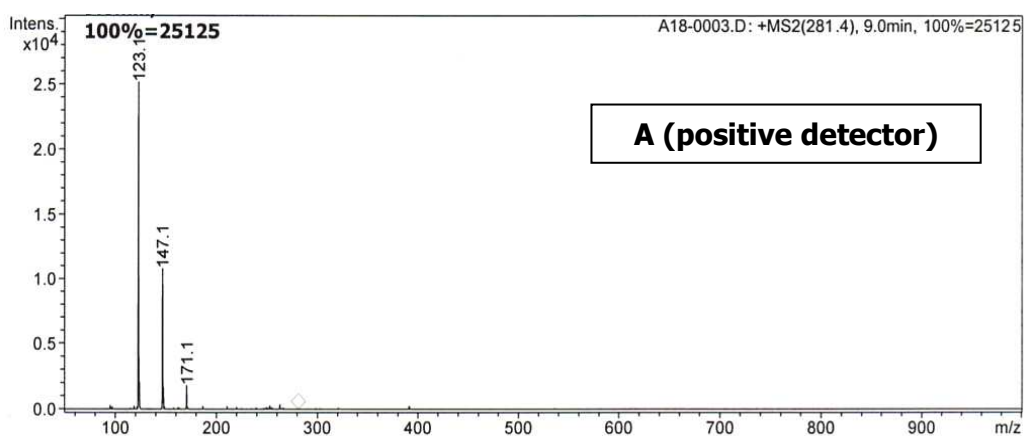


Fig.III.10b. ESI-MS spectrum of fragmentation of compound A182

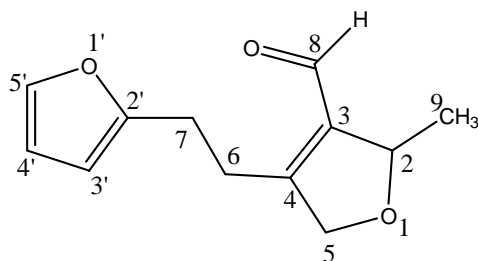
III.12. Compound HWu10**4-(2-(Furane-2-yl)ethyl)-2-methyl-2,5-dihydrofurane-3-carbaldehyde**

Fig.III.12.1. The chemical structure of compound HWu10 4-(2-(furane-2-yl)ethyl)-2-methyl-2,5-dihydrofurane-3-carbaldehyde

Compound (HWu10) was obtained from the ethyl acetate extract as yellow powder. The GC/MS chromatogram of this compound (Fig.III.12.4) shows two peaks at 19.2 and 21.7 minutes which have molecular ion signals at m/z 126 and 206, respectively, as described in Fig III.12.9. The molecular formula was confirmed as $C_7H_{10}O_2$ for m/z 126 and $C_{12}H_{14}O_3$ for m/z 206. The molecule which has a molecular mass of 126 might be 2,4-dimethyl-2,5-dihydrofurane-3-carbaldehyde as a degradation product of the main molecule (4-(2-(furane-2-yl)ethyl)-2-methyl-2,5-dihydrofurane-3-carbaldehyde) during process in the gas chromatography.

Inst.f.Pharmazie
Instrument Serial Number ER00093766

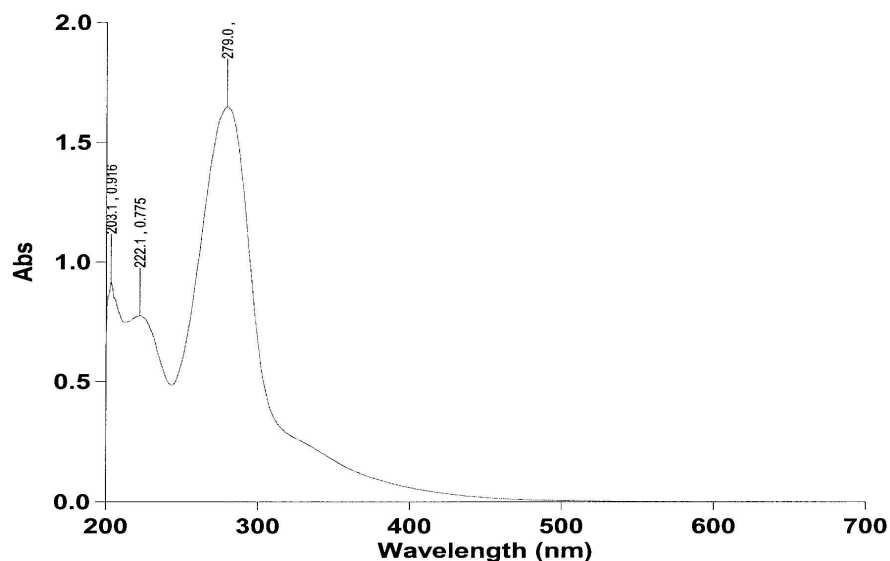


Fig. III.12.2. UV spectrum of compound HWu10

The IR spectrum (Fig.III.12.3) indicates the presence of C-C double bond or C=O (1668 cm^{-1}), a -CH aliphatic group (2930 cm^{-1}), and a -CH₂ (1446 cm^{-1}). Additionally, the IR spectrum shows 1021 cm^{-1} (-C-O-C group). The presence of aldehyde group could be deduced from the signals at δ_{H} 9.45 ppm and from the chemical shift value of ^{13}C NMR at δ 178.56 ppm. An intense cross peaks observed in ^1H - ^{13}C HMBC diagram correlates δ 158.23 (C⁸) to δ 9.45 (H⁸) ($^2J_{\text{C-H}}$). The evidence suggested that the aldehyde group was attached to C-C double bond of a dihydrofuran ring (C³).

The signals at δ_{H} 7.27 ppm and 6.56 ppm were characteristic for hydrogens that were bound to the C-C double bond in the furane ring. The presence of a pair of triplets at δ 2.49 and δ 2.70 was due to the protons at C⁶ and C⁷ in molecule HWu10. The complete data of the chemical shift value can be found in Table III.12.1.

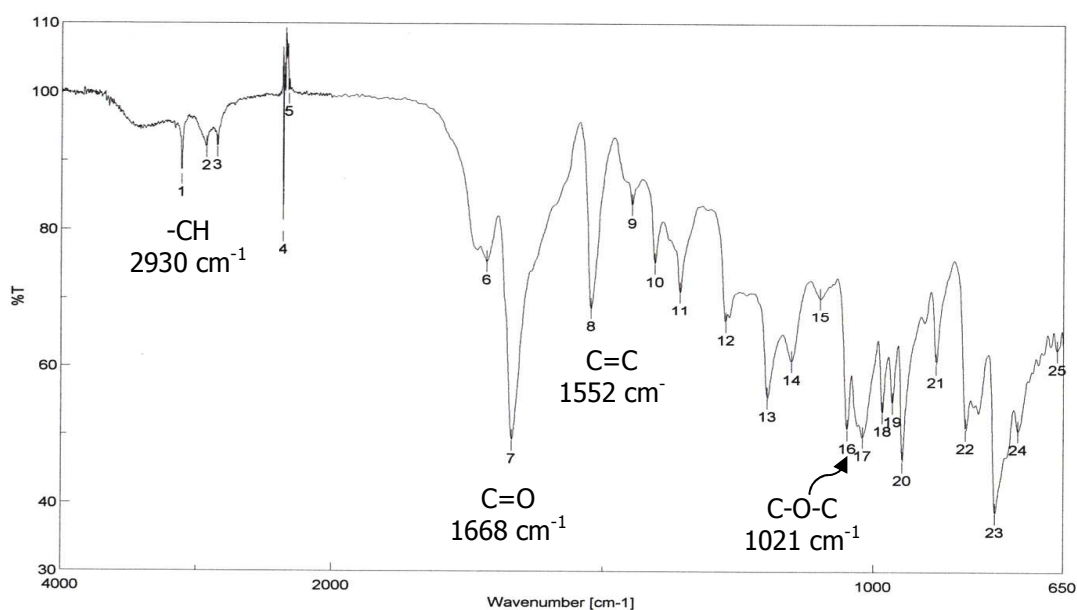


Fig. III.12.3. IR spectrum of compound HWu10

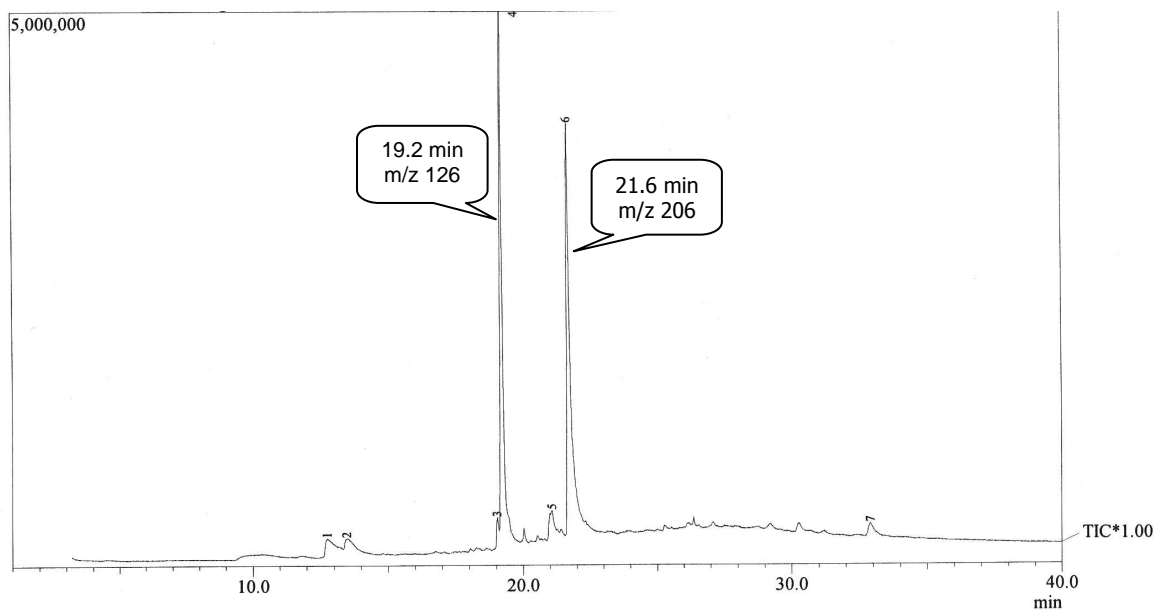


Fig.III.12.4. GC/MS chromatogram of compound HWu10

Table III.12.1. ^1H NMR and ^{13}C NMR spectroscopic data of the compound HWu10 measured in MeOH-d_4

C/H	δ C (ppm)	δ H (ppm)
2	58.00	5.05 (1H, s)
3	158.29	-
4	173.28	-
5	64.15	4.54 (2H, d)
6	27.43	2.49 (2H, t)
7	37.40	2.70 (2H, t)
8	178.56	9.45 (1H, s)
9	28.24	2.05 (3H, s)
2'	153.28	-
3'	112.06	7.27 (1H, d)
4'	123.36	6.56 (1H, dd)
5'	123.36	7.27 (1H, d)

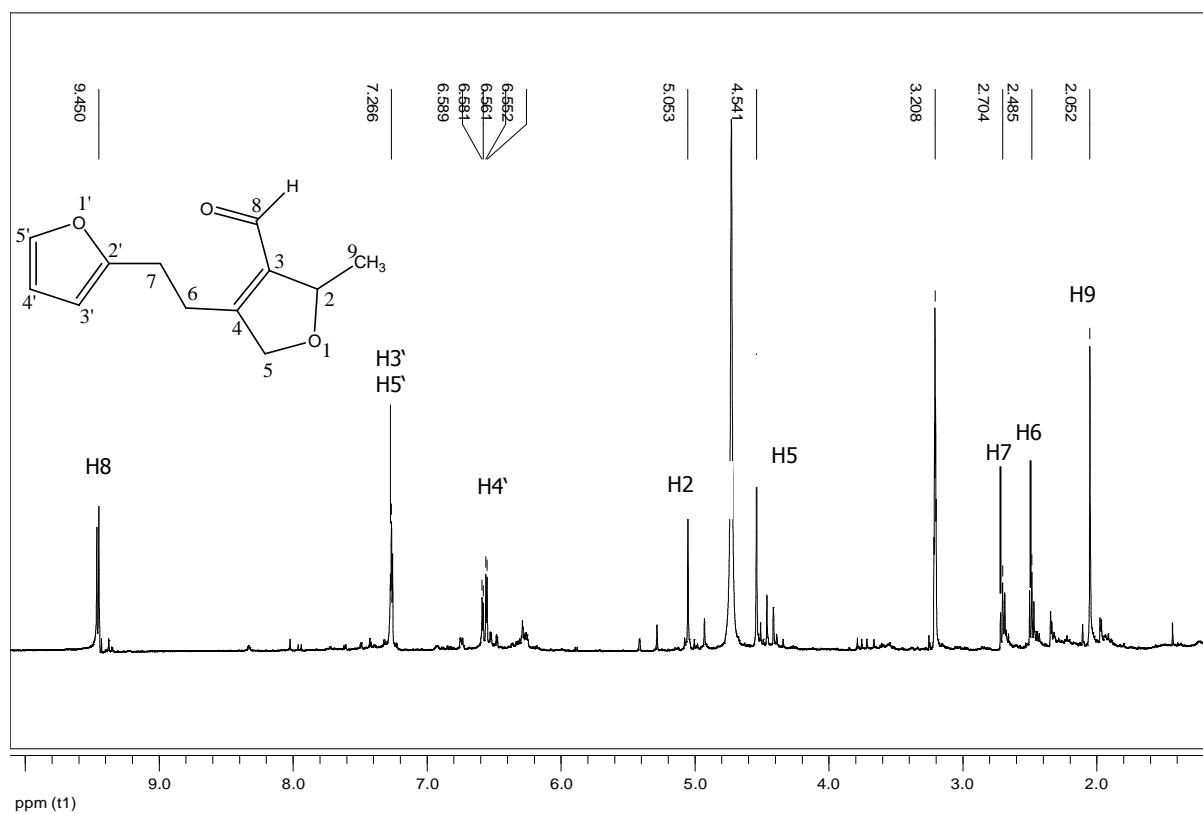


Fig. III.12.5. ¹H NMR spectrum of compound HWu10 (MeOH-d₄, 500 MHz)

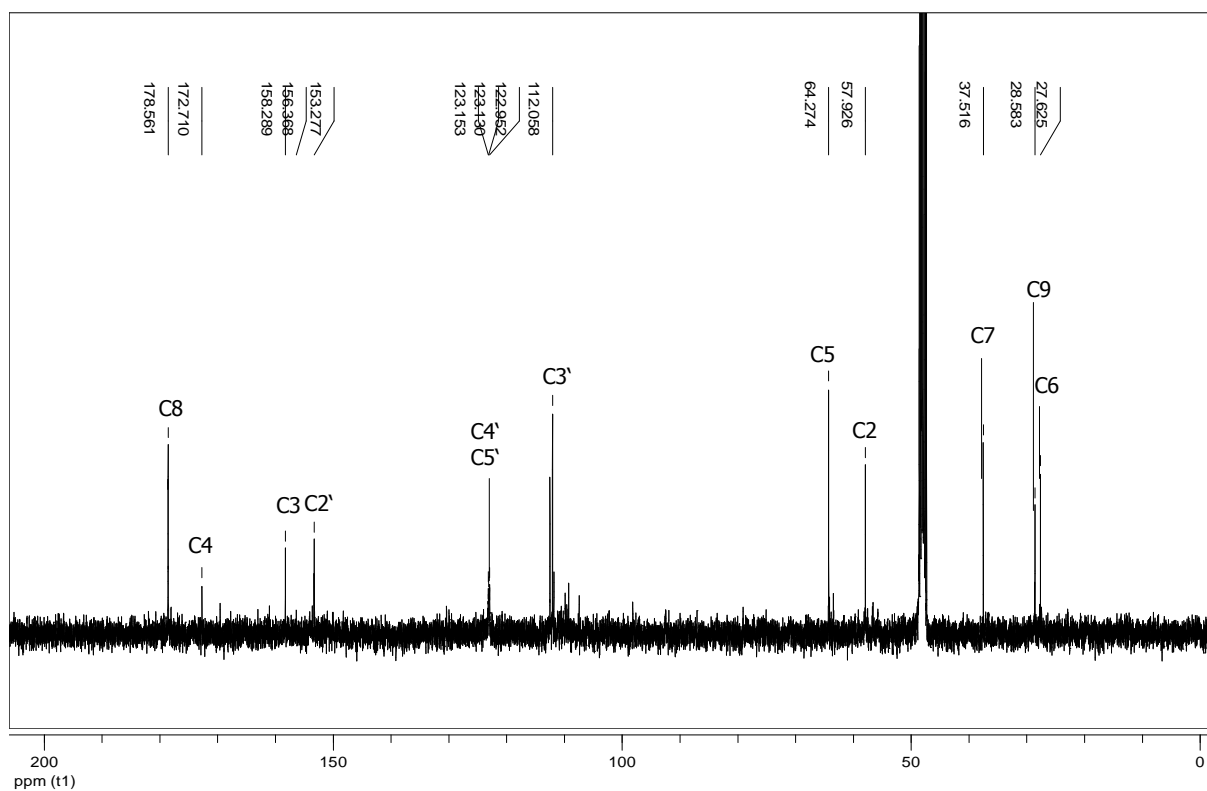


Fig. III.12.6. ¹³C NMR spectrum of compound HWu10 (MeOH-d₄, 125 MHz)

The COSY diagram in Fig III.12.7 shows the correlation of H⁶-H⁷ and H^{4'}-H^{5'}. The correlation between δ 7.27 ppm (d, H^{3'} and H^{5'}) and δ 6.56 ppm (dd, H^{4'}) is characteristic for three protons in the furane ring, i.e. H^{3'}, H^{5'} and H^{4'}, respectively. Some of the ¹H-¹³C-long range correlations (Figure III.12.8.) observed in the HMBC spectrum confirmed that the structures of HWu10 to be 4-(2'-(furane-2-yl)ethyl)-2-methyl-2,5-dihydrofurane-3-carbaldehyde.

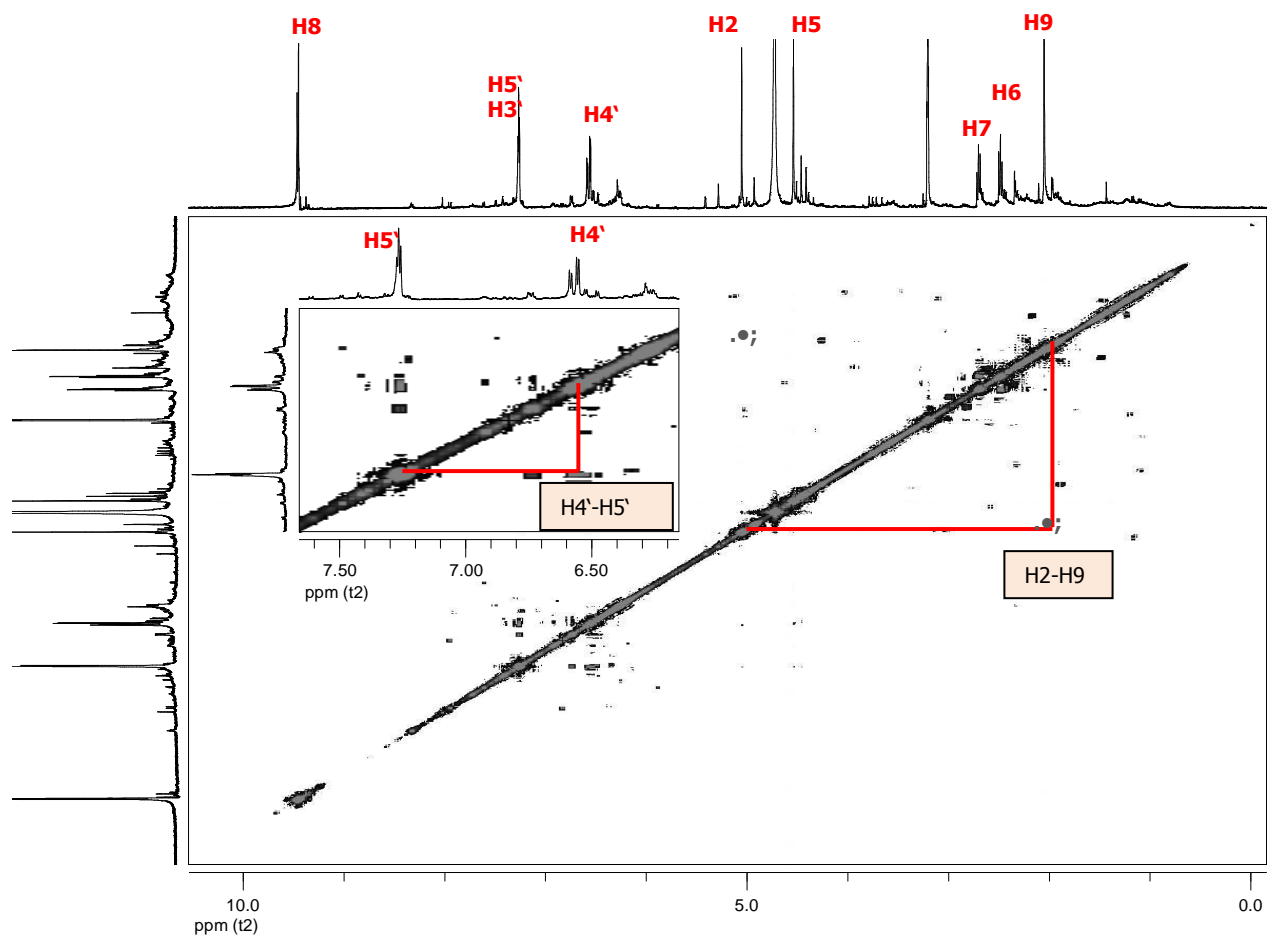


Fig.III.12.7. COSY diagram of compound HWu10

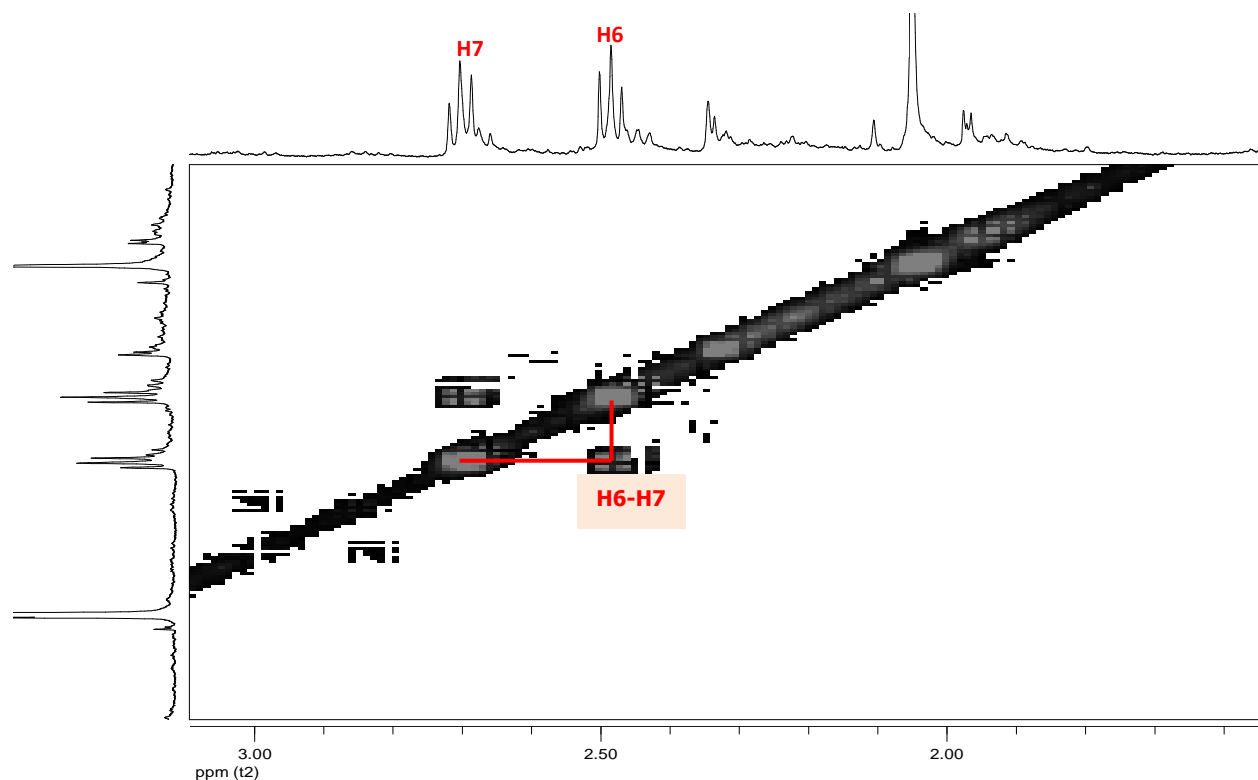


Fig.III.12.7. COSY diagram of compound HWu10

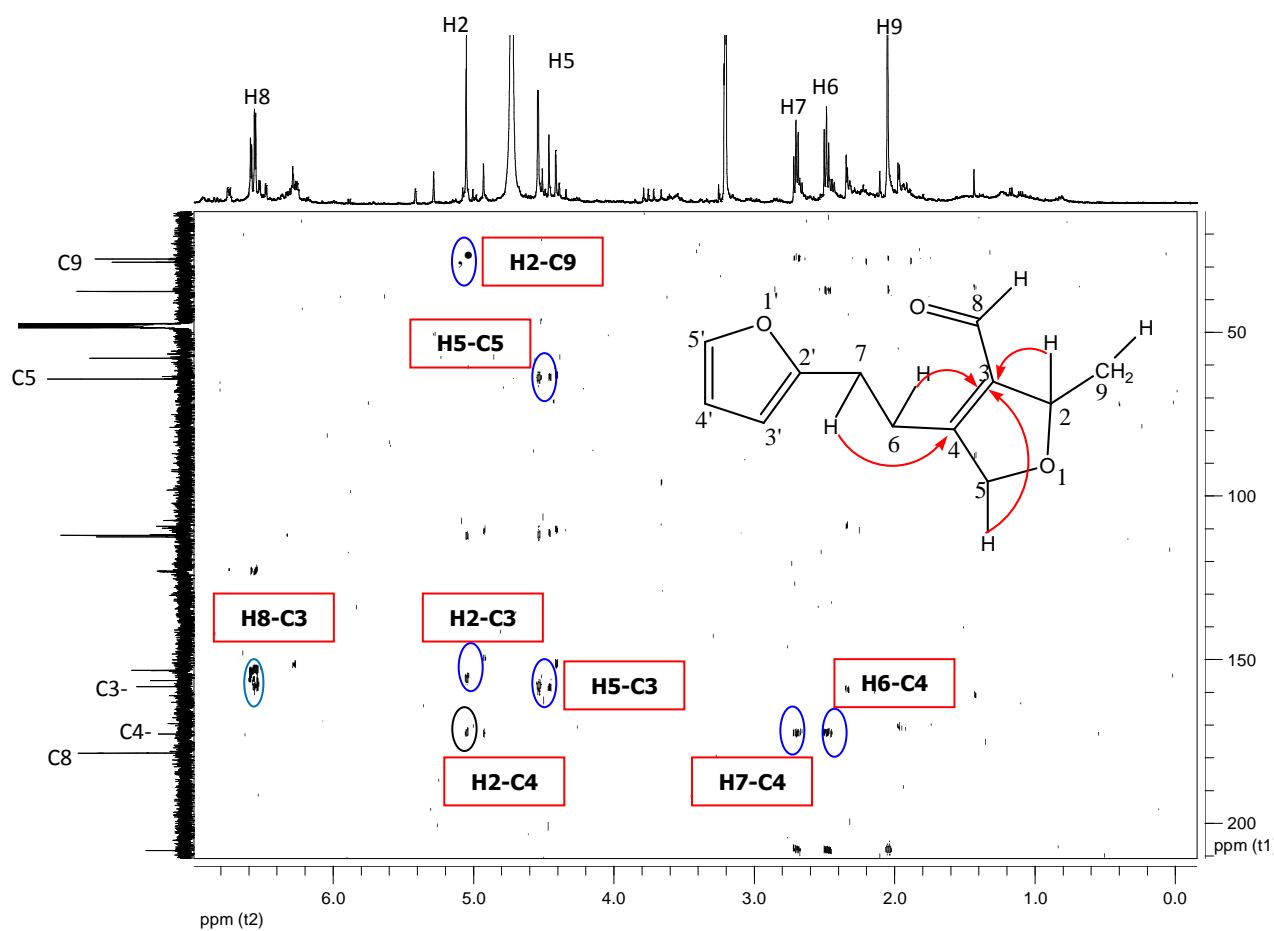


Fig. III.12.8. The HMBC diagram of the compound Hwu10

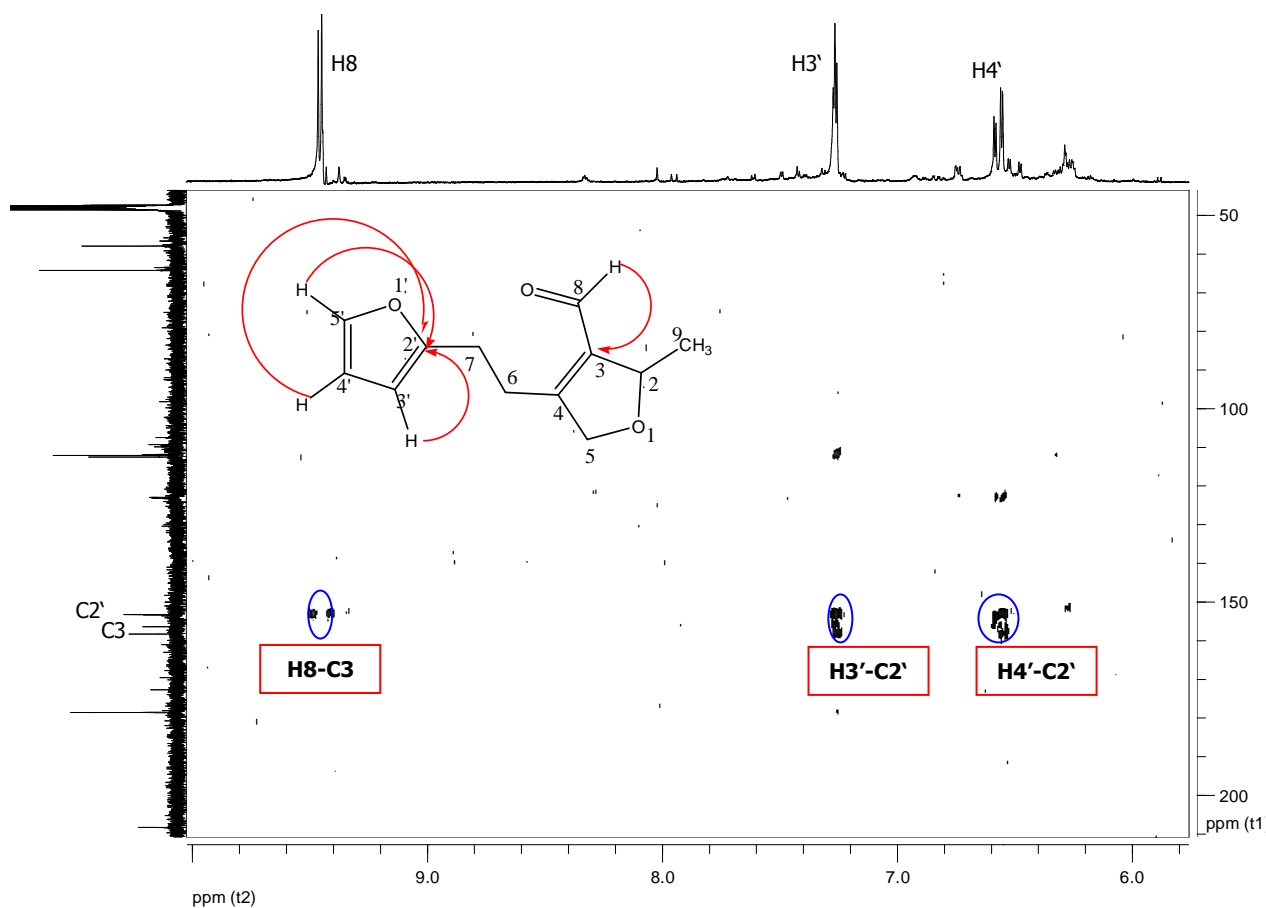


Fig. III.12.8. The HMBC diagram of the compound HWu10

Figure III.12.10 displayed the mass fragmentation pattern of compound HWu10 based on the EI-MS spectrum.

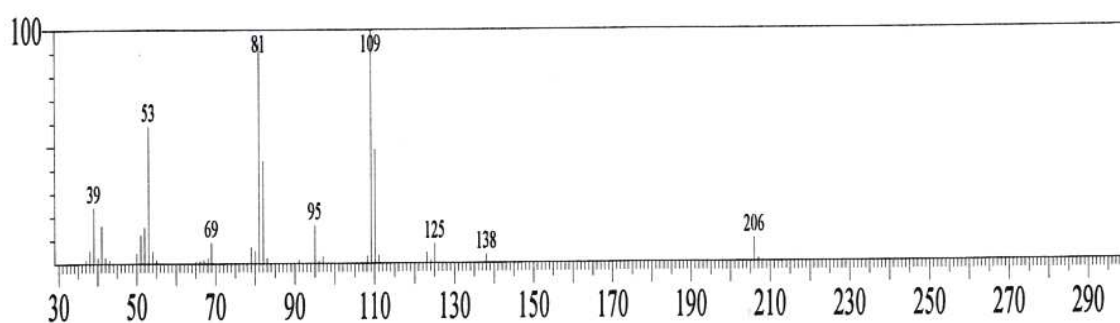


Fig.III.12.9. EI-MS spectrum of compound HWu10

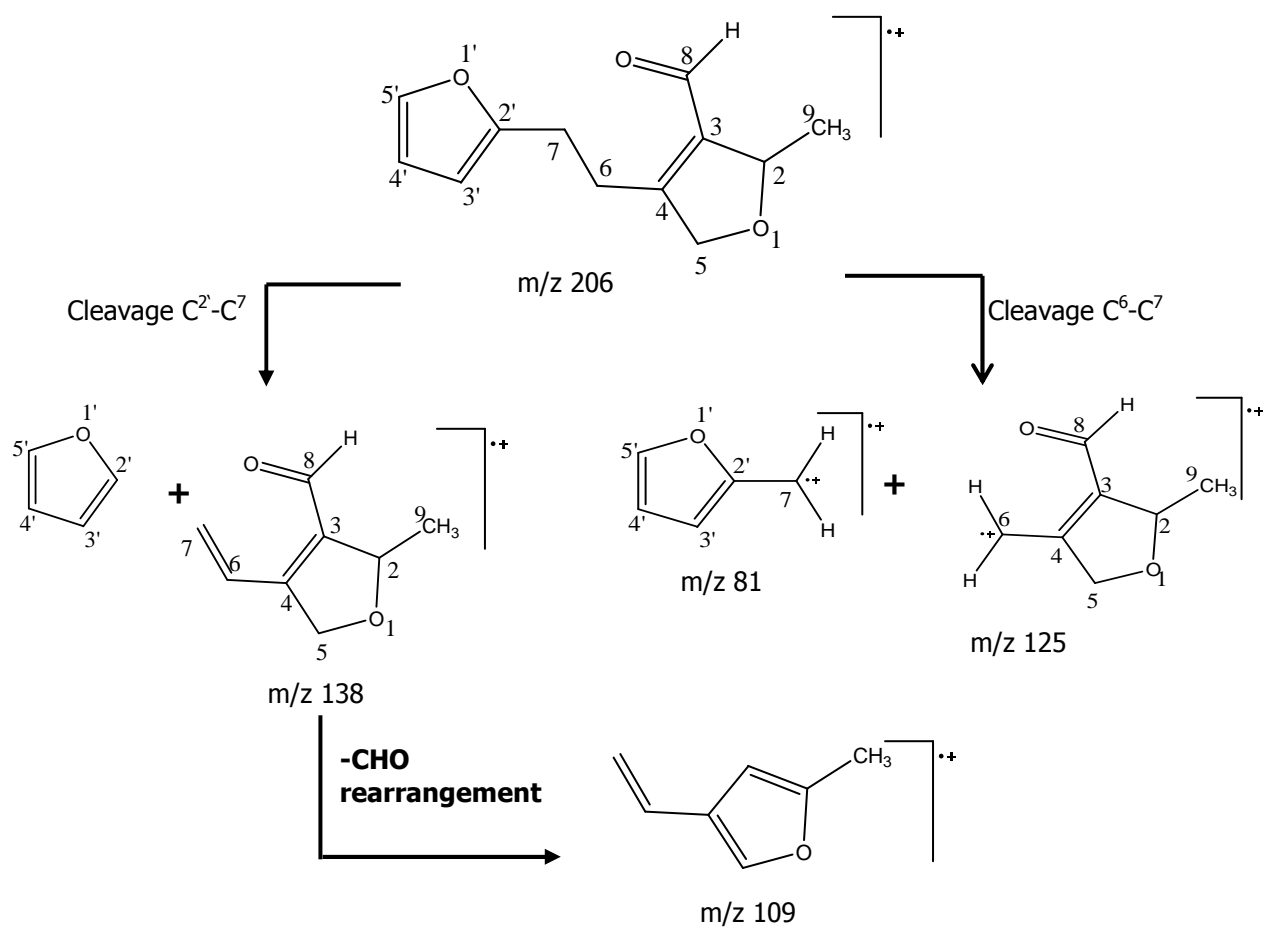


Fig.III.12.10. The fragmentation pattern of compound HWu10

The signal at m/z 206 in the EI-MS spectrum of compound HWu10 (Fig.III.12.9) was assigned to $[M]^+$. During the process in EI-MS, compound HWu10 was fragmented producing signal at m/z 138 because of cleavage at $C^{2'}-C^7$. This fragment was further fragmented by loss the $-CHO$ and followed by rearrangement producing signal at m/z 109. Additionally, compound HWu10 could be fragmented by cleavage at C^6-C^7 producing signal at m/z 81 and 125.

Based on all data, the compound HWu10 was identified as 4-(2-(furan-2-yl)ethyl)-2-methyl-2,5-dihydrofuran-3-carbaldehyde.

III.13. Compound WuBuOH (2-Butoxy-2,5-bis(hydroxymethyl)-tetrahydrofuran-3,4-diol)

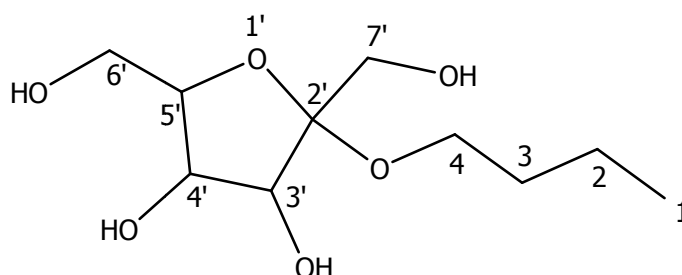


Fig. III.13.1. Chemical structure of compound WuBuOH

Compound WuBuOH was isolated from the butanol extract as a brown powder which was able to reduce the DPPH and absorb the UV light. Figure III.13.2 shows the HPLC chromatogram of fraction containing the compound WuBuOH and some other impurity. This compound has a retention time of 8.9 min. The EI-MS spectrum (Fig.III.13.9) shows the molecular ion peak at m/z 236 consistent with the molecular formula $C_{10}H_{20}O_6$. The IR spectrum (Fig.III.13.3) shows a band at 3316 cm^{-1} is due to the presence of a hydroxyl group (-OH). The absorption band at 1033 cm^{-1} is due to ether group (-C-O-C-) or in this case an acetal group at $C^{2'}$. The presence of the acetal group is supported by a signal of the ^{13}C NMR spectrum at δ_c 107.7 ppm (C quaternary) and two signals of the HMBC diagram (correlations between $H^{7'}-C^{2'}$ and $H^{3'}-C^{2'}$). The signal at 1622 cm^{-1} might be due to the contamination of the glycosidic daidzein. Since the glycosidic daidzein is a polar substance, it can be extracted with butanol.

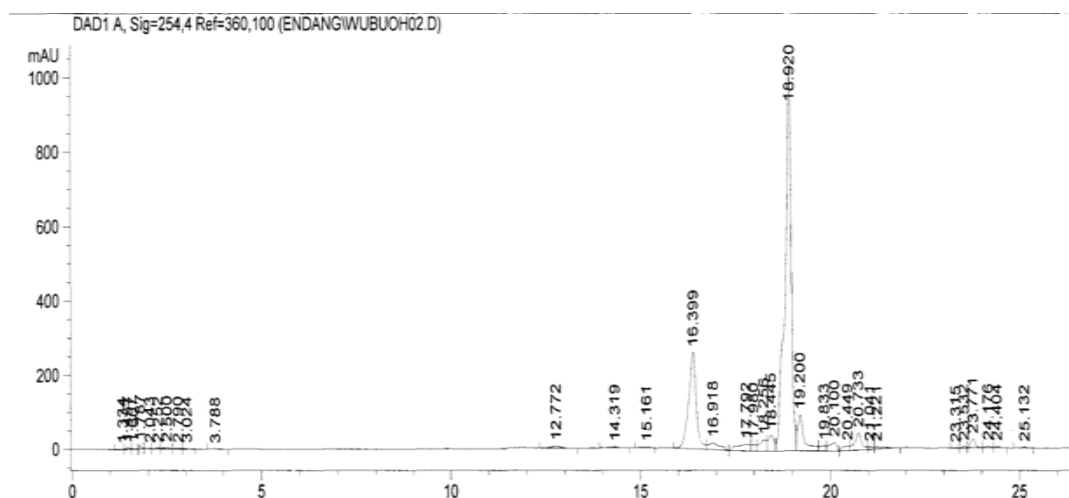


Fig.III.13.2. The HPLC chromatogram of compound WuBuOH

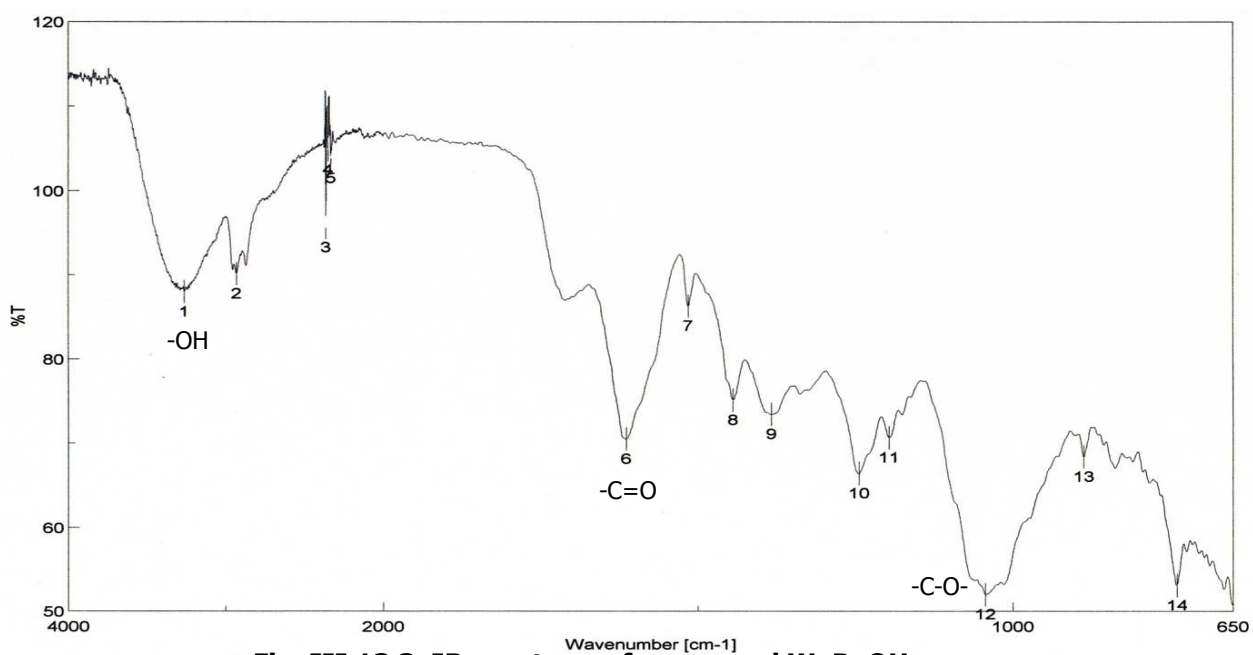


Fig. III.13.3. IR spectrum of compound WuBuOH

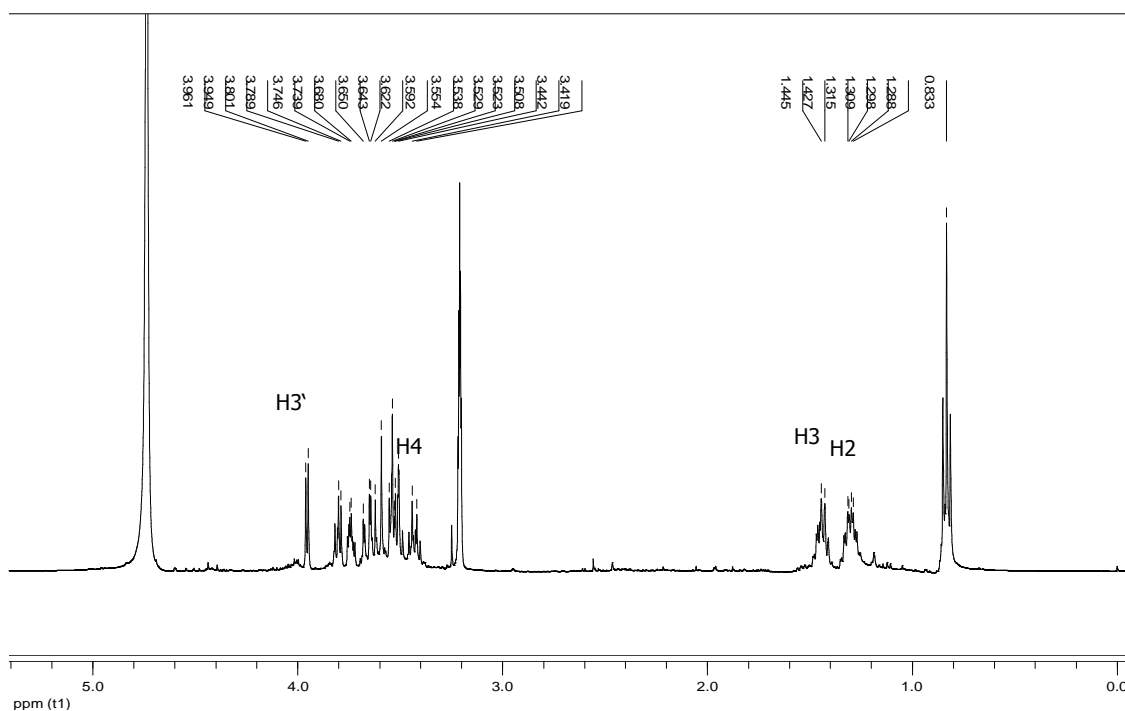


Fig. III.13.4. ¹H NMR spectrum of compound WuBuOH (MeOH-d₄, 500 MHz)

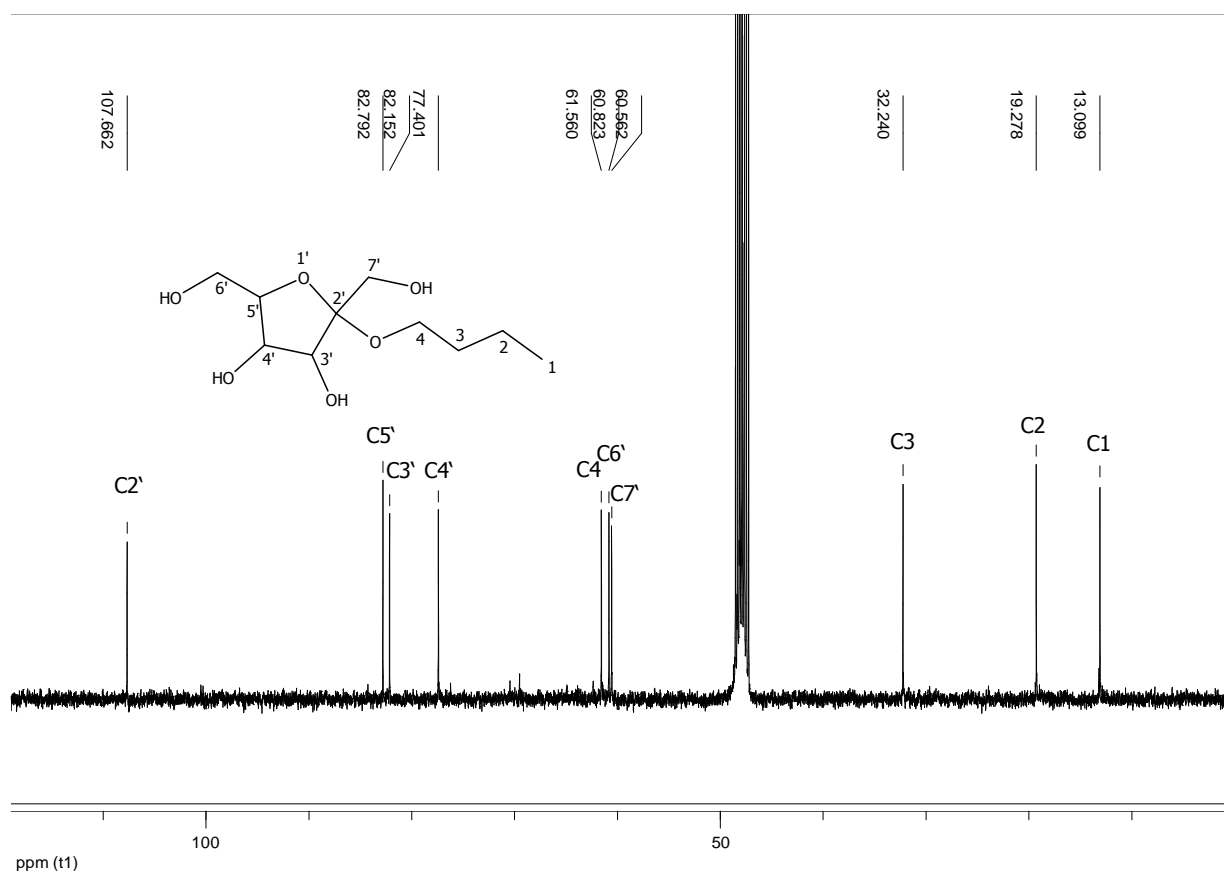


Fig. III.13.5. ^{13}C NMR spectrum of compound WuBuOH (MeOH- d_4 , 125 MHz)

In the ^1H NMR spectrum (Fig.III.13.4), the signals could be divided into two groups. The first group was signals at δ 3.59 – 3.96 ppm, and the other group was the signals at δ 0.83 – 1.45 ppm. The presence of signals at δ 3.59 – 3.96 ppm of the ^1H NMR spectrum was typical of sugar moiety. Thus, the compound WuBuOH was assigned to a glycosidic derivative. Since a signal at δ 5.02 ppm didn't appear, the sugar group didn't have an anomeric proton. The sugar was concluded as a fructose. While the signals at δ 0.83 – 1.45 ppm was characteristic for the alkane group. They were also in accordance with the signals in ^{13}C NMR spectrum. Based on the NMR signals, both in ^1H NMR and ^{13}C NMR, the alkane group was assigned to butyl group. The presence of butyl was also supported by the signal at m/z 73 in EI-MS spectrum. The signal at m/z 73 in the EI-MS spectrum described that the butyl group was bound to an oxygen of the fructose ($-\text{O}-\text{C}_4\text{H}_9$). Table III.13.1 displays the spectroscopic data of the compound WuBuOH. The fragmentation pattern of this compound can be seen in scheme (Fig.III.13.10).

Table. III.13.1. The spectroscopic data of compound WuBuOH (measured in MeOH-d₄)

C/H	δ C (ppm)	δ^* C (ppm)	δ H (ppm)	δ^* H database (ppm)
1	13.09	14.1	0.83 (3 H, t, J = 0.8)	0.96
2	19.05	19.0	1.31 (2H, m, J = 1.3)	1.33
3	32.81	32.8	1.45 (2H, m, J = 1.5)	1.46
4	61.33	64.3	3.42 (2H, m, J = 3.5)	3.37
1'	-	-	-	-
2'	107.66	110.2	-	-
3'	82.15	76.9	3.96 (1H, d, J = 4.0)	3.97
4'	77.40	72.1	3.80 (1H, t, J = 3.8)	3.65
5'	82.79	80.7	3.76 (1H, m, J = 3.7)	3.91
6'	60.59	62.2	3.65 (1H, m, J = 3.6)	3.54
			3.68 (1H, m, J = 3.6)	3.79
7'	60.33	61.9	3.59 (1H, s)	3.66
			3.53 (1H, s)	3.91

The COSY experiments (Fig.III.13.6) showed the expected correlations between the protons of H¹-H², H²-H³, H³-H⁴ and H^{3'}-H^{4'}. Some of the ¹H-¹³C- long-range correlations can be found in Fig.III.13.8. The correlation ³J_{C-H} in HMBC diagram between δ 107.66 (C^{2'}) with δ 3.44 (H⁴) showed that the butyl group was attached to oxygen of C^{2'}.

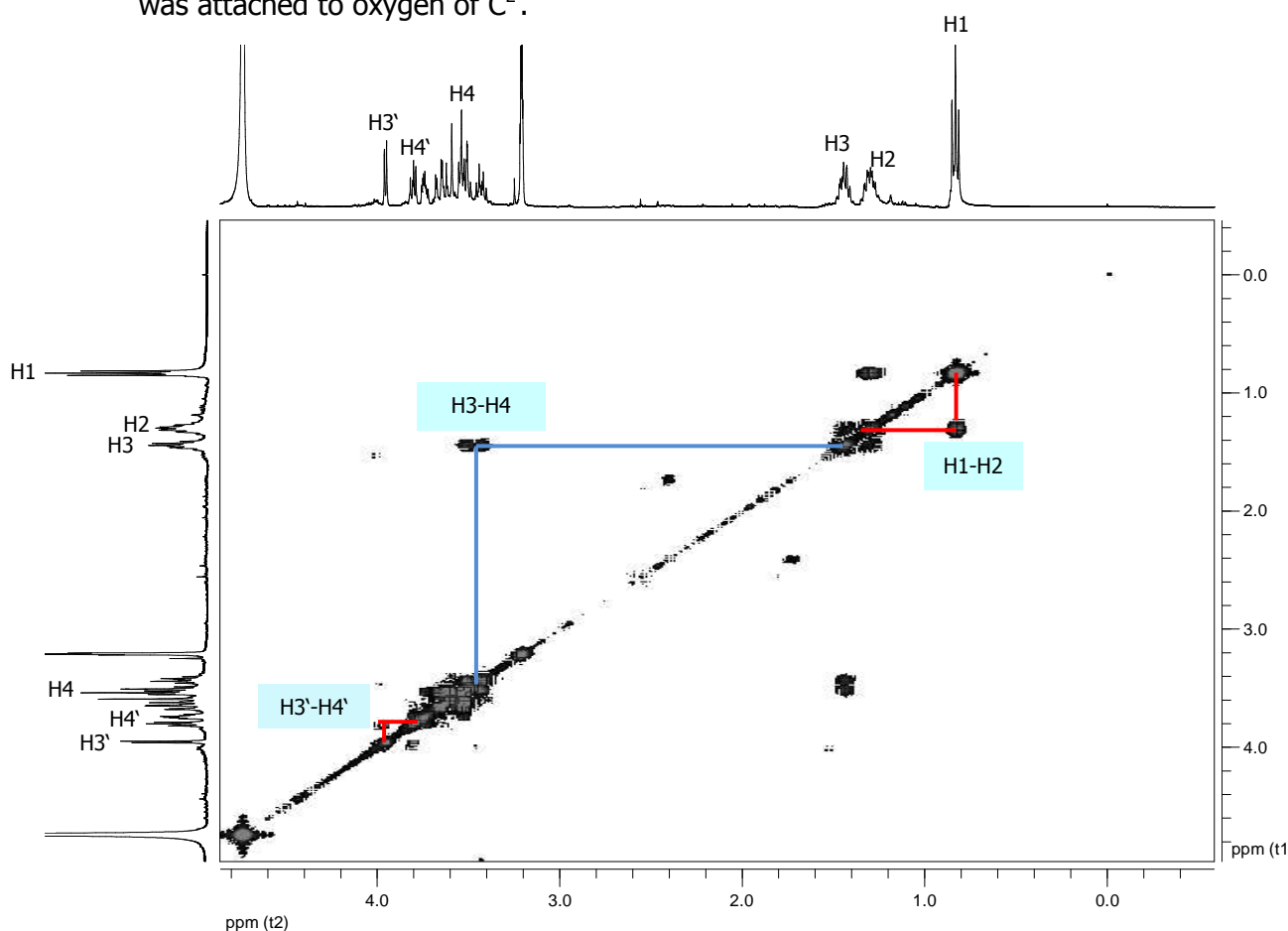


Fig.III.13.6. The COSY diagram of compound WuBuOH

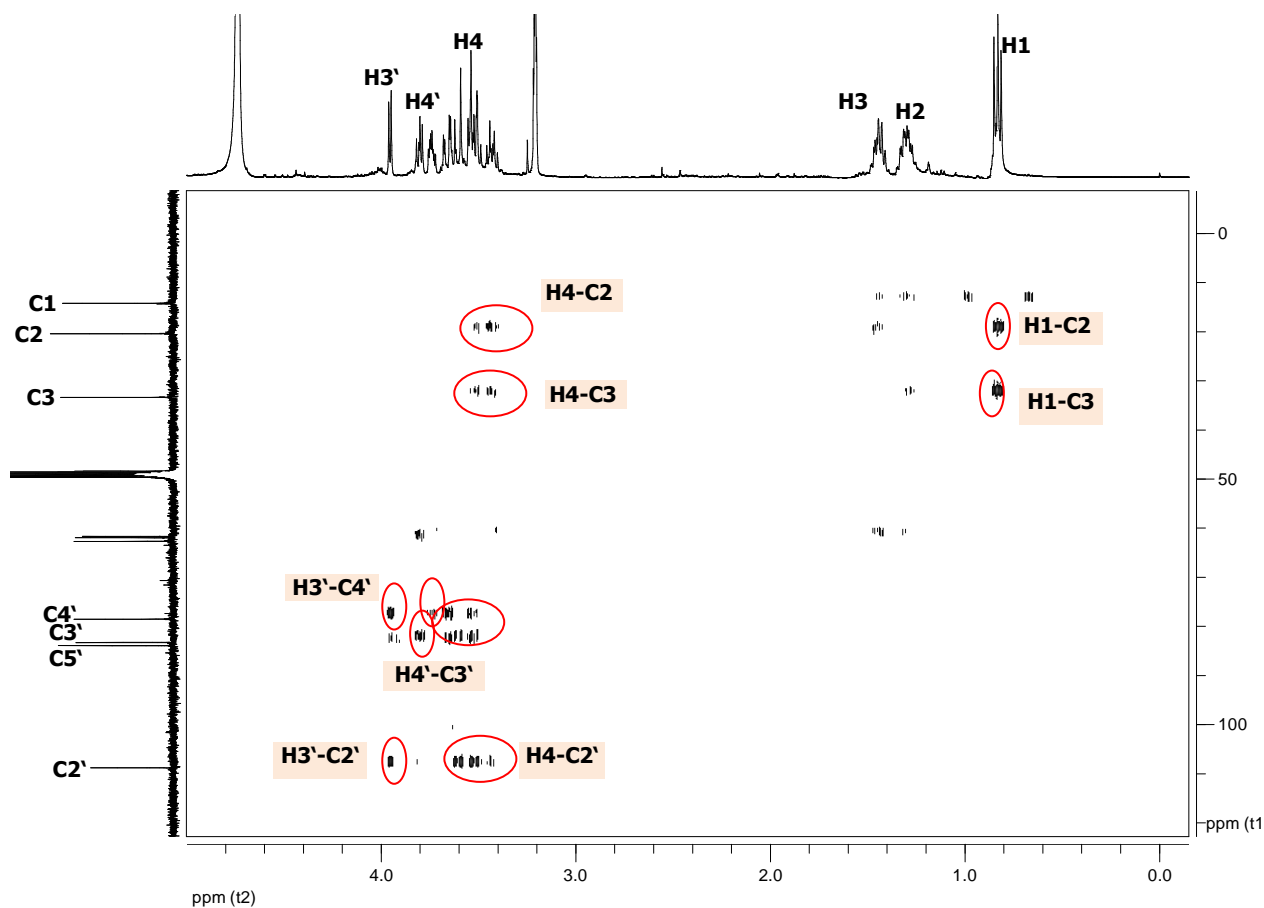


Fig.III.13.7. The HMBC diagram of compound WuBuOH

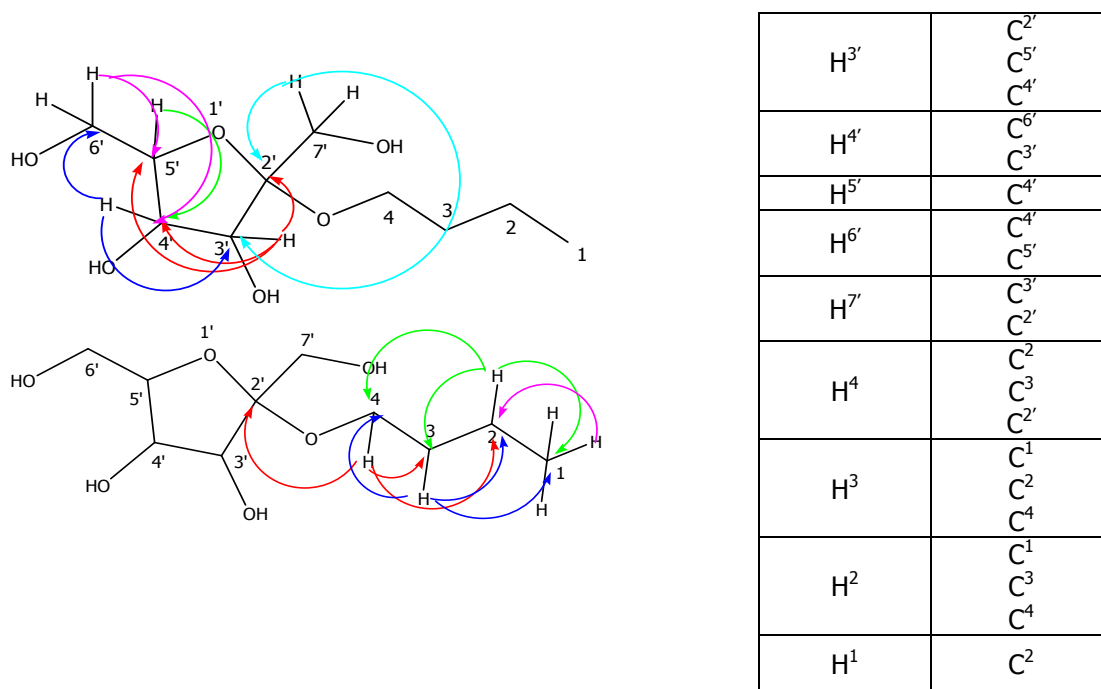


Fig.III.13.8. Some of the ¹H-¹³C long-range correlations of the compound WuBuOH

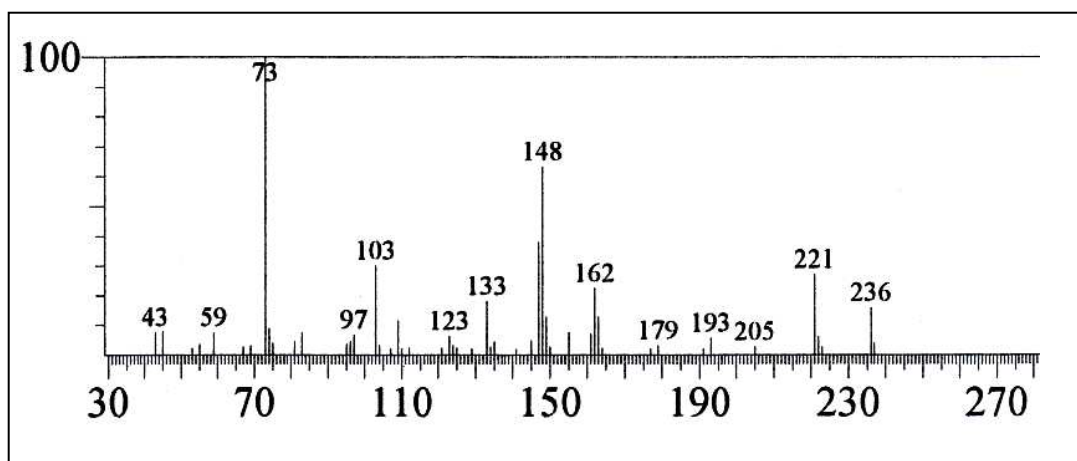


Fig.III.13.9. EI-MS spectrum of compound WuBuOH

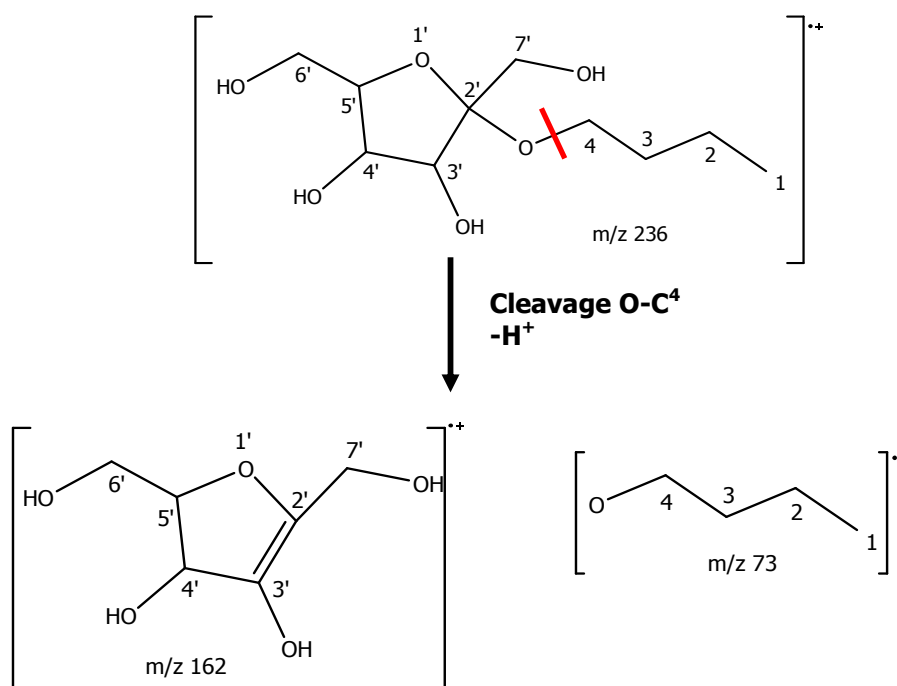


Fig.III.13.10. Fragmentation pattern of compound WuBuOH

The signal at 236 in the EI-MS spectrum of compound WuBuOH was assigned to the positively charged radical of compound WuBuOH $[M]^+$ which was fragmented by cleavage at O-C⁴ producing signal at m/z 73 and 162 that were assigned to butoxy and 2,5-bis(hydroxymethyl)-2,3-dihydrofuran-3,4-diol.

Based on the informations from NMR spectrum, IR spectrum and EI-MS spectrum, the compound WuBuOH was confirmed as **2-butoxy-2,5-bis(hydroxymethyl)-tetrahydrofuran-3,4-diol**.

III.14. UV absorption activity assay

The activity to absorb UV light has been investigated by using the UV/Vis spectrophotometer for apolar substances and an analytical HPLC equipped with a UV detector for semipolar and polar substances, which was performed because of the limited amount of active compounds obtained and of their limited solubility. The UV absorption activity was expressed as Absorbance Unit (AU)/concentration of sample (in the case the data was recorded on spectrophotometer) or Absorbance Unit.Second/concentration of sample (in the case the data obtained by HPLC). p-Aminobenzoic acid (PABA) was used as a reference compound, because it has been used as a sun screening compound in several cosmetic products. The results are summarized in Table III.14.1.

Table III.14.1. The results of the UV absorption activity assay

Compound	UV absorption activity	
	Measured by HPLC (AU*S/mmol)	Measured by UV spectrophotometer (AU/mM)
PABA	21.091	
Daidzein	24.401	
4-(2-(Furane-2-yl)ethyl)-2-methyl-2,5-dihydrofurane-3-carbaldehyde	2.883	
Dihydrofurane-2,5-dione	0.039	
2-Butoxy-2,5-bis(hydroxymethyl)-tetrahydrofurane-3,4-diol	0.211	
β -Sitosterol and Stigmasterol	0.094	
Daidzein-7-O- β -glucopyranose	1.428	
5-Hydroxy-daidzein-7-O- β -glucopyranose	1.016	
(8,9)-Furanyl-pterocarpan-3-ol	4.018	
Tricosandiene		0.003
Hexadecyl pentanoate		0.048
Palmitic acid		0.011
Trilinolein		0.002

The results show that compound daidzein has a highest activity among the other isolated compounds, with activity value of 24,401 AU*S/mmol. This fact might be due to the presence of phenol groups in daidzein. Therefore, daidzein can be further developed as a sun screening material in cosmetic products.

III.15. Total phenol contents assay

The amount of phenol compounds in the extracts was determined by the Folin-Ciocalteu colorimetric method using spectrophotometer at wavelength 755 nm (obtained from Figure III.15.1) (Singleton and Rossi 1965). Determinations were carried out in triplicate and calculated from a calibration curve obtained with gallic acid. The total phenol contents were expressed as mg gallic acid equivalents (GAE)/g extract. Figure III.15.2 displays a calibration curve of the gallic acid and the total phenol contents of extracts can be seen in Table III.15.1.

The Folin-Ciocalteu reagent is a solution of complex polymeric ions formed from phosphomolybdic and phosphotungstic heteropoly acids. It oxidises phenolates, reducing heteropoly acids to a blue Mo-W complex with an absorbance maximum at 750-775 nm. The phenolates are only present in alkaline solution but the reagent and products are alkali unsuitable. Hence a moderate alkalinity and a high reagent concentration are used in the procedure.

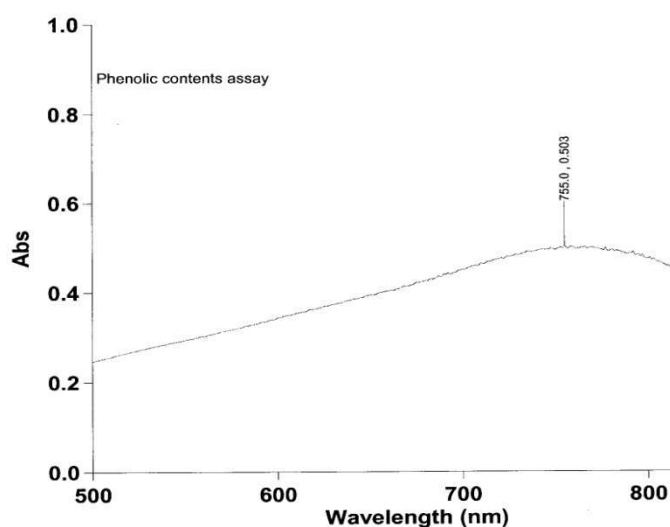


Fig. III.15.1. Wavelength scans of the reaction gallic acid with Folin-Ciocalteu reagent

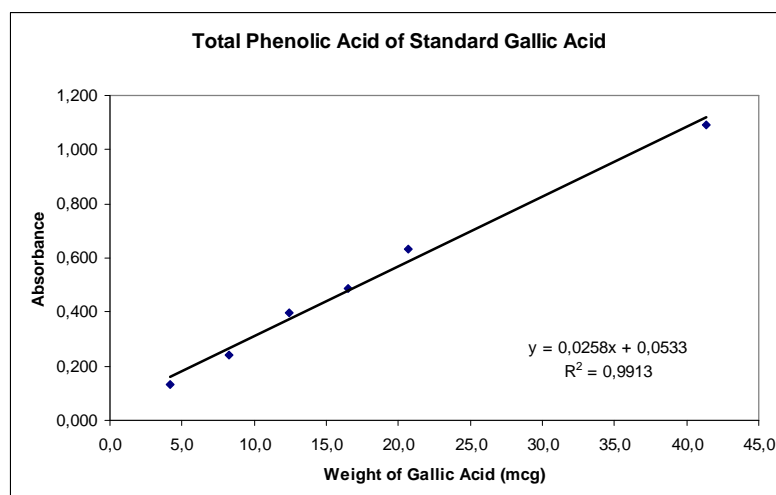


Fig. III.15.2. Calibration curve of the gallic acid

Table III.15.1. The total phenol contents in some crude extracts (mg GAE/g extract)

Extract	Total phenol contents (mg GAE/g extract)	
	Mean	SD
Methanol	4.38	0.67
Ethyl acetate	140.76	14.87
Ethyl acetate after hydrolysis	11.68	3.56
n-Butanol	13.24	1.76
Petroleum ether	Not detectable	

Phenol compounds have been found to be one of the most ubiquitous classes of constituents in the plant kingdom, and they have been reported to have multiple biological effects. Previous papers have also noted that many phenol compounds found in plants show tyrosinase inhibitory activity and can be used as a cosmetics material primarily as skin whitening material (Sugumuran 2002; Boissy and Manga 2004; Victor et al. 2004). Additionally, it was also reported that phenol compounds might be used as depigmenting agents because they have a chemical structure similar to tyrosine, the substrate of tyrosinase (Boissy and Manga 2004). The result in Table III.15.1 showed that the ethyl acetate extract had a significantly higher total phenol content than other extracts, while there was almost no phenol compounds in the petroleum extract, which is expected.

III.16. Total Flavonoid Contents Assay

Total flavonoid content was measured by the aluminium chloride colorimetric assay (Zhisen et al. 1999) using spectrophotometer at 750 nm

(obtained from Figure III.16.1). Determinations were carried out in triplicate and calculated from a calibration curve obtained with catechin. The total flavonoid contents were expressed as mg catechin equivalents (CE)/g extract. Figure III.16.2 displays the principle of the reaction of catechin with aluminum chloride, while Figure III.16.3 displays a calibration curve of the catechin and the total flavonoid contents in extracts can be seen in Table III.16.1

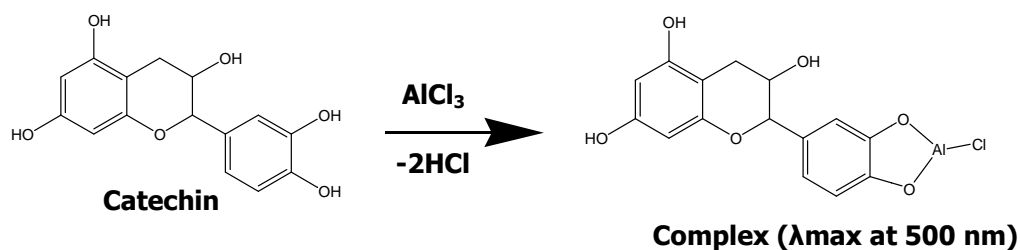


Fig. III.16.1. The reaction of catechin with AlCl_3

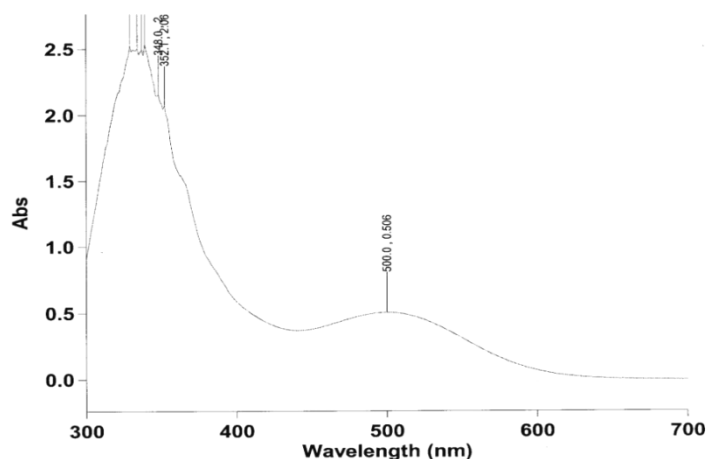


Fig. III.16.2. Wavelength scans of the reaction catechin with aluminum chloride

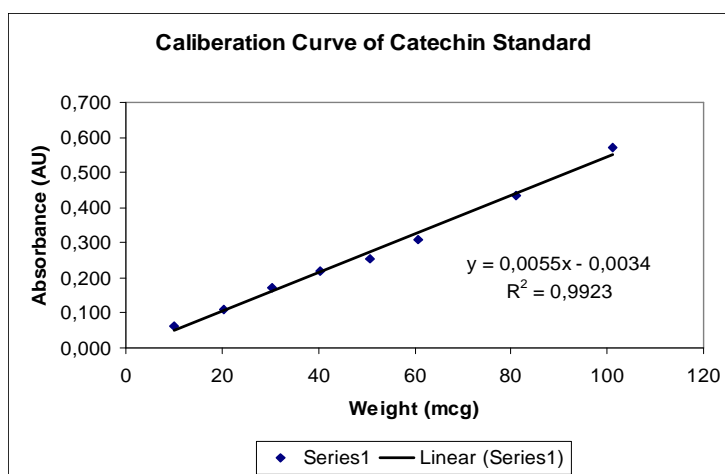


Fig. III.16.3. Calibration curve of the catechin

Table III.16.1. The total flavonoid contents in crude extracts (mg CE/g extract)

Extract	Total flavonoid contents (mg CE/g extract)	
	Mean	SD
Methanol	1.31	0.02
Ethyl acetate	16.22	0.10
Ethyl acetate after hydrolysis	3.14	0.12
n-Butanol	6.49	0.05
Petroleum ether	Not detectable	

Flavonoids as one of the most diverse and widespread group of natural compounds are probably the most important natural phenols (Miliauskus et al. 2003). These compounds possess a broad spectrum of chemical and biological activities including radical scavenging properties (see Chapter I.2.2). Therefore, the content of both groups of phenols was determined. As shown in Table III.16.1, the ethyl acetate extract had the highest amount of flavonoids (16.22 ± 0.10 mg CE/g extract) while the petroleum extract didn't contain flavonoids as expected. The phenol and flavonoid content correlate. The ethyl acetate extract had also the highest amounts of phenol contents with its concentration 140.76 ± 14.87 mg GAE/ g extract.

III.17. Antioxidative Activity Assay

The antioxidative activities of crude extracts and some of isolated compounds were evaluated by means of scavenging activity assay using DPPH radical and ascorbic acid as a positive control (IC₅₀ 7.24 ppm or 0.041 mM). The reduced DPPH form was determined using the UV/Vis spectrophotometer at maximum wavelength of 515 nm (Figure III.17.2). The results were expressed as the concentration of the extracts or isolated compounds which scavenged free radicals by 50% (SC₅₀). All tests were done in triplicate.

The molecule DPPH was characterised as a stable free radical by virtue of the delocalisation of the spare electron over the molecule as a whole, so that the molecules did not dimerise, as would be the case with most of the free radicals. The delocalisation also gave rise to the deep violet colour, characterised by an absorption band in ethanol solution centred about 520 nm (Molyneux 2004).

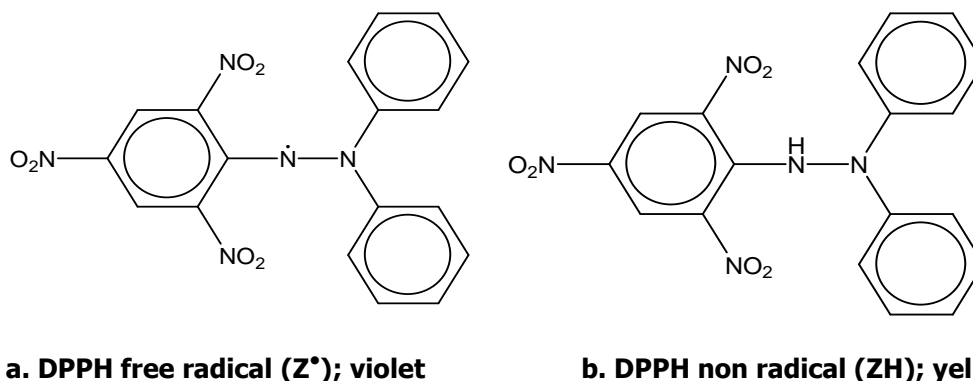
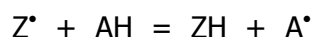


Fig.III.17.1. The structure of DPPH free radical and DPPH non radical or in reduced form (Songklanakarín 2004)

When a solution of DPPH was mixed with a solution of a substance being able to donate a hydrogen atom, this gave rise to the reduced form (Fig. III.17.1b) with the loss of the violet colour (although there would be expected to be a residual pale yellow colour from picryl group still present). Representing the DPPH radical by Z^{\bullet} and the donor molecule by AH, the primary reaction was



Where ZH was the reduced form of DPPH and A^{\bullet} was free radical produced in the first step. The latter radical would undergo further reactions which control the overall stoichiometry, that was, the number of molecules of DPPH reduced (decolourised) by one molecule of the reductant.

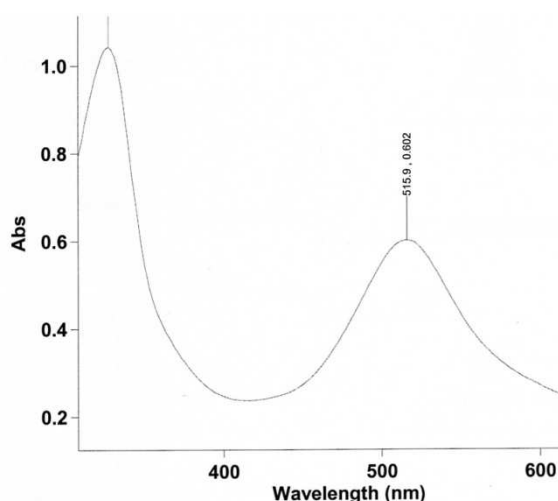


Figure III.17.2. Wavelength scans of the product reaction of ascorbic acid and DPPH

One of parameter for interpretation of the results from the DPPH method, was the "scavenging free radical concentration" or SC_{50} value (otherwise called the IC_{50} value). This was defined as the concentration of substance that causes 50% loss of the DPPH activity (colour), i. e. the higher the antioxidative activity, the lower was the value of SC_{50} . The correlation of the scavenging free radical of extracts and isolated compounds is displayed in Figures III.17.3a and III.17.3b below, while the corresponding SC_{50} value can be seen in Table III.17.1.

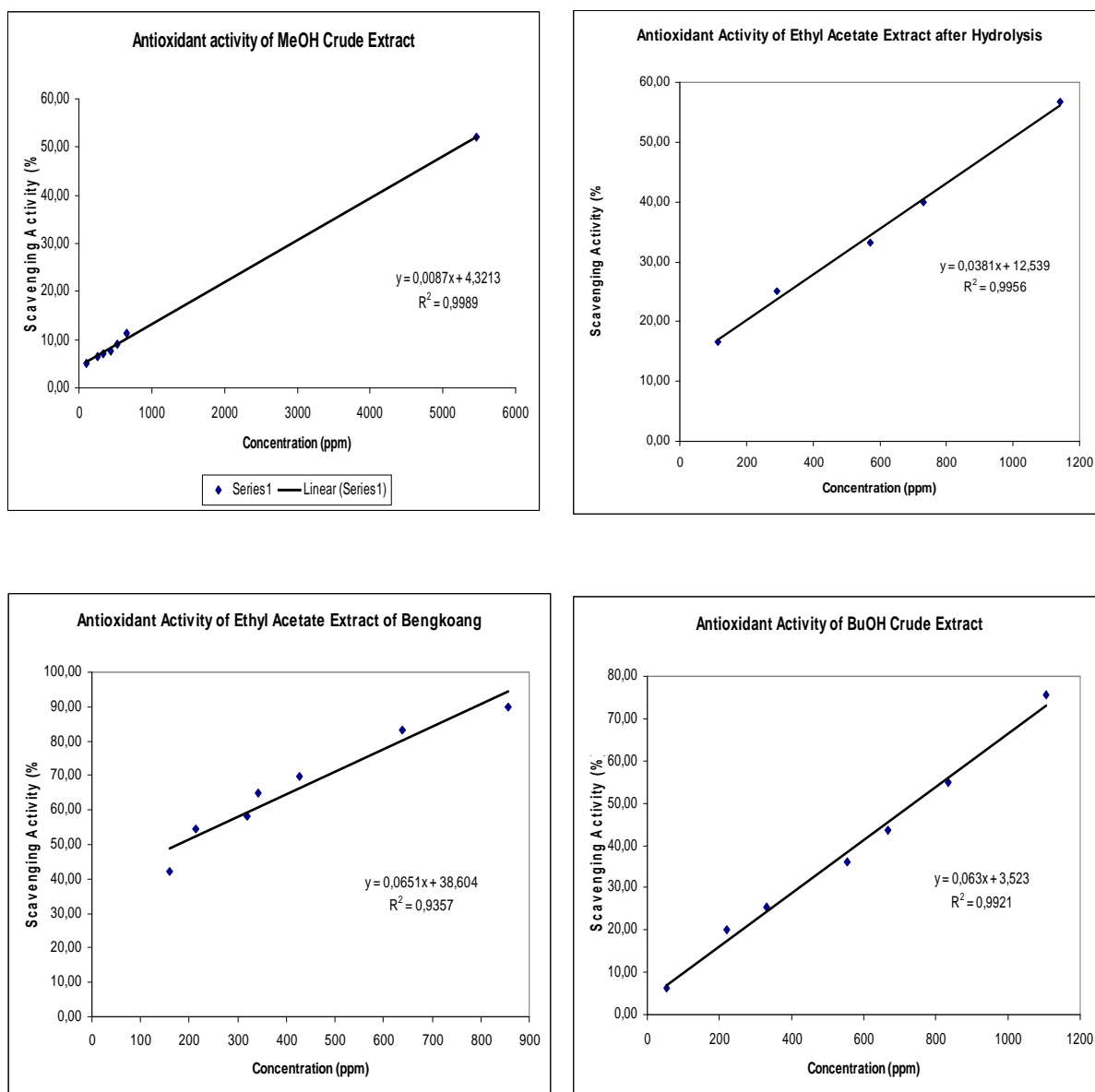
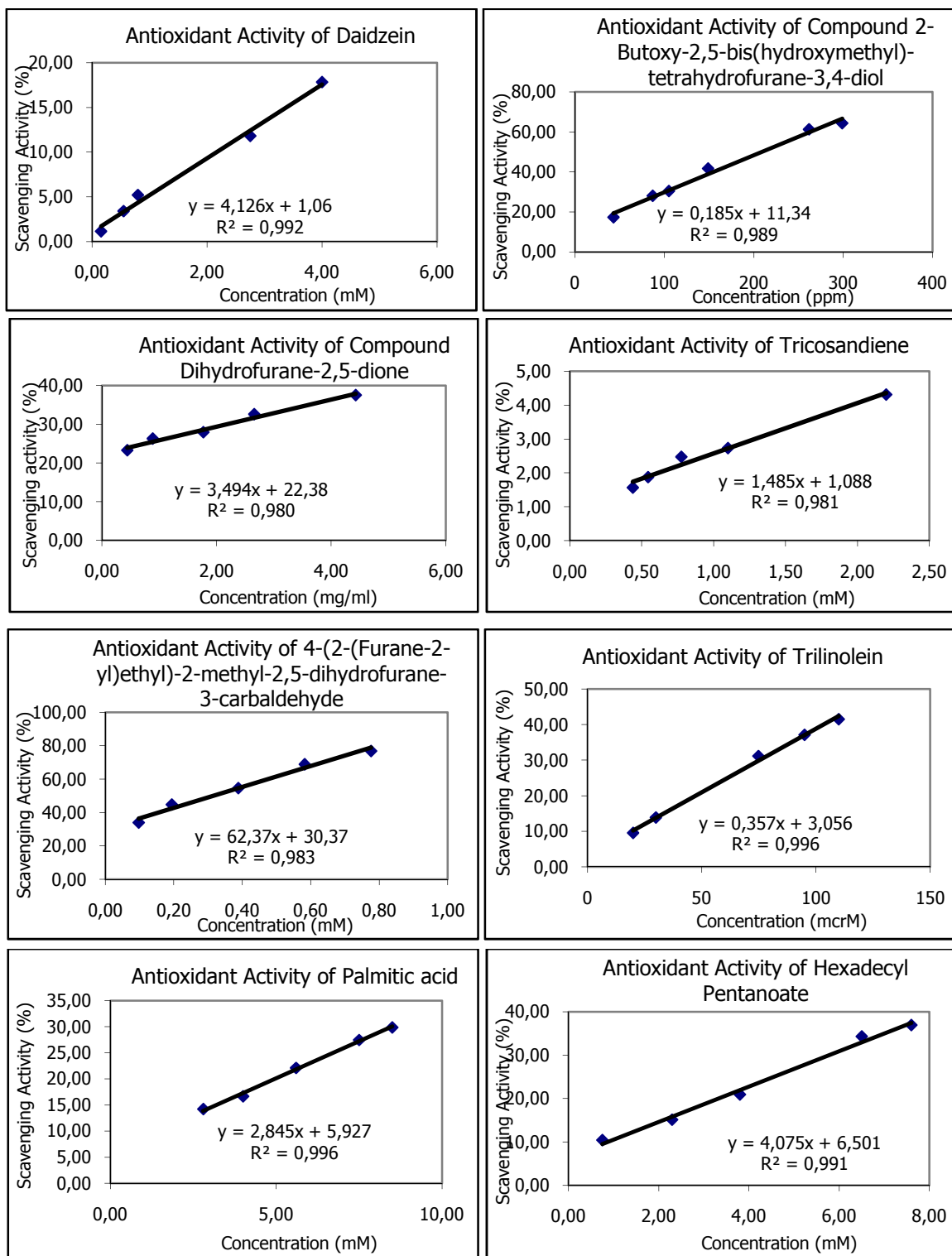
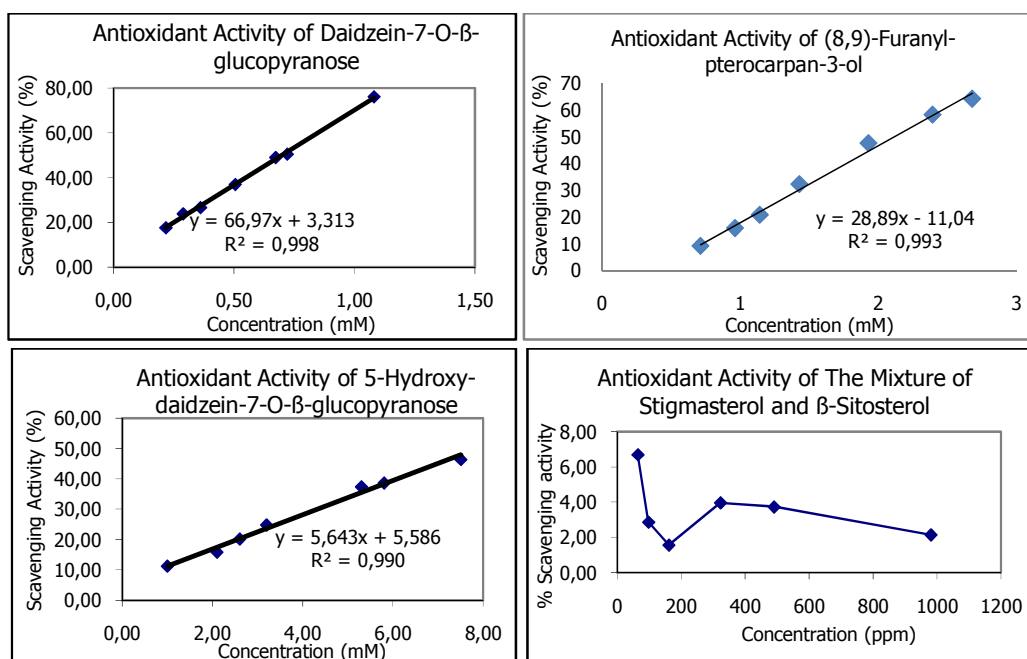


Fig. III.17.3a. Concentration-scavenging activity (%) curve of crude extracts

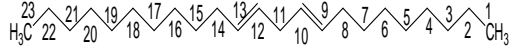
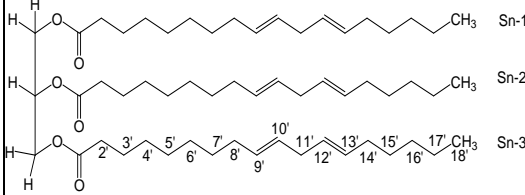
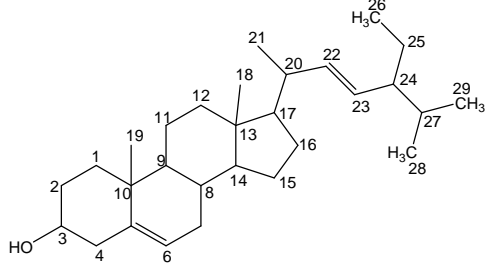
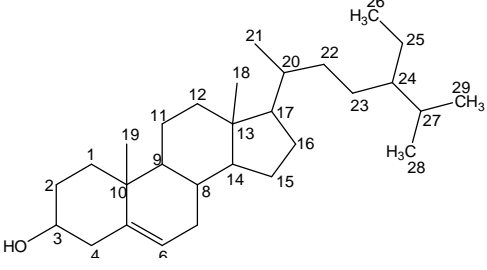
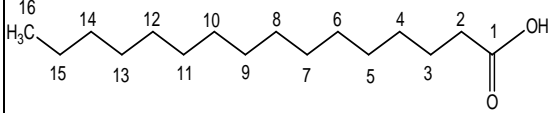
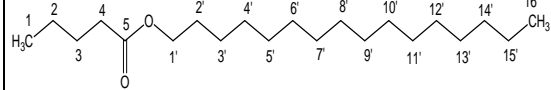


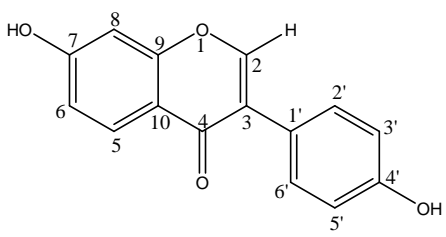
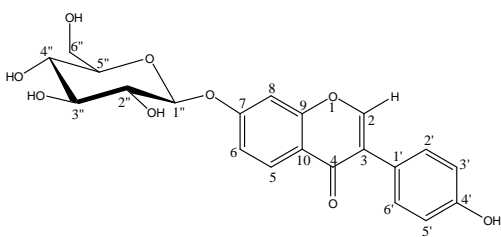
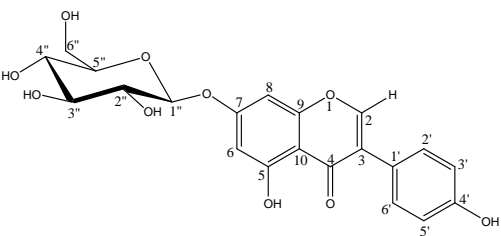
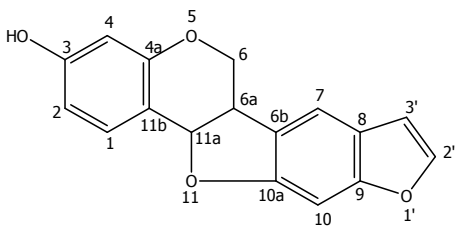
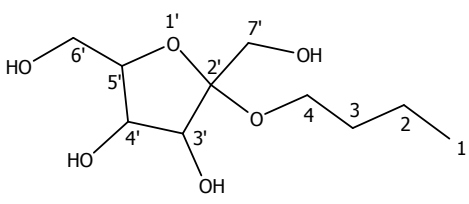
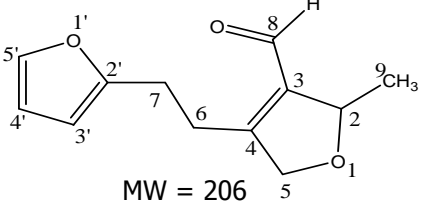
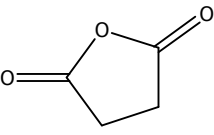


Note : The mixture of compound 109a and 109b didn't have correlation between antioxidative activity with their concentrations.

Fig. III.17.3b. Concentration-Scavenging Activity (%) curve of isolated compounds

Table III.17.1. The SC₅₀ of antioxidative activity of crude extracts and isolated compounds

Name		SC ₅₀ value (Mean ± SD)
Standard		
Ascorbic acid (vit C)		0.041 ± 0.001 mM
Extracts		
Ethyl acetate		175.06 ± 3.28 ppm
Methanol		4120.3 ± 147 ppm
Ethyl acetate (after hydrolysis)		983.23 ± 3.42 ppm
n-Butanol		737.73 ± 4.931 ppm
Petroleum ether		21794 ± 43 ppm
Isolated compounds		
(9,12)-Tricosandiene		31.38 ± 9.44 mM
Trilinolein		0.131 ± 0.004 mM
Stigmasterol		Not detectable
β-Sitosterol		Not detectable
Palmitic acid		60.51 ± 0.66 mM
Hexadecyl pentanoate		10.76 ± 0.12 mM

Daidzein		$11.86 \pm 0.23 \text{ mM}$
Daidzein-7-O- β -glucopyranose		$0.697 \pm 0.002 \text{ mM}$
5-Hydroxy-daidzein-7-O- β -glucopyranose		$7.857 \pm 0.069 \text{ mM}$
(8,9)-Furanyl-pterocarpan-3-ol		$2.113 \pm 0.001 \text{ mM}$
2-Butoxy-2,5-bis(hydroxymethyl)-tetrahydrofuran-3,4-diol		$0.885 \pm 0.003 \text{ mM}$
4-(2-(Furane-2-yl)ethyl)-2-methyl-2,5-dihydrofuran-3-carbaldehyde	 MW = 206	$0.314 \pm 0.002 \text{ mM}$
Dihydrofuran-2,5-dione	 MW = 100	$79.07 \pm 2.19 \text{ mM}$

These data clearly showed that the scavenging activity of the ethyl acetate extract was significantly higher than that of other extracts; the SC_{50} value amounts to 175.06 ppm. The mixture of stigmasterol and β -sitosterol didn't have any scavenging activity, while trilinolein had the highest activity of all isolated compounds with a SC_{50} value of 0.131 mM and followed by compound 4-(2-(furan-2-yl)-2-methyl-2,5-dihydrofuran-3-carbaldehyde, daidzein-7-O- β -glucopyranose and 2-butoxy-2,5-bis(hydroxymethyl)-tetrahydrofuran-3,4-diol. The antioxidative activity of trilinolein was lower than ascorbic acid, because the SC_{50} of trilinolein (0.131 mM) still higher than SC_{50} of ascorbic acid (0.041 mM). The reducing properties were generally associated with the presence of compounds with strong proton-donating abilities (Sawai and Moon 2000) and their antioxidative activity was based on the breaking of the free radical chain reaction by donating a hydrogen atom (Gordon 1990). Trilinolein had many carbonyl groups and double bonds C-C which play a major role as antioxidative agent. On the other hand, the isoflavonoid compounds, daidzein and daidzein-7-O- β -glucopyranose contain phenol groups which were responsible to their antioxidative activity. According to Jayaprakasha et al. (2003), the antioxidative activity of some natural products may depend on the presence of polyphenols which may act as reductors.

Based on the results, it was clear that isolated compounds with exception of the phytosterol group (β -sitosterol and stigmasterol) have antioxidative activity and could be developed as an antioxidative material in cosmetics products.

III.18. Tyrosinase Inhibitory Activity Assay

Tyrosinase inhibitory activity of crude extracts and isolated compounds was measured using mushroom tyrosinase as the enzyme, L-DOPA as a substrate and kojic acid as a positive control. UV detection at a maximum wavelength of 475 nm was applied (Figure III.18.2). All tests were done in triplicate. The tyrosinase inhibitory activity is expressed as IC_{50} value that defined as the concentration of the extracts or isolated compounds that causes 50% loss of the enzyme tyrosinase activity.

The catalytic action of tyrosinase enzyme was the conversion of tyrosine with oxygen to give DOPA which was then converted to dopaquinone and water. Subsequently, dopaquinone was converted through autooxidation to

dopachrome, an orange to red pigment with an absorbance maximum at 475 nm. Dopachrome could be found in human red hair, which can then be converted to the black or brown melanin pigments (found in virtually all human pigments) (Parvez et al. 2007; Rangkadilok et al. 2006). The catalytic reaction of tyrosinase enzyme with L-Dopa as a substrate is shown in Figure III.18.1, while the wavelength scan of DOPACHrome can be seen in Figure III.18.2 and all of the results are displayed in Figure III.18.3.

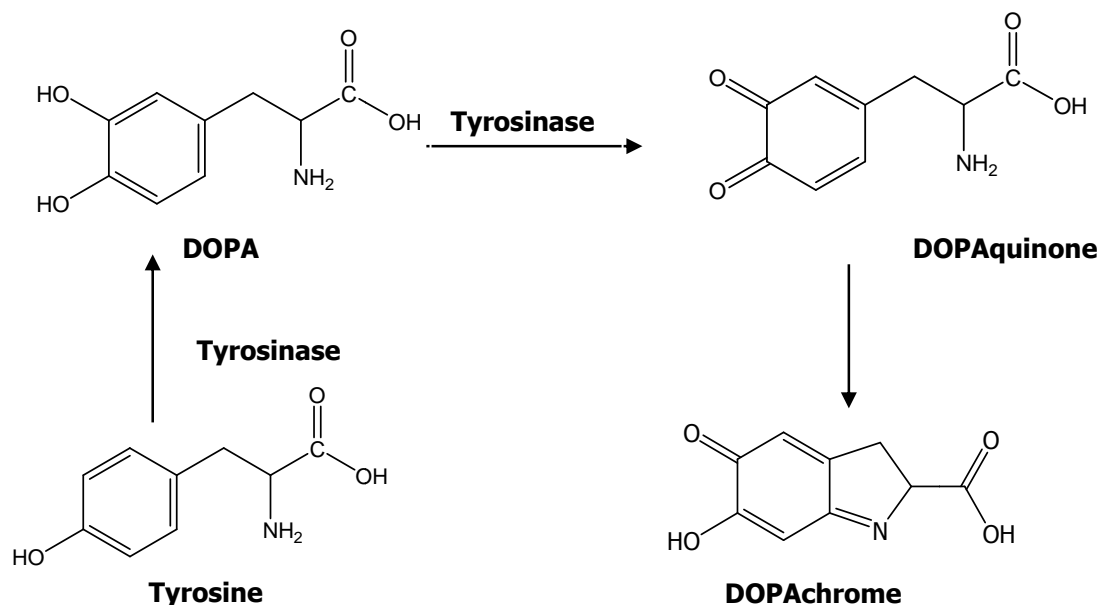


Fig. III.18.1. The oxidation pathway of tyrosine catalysed by tyrosinase enzyme

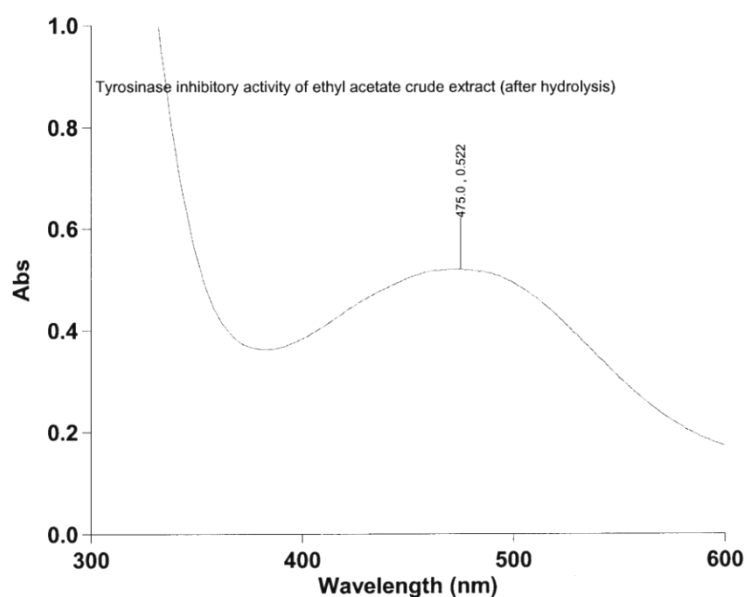
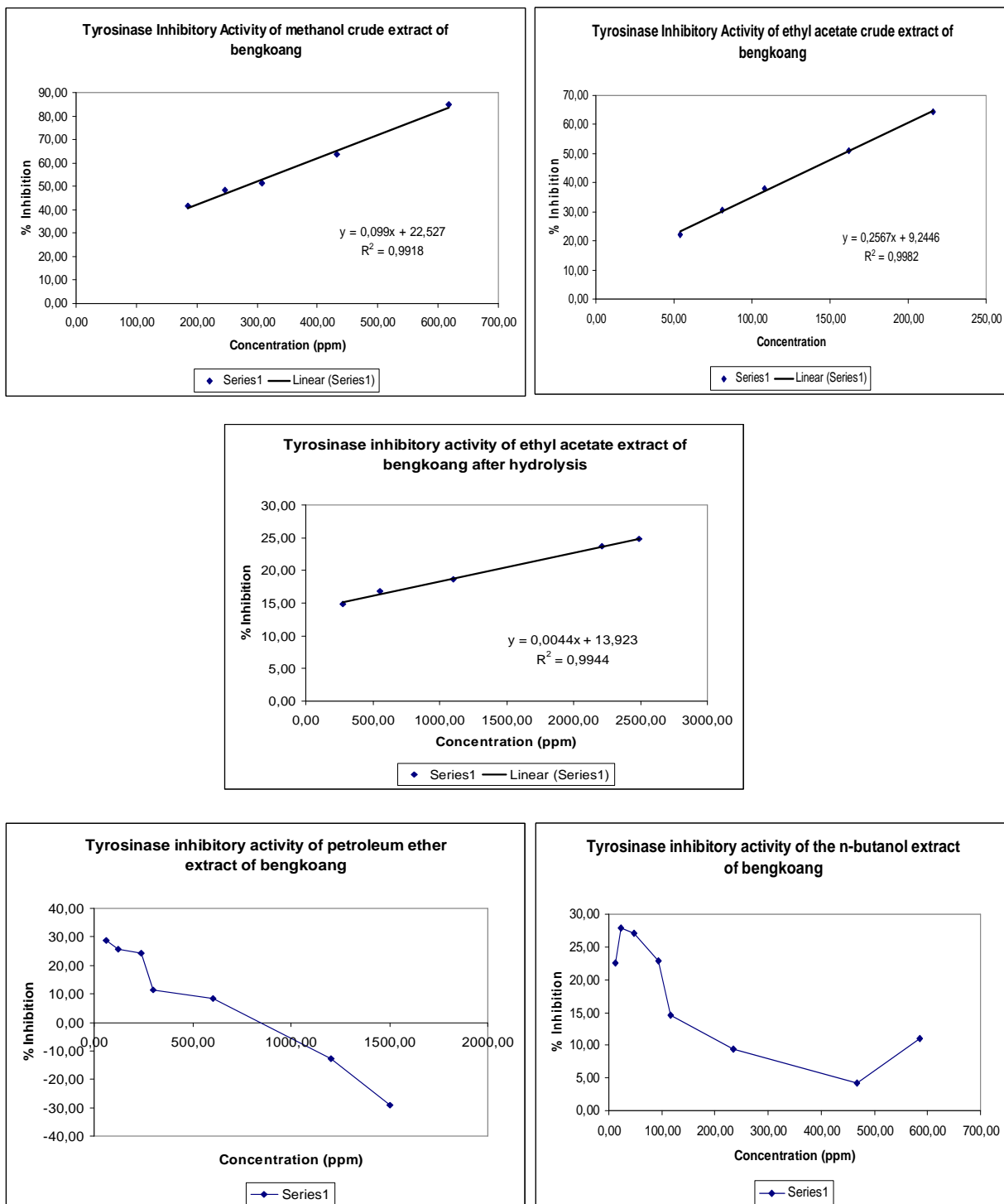


Fig.III.18.2. Wavelength scans of the product reaction DOPACHrome in the ethyl acetate extract



Note : The petroleum ether extract and the butanol extract didn't have any tyrosinase inhibitory activity

Fig. III.18.3a. Concentration-tyrosinase inhibition (%) curve of five crude extracts of bengkoang

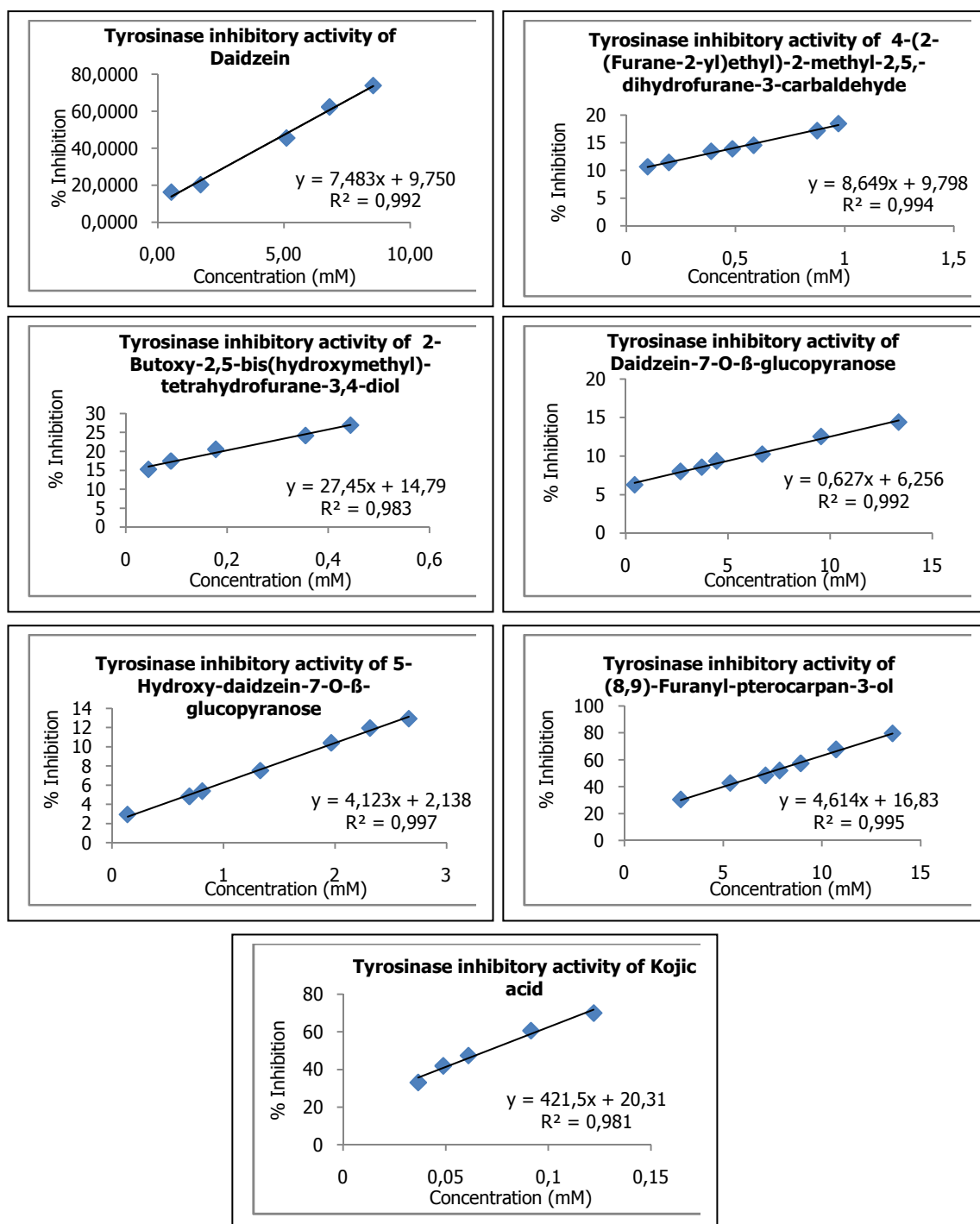
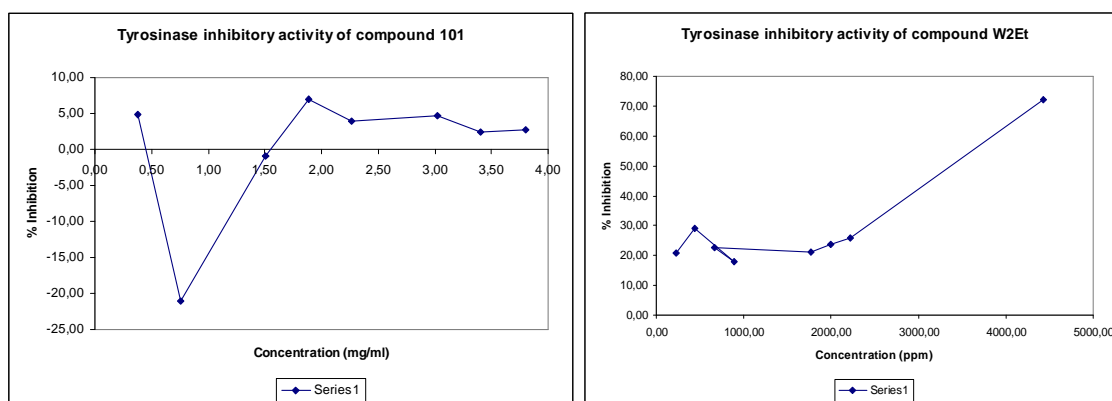


Fig. III.18.3b. Concentration-tyrosinase inhibition (%) curve of isolated compounds and kojic acid



Note : The compound 101 and W2Et didn't have any tyrosinase inhibitory activity

Fig. III.18.3b. Concentration-Tyrosinase Inhibition (%) curve of isolated compounds and kojic acid standard

The results provided in Figure III.18.3a demonstrate that only the ethyl acetate extract, the ethyl acetate extract after hydrolysis and the methanol extract show a significant correlation between the concentration and the tyrosinase inhibitory activity, but this correlation can not be seen in petroleum ether extract and n-butanol extract. Figure III.18.3b shows that 9,12-tricosandiene and dihydrofurane-2,5-dione do not have any tyrosinase inhibitory activity. The IC_{50} value of active extracts and the isolated compounds are displayed in Table III.18.1.

Table III.8.1. The IC_{50} of tyrosinase inhibitory activity of crude extracts and isolated compounds

Name	IC_{50} value
Extracts	
Ethyl acetate	158.13 ± 1.36 ppm
Methanol	277.50 ± 0.69 ppm
Ethyl acetate (after hydrolysis)	8.540 ± 0.028 ppm
n-Butanol	Not detectable
Petroleum ether	Not detectable
Isolated compounds	
Daidzein	5.35 ± 0.03 mM
4-(2-(Furane-2-yl)ethyl)-2-methyl-2,5-dihydrofurane-3-carbaldehyde	1.21 ± 0.02 mM
2-Butoxy-2,5-bis(hydroxymethyl)-tetrahydrofurane-3,4-diol	0.198 ± 0.004 mM
Dihydrofurane-2,5-dione	Not detectable
β -Sitosterol and Stigmasterol	Not detectable
9,12-Tricosandiene	Not detectable
Trilinolein	Not detectable
Palmitic acid	Not detectable
Hexadecyl pentanoate	Not detectable
Daidzein-7-O- β -glucopyranose	22.20 ± 0.27 mM
5-Hydroxy-daidzein-7-O- β -glucopyranose	4.38 ± 0.01 mM
(8,9)-Furanyl-pterocarpan-3-ol	7.19 ± 0.11 mM
Kojic acid standard	0.070 ± 0.001 mM

When we compared the tyrosinase inhibitory activity of the isolated compounds, 2-butoxy-2,5-bis(hydroxymethyl)-tetrahydrofuran-3,4-diol had greatest activity and followed by 4-(2-(furan-2-yl)ethyl)-2-methyl-2,5-dihydrofuran-3-carbaldehyde, 5-Hydroxy-daidzein-7-O- β -glucopyranose and daidzein. However, the activity of 2-butoxy-2,5-bis(hydroxymethyl)-tetrahydrofuran-3,4-diol was lower than kojic acid.

In cosmetic fields, the ethyl acetate extract can be developed as a natural skin-whitening agent, because it contained several active compounds of antioxidative property, namely the isoflavonoids daidzein, daidzein-7-O- β -glucopyranose, 5-Hydroxy-daidzein-7-O- β -glucopyranose, the pterocarpan ((8,9)-furan-yl-pterocarpan-3-ol), the furanes (2-butoxy-2,5-bis(hydroxymethyl)-tetrahydrofuran-3,4-diol) and 4-(2-(furan-2-yl)ethyl)-2-methyl-2,5-dihydrofuran-3-carbaldehyde, which have activities to inhibit tyrosinase enzyme. The results also showed that the phenol content in the ethyl acetate was higher than in the other extracts, thus the presence of phenol in the extracts might play a pivotal role in tyrosinase inhibition. On the other hand, the petroleum ether extract was suitable only as an antioxidative material, because it possessed antioxidative activity without tyrosinase inhibitory activity. Antioxidative activity in the petroleum ether might be due to compounds with unsaturated carbon chains and/or carbonyl functional group, such as trilinolein, 9-12 tricosandiene, palmitic acid and hexadecyl pentanoate. According to some previously papers (Seo et al. 2003, and Karg et al. 1993), antioxidatives might prevent or delay pigmentation by different mechanisms, such as by scavenging reactive oxygen species and reactive nitrogen species (Seo et al. 2003), or by reducing DOPAquinone or other intermediates in melanin biosynthesis, thus delaying oxidative polymerization (Karg et al. 1993). Therefore, it was important to combine compounds which have tyrosinase inhibitory activity and antioxidative compounds in skin whitening products.

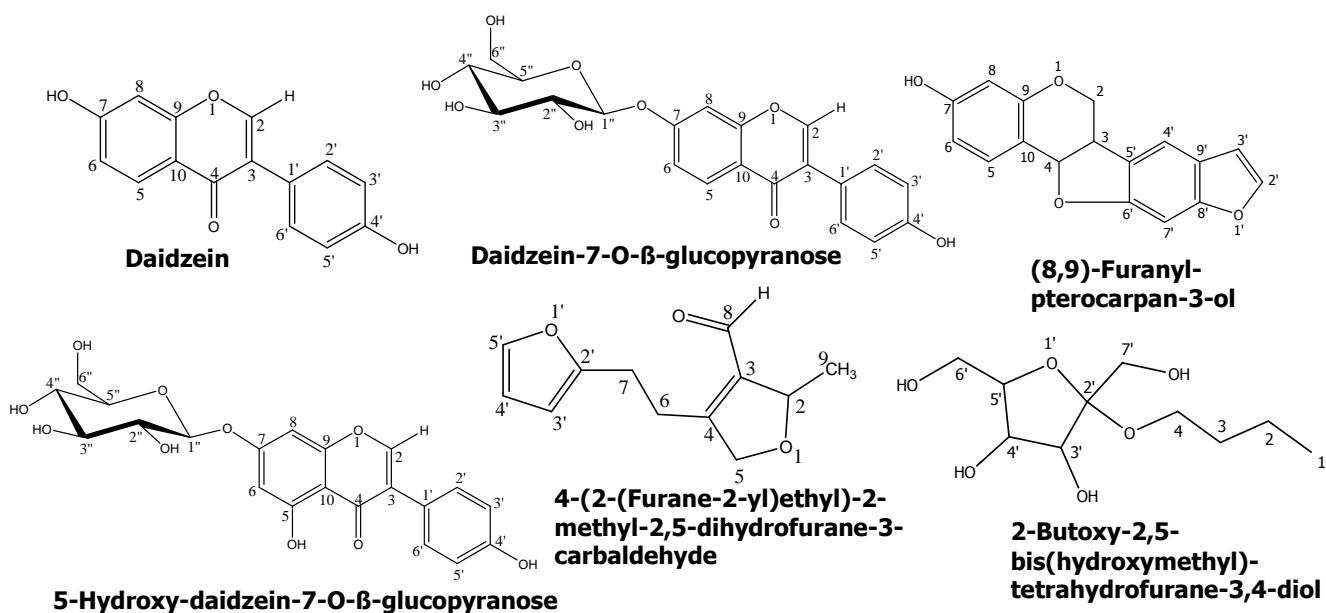


Fig.18.4. Chemical structures of isoflavonoids and a pterocarpan isolated from the bengkoang root

The compounds of daidzein, daidzein-7-O-β-glucopyranose, 5-Hydroxy-daidzein-7-O-β-glucopyranose were isoflavonoids and (8,9)-furanyl-pterocarpan-3-ol was a pterocarpan (Fig.III.18.4). Comparison of the tyrosinase inhibition potency of isoflavonoids, revealed that 5-Hydroxy-daidzein-7-O-β-glucopyranose had the greatest inhibition activity, followed by daidzein, (8,9)-furanyl-pterocarpan-3-ol and daidzein-7-O-β-glucopyranose, respectively. The decrease of the activities from daidzein to daidzein-7-O-β-glucopyranose might be reasoned by the glucose substituent providing steric bulk. The result is in accordance with findings reported by Chang (2007). The active site of enzyme tyrosinase (see Fig.I.2.3.2 in Chapter I) consisted of two copper atoms that were each coordinated with three histidine residue (Mirica et al. 2005). The compounds having phenol or diphenol group could form a chelat complex with copper in the enzyme and thus irreversibly inactivated the tyrosinase. Daidzein-7-O-β-glucopyranose having one of phenol group because the other phenol groups bond to a glucose molecule forms only a weak complex resulting in a lower inhibitory activity.

The compound of 5-Hydroxy-daidzein-7-O-β-glucopyranose is also a glycoside having an extra hydroxyl group at position C⁴ beside the -OH group at position C^{4'}. However, the tyrosinase inhibition activity was still greater than that of daidzein compound. The hydroxyl group (-OH) at position 4 adjacent to the carbonyl group (-C=O) enables this compound to form a strong chelation with

the copper of the active site enzyme, so that the inhibition power was greater than the aglycon molecule of daidzein. The molecule of (8,9)-furanyleptero-carpan-3-ol has only one hydroxyl -OH at position C⁷ and no carbonyl group (-C=O), thus the activity was much lower than the aglycon daidzein.

The compound of 4-(2-(furan-2-yl)ethyl)-2-methyl-2,5-dihydrofuran-3-carbaldehyde is an aldehyde and does not have a phenol group. However, this compound also shows the inhibitory activity towards tyrosinase. Some authors (Parvez et al. 2007; Kubo and Kinst-Hori 1999) mentioned that the aldehyde compound can inhibit the enzyme tyrosinase via the different mechanism, i. e. the formation of a Schiff base with histidine residue in the active site of the enzyme, explaining the observed activity.

The compound of 2-butoxy-2,5-bis(hydroxymethyl)-tetrahydrofuran-3,4-diol does neither have phenol or aldehyde groups, but its activity is much greater than the other isolated compounds. The inhibition activity of 2-butoxy-2,5-bis(hydroxymethyl)-tetrahydrofuran-3,4-diol may be due to the interaction of two hydroxyl groups (-OH) at the position 3 and 4 with the active site of the enzyme or ring-opened followed by forming an aldehyde.

III.19. Determination of Tyrosinase Inhibition Type of isolated compounds

This study was conducted to determine the inhibition type of the isolated active compounds. An inhibitor molecule affects an enzyme either as a competitive inhibitor and non-competitive inhibitor. Competitive inhibition takes place when a molecule that is structurally similar to the substrate for a particular reaction competes for a position at the active site on the enzyme. Competitive inhibition can be reversed by raising the concentration of substrate to sufficiently high levels while the concentration of the inhibitor is held constant. The presence of the competitive inhibitor can reduce the maximum rate of a chemical reaction (V_{max}) without changing the apparent binding affinity of the active site to substrate. A non-competitive inhibitor always binds to a site that is not the active site (an allosteric site). The presence of non-competitive inhibitor changes the nature and shape of the enzyme so that its catalytic properties are lost. This can happen in two ways. Either the non-competitive inhibitor itself physically blocks the access to the active site, or it causes a conformational change in the protein,

thus inactivating the active site. Because the substrate molecules cannot reverse the binding of a non-competitive inhibitor, increasing the concentration of substrate will not reverse the inhibition.

To analyze the inhibition type of the present isolated compounds for tyrosinase, a steady-state analysis was performed. Lineweaver-Burk plots for the inhibition of tyrosinase by isolated compounds were obtained with variable concentrations of them and substrate (L-DOPA). The Lineweaver-Burk plots of the isolated compounds displayed in Figure III.19.2.

The intersections of the lines on the vertical axis in Lineweaver-Burk plots of daidzein, 4-(2-(furane-2-yl)ethyl)-2-methyl-2,5-dihydrofurane-3-carbaldehyde, daidzein-7-O- β -glucopyranose, 2-butoxy-2,5-bis(hydroxymethyl)-tetrahydrofurane-3,4-diol and 5-Hydroxy-daidzein-7-O- β -glucopyranose indicates that these compounds could be included in the group of competitive inhibitors. Meanwhile the Lineweaver-Burk plot of (8,9)-furanyl-pterocarpan-3-ol produced the lines which have the same intersection on the horizontal axis indicating that this compound had to be included in the group of non-competitive type.

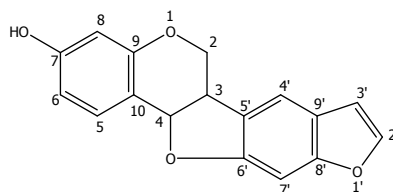


Fig.19.1. Chemical structure of compound (8,9)-furanyl-pterocarpan-3-ol

The presence of hydroxyl (-OH) at position C^{4'} in the isoflavonoid compounds and aldehyde in the furane carbaldehyde compounds might be responsible for the competitive inhibition activity. The compound (8,9)-furanyl-pterocarpan-3-ol (Fig.III.19.1) didn't have hydroxyl (-OH) at position C^{4'}, therefore it wasn't be able to bind with the active site of tyrosinase enzyme. The inhibition activity of (8,9)-furanyl-pterocarpan-3-ol might be due to its ability to bind with tyrosinase at a site other than the enzyme's active site (at allosteric site). This fact was in agreement with Khatib et al. (2005) showing that the position of hydroxyl in the molecule played an important role in the type inhibition activity rather than the number of hydroxyl group. Chang (2007) has reported that the isoflavone skeleton in the compounds was absolutely necessary for the compounds to suicide substrates of mushroom tyrosinase (as a competitive tyrosinase inhibitor).

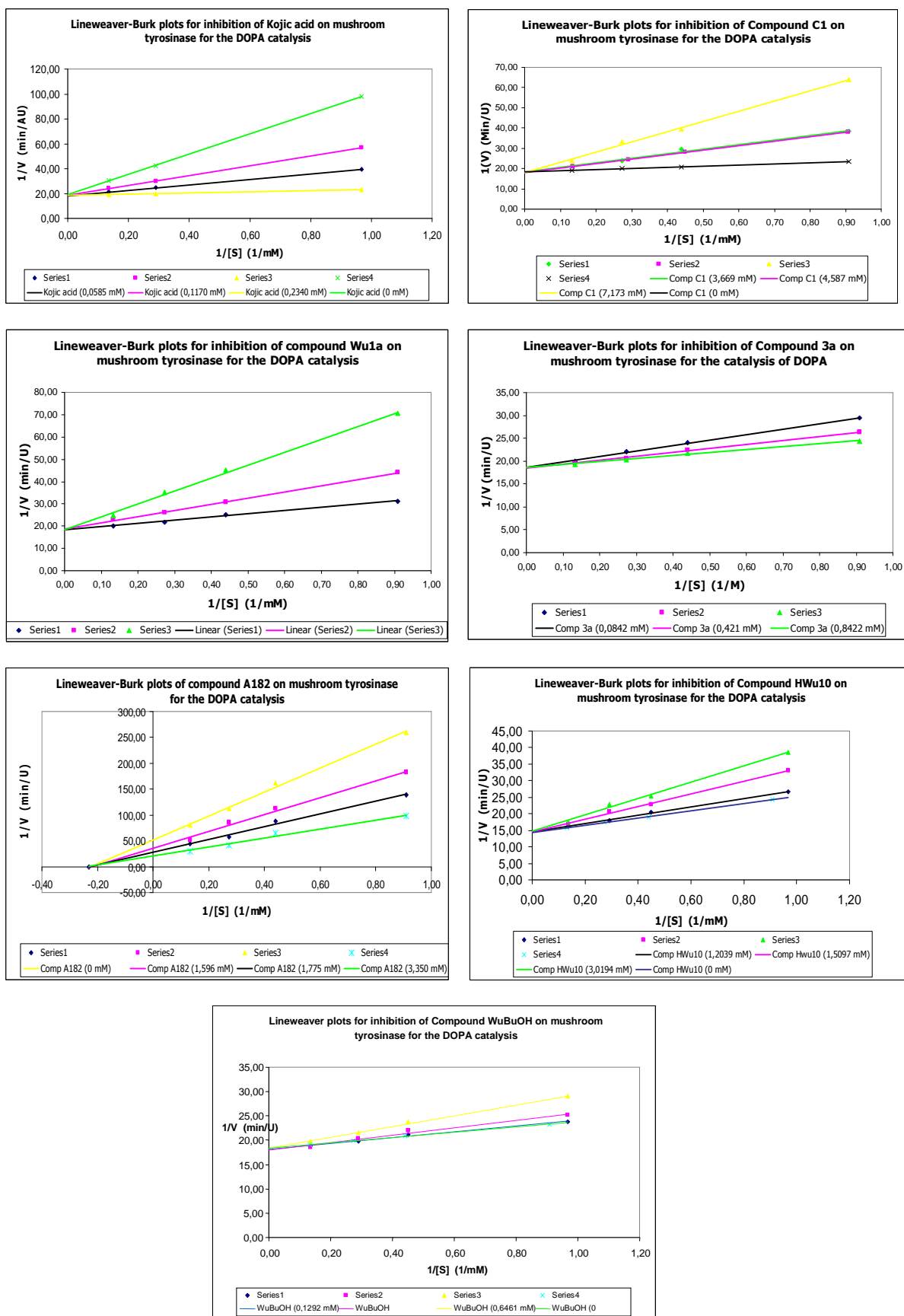


Fig. III.19.2. The Lineweaver-Burk plots of isolated compounds

Table III.19.1. Result of the determination of the tyrosinase inhibition type of isolated compounds

Compound	L-DOPA (IC ₅₀ ,mM)	Type of inhibition
Daidzein	5.35 ± 0.03 mM	Competitive V _m = 55.16 ± 0.33 U/min
Daidzein-7-O-β-glucopyranose	22.20 ± 0.27 mM	Competitive V _m = 56.64 ± 0.53 U/min
5-Hydroxy-daidzein-7-O-β-glucopyranose	4.38 ± 0.01 mM	Competitive V _m = 53.91 ± 0.29 U/min
(8,9)-Furanyl-pterocarpan-3-ol	7.19 ± 0.11 mM	Non-competitive K _m = 4.48 ± 0.11 mM
2-Butoxy-2,5-bis(hydroxymethyl)-tetrahydrofurane-3,4-diol	1.21 ± 0.02 mM	Competitive V _m = 54.72 ± 0.66 U/min
4-(2-(Furane-2-yl)ethyl)-2-methyl-2,5-dihydrofurane-3-carbaldehyde	0.198 ± 0.004mM	Competitive V _m = 56.94 ± 0.43 U/min

CHAPTER IV SUMMARY

The exploration of the bengkoang root (*Pachyrhizus erosus*) collected from Purworejo, Indonesian has been conducted for their chemical constituents and their activities in cosmetics field (UV absorption activity, antioxidative activity, tyrosinase inhibitory activity and the type of tyrosinase inhibition activity).

Thirteenth compounds have been obtained from the bengkoang root. The structures of the compounds were estimated on the basis of NMR spectroscopic (^1H , ^{13}C , COSY, ^1H -detected direct and long range ^{13}C - ^1H correlations) and mass spectroscopic data. The identified of the compounds were also established by comparison with the published data.

By using bioassay-guided isolated components, six compounds obtained in petroleum ether extract (9,12-tricosandiene; trilinolein; β -sitosterol; stigmasterol; hexadecyl pentanoate; palmitic acid), five compounds obtained in ethyl acetate extract (daidzein; daidzein-7-O- β -glucopyranose, 5-hydroxyl-daidzein-7-O- β -glucopyranose; dihydrofurane-2,5-dione; (8,9)-furanly-pterocarpan-3-ol, one compound in the ethyl acetate extract after hydrolysis (4-(2-(furan-2-yl)-2-methyl-2,5-dihydrofurane-3-carbaldehyde) and one compound in the butanol extract (2-butoxy-2,5-bis(hydroxymethyl)-tetrahydrofurane-3,4-diol) have been found.

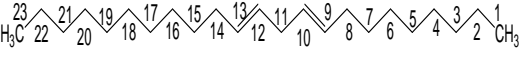
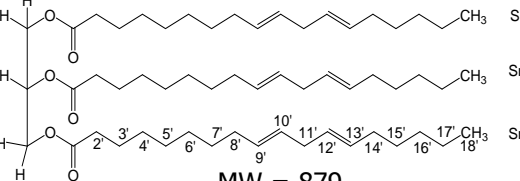
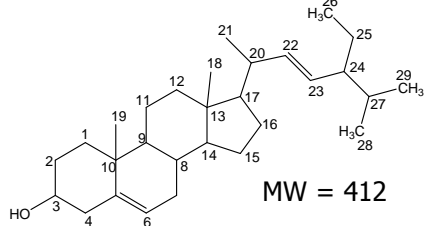
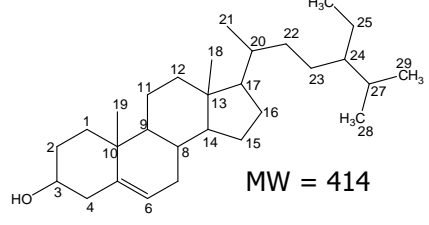
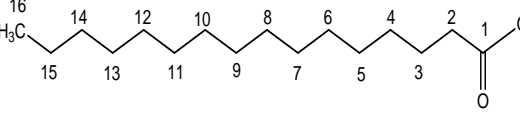
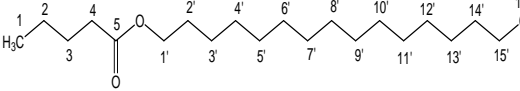
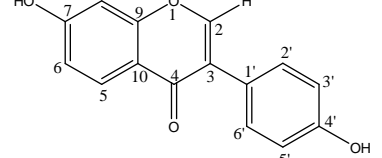
Three isolated isoflavonoids (daidzein, daidzein-7-O- β -glucopyranose; 5-hydroxyl-daidzein-7-O- β -glucopyranose), (8,9)-furanly-pterocarpan-3-ol, 2-butoxy-2,5-bis(hydroxymethyl)-tetrahydrofurane-3,4-diol and 4-(2-(furan-2-yl)-2-methyl-2,5-dihydrofurane-3-carbaldehyde) showed interesting antioxidative and tyrosinase inhibitory activities. These compounds were significantly inhibiting tyrosinase enzyme. The IC_{50} values (in mM) to inhibit tyrosinase of compounds were 5.35 ± 0.03 ; 22.20 ± 0.27 ; 4.39 ± 0.01 ; 7.18 ± 0.11 ; 0.198 ± 0.004 ; 1.21 ± 0.02 , respectively.

Four isolated compounds obtained in petroleum ether extract (9,12-tricosandiene, trilinolein, hexadecyl pentanoate and palmitic acid) and dihydrofurane-2,5-dione showed antioxidative activity against the DPPH reagent. However, they didn't have the tyrosinase inhibitory activity. The SC_{50} values (in

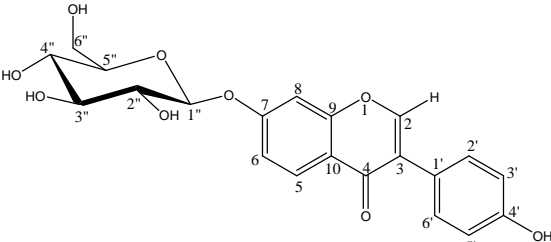
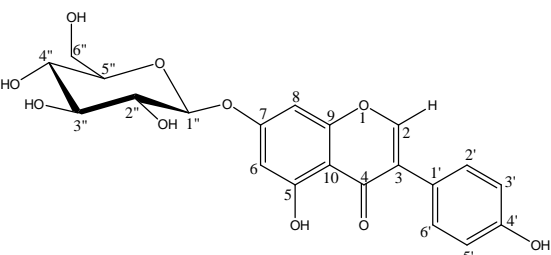
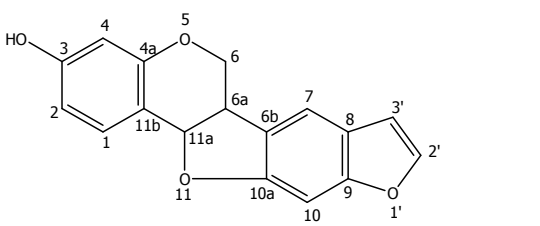
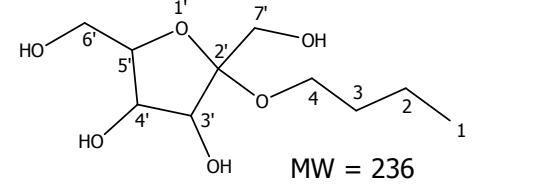
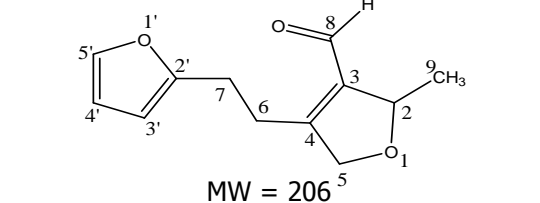
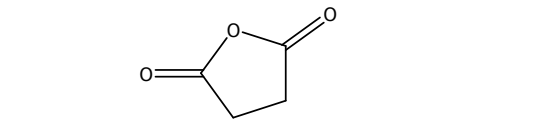
mM) of these compounds were 31.38 ± 9.44 ; 0.131 ± 0.004 ; 1076 ± 0.12 and 60.51 ± 0.66 , respectively. The compounds having antioxidative activity could also prevent or delay pigmentation by different mechanisms than tyrosinase inhibition, such as by scavenging reactive oxygen species and reactive nitrogen species (Seo et al. 2003), or by reducing DOPAquinone or other intermediates in melanin biosynthesis, thus delaying oxidative polymerization (Karg et al. 1993). Therefore, these compounds were important to combine with the tyrosinase inhibitor in whitening cosmetics product to get a synergic effect.

Based on all the results, isolated compounds could be classified into three groups, i. e. **(1)** the UV absorption group (all compounds), **(2)** antioxidative group (Trilinolein; 9,12-tricosandiene; daidzein; daidzein-7-O- β -glucopyranose; 5-hydroxyl-daidzein-7-O- β -glucopyranose; (8,9)-furan-yl-pterocarpan-3-ol; dihydrofuran-2,5-dione; 2-butoxy-2,5-bis(hydroxymethyl)-tetrahydrofuran-3,4-diol; 4-(2-(furan-2-yl)ethyl)-2-methyl-2,5-dihydrofuran-3-carbaldehyde), and **(3)** antityrosinase group (the compounds of daidzein, daidzein-7-O- β -glucopyranose, 5-hydroxyl-daidzein-7-O- β -glucopyranose, (8,9)-furan-yl-pterocarpan-3-ol, 2-butoxy-2,5-bis(hydroxymethyl)-tetrahydrofuran-3,4-diol and 4-(2-(furan-2-yl)ethyl)-2-methyl-2,5-dihydrofuran-3-carbaldehyde).

Table. IV.1. Summary of isolated compounds and their activities from the bengkoang root extract

Name	Chemical Structure MW (g/mol)	UV absorption activity	Antioxidative activity (SC ₅₀ , mM)	Type of Tyrosinase inhibition
101 (9,12- Tricosandiene)	 MW = 320	0.003 AU/mM	31.38 ± 9.44	Not detectable
102 (Trilinolein)	 MW = 879	0.002 AU/mM	0.131 ± 0.004	Not detectable
109 a (Stigmasterol)	 MW = 412	0.094 mAU*S/mmol	Not detectable	Not detectable
109 b (β-Sitosterol)	 MW = 414	0.094 mAU*S/mmol	Not detectable	Not detectable
WuPe (Palmitic acid)	 MW = 256	0.011 AU/mM	60.51 ± 0.66	Not detectable
G1 (Hexadecyl pentanoate)	 MW = 326.7	0.048 AU/mM	10.76 ± 0.12	Not detectable
C1 (Daidzein)	 MW = 254	21.091 mAU*S/mmol	11.86 ± 0.23	Competitive IC ₅₀ = 5.35 ± 0.03 mM V _m = 55.16 ± 0.33 U/min

Summary

<p>Wu1a (Daidzein-7-O-β-glucopyranose)</p>	 <p>MW = 416</p>	<p>1.428 mAU*S/mmol</p>	<p>0.697 \pm 0.002</p>	<p>Competitive IC₅₀ = 22.20 \pm 0.27 mM V_m = 56.64 \pm 0.53 U/min</p>
<p>Wu3a (5-Hydroxydaidzein-7-O-β-glucopyranose)</p>	 <p>MW = 432</p>	<p>1.016 mAU*S/mmol</p>	<p>7.857 \pm 0.069</p>	<p>Competitive IC₅₀ = 4.38 \pm 0.01 mM V_m = 53.91 \pm 0.29 U/min</p>
<p>A182 (8,9)-Furanylpterocarpan-3-ol</p>	 <p>MW = 280</p>	<p>4.018 mAU*S/mmol</p>	<p>2.113 \pm 0.001</p>	<p>Non Competitive IC₅₀ = 7.19 \pm 0.11 mM K_m = 4.48 \pm 0.11 mM</p>
<p>WuBuOH (2-Butoxy-2,5-bis(hydroxymethyl)-tetrahydrofurane-3,4-diol)</p>	 <p>MW = 236</p>	<p>0.211 mAU*S/mmol</p>	<p>0.885 \pm 0.003</p>	<p>Competitive IC₅₀ = 1.21 \pm 0.02 mM V_m = 54.72 \pm 0.66 U/min</p>
<p>HWu10 (4-(2-(Furane-2-yl)ethyl)-2-methyl-2,5-dihydrofurane-3-carbaldehyde)</p>	 <p>MW = 206</p>	<p>2.883 mAU*S/mmol</p>	<p>0.314 \pm 0.002</p>	<p>Competitive IC₅₀ = 0.198 \pm 0.004mM V_m = 56.94 \pm 0.43 U/min</p>
<p>W2Et (Dihydrofurane-2,5-dione)</p>	 <p>MW = 100</p>	<p>39 mAU*S/mmol</p>	<p>79.07 \pm 2.19</p>	<p>Not detectable</p>

Zusammenfassung

Die Wurzeln der Bengkoang (*Phacyrhizus erosus*) werden im Bereich der Kosmetik, speziell zum Schutz vor UV-Strahlung und zum Bleichen der Haut, verwendet. Indonesien ist ein tropisches Land, in dem täglich die Sonne scheint. Die Sonnenstrahlung, insbesondere die UV-Strahlung hat negative Auswirkungen, wie z. B. Sonnenbrand, Krebserzeugung und Hyperpigmentation. Deshalb brauchen die Menschen in Indonesien „sunscreen and whitening“-Kosmetik zum Schutz der Haut vor der Sonneneinstrahlung.

Bis heute gibt es keine wissenschaftlichen Beweise, ob Bengkoang Wirkstoffe enthält, die die UV-Strahlung absorbieren und die Haut bleichen können. Ziel der Arbeit war die Suche nach Substanzen mit diesen Eigenschaften. Deshalb stand die Isolierung und Strukturaufklärung von Inhaltsstoffen aus Bengkoang-Wurzeln sowie die Analyse der UV-Absorptionsfähigkeit und Analyse der Hautbleichungs-Fähigkeit der gefundenen Verbindungen im Mittelpunkt der Arbeit. Die Hautbleichungs-Fähigkeit wurde durch die Analyse der antioxidativen Aktivität und Tyrosinase-Inhibitor-Aktivität getestet.

Aus Extrakten unterschiedlicher Polarität wurden Sekundärstoffe durch unterschiedliche chromatographische Trenn-Methoden (Säulenchromatographie mit verschiedenen stationären Phasen) isoliert, deren Struktur mittels Massenspektrometrie und ein- und zweidimensionalen Kernresonanz-Spektroskopie-Experimente aufgeklärt wurde. Insgesamt wurden 13 Naturstoffe isoliert, von denen 11 die antioxidative Aktivität haben. Nur β -Sitosterol und Stigmasterol zeigten keine die antioxidative Aktivität.

Drei Verbindungen der Isoflavonoid-Gruppe, nämlich *Daidzein*, *Daidzein-7-O- β -glucopyranose*, *5-hydroxy-daidzein-7-O- β -glucopyranose* und eine Verbindung der Pterocarpan-Gruppe, nämlich *(8,9)-Furanyl-pterocarpan-3-ol*, wurde aus dem Essigsäureethylacetat-Extrakt isoliert. Alle haben starke Tyrosinase-Inhibitions-Aktivität mit IC_{50} -Werten von 4.38 mM bis 22.20 mM. Die andere Verbindungen, nämlich *2-Butoxy-2,5-bis(hydroxymethyl)-tetrahydrofuran* aus dem Butanol-Extrakt und *4-(2-(Furan-2-nyl)ethyl)-2-methyl-2,5-dihydrofuran-3-carbaldehyd* aus dem Essigsäureethylacetat-Extrakt nach-

Hydrolyse, haben eine Tyrosinase-Inhibitions-Aktivität mit IC_{50} -Werten von 1.21 mM und 0.20 mM.

Zusammenfassend kann festgestellt werden, dass Bengkoang viele aktive Verbindungen im Bereich der UV Absorption, antioxidative Aktivität und Tyrosinase-Inhibitions-Aktivität haben. Deshalb kann Bengkoang für Kosmetik, speziell als Material, das vor UV-Strahlung schützt und die Haut bleicht, verwendet werden.

Abstract

Bengkoang roots (*Phacyrhizus erosus*) have been used as cosmetics materials, primarily as sun screening and skin whitening materials. Indonesia is a tropical country, which has high sunlight intensities every day. Sunlight, primarily the ultraviolet ray, causes several damages on skin; for examples, sunburn, cancer, and hyperpigmentation. Therefore, the Indonesian people need sun screening and skin whitening preparations to avoid the negative effects of ultraviolet.

Up to now, active compounds in bengkoang roots which have skin whitening and sun screening activity have not been discovered yet. Therefore, the study on isolation, structure elucidation, antioxidative and anti-tyrosinase assay of active compounds in bengkoang roots has been conducted. The isolation of active compounds has been carried out by Soxhlet extraction using solvents (petroleum ether, ethyl acetate and butanol) followed by fractionated using column chromatography. The structures of the compounds were elucidated using 1D and 2D NMR spectroscopy and mass spectrometry. 13 compounds were isolated. All compounds have an antioxidative activity with the exceptions of β -sitosterol and stigmasterol.

Three isoflavonoids (i.e. daidzein; daidzein-7-O- β -glucopyranose; 5-Hydroxy-daidzein-7-O- β -glucopyranose), and a pterocarpan (i. e. (8,9)-Furanyl-pterocarpan-3-ol) were isolated from the ethyl acetate extract. All compounds showed tyrosinase inhibitory activity with IC_{50} values from 4.38 to 22.20 mM. The other compounds, i. e. 2-Butoxy-2,5-bis(hydroxymethyl)-tetrahydrofurane from the butanol extract and 4-2-(Furane-2-nyl)ethyl)-2-methyl-2,5-dihydrofurane-3-carbaldehyde from the ethyl acetate after hydrolysis extract have the tyrosinase inhibitory activity with IC_{50} values of 1.21 mM and 0.20 mM, respectively.

Based on the results, it can be concluded that bengkoang root can be used as sun screening and skin whitening materials for cosmetics preparations, because the bengkoang root posseses many compounds which have UV absorption, antioxidative and tyrosinase inhibitory activities.

List of References

- Abdalla, A.E., Roozen, J.P., Effect of plant extracts on the oxidative stability of sunflower oil and emulsion, *Food Chem.*, 64, **1999**, 323-329
- Abdel-Halim, O.B., Mothana, A.M., awadh, N., A new tyrosinase inhibitor from *Crinum yemense* as potential treatment for hyperpigmentation, *Pharmazie*, 63, **2008**, 405-407
- Ando, H., Funasaka, Y., Possible involvement of proteolytic degradation of tyrosinase in the regulatory effect of fatty acids on melanogenesis, *Lipid Res.*, 40, **1999**, 1312-1316
- Anonim, Jicama, http://en.wikipedia.org/wiki/Pachyrhizus_erosus, accessed on 10. 10. 2006
- Aridogan, B.C., Baydar, H., Kaya, S., Demirci, M., Özbasar, D., Mumcu, E., Antimicrobial activity and chemical composition of some essential oils, *Arch. Pharm. Res.*, 25, **2002**, 860-864
- Berezin, M.Y., Dzenitis, J.M., Hughes, B.M., Ho, S.V., Separation of sterols using zeolites, *Phys. Chem.*, 3, **2001**, 2184-2189
- Blair, H.C., Jordan, S.E., Peterson, T.G., Barnes, S., Variable effects of tyrosinase kinase inhibitors on avian osteoclastic activity and reduction of bone loss in ovariectomized rats, *J. Cell. Biochem.*, 61, **1996**, 629-637
- Bland, J.M., Park, Y.I., Raina, A.K., Dickens, J.C., Hollister, B., Trilinolein identified as a sex-specific component of tergal glands in alates of *Coptotermes formosanus*, *J. Chem. Ecol.*, 30, **2004**, 835-849
- Bleehen, S.S., Ebling, F.J.G., Champion, R.H., Disorders of skin Colour, *Textbook of dermatology*, Vol.3, Ed.5., **1995**, 1561-1577
- Blomquist, G.J., Howard, R.W., McDaniel, C.A., Remaley, S., Dwyer, L.A., Nelson, D.R., Application of methoxymercuration-demercuration followed by mass spectrometry as a convenient microanalytical technique for double-bond location in insect-derived alkenes, *J. Chem. Ecol.*, 6, **1980**, 257-269
- Boissy, R.E., Manga, P., On the etiology of contact/occupational vitiligo, *Pigment Cell Res.*, 17, **2004**, 208-214
- Briganti, S., Camera, E., Picardo, M., Chemical and instrumental approaches to treat hyperpigmentation, *Pigment Cell Res.*, 16, **2003**, 101-110
- Brown, A.J. and Jessup, W., Review article Oxysterols and Atherosclerosis, *Atherosclerosis*, 142, **1999**, 1-28

- Cacha, M., Gojuse-Moletta, G., Majind, R.R.T., Antimicrobial and radical scavenging flavonoids from the steam wood of *Erithrina latissima*, *Phytochem.*, 66, **2005**, 99, 104
- Cavaliere, C., Cucci, F., Foglia, P., Guarino, C., Samperi, R., Lagana, A., Flavonoid profile in soybeans by high-performance liquid chromatography/tandem mass spectrometry, *Rapid Commun. Mass Spectrom.*, 21, **2007**, 2177-2187
- Chan, P., Thomas, G.N., Tomlinson, B., Protective effects of trilinolein extracted from *Panax notoginseng* against cardiovascular disease, *Acta Pharmacol. Sin.*, 3, **2002**, 1157-1162
- Chang, T.S., Two potent suicide substrate of mushroom tyrosinase: 7,8,4'-trihydroxyisoflavone and 5,7,8,4'-tetrahydroxyisoflavone, *J. Agric. Food Chem.*, 55, **2007**, 2010-2015
- Chaves, M.H., Roque, N.F., Ayres, C.C., Steroids and flavonoids of *Porcelia macrocarpa*, *J. Braz. Chem. Soc.*, 15, **2004**, 608-613
- Chen, L.J., Zhao, X., Plummer, S., Tang, J., Games, D.E., Quantitative determination and structural characterization of isoflavones in nutrition supplements by liquid chromatography-mass spectrometry, *J. Chromatogr. A.*, 1082, **2005**, 60-70
- Chen, Q., Kubo, I., Kinetics of mushroom tyrosinase inhibition by quercetin, *J. Agric. Food Chem.*, 50, **2002**, 4108-4112
- Choi, E.J., The prooxidant, rather than antioxidant, acts of daidzein in vivo and in vitro: Daidzein suppresses glutathione metabolism, *Eur. J. Pharmacol.*, 542, **2006**, 162-169
- De-Eknamkul, W. and Potduang, B., Biosynthesis of β -sitosterol and stigmaterol in *Croton sublyratus* proceeds via a mixed origin of isoprene units, *Phytochem.*, 62, **2003**, 389-398
- Dewick, P.M., *Medicinal Natural Products: a biosynthetic approach*, 2nd Ed., John Wiley and Sons Ltd, **2002**, 247-272
- Dickson, R.A., Houghton, P.J., Hylands, P.J., Antibacterial and antioxidant cassane diterpenoids from *Caesalpinia benthamiana*, *Phytochem.*, 68, **2007**, 1436-1441
- Eisenreich, W., Schwarz, M., Cartarayde, A., Arigoni, D., Zenk, M.H., Bacher, A., The deoxyxylulose phosphate pathway of terpenoid biosynthesis in plants and microorganisms, *Chem. Biol.*, 5, **1998**, 21-23
- Falco, M.J.C., Pouliquem, Y.B.M., Lima, M.A.S., Gramosa, N.V., Costa-Lotufo, L.V., Milito, G.C.G., Pessoa, C., de Moraes, M.O., Silveira, E.R., Cytotoxic

- Flavonoids from *Platymiscium floribundum*, *J. Nat. Prod.*, 68, **2005**, 423-426
- Fassbender, K., Lütjohann, D., Dik, M.G., Bremmer, M., König, J., Walter, S., Liu, Y., Letiembre, M., von Bergmann, K., Jonker, C., Moderately elevated plant sterol levels are associated with reduced cardiovascular risk-The LASA study, *Atherosclerosis*, 196, **2006**, 283-288
- Frankel, E.N., Lipid oxidation: Mechanism, products and biological significance, *J. Am. Oil Chem. Soc.*, 61, **1984**, 1908-1917
- Friedman, M., Food browning and its prevention : An overview, *J. Agric. Food Chem.*, 44, **1996**, 631-653
- Geahlen, R.L., Koonchanok, N.M., McLaughlin, J.L., Pratt, D.E., Inhibition of protein-tyrosinase kinase activity by flavonoids and related compounds, *J. Nat. Prod.*, 52, **1989**, 982-986
- Gibb, A.R., Pinese, B., Tenakanai, D., Kawi, A.P., Bunn, B., Ramankutty, P., Suckling, D.M., (Z)-11-Hexadecenal and (3Z,6Z,9Z)-Tricosatriene: Sex pheromone components of the red banded Mango Caterpillar *Deanolis sublimbalis*, *J. Chem. Ecol.*, 34, **2008**, 1125-1133
- Gibb, A.R., Suckling, D.M., Morris, B.D., Dawson, T.E., Bunn, B., Comeskey, D., Dymock, J.J., (Z)-7-Tricosene and monounsaturated ketones as sex pheromone components of the Australian guava moth *Coscinoptycha improbana*: identification, field trapping and phenology, *J. Chem. Ecol.*, 32, **2006**, 221-237
- Gilly, R., Mara, D., Oded, S., Zohar, K., Resveratrol and a Novel Tyrosinase in Carignan Grape Juice, *J. Agric. Food Chem.*, 49, **2001**, 1479-1485
- Gomes, A., Saha, A., Chatterjee, I., Chakravarty, A.K., Viper and cobra venom neutralization by β -sitosterol and stigmasterol isolated from the root extract of *Pluchea indica* Less. (Asteraceae), *Phytomedicine*, 14, **2007**, 637-643
- Gordon, M.F., The mechanism of antioxidant action in vitro, In: Hudson, B.J.F. (ed), *Food Antioxidants*, London: Elsevier Applied Science, **1990**, 1-18
- Goto, H., Terao, Y., Akai, S., Synthesis of various kinds of isoflavones, isoflavanes, and biphenyl-ketones and their 1,1-diphenyl-2-picrylhydrazyl radical-scavenging activities, *Chem. Pharm. Bull.*, 57, **2009**, 346-360
- Gregg, C.D., Nelson, J.M., The action of tyrosinase on hydroquinone, *J. Am. Chem. Soc.*, 62, **1940**, 2510-2512

- Hac-Wydro, K., Wydro, P., Jagoda, A., Kapusta, J., The study on the interaction between phytosterols and phospholipids in model membranes, *Chem. Phys. Lipids*, 150, **2007**, 22-34
- Han, R-M., Tian, Y-X., Chen, C-H., Ai, X-C, Zhang, J-P., Skibsted, L.H., Comparison of flavonoids as antioxidants, *J. Agric. Food Chem.*, 57, **2009**, 3780-3785
- Harborne, J.B. and Baxter, H., *Handbook of Natural Flavonoids*, 2 vols., **1999**, Wiley, Chichester
- Hearing, V.J.Jr., In: *Methods in Enzymology*, Academic Press, New York, 142, **1987**, 154-165
- Hirota, S., Kawahara, T., Lonardi, E., de Waal, E., Funasaki, N., Canters, G.W., Oxygen binding to tyrosinase from *Streptomyces antibioticus* studied by laser flash photolysis, *J. Am. Chem. Soc.*, 127, **2005**, 17966-17967
- Huang, L., Zhong, T., Ye, Z., Chen, G., Identification of β -sitosterol, stigmasterol and ergosterin in *A. roxburghii* using supercritical fluid extraction followed by liquid chromatography/atmospheric pressure chemical ionization ion trap mass spectrometry, *Rapid Commun. Mass Spectrom.*, 21, **2007**, 3024-3032
- Hvattum, E., Analysis of triacylglycerols with non-aqueous reversed-phase liquid chromatography and positive ion electrospray tandem mass spectrometry, *Rapid Commun. Mass Spectrom.*, 15, **2001**, 187-190
- Imokawa, G., Tejima, T., Kirii, N., Kawai, M., Efficacy of 4-methoxydibenzoylmethane-2-carboxylic acid as a new broad spectrum sunscreen, *J. Soc. Cosmetic Chem.*, 42, **1990**, 67-84
- Ito, C, Itoigawa, M., Kumagaya, M., Okamata, Y., Ueda, K., Nishihara, T., Kojima, N., Furukawa, H., Isoflavonoids with Antiestrogenic Activity from *Millettia pachycarpa*, *J. Nat. Prod.*, 69, **2006**, 138-141
- Jackman, M.P., Hajnal, A., Lerch, K., Albino mutants of *Streptomyces glaucescens* tyrosinase, *Biochem.*, 274, **1991**, 707-713
- Jayaprakasha, G.K., Selvi, T., Sakariah, K.K., Antibacterial and Antioxidant Activities of Grape (*Vitis vinifera*) Seed Extracts, *Food Res. Internat.*, 36, **2003**, 117-122
- Joung-Ha, T., Tamura, S., Kubo, I., Effects of Mushroom tyrosinase on anisaldehyde, *J. Agric. Food Chem.*, 53, **2005**, 7024-7028
- Kahn, V., Ben-Shalom, N., Zakin, V., Effect of Kojic acid on the oxidation of N-acetyldopamine by mushroom tyrosinase, *J. Agric. Food Chem.*, 45, **1997**, 4460-4465

- Kang, J., Hick, L.A., Price, W.E., A fragmentation study of isoflavones in negative electrospray ionization by MSⁿ ion trap mass spectrometry and triple quadrupole mass spectrometry, *Rapid Commun. Mass Spectrom.*, 21, **2007**, 857-868
- Kanner, J., German, J.B., Kinsella, J.C., Initiation of lipid peroxidation in biological systems, *CRC Crit. Rev. Food. Sci. Nutr.*, 25, **1987**, 317-364
- Karg, E., Odh, G., Wittbjer, A., Rosengren, E., Rorsman, H., Hydrogen peroxide as an inducer of elevated tyrosinase level in melanoma cells, *Ethnopharmacol.*, 106, **2006**, 353-359
- Khan, M.T.H., Choudary, M.I., Atta.ur-Rahman, Mamedova, R.P, Agzamova, M.A., Sultankhodzhaev, M.N., Isaev, M.I., Tyrosinase inhibition studies of cycloartane and cucurbitane glycosides and their structure-activity relationships, *Bioorg. Med. Chem.*, 14, **2006**, 6085-6088
- Khatib, S., Nerya, O., Musa, R., Shmuel, M., Tamir, S., Vaya, J., Chalcones as potent tyrosinase inhibitors: the importance of a 2,4-substituted resorcinol moiety, *Bioorg. Med. Chem.*, 13, **2005**, 433-441
- Kim, D., Park, J., Kim, J., Han, C., Yoon, J., Kim, N., Seo, J., Lee, C., Flavonoids as mushroom inhibitors: A Fluorescence quenching study, *J. Agric. Food Chem.*, 54, **2006**, 935-941
- Kim, H, Choi, J., Cho., J.K., Kim, S.Y., Lee, Y-S., Solid-phase synthesis of kojic acid-tripeptides and their tyrosinase inhibitory activity, storage stability, and toxicity, *Bioorg. Med. Chem. Letter*, 14, **2004a**, 2843-2846
- Kim, Y-J., Chung, J.E., Kurisawa, M., Uyama, H., Kobayashi, S., New Tyrosinase Inhibitors, (+)-Catechin-Aldehyde Polycondensates, *Biomacromolecules*, 5, **2004b**, 474-479
- Knight, D.C., Eden, J.A., A review of the clinical effects of phytoestrogens, *Obstet. Gynecol.*, 87, **1996**, 897-904
- Kobayashi, T., Urabe, K., Winder, A., Jimenez-Cervantes, C., Imokawa, G., Brewington, T., Solano, F., Garcia-Borron, J.C., Hearing, V.J., Tyrosinase related Protein 1 (TRP1) functions as a DHICA oxidase in melanin biosynthesis, *EMBO Journal*, 13, **1994**, 5818-5825
- Koleva, I.I., van Beek, T.A., Linssen, J.P.H., de Groot, A., Evstatieva, L.N., Screening of plant extracts for antioxidant activity: a comparative study on three testing methods, *Phytochem. Anal.*, 13, **2001**, 8-17
- Konzen, M., De Marco, D., Cordova, C.A.S., Vieira, T.O., Antonio, R.V., Creczynski-Pasa, T.B., Antioxidant properties of violacein: Possible

- relation on its biological function, *Bioorg. Med. Chem.*, 14, **2006**, 8307-8313
- Kubo, I. and Kinst-Hori, I., Tyrosinase Inhibitors from Cumin, *J. Agric. Food Chem.*, 46, **1998a**, 5338-5341
- Kubo, I., Kinst-Hori, I., Nihei, K-I., Soria, F., Takasaki, M., Calderon, J.S., Cespedes, C.L., Tyrosinase inhibitors from galls of *Rhus javanica* leaves and their effects on insects, *Z. Naturforsch*, 58C, **2003**, 719-725
- Kubo, I., Kinst-Hori, I., Tyrosinase inhibitors from Anise oil, *J. Agric. Food Chem.*, 46, **1998b**, 1268-1271
- Kubo, I., Kinst-Hori, I., Tyrosinase inhibitory activity of the Olive oil flavor compounds, *J. Agric. Food Chem.*, 47, **1999**, 4574-4578
- Kubow, S., Routes of formation and toxic consequences of lipid oxidation products in foods, *Free Radical Biol. Med.*, 12, **1992**, 63-81
- Kulisic, T., Radonic, A., Katalinic, V., Milos, M., Use of different methods for testing antioxidative activity of oregano essential oil, *Food Chem.*, 85, **2004**, 633-640
- Kumar, V., Rani, A., Dixit, A.K., Bhatnagar, D., Chauhan, G.S., Relative changes in tocopherols, isoflavones, total phenolic content, and antioxidative activity in soybean seeds at different reproductive stages, *J. Agric. Food Chem.*, 57, **2009**, 2705-2710
- Land, E.J., Ramsden, C.A., Riley, P.A., Tyrosinase autoactivation and the chemistry of ortho-quinone amines, *Acc. Chem. Res.*, 36, **2003**, 300-308
- Lang'at-Thoruwa, C., Song, T.T., Hu, J., Simons, A.L., Murphy, P.A., A simple synthesis of 7,4'-dihydroxy-6-methoxyisoflavone, glycitein, the third soybean isoflavone, *J. Nat. Prod.*, 66, **2003**, 149-151
- Laufer, Z., Beckett, R.P., Minibayeva, F., Co-occurrence of the multicopper oxidases tyrosinase and laccase in Lichens in sub-order Peltigerineae, *Annals of Botany*, Oxford University Press, **2006**, 1-8
- Lee, H.S., Tyrosinase inhibitors of *Pulsatilla cernua* root-derived materials, *J. Agric. Food Chem.*, 50, **2002**, 1400-1403
- Lee, J-H., Lee, J.Y., Park, J.H, Jung, H.S., Kim, J.S., Kang, S.S., Kim, Y.S., Han, Y., Immunoregulatory activity by daucosterol, a β -sitosterol glycoside, induces protective Th1 immune response against disseminated Candidiasis in mice, *Vaccine*, 25, **2007**, 3834-3840
- Lerch, K., Neurospora tyrosinase: structural, spectroscopic and catalytic properties, *Mol. Cell. Biochem.*, 52, **1983**, 125-138

- Likhitwitayawuid, K., Stilbenes with tyrosinase inhibitory activity, *Current Sci.*, 94, **2008**, 44-52
- Liu, J-C., Chan, P., Chen, J-J., Lee, H-M., Lee, W-S., Shih, N-L., Chen, Y-L., Hong, H-J., Cheng, T-H., The inhibitory effect of trilinolein on norepinephrine-induced β -myosin heavy chain promptor activity, reactive oxygen species generation, and extracellular signal-regulated kinase phosphorylation in neonatal rat cardiomyocytes, *J. Biomed. Sci.*, 11, **2004**, 11-18
- Maeda, K., Fukuda, M., In vitro effectiveness of several whitening cosmetics components in human melanocytes, *J. Soc. Cosmet. Chem.*, 42, **1991**, 361-368
- Mahungu, S.M., Hansen, S.L., Artz, W.E., Identification and quantification of volatile compounds in two heated model compounds, trilinolein and linoleic acid esterified propoxylated glycerol, *J. Agric. Food Chem.*, 47, **1999**, 690-694
- Martens, S. and Mithöfer, A., Flavones and flavone synthases, *Phytochem.*, 66, **2005**, 2399-2407
- Martinez, M.V., Whittaker, J.R., The biochemistry and control of enzymatic browning, *Trends Food Sci. Technol.*, 6, **1995**, 1995-2000
- Marxen, K., Vanselow, K.H., Lippemeier, S., Hintze, R., Ruser, A., Hansen, U-P., Determination of DPPH radical oxidation caused by methanolic extracts of some Microalga species by linear regression analysis of spectrophotometric measurements, *Sensors*, 7, **2007**, 2080-2095
- Matoba, Y., Kumagai, T., Yamamoto, A., Yoshitshu, H., Sugiyama, M., Crystallographic evidence that the dinuclear copper center of tyrosinase is flexible during catalysis, *J. Biol. Chem.*, 281, **2006**, 8981-8990
- Matsuura, R., Ukeda, H., Sawamura, M., Tyrosinase inhibitory activity of Citrus essential oils, *J. Agric. Food Chem.*, 54, **2006**, 2309-2313
- Maver, M., Queiroz, E.F., Wolfender, J-L., Hostettmann, K., Flavonoids from the Stem of *Eriophorum scheuchzeri*, *J. Nat. Prod.*, 68, **2005**, 1094-1098
- Mayer, A.M., Polyphenol oxides in plants, Recent progress, *Phytochem.*, 26, **1987**, 11-20
- McCarthy, F.O., Chopra, J., Ford, A., Hogan, S.A., Kerry, J.P., O'Brien, N.M., Ryan, E., Maguire, A.R., Synthesis, isolation and characterization of β -sitosterol and β -sitosterol oxide derivatives, *Org. Biomol. Chem.*, 3, **2005**, 3059-3065

- Miliauskas, G., van Beek, T. A., de Waard, P., Venskutonis, R. P., Sudhölter, E. J. R., Comparison of analytical and semi-preparative columns for high-performance liquid chromatography - solid phase extraction - nuclear magnetic resonance, *J. Chromatogr. A*, 1112, **2006**, 276-284
- Miliauskas, G., Venskutonis, P.R., van Beek, T.A., Screening of radical scavenging activity of some medicinal and aromatic plant extracts, *Food Chem.*, **2003**
- Mirica, L.M., Vance, M., Rudd, D.J., Hedman, B., Hodgson, K.O., Solomon, E.I, Stack, T.D.P., Tyrosinase reactivity in a model complex: An alternative hydroxylation mechanism, *Science*, 308, **2005**, 1890-1892
- Molyneux, P., The use of the stable free radical diphenylpicrylhydrazyl (DPPH) for estimating antioxidant activity, *Songklanakari J. Sci. Technol.*, 26, **2004**, 211-219
- Moon, D-O., Lee, K-J., Choi, Y.H., Kim, G-Y., β -sitosterol-induced-apoptosis is mediated by the activation of ERK and the downregulation of Akt in MCA-102 murine fibrosarcoma cells, *Internatl. Immunopharmacol.*, 7, **2007**, 1044-1053
- Murthy, M.S.R., Rao, E.V., Ward, R.S., Carbon-13 Nuclear Magnetic Resonance Spectra of Isoflavones, *Magn. Reson. Chem.*, 24, **1986**, 225-230
- Mximo, P., Loureno, A., Feio, S.S., Roseiro, J.C., Flavonoids from *Ulex airensis* and *Ulex europaeus ssp. europaeus*, *J. Nat. Prod.*, 65, **2002**, 175-178
- Neff, W.E., Byrdwell, W.C., Characterization of model triacylglycerol (triolein, trilinolein and trilinolein) autooxidation products via high-performance liquid chromatography coupled with atmospheric pressure chemical ionization mass spectrometry, *J. Chromatogr. A*, 818, **1998**, 169-186
- Nerya, O., Musa, R., Khatib, S., tamir, S., Vaya, J., Chalcones as potent tyrosinase inhibitors: the effect of hydroxyl positions and numbers, *Phytochem.*, 65, **2004**, 1389-1395
- Nes, W.D. and Venkatramesh, M., Enzymology of phytosterol transformations, *Critical Rev. Biochem. Molc. Biol.*, 34, **1999**, 81-93
- Nithitanakool, S., Pithayanukul, P., Bavovada, R., Patchreenart, S., Molecular docking studies and anti-tyrosinase activity of Thai Mango Seed Kernel Extract, *Molecules*, 14, **2009**, 257-265
- Ogawa, M., Perdiago, N.B., Santiago, M.E., Kozima, T.T., On physiological aspects of black spot appearance in Shrimp, *Bull. Jpn. Soc. Sci. Fish*, 50, **1984**, 1763-1769

- Ohguchi, K., Tanaka, T., Iliya, I., Ito, T., Iinung, M., Matsumoto, K., Akao, Y., Nozawa, Y., Gnetol as a potent tyrosinase inhibitor from Genus Gnetum, *Biosci. Biotechnol. Biochem.*, 67, **2003**, 663-665
- Ohslugi, M., Fan, W., Hase, K., Xiong, Q., Tezuka, Y., Komatsu, K., Namba, T., Saitoh, T., Tazawa, K., Kadota, S., Active-oxygen scavenging activity of traditional nourishing-tonic herbal medicines and active constituents of *Rhodiola sacra*, *J. Ethnopharmacol.*, 67, **1999**, 111-119
- Okombi, S., Rival, D., Bonnet, S., Mariotte, A.M., Perrier, E., Boumendjel, A., Analogues of N-hydroxycinnamoylphenalkylamides as inhibitors of human melanocyte-tyrosinase, *Bioorg. Med. Lett.*, 16, **2006**, 2252-2255
- Özkan, G., Sagdic, O., Baydar, N.G., Baydar, H., Antioxidant and antibacterial activities of *Rosa damascene* flower extracts, *Food Sci. Technol. Internat.*, 10, **2004**, 277-281
- Palavicini, S., Granata, A., Monzani, E., Casella, L., Hydroxylation of phenolic compounds by a peroxodicopper(II) Complex: Further Insight into the mechanism of tyrosinase, *J. Am. Chem. Soc.*, 127, **2005**, 18031-18036
- Park, C., Moon, D-O., Rhu, C-H., Choi, B.T., Lee, W.H., Kim, Y.G., Choi, Y.H., β -sitosterol induces anti-proliferation and apoptosis in human leukemic U937 cells through activation of Caspace-3 and induction of Bax/Bcl-2 Ratio, *Biol. Pharm. Bull.*, 30, **2007**, 1317-1323
- Parra-Delgado, H., Ruiz, G.G., Camacho, A.N., Martinez-Vazquez, M.M., Anti-inflammatory activity of some extracts and isolates from *Leonotis nepetaefolia* on TPA-induced edema model, *Rev. Soc. Quim. Mex.*, 48, **2004**, 293-295
- Parvez, S., Kang, M., Chung, H.S., Bae, H., Naturally occurring tyrosinase inhibitors: mechanism and applications in skin health, cosmetics and agriculture industrie, *Phytother. Res*, 21, **2007**, 805-816
- Patrick, J.D., Lamprecht, J.H., Plant sterols and sterolin: a review of their immune-modulating properties, *Altern. Med. Rev.*, 4, **1999**, 170-177
- Prior, R.L., Wu, X., Schaih, K., Standardized methods for the determination of antioxidant capacity and phenolics in foods and dietary supplements, *J. Agric. Food Chem.*, 53, **2005**, 4290-4303
- Qian, J. Y., Liu, D, Huang, A.G., The efficiency of flavonoids in polar extracts of *Lycium chinense* mill fruits as free radical scavenger, *Food Chem.*, 87, **2004**, 283-288
- Qu, J., Tu, H., Shan, B., Luk, A., deBose-Boyd, R.A., Bashmakov, Y., Goldstein, J.L., Brown, M.S., Unsaturated fatty acids inhibit transcription of the sterol

- regulatory element-binding protein-1c (SREBP-1c) gene by antagonizing ligand-dependent activation of the LXR, *Proc. Natl. Acad. Sci.*, 98, **2001**, 6027-6032
- Rangkadilok, N., Sitthimonchai, S., Worasuttayangkurn, L., Mahidol, C., Ruchirawat, M., Satayavivad, J., Evaluation of free radical scavenging and antityrosinase activities of standardized longan fruit extract, *Food Chem. Toxicol.*, **2006**, 1016-1024
- Raynal, N., J-M., Momparler, L., Charbonneau, M., Momparler, R.L., Antileukemic activity of Genistein, a major isoflavone present in soy products, *J. Nat. Prod.*, 71, **2008**, 3-7
- Re, R., Pellegrini, N., Proteggente, A., Pannala, A., Yang, M., Rice-Evans, C., Antioxidant activity applying an improved ABTS radical cation decolorization assay, *Free Radical Biol. Med.*, 26, **1999**, 1231-1237
- Rohmer, M., The discovery of a mevalonate-independent pathway for isoprenoid biosynthesis in bacteria, algae and higher plants, *Nat. Prod. Rep.*, 16, **1999**, 565-574
- Ruiz-Larrea, M.B., Mohan, A.R., Paganga, G., Miller, N.J., Bolwel, G.P., Rice-Evans, C.A., Antioxidant activity of phytoestrogenic isoflavones, *Free Rad. Res.*, 26, **1997**, 63-70
- Salzbrunn, K. U., Über die Funktion und Struktur Tyrosinase aus *Streptomyces antibioticus*, *Dissertation*, The Johannes Gutenberg-Mainz University, Germany, **2007**, 1-18
- Sandler, J. A., *The Phytochemical Extraction and analysis of new flavonoids and saponins from the genus Silphium*, *Dissertation*, The University of Texas at Austin, **2005**, 1-23
- Santos, L.S., Catharino, R.R., Aguiar, C.L., Tsai, S.M., Eberlin, M.N., Chemotaxonomic markers of organic, natural, and genetically modified soybeans detected by direct infusion electrospray ionization mass spectrometry, *J. Radioanal. Nucl. Chem.*, 269, **2006**, 505-509
- Sasaki, K. and Yoshizuki, F., Nobiletin as a tyrosinase inhibitor from the peel of Citrus fruit, *Biol. Pharm. Bull.*, 25, **2002**, 806-808
- Sawai, Y., Moon, J.H., NMR analytical approach to clarify the molecular mechanisms of the antioxidative and radical-scavenging activities of antioxidants in tea using 1,1-diphenyl-2-picrylhydrazyl, *J. Agric. Food Chem.*, 48, **2000**, 6247-6253

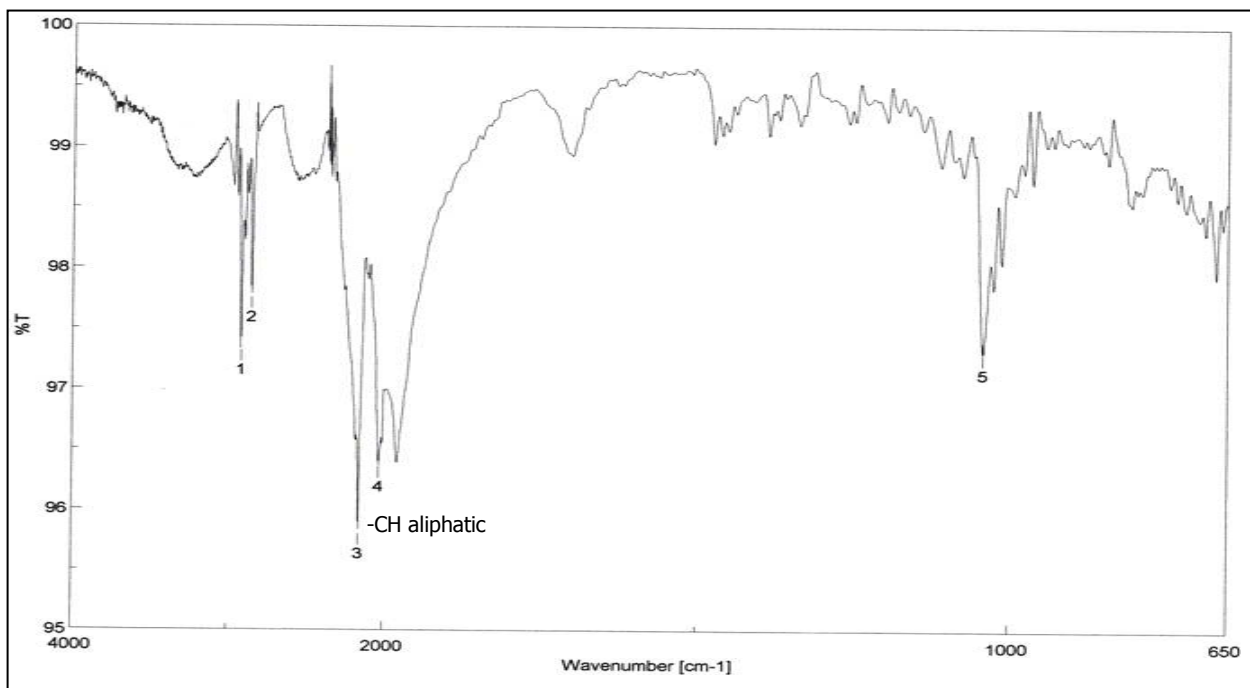
- Sayre, L.M., Nadkarni, D.V., Direct conversion of phenols to o-quinones by copper(I)dioxygen. Questions regarding the monophenolase activity of tyrosinase mimics, *J. Am. Chem. Soc.*, 116, **1994**, 3157-3158
- Schauenstein, E., Esterbauer, H., Zollner, H., In aldehydes in biological systems, Pion, London, 1977
- Seiberg, M., Paine. C., Sharlow, E., Andrade-Gordon., P., Costanzo, M., Eisinger, M., Shapiro, S.S., Inhibition of melanosome transfer results in skin lightening, *J. Invest. Dermatol.*, 115, **2000**, 162-167
- Seo, S.Y., Sharma, V.K., Sharma, N., Mushroom tyrosinase: recent prospect, *J. Agric. Food Chem.*, **2003**, 2837-2853
- Setchel, K.D.R., and Welsh, M.B., High-performance liquid chromatography analysis of phytoestrogens in soy protein preparations with ultraviolet, electrochemical and thermospray mass spectrometric detection, *J. Chromatogr.*, 386, **1987**, 313-323
- Sharma, K.R., Seenivasagan, T., Rao, A.N., Ganeson, K., Agarwal, O.P., Malhotra, R.C., Prakash, S., Oviposition responses of *Aedes aegypti* and *Aedes albopictus* to certain fatty acid esters, *Parasitol. Res.*, 103, **2008**, 1065-1073
- Shen, Y.C. and Hong, C.Y., Effect of trilinolein on cyclic nucleotide formation in human platelets: relationship with its antiplatelet effect and nitric oxide synthesis, *Br. J. Pharmacol.*, 116, **1995**, 1644-1648
- Shimoda, K., Sato, N., Kobayashi, T., Hamada, H., Hamada, Hi., Glycosylation of daidzein by the *Eucalyptus* cell cultures, *Phytochem.*, 69, **2008**, 2303-2306
- Silva, B. A., Ferreres, F., Malva, J. O., Dias, A. C. P., Phytochemical and antioxidant characterization of *Hypericum perforatum* alcoholic extracts, *Food Chem.*, 90, **2005**, 157-167
- Simonova, M., Wall, A., Weissleder, R., Bogdanov, A.Jr., Tyrosinase mutants are capable of prodrug activation in transfected nonmelanotic cells, *Cancer Res.*, 60, **2000**, 6656-6662
- Singleton, V.L., Rossi, J.R., Colorimetry of Total Phenolics with Phosphomolibdat-Phosphothungstic acid, *Am. J. Enol. Viticulture*, 16, **1965**, 144-158
- Solano, F., Martinez-Liarte, J.H., Jimenez-Cervantes, C., Garcia-Borrón, J.C., Lozano, J.A., Dopachrome Tautomerase is a Zinc-containing Enzyme, *Biochem. Biophys. Res. Comm.*, 204, **1994**, 1243-1250
- Soma, M.R., Mims, M.P., Chari, M.V., Rees, D., Morrisett, J.D., Triglyceride Metabolism in 3T3-L1 Cells, *J. Biol. Chem.*, 267, **1992**, 11168-11175

- Sudjaroen, Y., Haubner, R., Würtele, G., Hull, W. E., Erben, G., Spiegelhalder, B., Changbumrung, S., Bartsch, H., Owen, R. W., Isolation and structure elucidation of phenolic antioxidants from Tamarind (*Tamarindus indica* L.) seeds and pericarp, *Food Chem. Toxicol.*, 43, **2005**, 1673-1682
- Sugumuran, M., Comparative biochemistry of eumelanogenesis and the protective roles of phenoloxidase and melanin in insects, *Pigment cell Res.*, 15, **2002**, 2-9
- Tanimoto, S., Tominaga, H., Okada, Y., Nomura, M., Synthesis and cosmetic whitening effect of glycosides derived from several phenylpropanoids, *Pharm. Soc.*, 126, **2006**, 173-177
- Thayer, A.M., Food additives, *Chem. Eng. News*, 70, **1992**, 92-97
- Torres, R., Fanii, F., Modak, B., Urbina, F., Labbe, C., Guerrero, J., Antioxidant activity of coumarins and flavonols from resinous exudates of *Haplopappus multifolius*, *Phytochem.*, 67, **2006**, 984-987
- Urasopon, N., Hamada, Y., Asaoka, K., Pongmali, U., Malaivijitnond, S., Isoflavone content of rodent diets and its estrogenic effect on vaginal cornification in *Pueraria mirifica*-treated rats, *Science Asia*, 34, **2008**, 371-376
- van Gelder, C.W.G., Flurkey, W.H., Wichers, H.J., Sequence and structural features of plant and fungal tyrosinases, *Phytochem.*, 45, **1997**, 1309-1323
- Victor, F.C., Gelber, J., Rao, B., Melasma: a Review, *J. Cutan. Med. Surg.*, 8, **2004**, 97-102
- Walters, C., Keeney, A., Wigal, C.T., Johnston, C.R., and Cornelius, R., The spectrophotometric analysis and modelling of sunscreens, *J. Chem. Edu.*, 74, **1997**, 99-101
- Wang, B.F., Wang, J.S., Lu, J.F., Kao, T.H., Chen, B.H., Antiproliferation effect and mechanism of prostate cancer cell lines as affected by isoflavones from soybean cake, *J. Agric. Food Chem.*, 57, **2009**, 2221-2232
- Wang, K.H., Lin, R.D., Hsu, F.L., Huang, Y.H., Chang, H.C., Huang, C.Y., Lee, M.H., Cosmetic applications of selected traditional Chinese herbal medicines, *J. Ethnopharmacol.*, 106, **2006**, 353-359
- Wang, N., Hebert, D.N., Tyrosinase maturation through the mammalian secretory pathway: bringing color to life, *Pigment Cell Res.* 19, **2006**, 3-18
- Whitaker, J.R., Polyphenol oxidase, in *Food Enzymes, Structure and Mechanism*; Wong, D.W.S., Ed.; Chapman&Hall: New York, **1995**, 271-307

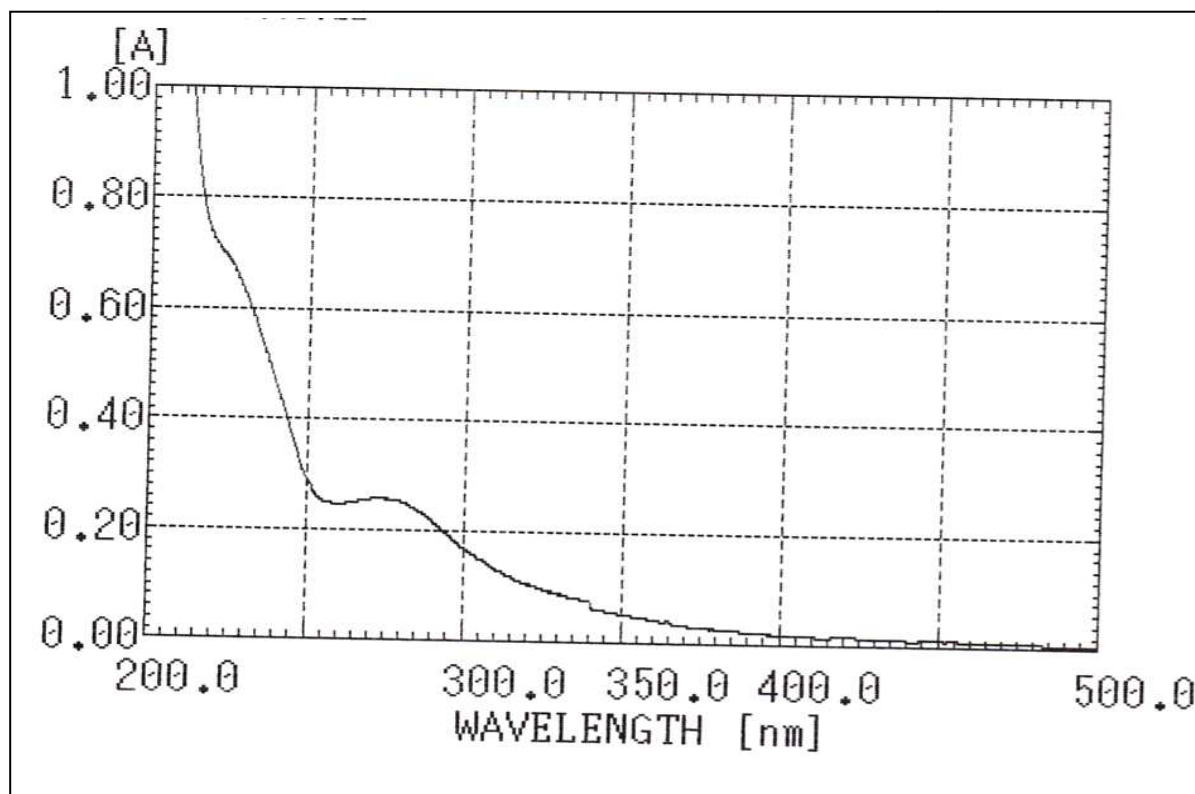
- Williams, P.L., Bannister, L.H., Berry, M.M., Collins, P., Dyson, M., Dussek., J.E., Ferguson, M.W.J., Integumental system, *Gray's Anatomy*, **1995**, 376-417
- Wink. M., *Biochemistry of plant secondary metabolism*, England: Sheffield Academic Press, **1999**, 1-16
- Wu, C., Chen, F., Wang, X., Jim, H. J., Guo-qing He, Zitlin, V. H., Huang, G., Antioxidant constituents in feverfew (*Tanacetum parthenium*) extract and their chromatographic quantification, *Food Chem.*, 96, **2006**, 220-227
- Wu, C., Chen, F., Wang, X., Kim, H-J., He, G-q., Haley-Zittlin, V., Huang, G., Antioxidant constituents in feverfew (*Tanacetum parthenium*) extract and their chromatography quantification, *Food Chem.*, 96, **2006**, 220-227
- Wu, Q., Wang, M., Simon, J.E., Analytical methods to determine phytoestrogenic compounds, *J. Chromatogr. B.*, 812, **2004**, 325-355
- Yuk, J.E., Woo, J.S., Yun, C-Y., Lee, J-S., Kim, J-H., Song, G-Y., Yang, J.E., Hur, I.K., Kim, I.S., Effects of lactose- β -sitosterol and β -sitosterol on ovalbumin-induced lung inflammation in actively sensitized mice, *Internatl. Immunopharmacol.*, 7, **2007**, 1517-1527
- Zhang, X., et al., Identification and quantitative analysis of β -sitosterol oxides in vegetables oil by capillary gas chromatography-mass spectrometry, *Steroids*, 70, **2005**, 896-906
- Zheng, Z.P., Cheng, K.W., Kinto, J.K., Li, H., Wang, M., Isolation of tyrosinase inhibitors from *Artocarpus heterophyllus* and use of its extract as antibrowning agent, *Mol. Nutr. Food. Res.*, 52, **2008**, 1530-1538

APPENDIX 1

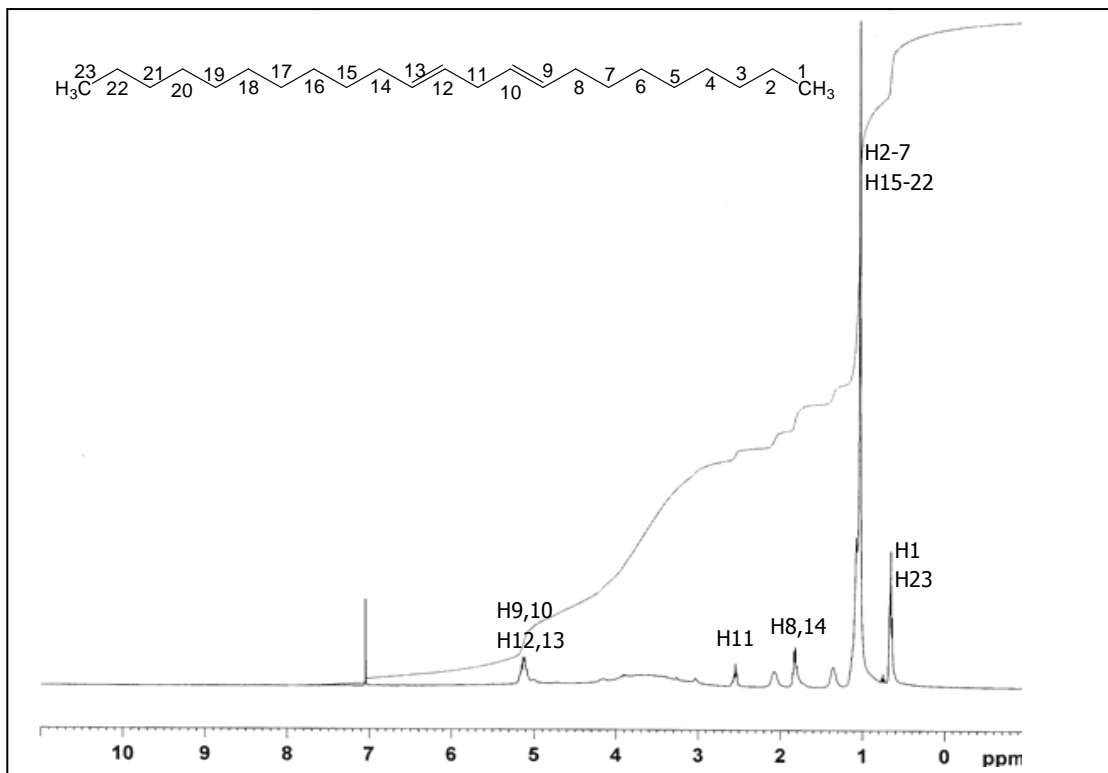
IR spectrum, UV spectrum, ^1H NMR and ^{13}C NMR of compound 101



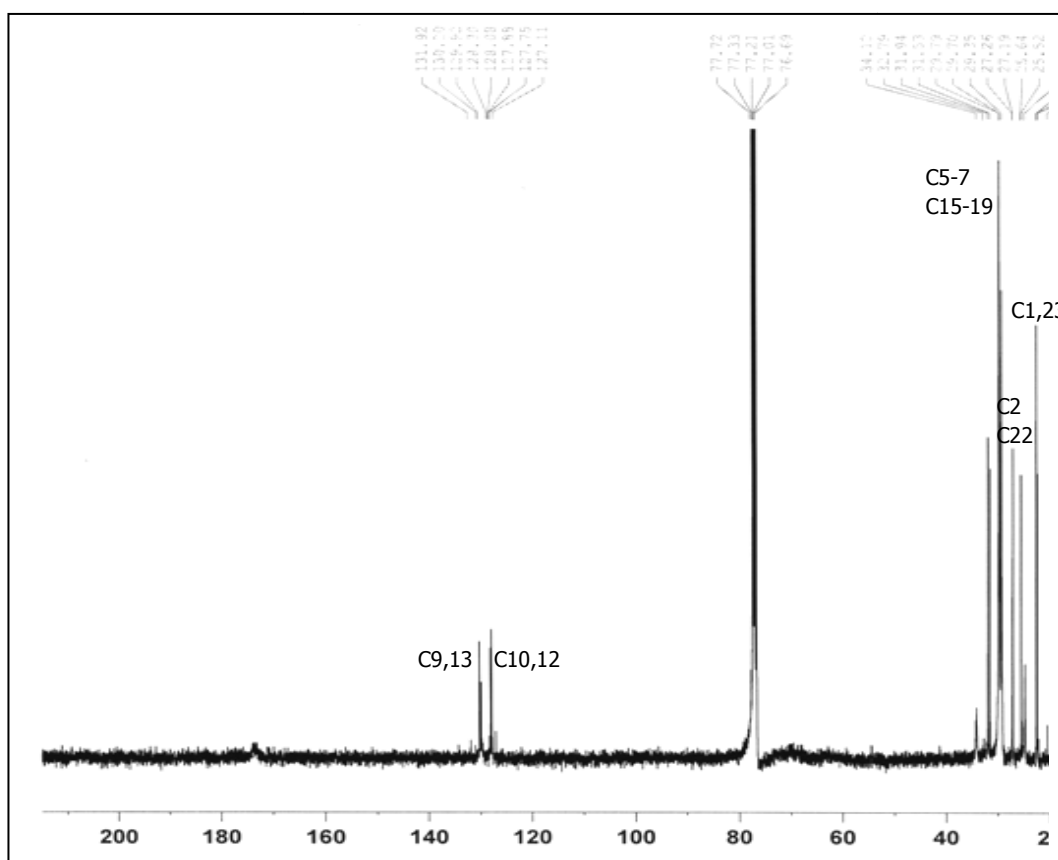
App.1.1. IR spectrum of compound 101 (9,12-Tricosandiene)



App.1.2. UV spectrum of compound 101 (9,12-Tricosandiene)



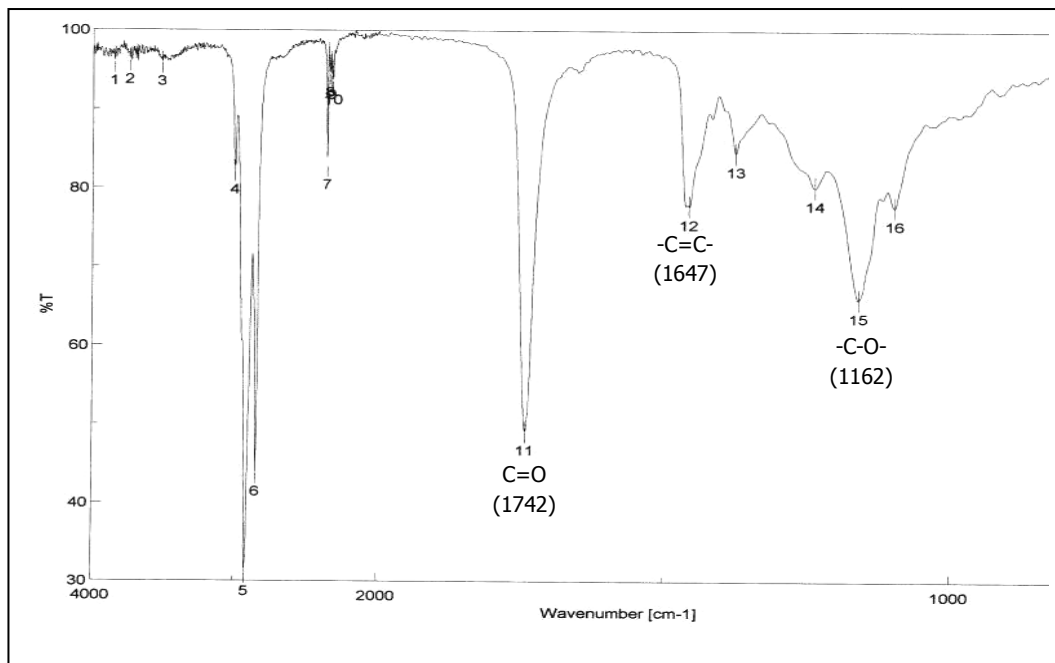
App.1.3. ^1H NMR spectrum of compound 101 (9,12-Tricosandiene) measured in CDCl_3 (500 MHz)



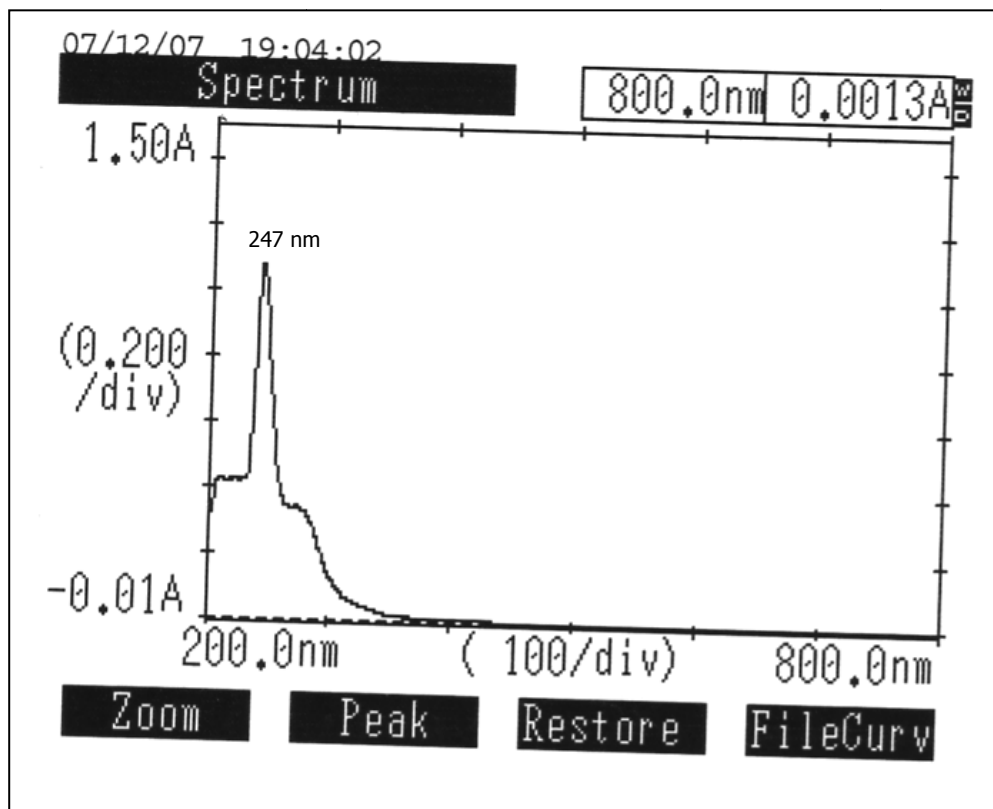
App.1.4. ^{13}C NMR of compound 101 (9,12-Tricosandiene) measured in CDCl_3 (125 MHz)

APPENDIX 2

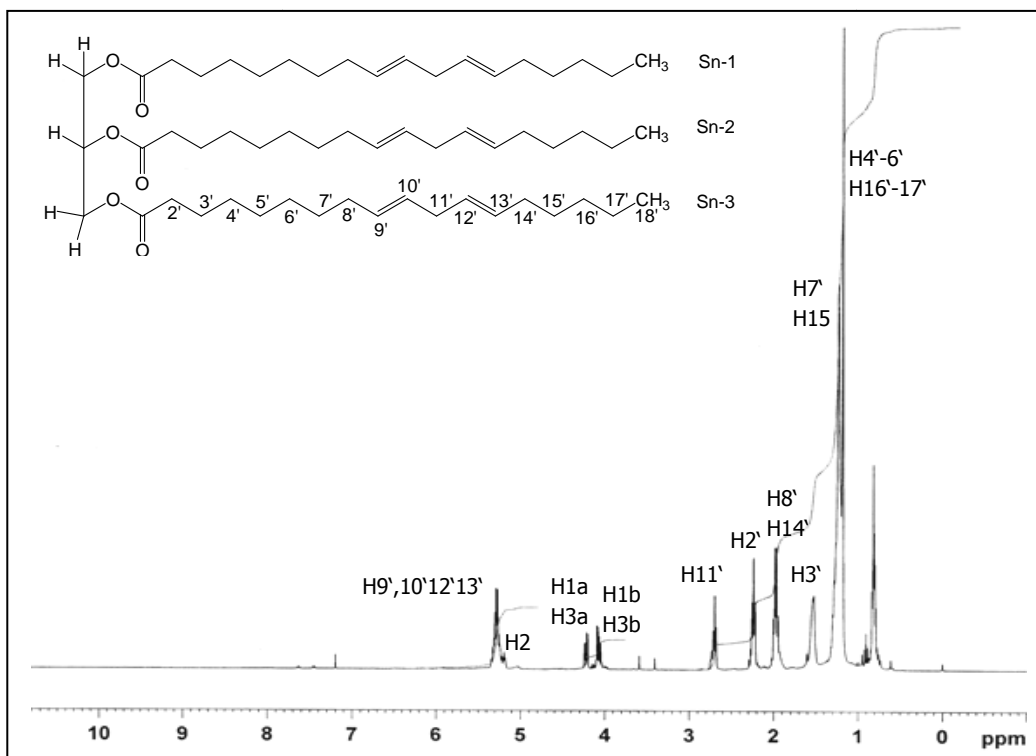
IR spectrum, UV spectrum, ^1H NMR and ^{13}C NMR of compound 102



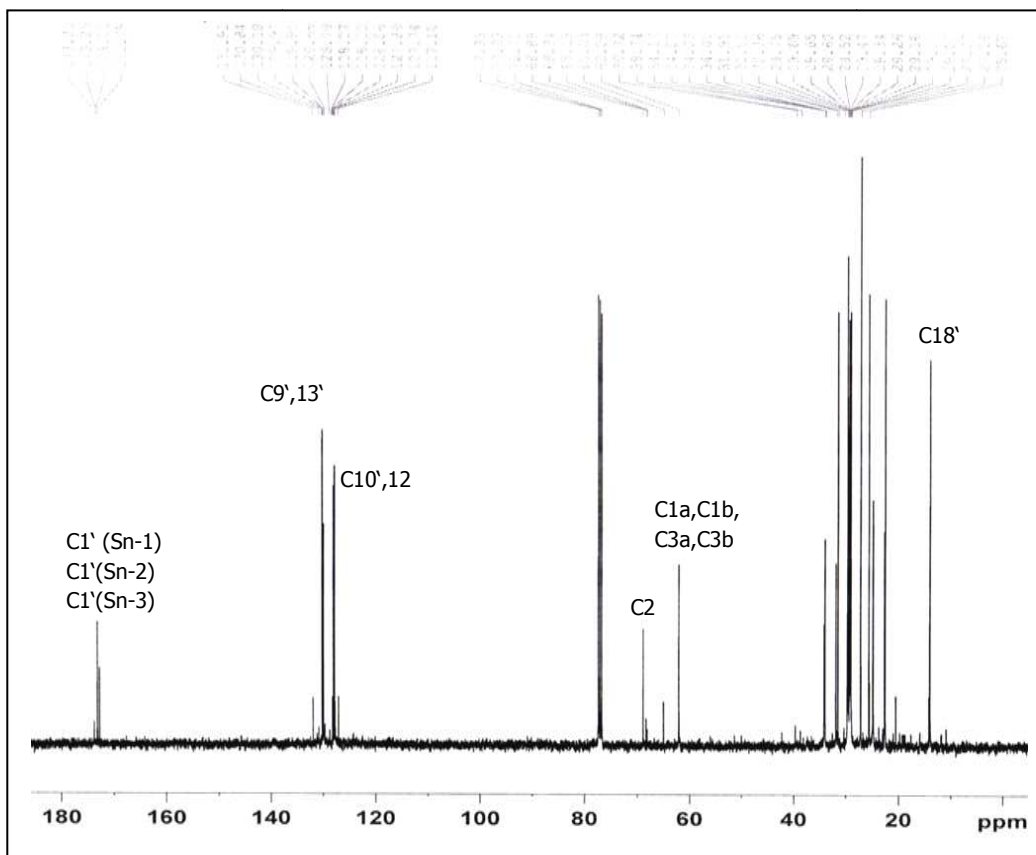
App.2.1. IR Spectrum of compound 102 (Trilinolein)



App.2.2. UV spectrum of compound 102 (Trilinolein)



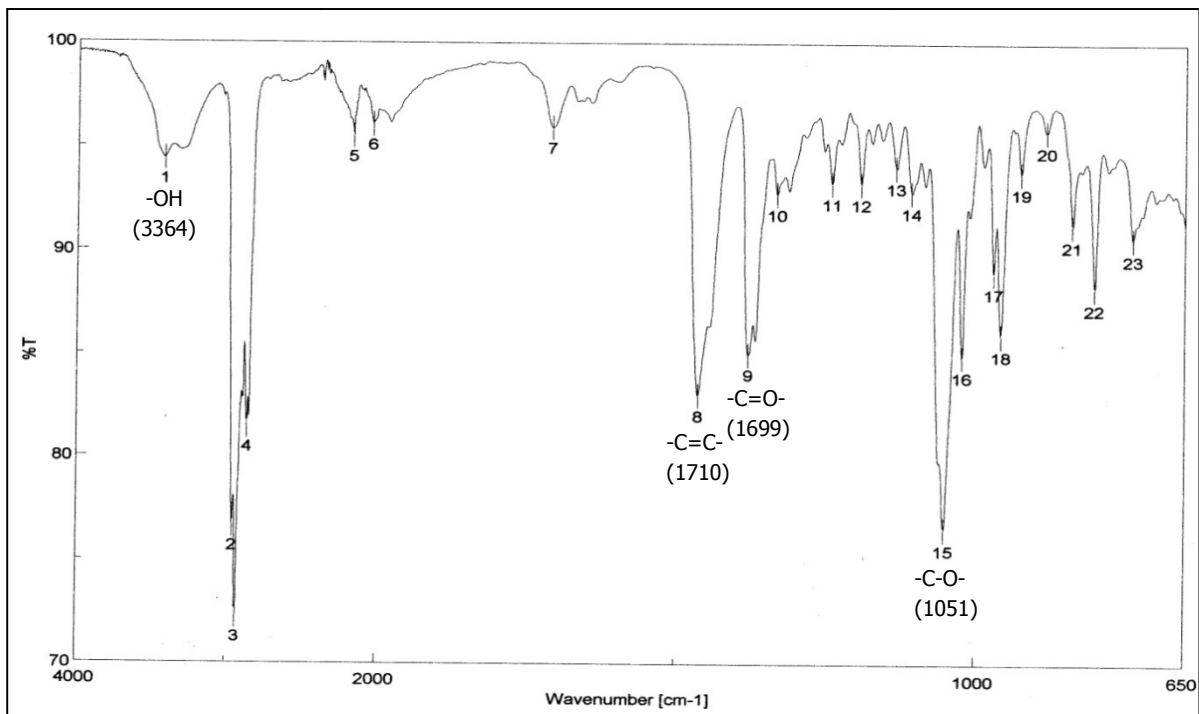
App.2.3. ^1H NMR of compound 102 (Trilinolein) measured in CDCl_3 (500 MHz)



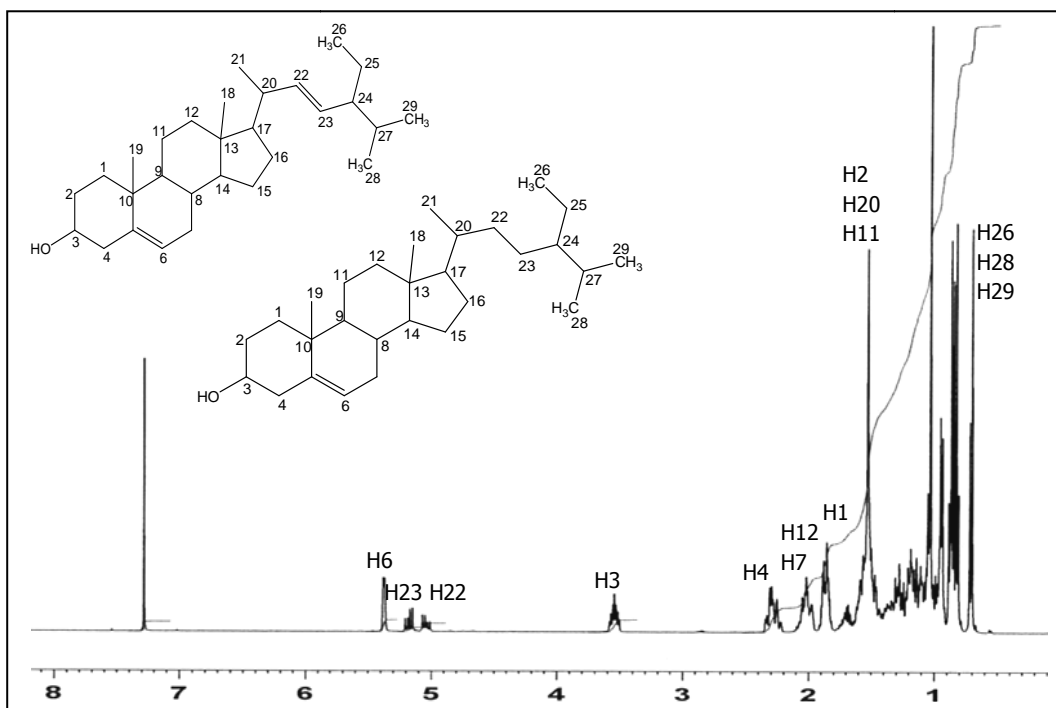
App.2.4. ^{13}C NMR of compound 102 (Trilinolein) measured in CDCl_3 (125 MHz)

APPENDIX 3

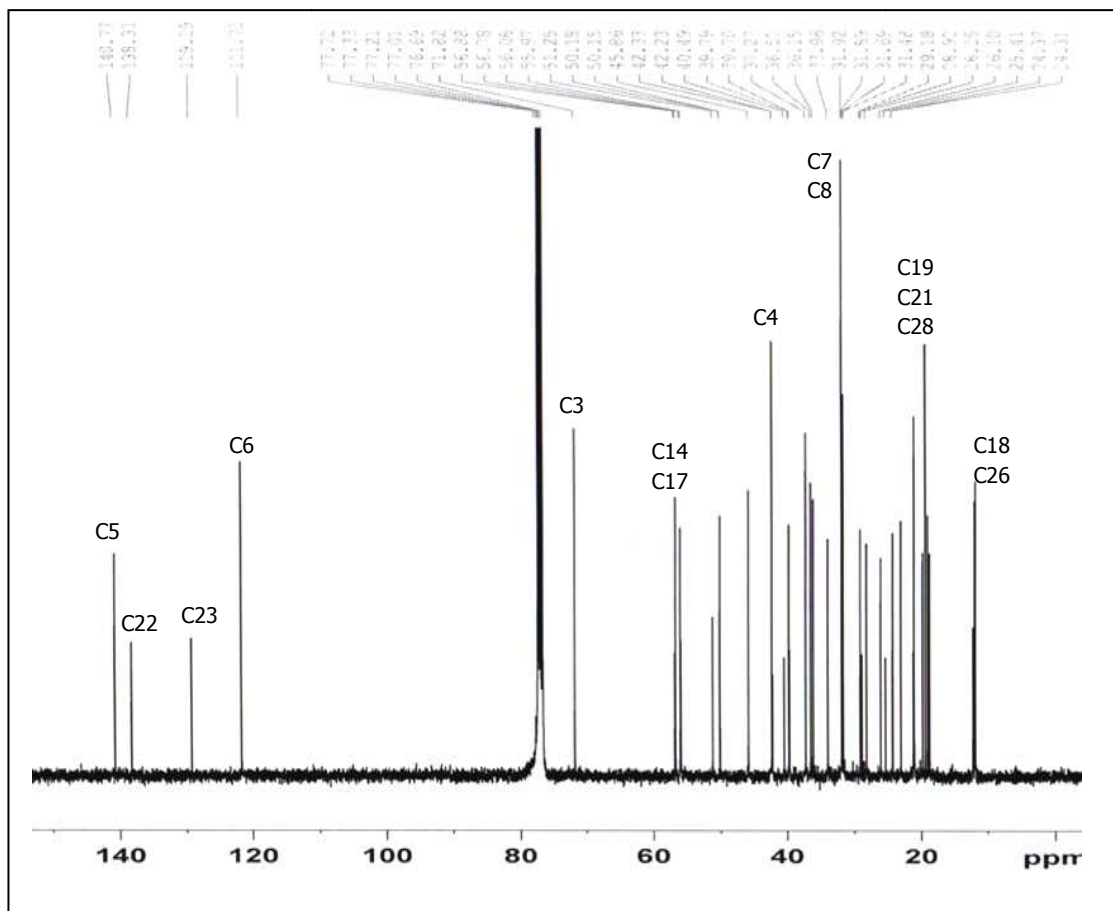
IR spectrum, ^1H NMR and ^{13}C NMR of the mixture of compound 109a and 109b



App.3.1. IR spectrum of the mixture of compound 109a and 109b (stigmasterol and β -sitosterol)



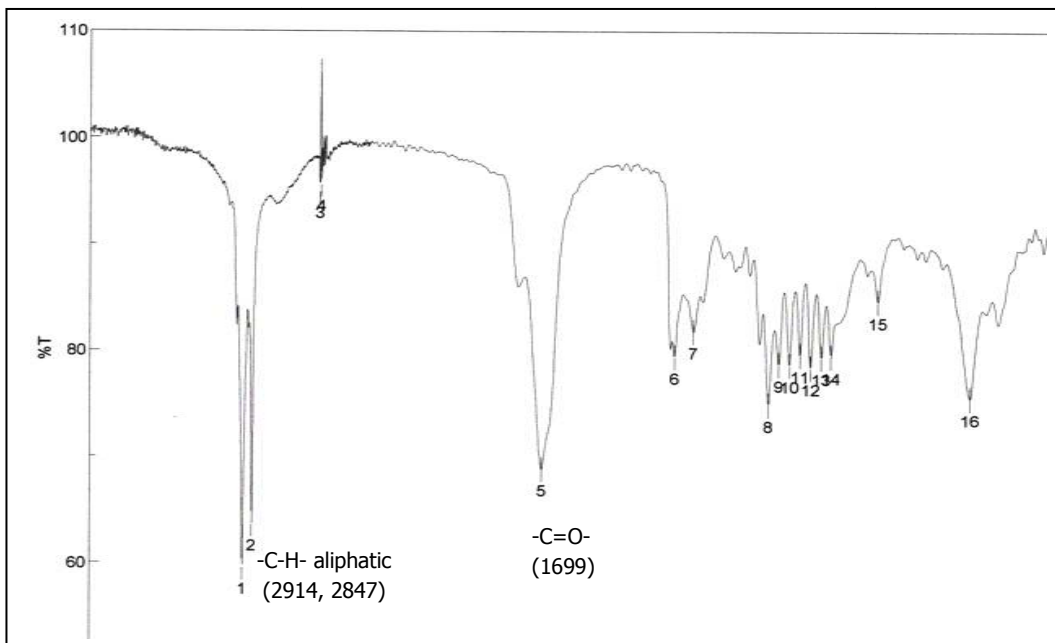
App.3.2. ^1H NMR of the mixture of compound 109a and 109b measured in CDCl_3 (500 MHz)



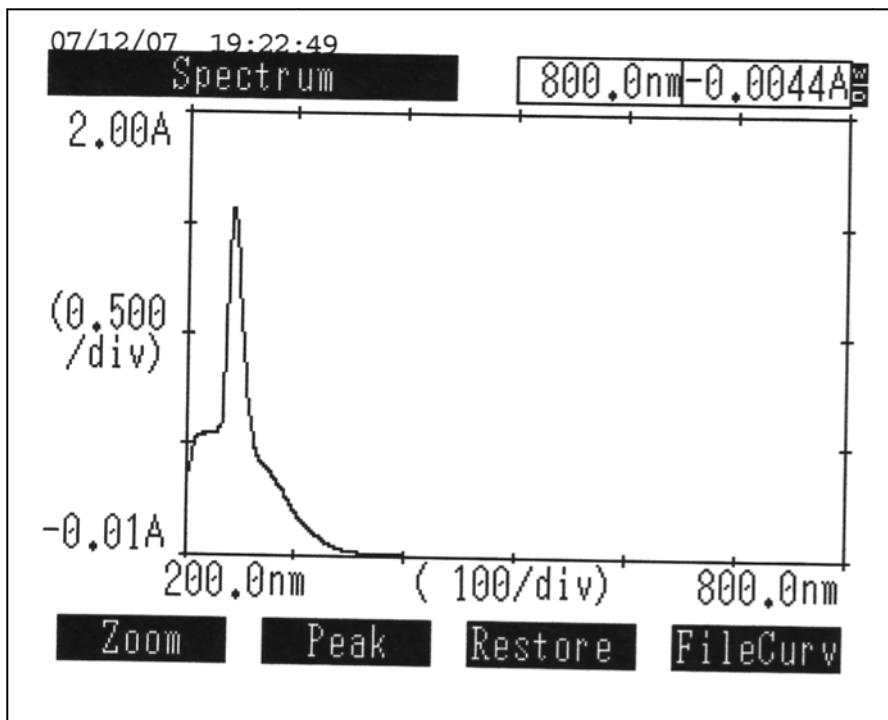
App. 3.3. ^{13}C NMR spectrum the mixture of compound 109a and 109b (stigmasterol and β -sitosterol) measured in CDCl_3 (125 MHz)

APPENDIX 4

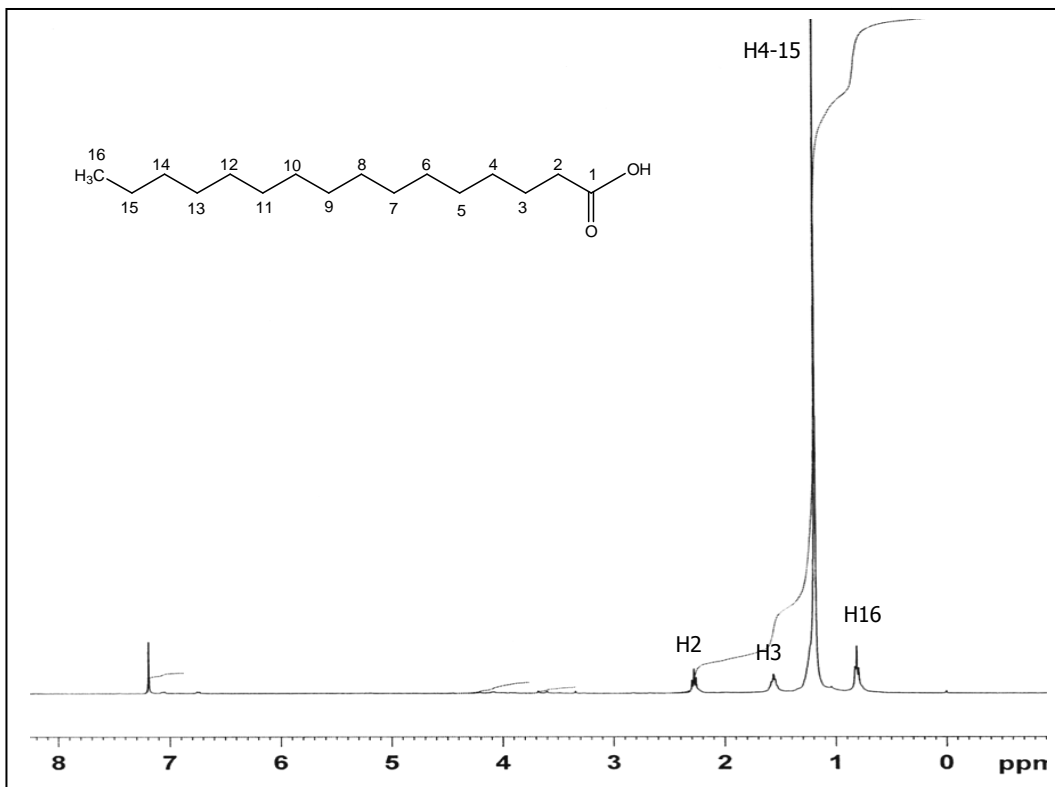
IR spectrum, UV spectrum, ¹H NMR and ¹³C NMR of compound WuPe



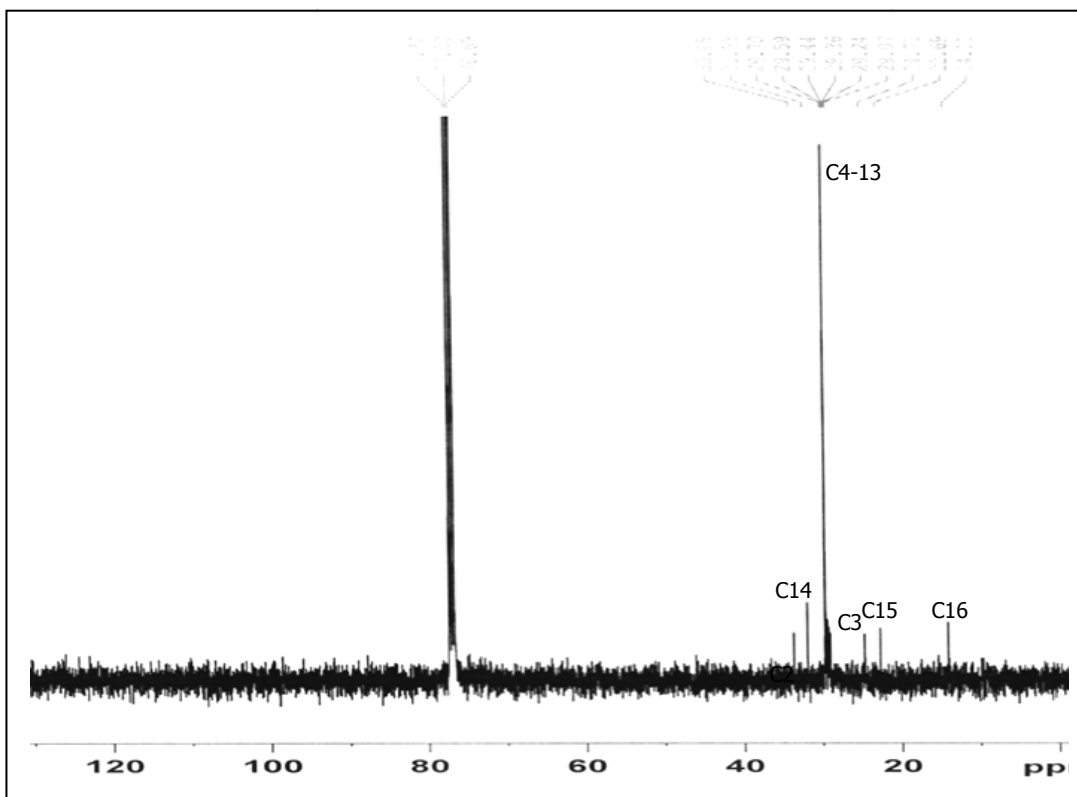
App.4.1. IR spectrum of compound WuPe (Palmitic acid)



App.4.2. UV spectrum of compound WuPe (Palmitic acid)



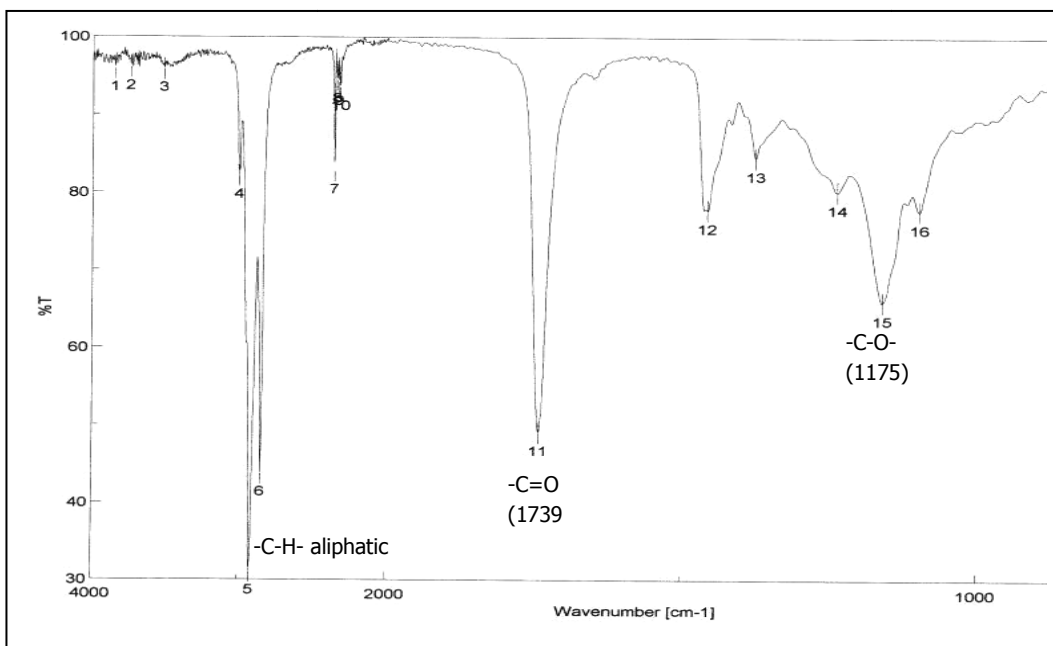
App.4.3. ¹H NMR of compound WuPe (Palmitic acid) measured in MeOH-d₄ (125 MHz)



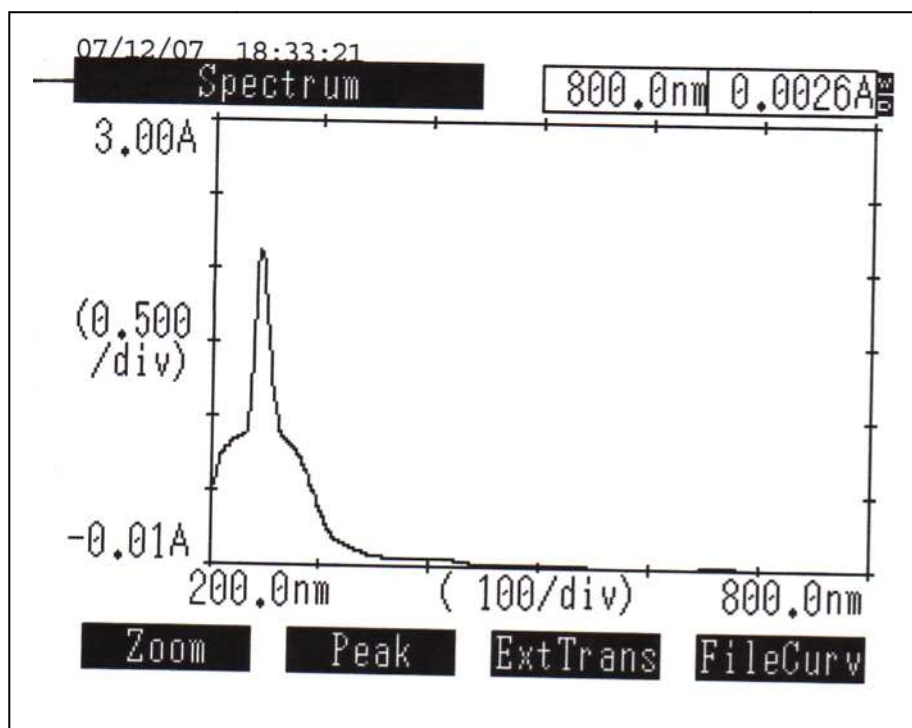
App.4.4. ¹³C NMR spectrum of compound WuPe (Palmitic acid) measured in MeOH-d₄ (125 MHz)

APPENDIX 5

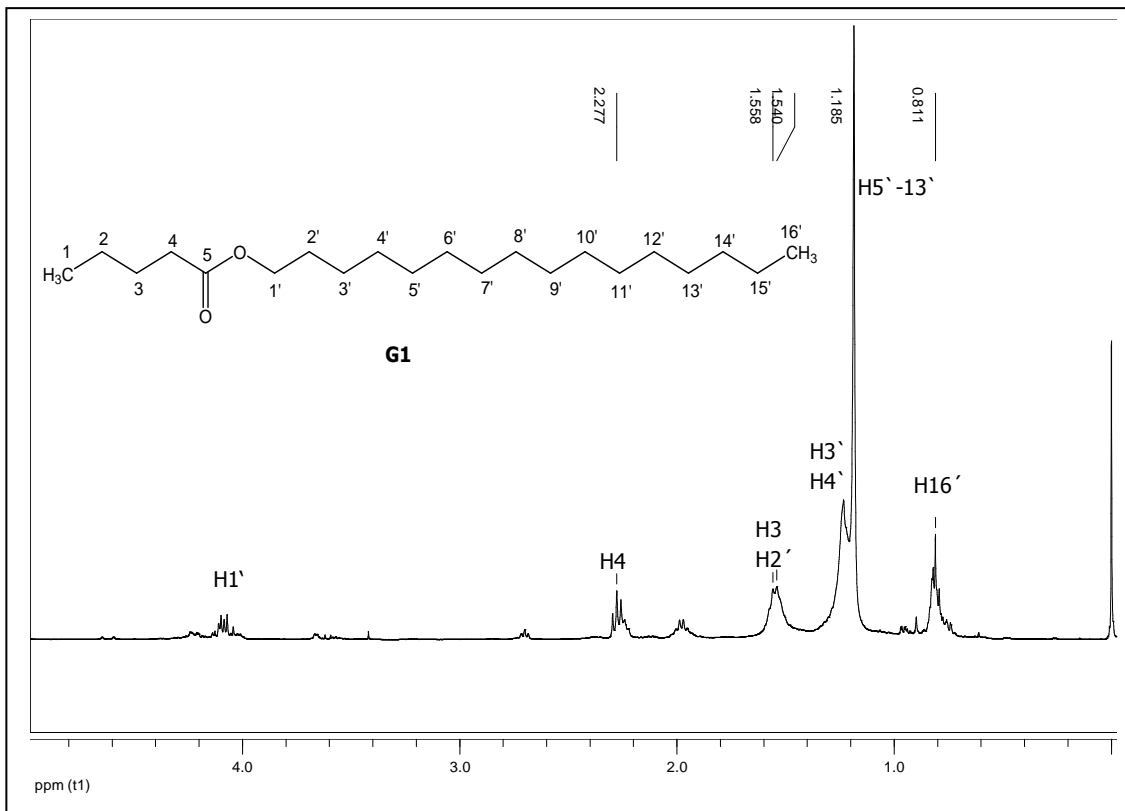
IR spectrum, UV spectrum, ¹H NMR and ¹³C NMR of compound G1



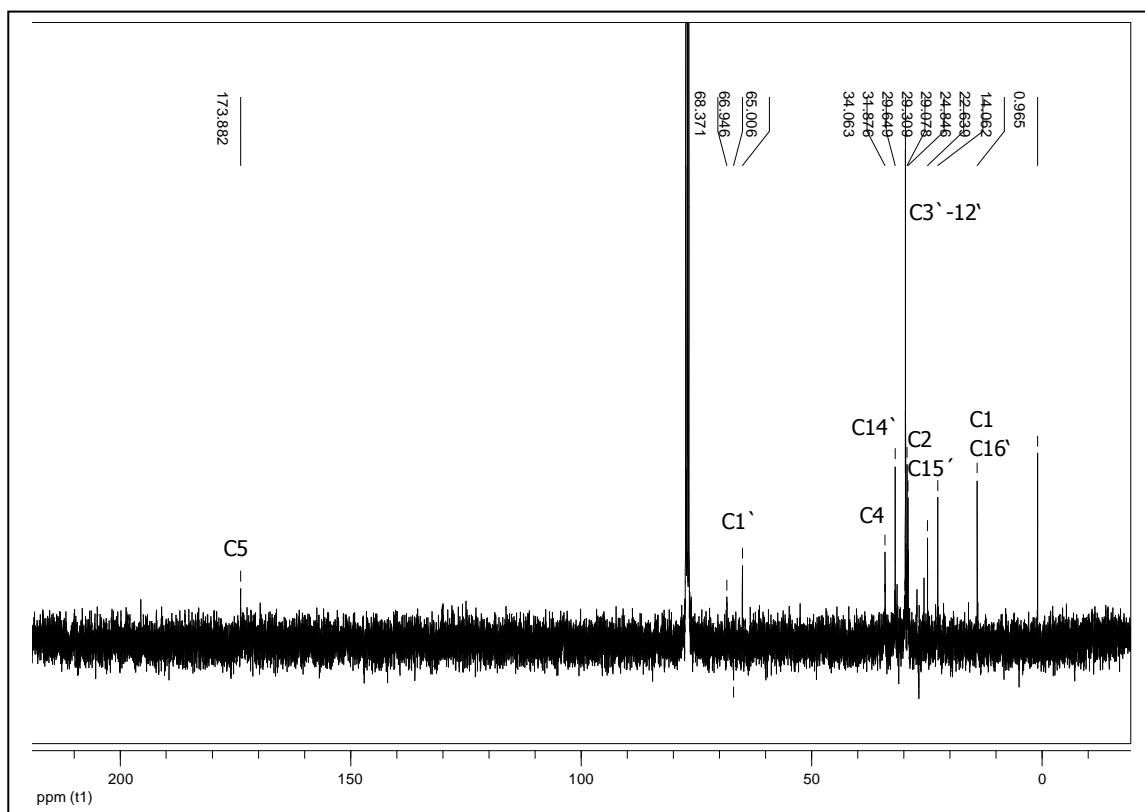
App.5.1. IR spectrum of compound G1 (Hexadecyl pentanoate)



App.5.2. UV spectrum of compound G1 (Hexadecyl pentanoate)



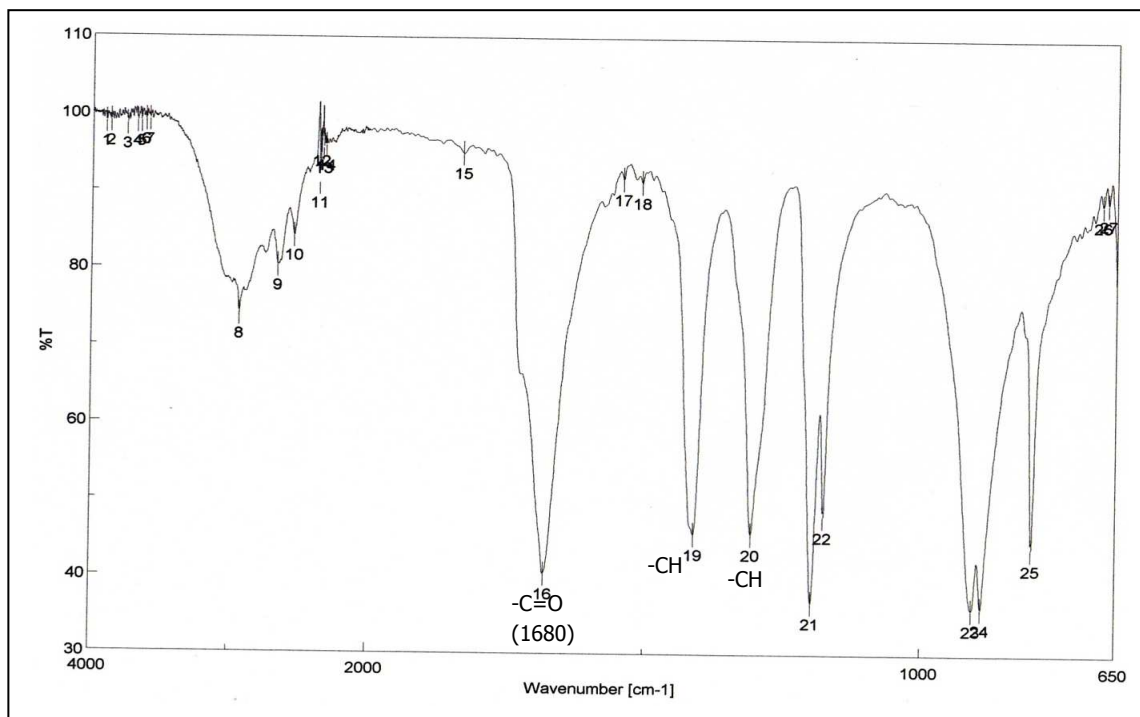
App.5.3. ¹H NMR of compound G1 (Hexadecyl pentanoate) measured in CDCl₃ (500 MHz)



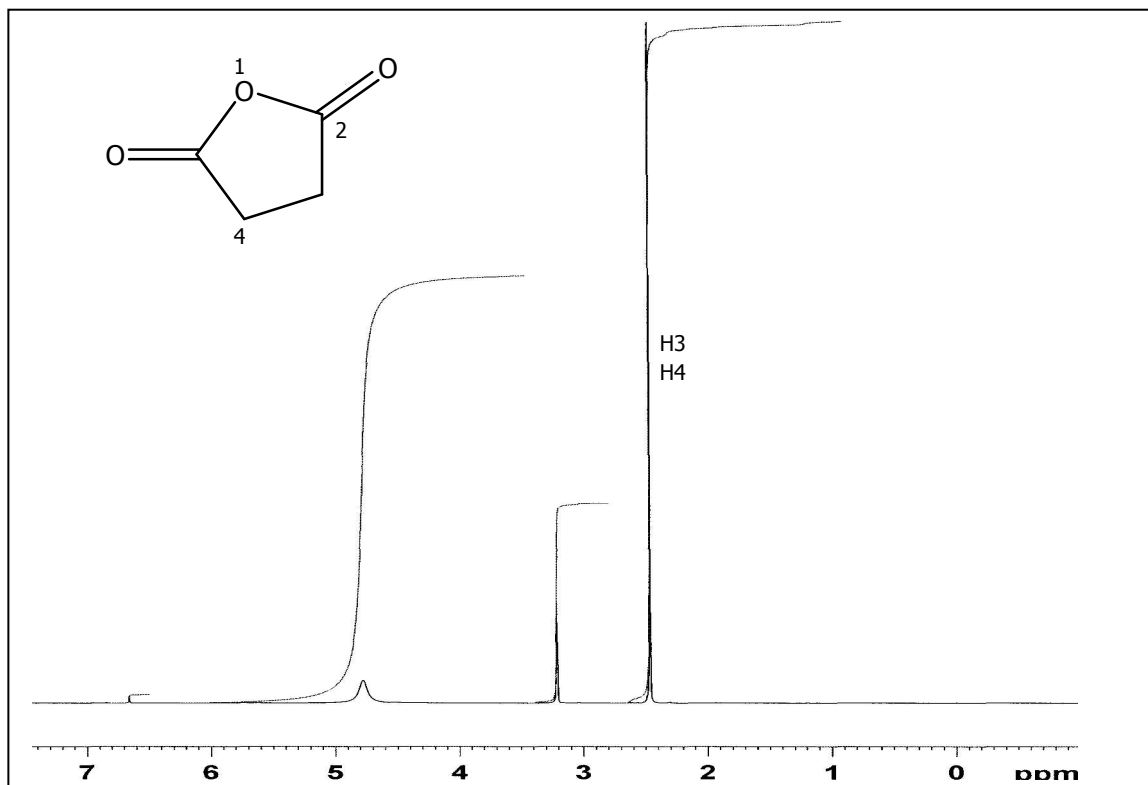
App.5.3. ¹³C NMR of compound G1 (Hexadecyl pentanoate) measured in CDCl₃ (125 MHz)

APPENDIX 6

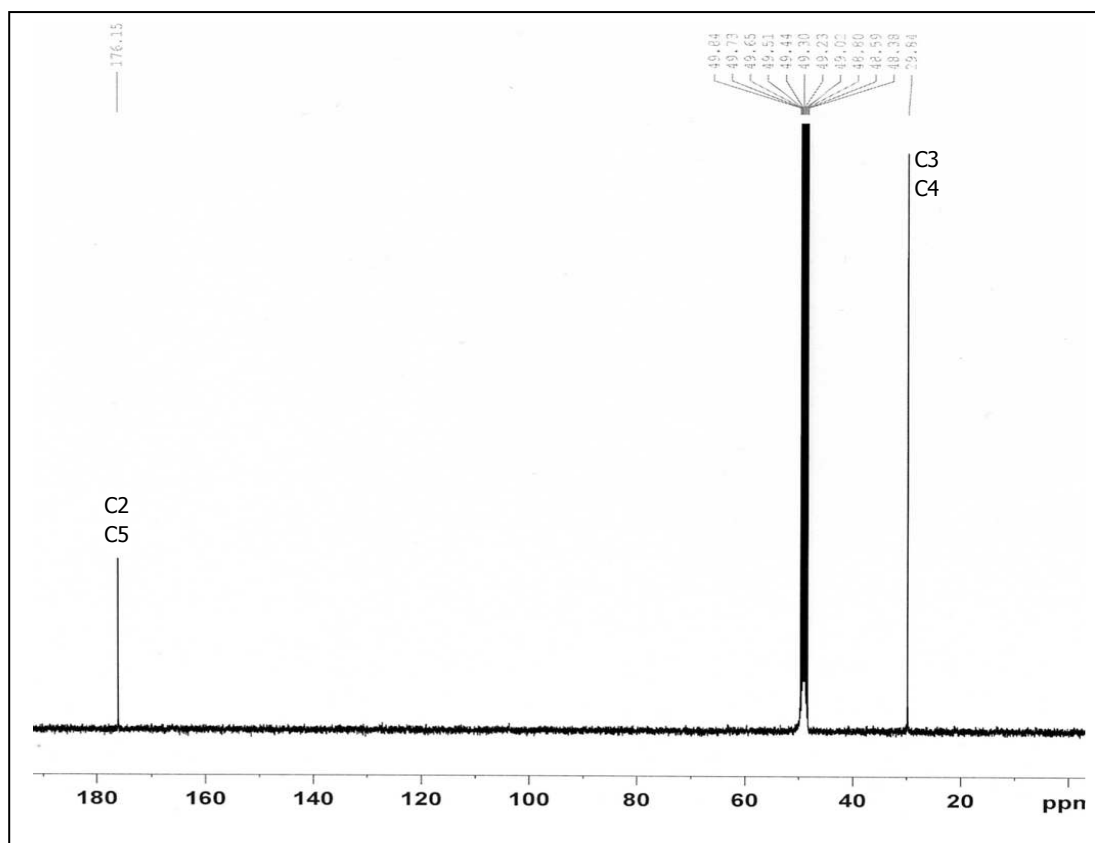
IR spectrum, ^1H NMR and ^{13}C NMR of compound W2Et



App.6.1. IR spectrum of compound W2Et (Dihydrofurane-2,5-dione)



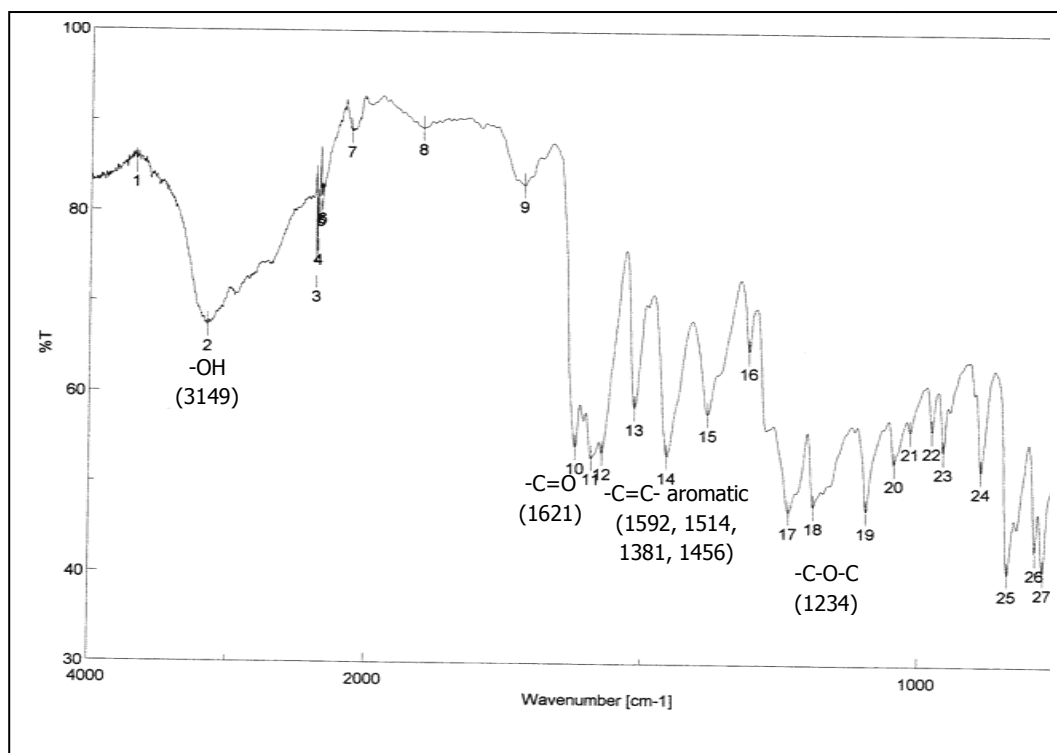
App.6.2. ^1H NMR spectrum of compound W2Et (Dihydrofurane-2,5-dione) measured in MeOH-d₄ (500 MHz)



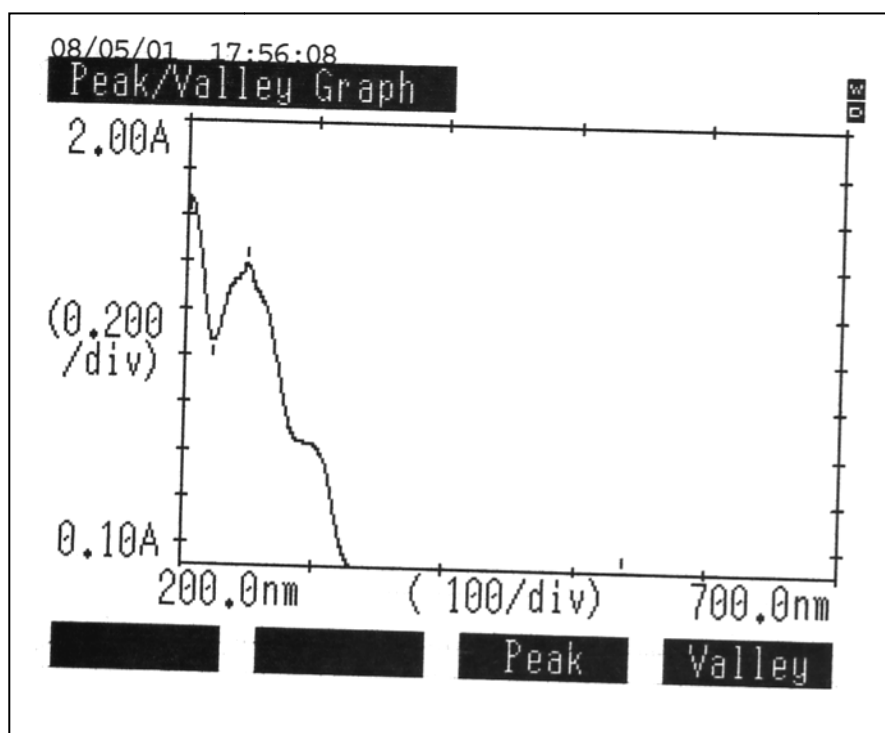
App.6.3. ^{13}C NMR spectrum of compound W2Et (Dihydrofurane-2,5-dione) measured in MeOH-d_4 , 125 MHz)

APPENDIX 7

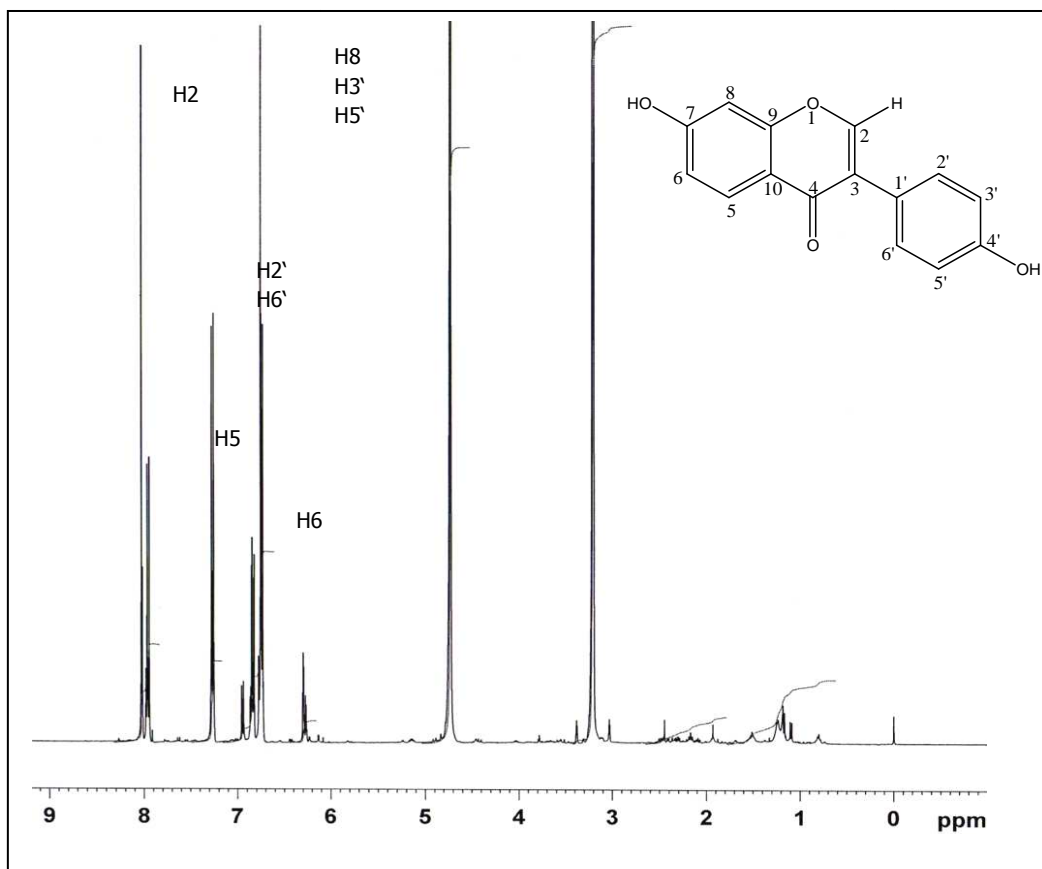
IR spectrum, UV spectrum, ¹H NMR and ¹³C NMR of compound C1



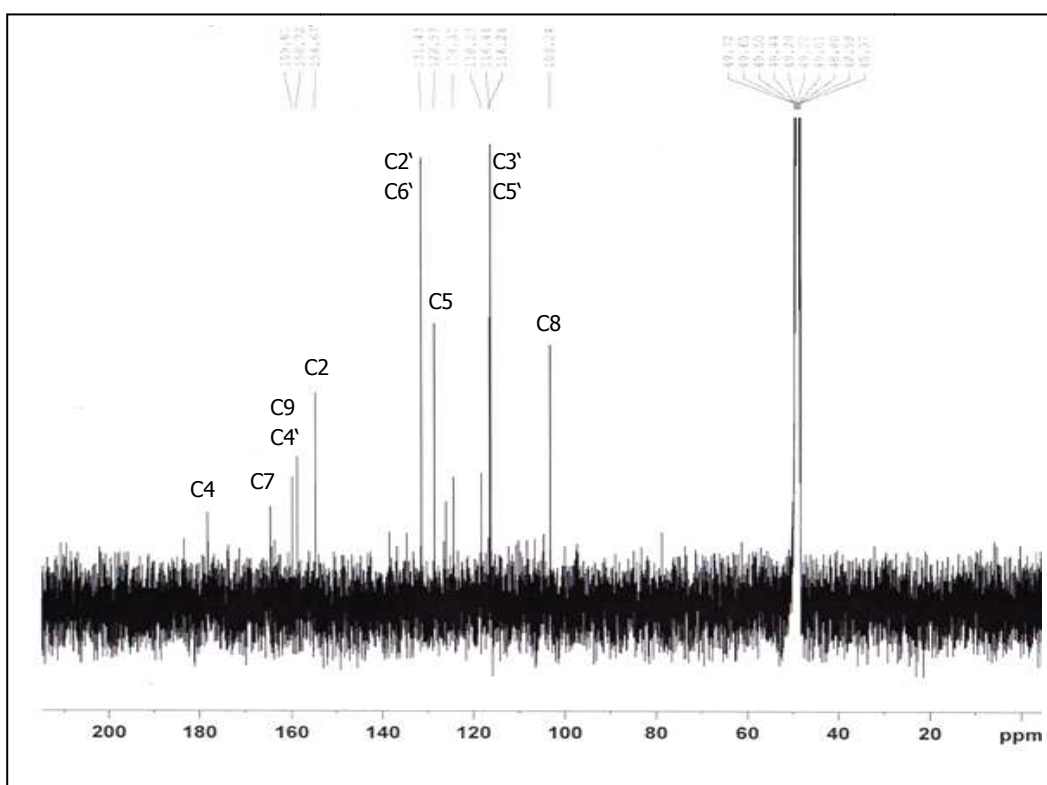
App.7.1. IR spectrum of compound C1 (Daidzein)



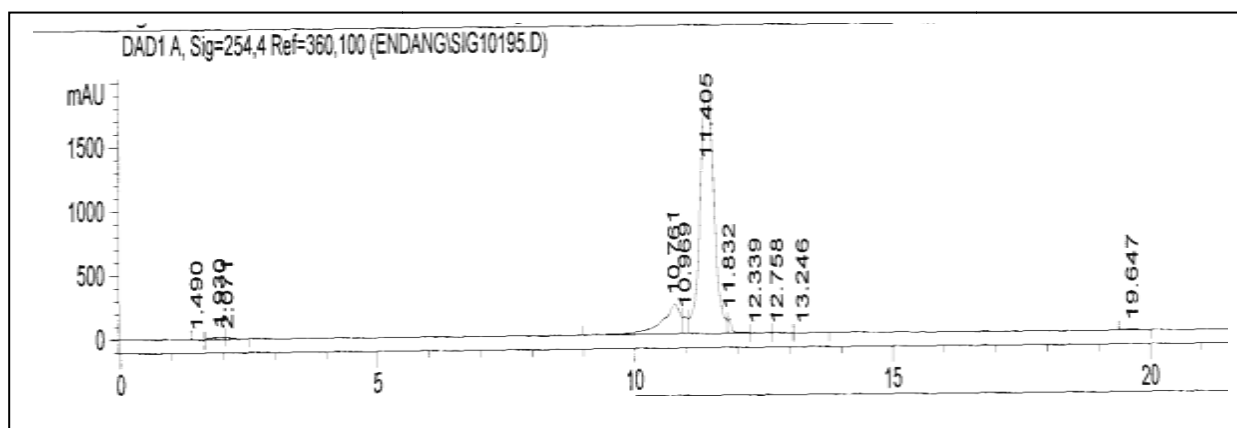
App.7.2. UV spectrum of compound C1 (Daidzein)



App.7.3. ^1H NMR of compound C1 (Daidzein) measured in MeOH-d_4 (500 MHz)



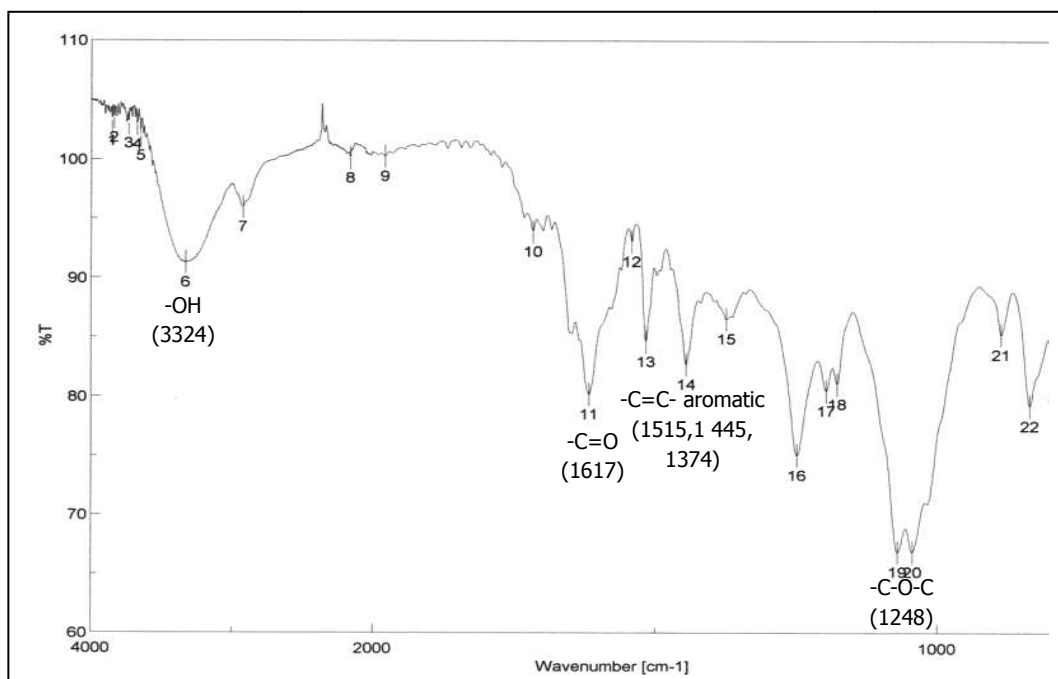
App.7.4. ^{13}C NMR spectrum of compound C1 (Daidzein) measured in MeOH-d_4 (125 MHz)



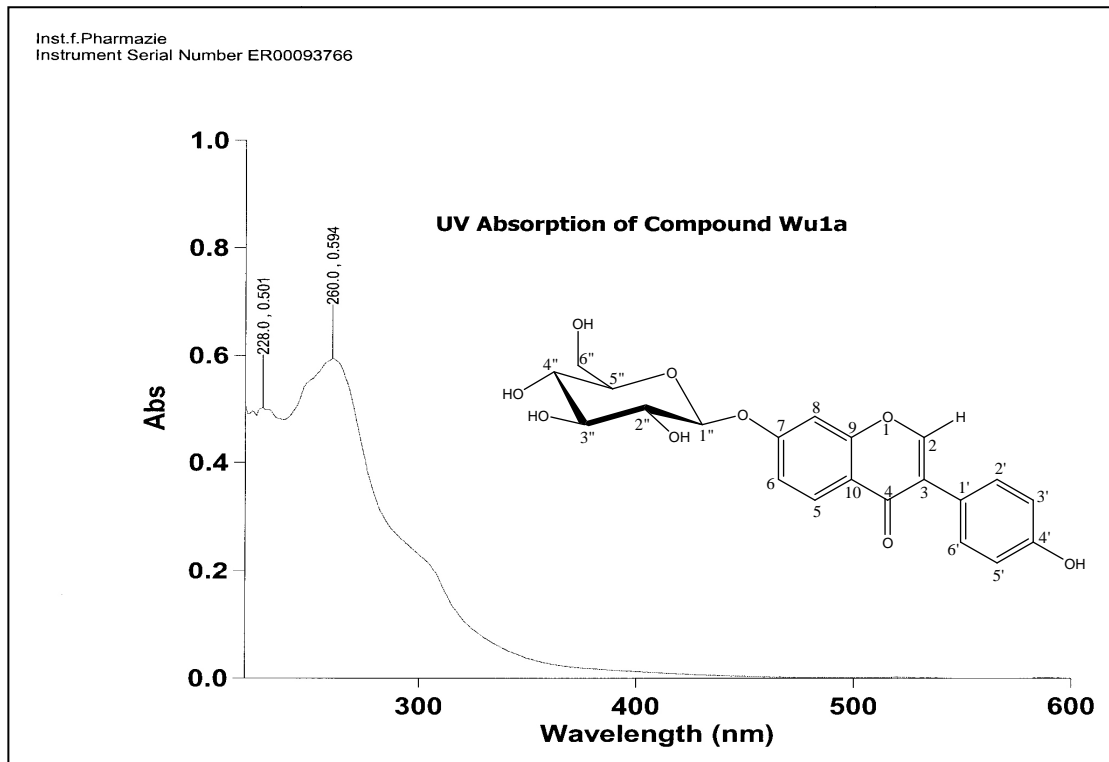
App.7.5. HPLC chromatogram of compound C1 (Daidzein) obtained with a column Zorbax SB-C18 (25 cm, i.d. 0,46 cm, 5 µm particle size) using a gradient mixture of MeOH-water as a mobile phase and UV detection at 254 nm

APPENDIX 8

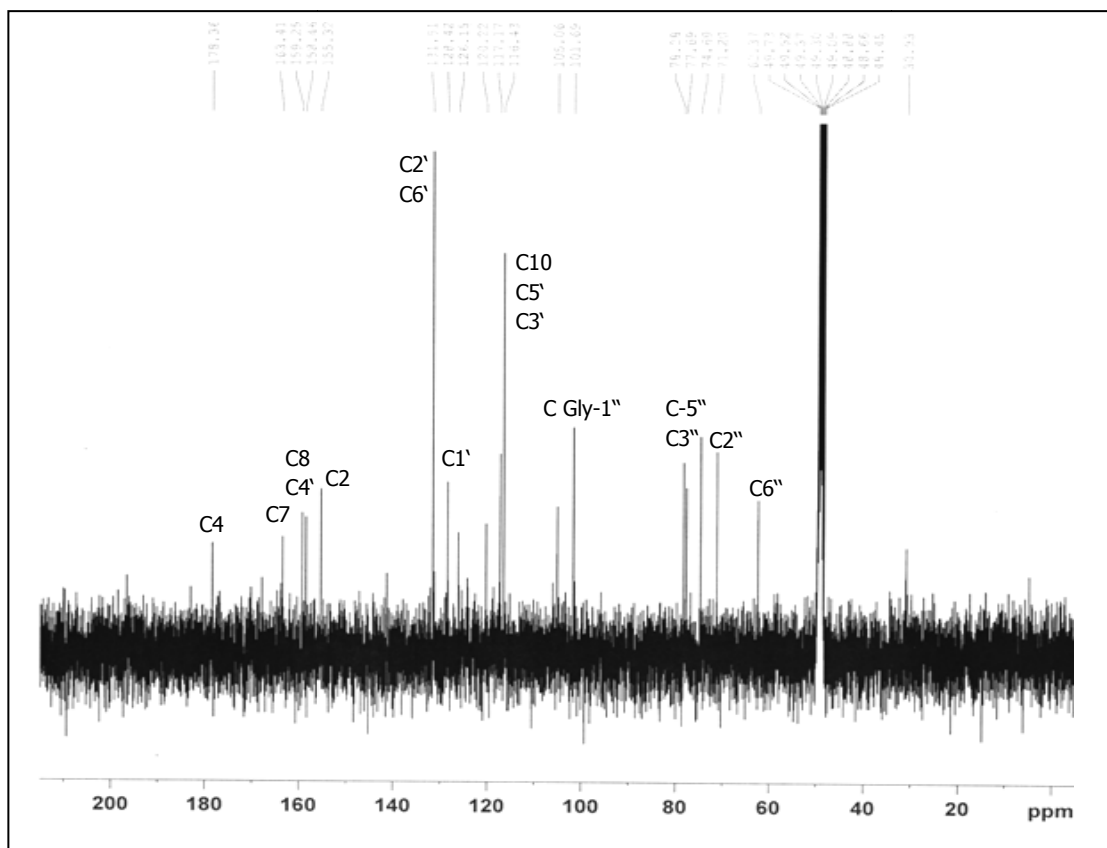
IR spectrum, UV spectrum, ¹H NMR and ¹³C NMR of compound Wu1a



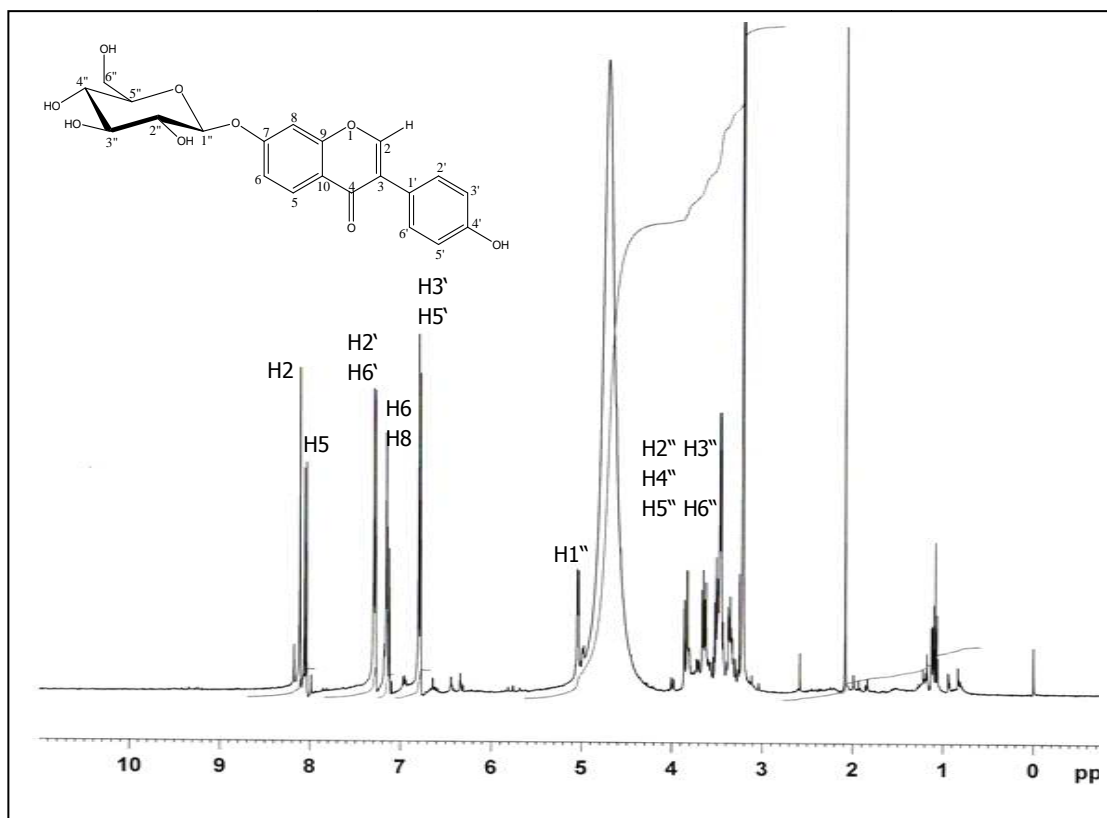
App.8.1. IR spectrum of compound Wu1a (Daidzein-7-O-β-glucopyranose)



App.8.2. UV spectrum of Wu1a (Daidzein-7-O-β-glucopyranose)



App.8.3. ^{13}C NMR of compound Wu1a (Daidzein-7-O- β -glucopyranose) measured in MeOH- d_4 (125 MHz)



App.8.4. ^1H NMR of compound Wu1a (Daidzein-7-O- β -glucopyranose) measured in MeOH- d_4 (500 MHz)